A STUDY OF DIFFRACTION CHANNELS

BY

Gilbert Everett Dares.

Submitted in partial fulfillment

of the requirements for the degree of

Doctor of Philosophy

Faculty of Graduate Studies

Department of Physics

The University of Ottawa

Ottawa, Canada

1972

ABSTRACT

A diffraction channel is a series of identical confocal lenses equipped with opaque diaphrams which have light transmitting annuli. The work in this thesis is a study of the properties of diffraction channels and an investigation into their possible use by a scanning process for "hyperresolution" - resolution beyond the Rayleigh limit. Since the object to be resolved can be considered as an infinite set of point sources, the problem was studied by investigating how diffraction patterns are formed through the system for a point source on axis and off axis. Analytical expressions, numerical calculations and photographs of diffraction patterns obtained experimentally are presented to illustrate certain properties of diffraction channels. Two systems were designed, constructed and studied both theoretically and experimentally for their hyperresolving properties.

ACKNOWLEDGEMENTS.

I wish to especially express my gratitude to my supervisor, Prof. Guy Lansraux, who suggested the project, for his constant interest and guidance throughout . His advice in various aspects of the work is much appreciated.

Also, I wish to thank the National Research Council for authorizing me to use the laboratory facilities of the Diffraction Optics Section. I am greatly appreciative of the help of Mr. M. Ranger who constructed most of the equipment and provided technical advice.

I am most grateful to the staff of the computation center of the University of Ottawa for making the computational work possible by generously providing time on the IBM 360.

I wish to thank Diane Perron for her excellent job of typing the thesis in a short period of time.

I also wish to thank the National Research Council for financial assistance through an NRC scholarship.

TABLE OF CONTENTS

page

page

page

LIST OF ILLUSTRATIONS.

page

page

page

page

page

LIST OF TABLES

page

CHAPTER 1

1.1 Introduction

Whenever coherent light is transmitted through any diaphram, it cannot be focused to a point but instead gives a diffraction pattern in which the central spot has a certain finite size inversely proportional to the size of the diaphram. For the special case of an aberration free lens limited by a circular diaphram, the image of a point source is a diffraction pattern known as the "Airy pattern". The Airy patterns of two point sources will not be resolved if the distance separating them is less than the radius of the central spot. Lord Rayleigh stated that two equally bright point sources could just be resolved by an optical system if the centre of one Airy pattern coincided with the first dark ring of the other. This condition is illustrated in figure 1.1

For quite some time it was widely accepted that this condition represented a fundamental limit to the resolution of an optical system and to resolve beyond the classical limit was a hopeless task. Recently, certain authors have found that it is in principle possible to surpass the limit of resolution set by the Rayleigh criterion. Toraldo di Francia (1952) stated, "... the classical limit of 1.22 λ/D, which has always been accepted as a theoretical limit, proved to be instead only a practical limit. Theoretically an optical instrument with a pupil of a given size can attain as high a resolving power as desired. The only limitation, if any, is set by the amount of luminous flux that we have at our disposal."

Other authors, for example Harris (1963), Barnes (1965), and Goodman (1968), have also shown that diffraction imposes a resolution limit determined by the noise of the system. Thus, the Rayleigh limit of resolution is of a practical, rather than a theoretical nature.

Some authors have had some success in the practical aspects of the problem by altering the transmission properties of the pupil. Using a series of light transmitting annuli, Toraldo di Francia (1952) was able to make the radius of the first dark ring of the image of a point source arbitrarily small and simultaneously, the dark ring zone arbitrarily large. However, this improvement was accompanied by an increase in the luminous energy outside this dark zone. Furthermore, for any substantial improvement in the resolution, the efficiency of the superresolving pupil would be poor and the tolerances on the radii would be severe. Boivin (1969) have used flux selectors to supress the outer rings of the Airy pattern at the sacrifice of a slight increase in the size of the central spot. This resulted in a very noticeable improvement in the resolving power for point sources as objects. A similar result was also obtained by Lansraux (1965) with the use of amplitude filters instead of flux selectors.

Part of the work in this thesis is an investigation into "hyper-resolution" - resolution beyond the classical limit. The method is new in its approach and it is necessary to present a brief description of the optical system before explaining its operation. The image formed by a conventional optical system is transmitted through an optical system called a Diffraction Channel consisting of identical confocal lenses (i.e. lenses spaced a distance equal to twice their focal length) limited by circular diaphrams or light transmitting annuli as illustrated in figure 1.2.

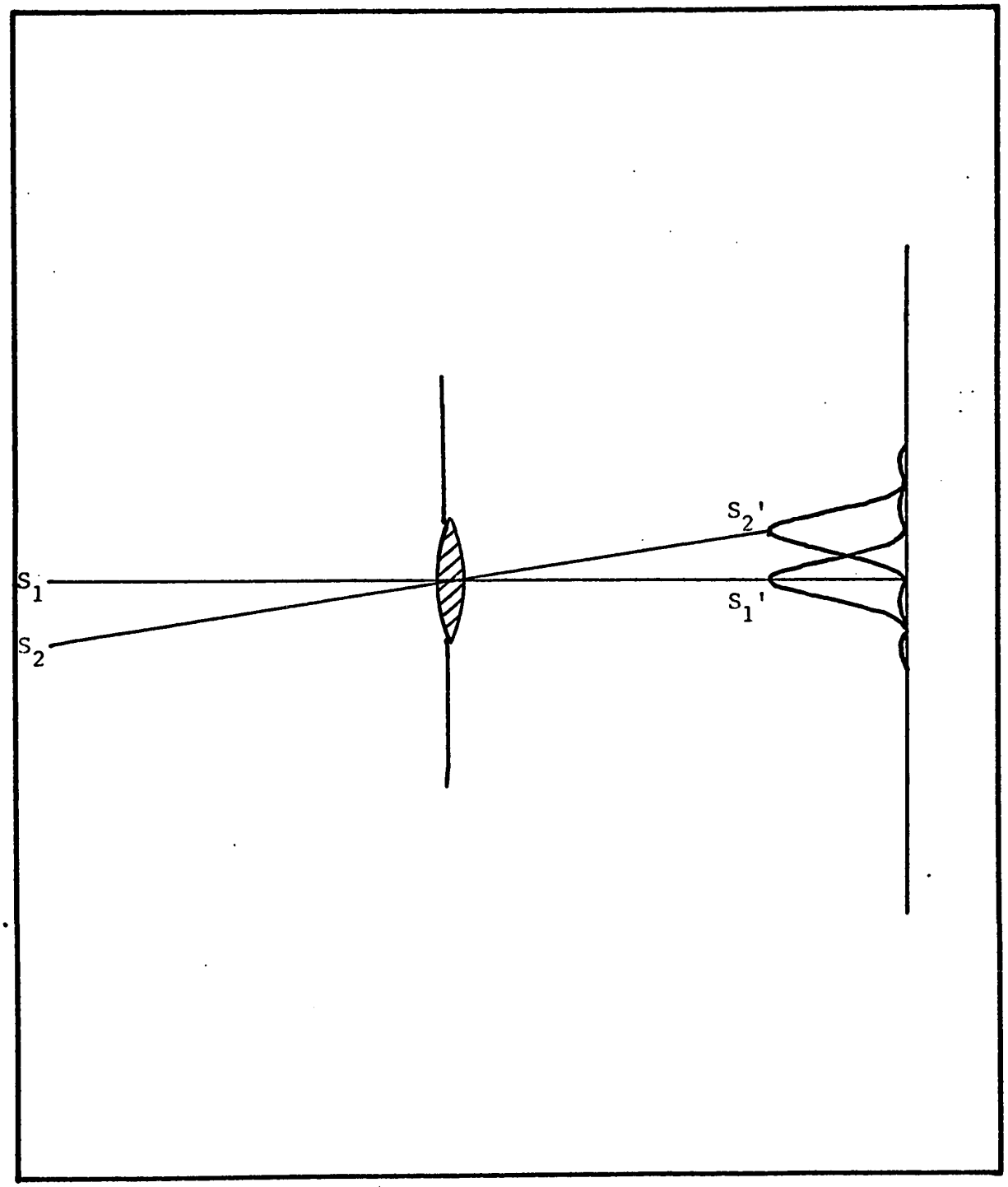

figure 1.1 Lord Rayleigh Criterion of Resolution.

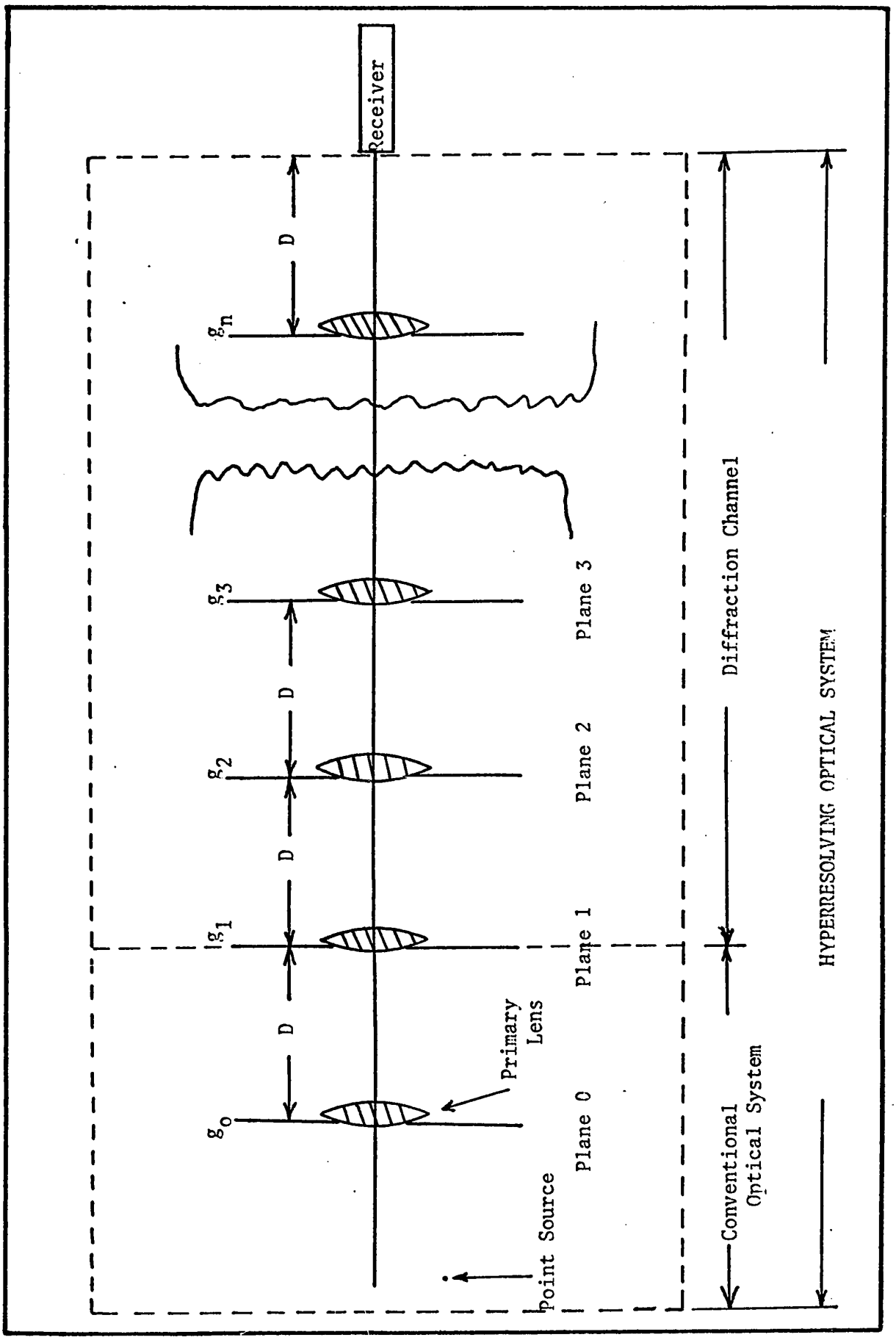

figure 1.2 A hyperresolving optical system.

The conventional optical system may be of any type, for example, the primary mirror of a telescope or the objective of a microscope, but for the purpose of this investigation will be represented by a lens limited by a circular diaphram. A "hyperresolving optical system" is formed by combining a conventional optical system with a diffraction channel in such a way that their axes are collinear and the conventional image is formed in the plane of the first channel lens as indicated in figure 1.2. The lens representing the conventional optical system then becomes the "primary lens" of the hyperresolving optical system.

To understand the process by which an image is constructed with a hyperresolving optical system, consider the region of the object plane inside a circle centered on the axis, of given radius much smaller than the Rayleigh limit of resolution. Suppose that the luminous energy emitted by this region is transmitted through the channel with a much lower loss than the luminous energy outside the region. In this case, the luminous energy received will be proportional to the luminous energy emitted from this region. If a hyperresolving optical system having a diffraction channel with such a characteristic is used to scan an object, a recording can be made of the output luminous energy at each position of the object and this information can then be used to construct an image of the object. In the scanning process, each position of the object is associated with three recorded parameters which together contain the necessary information - the two positional coordinates and the output luminous energy. In the image construction process, luminous spots may

be placed on a photosensitive screen such that their energy and positional coordinates are directly proportional to those recorded. This construction process is commonly used in modern technology, for example, in television. Since each region recorded is well within that defined by the Rayleigh limit, the constructed image will have a resolution beyond this limit.

The resolution of the constructed image depends on the energy characteristics of the hyperresolving system. These characteristics may be studied by considering the object as an infinite set of point sources. The transmission loss through the diffraction channel for each of these object point sources depends on the distance of the point source from the axis. Thus information on the performance of the hyperresolving system may be obtained by comparing the energy received from a point source on the optical axis to the energy received from the same point source at various positions off the axis. An ideal hyperresolving system would only transmit energy when the point source is exactly on the axis. In the design of a hyperresolving system attempts must be made to approach as closely as possible this ideal. However, in view of the fact that hyperresolution was for some time considered impossible, a demonstration of its possibility could be considered of major importance. The minimum requirement for a hyperresolving system may be stated in terms of the normalized energy - the ratio of the energy received from a point source off the axis to the energy received from the same point source on the axis. A hyperresolving optical system must at least satisfy the requirement that the normalized energy is negligible when the point source is at a greater distance from the axis than a chosen distance which must be smaller than the Rayleigh limit of resolution.

The work reported in this thesis is an investigation into diffraction channels. It consists of a broad study of the general properties of diffraction channels as well as a study of their possible use for hyperresolution.

1.2 Introductory theory.

This introductory theory will be restricted to the case of a diffraction channel equipped with diaphrams. The theory will be extended later to the more general case where annuli or diaphrams may be used.

To design a diffraction channel it is necessary to choose the diaphram radii so as to obtain the greatest possibl e decrease in output energy when the point source is moved off the axis. This choice must be based upon the distribution of the complex amplitude at each pupil for each position of the point source. To understand how these diffraction patterns may be calculated, suppose the complex amplitude distribution bounded by a diaphram or radius a_n on the spherical surface Σ_n is represented by $g_n(X,\phi)$ (see figure 1.3). It can be shown that the complex

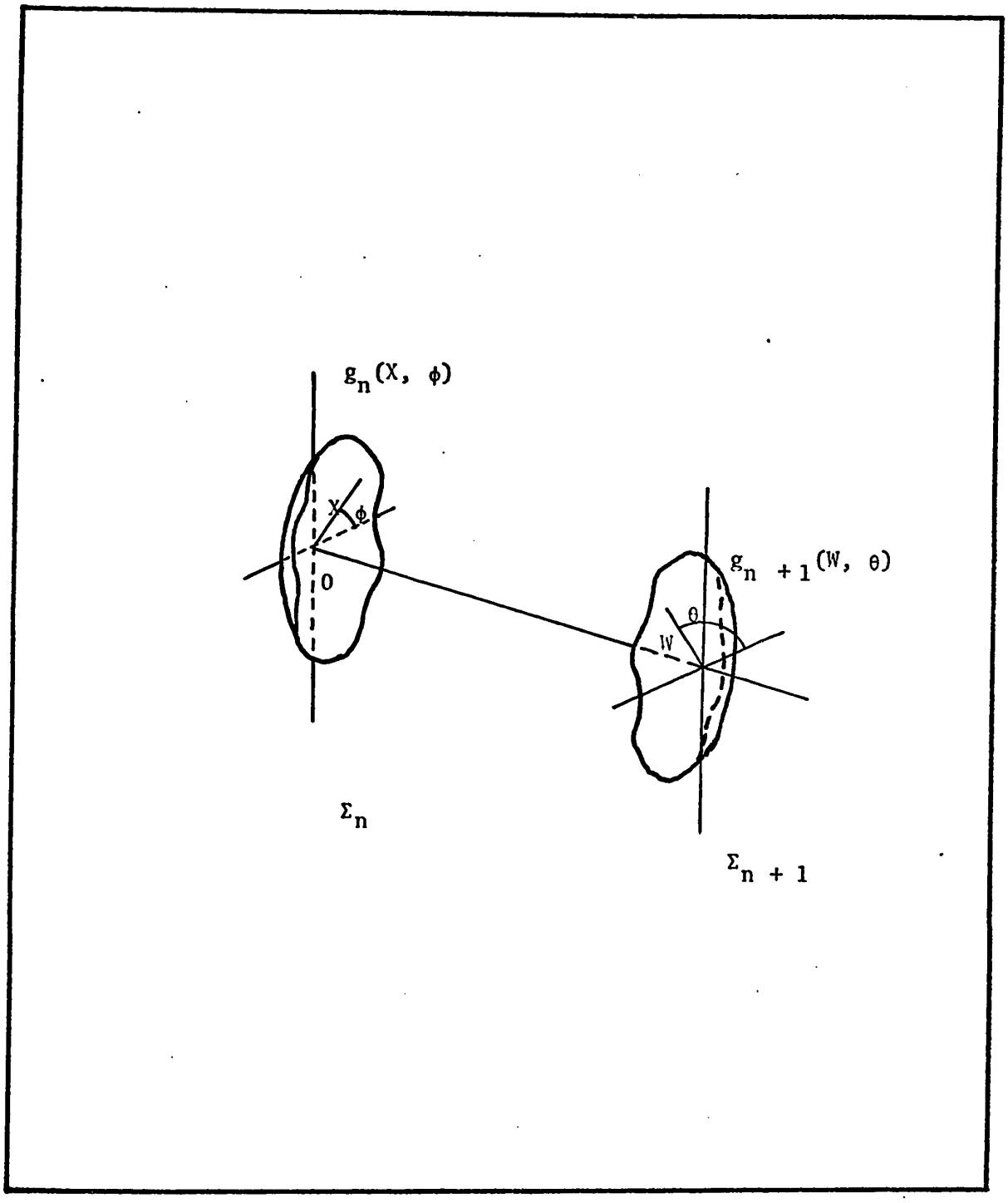

figure 1.3 Confocal spherical surfaces Σ_n and Σ_{n+1}

amplitude distribution on the spherical surface Σ_{n+1} which is confocal to Σ_n is given by the Fourier Transform.

$$g_{n+1}(W, \theta) = \frac{1}{2\pi} \int_0^{A_n} \int_0^{2\pi} g_n(X,\phi) e^{iWX \cos(\phi - \theta)} X dX d\phi \qquad 1.1$$

where $X = \bar{\rho}\sqrt{\frac{2\pi}{D\lambda}}$

$W = \bar{r}\sqrt{\frac{2\pi}{D\lambda}}$

$A_n = \bar{a}_n\sqrt{\frac{2\pi}{D\lambda}}$

ρ is the radial coordinate on surface Σ_n

r is the radial coordinate on surface Σ_{n+1}

ϕ is the angular coordinate on surface Σ_n

θ is the angular coordinate on surface Σ_{n+1}

D is the radius of curvature of the confocal spheres Σ_n and Σ_{n+1}

a_n is the radius of the diaphram at Σ_n

λ is the wavelength of the light

The amplitude distributions are expressed in terms of W and X instead of the radial coordinates r and ρ because of dependency on the parameters D and λ. The chosen definitions of W and X ensure a scaling of r and ρ by the same constant making interpretation simpler.

The distribution on the spherical surface Σ_{n+1} can be transformed by a lens of focal length D into the same distribution on the plane surface π_{n+1} as shown in figure 1.4. Similarly, the distribution on the surface Σ_n can be considered as resulting from a transformation by a lens of the same distribution on a plane surface π_n. Hence the distribution $g_n(X, \phi)$ on the plane π_n gives a corresponding distribution $g_{n+1}(W, \theta)$ on the plane π_{n+1}. That is, there exists a process, which may be called iteration, for transfering optical information from one plane to another plane. The optical system from the reference plane π_n to the reference plane π_{n+1} will be considered as a basic unit called a "cell". A linear succession of such cells constitute a Diffraction Channel as indicated in figure 1.5A. As indicated in figure 1.5B, the channel becomes effectively, then, a series of identical confocal lenses of focal length D/2. The complex amplitude distribution $g_n(X, \phi)$ on the plane π_n can be considered as an extended coherent source for the complex amplitude distribution $g_{n+1}(W, \theta)$ on the plane π_{n+1}. Hence by repeated use of the equation 1.1 the diffraction pattern in any plane of the channel may be obtained. To do this, it is necessary to know the hyperresolving optical system input function, which is the complex amplitude distribution in the plane of the primary lens. For a point source as object, this distribution is given by,

$$g_o(X, \phi, S) = e^{iSX \cos \phi} \qquad 1.2$$

where $S = d\sqrt{\frac{2\pi}{D\lambda}}$

d is the distance of the point source from the axis.

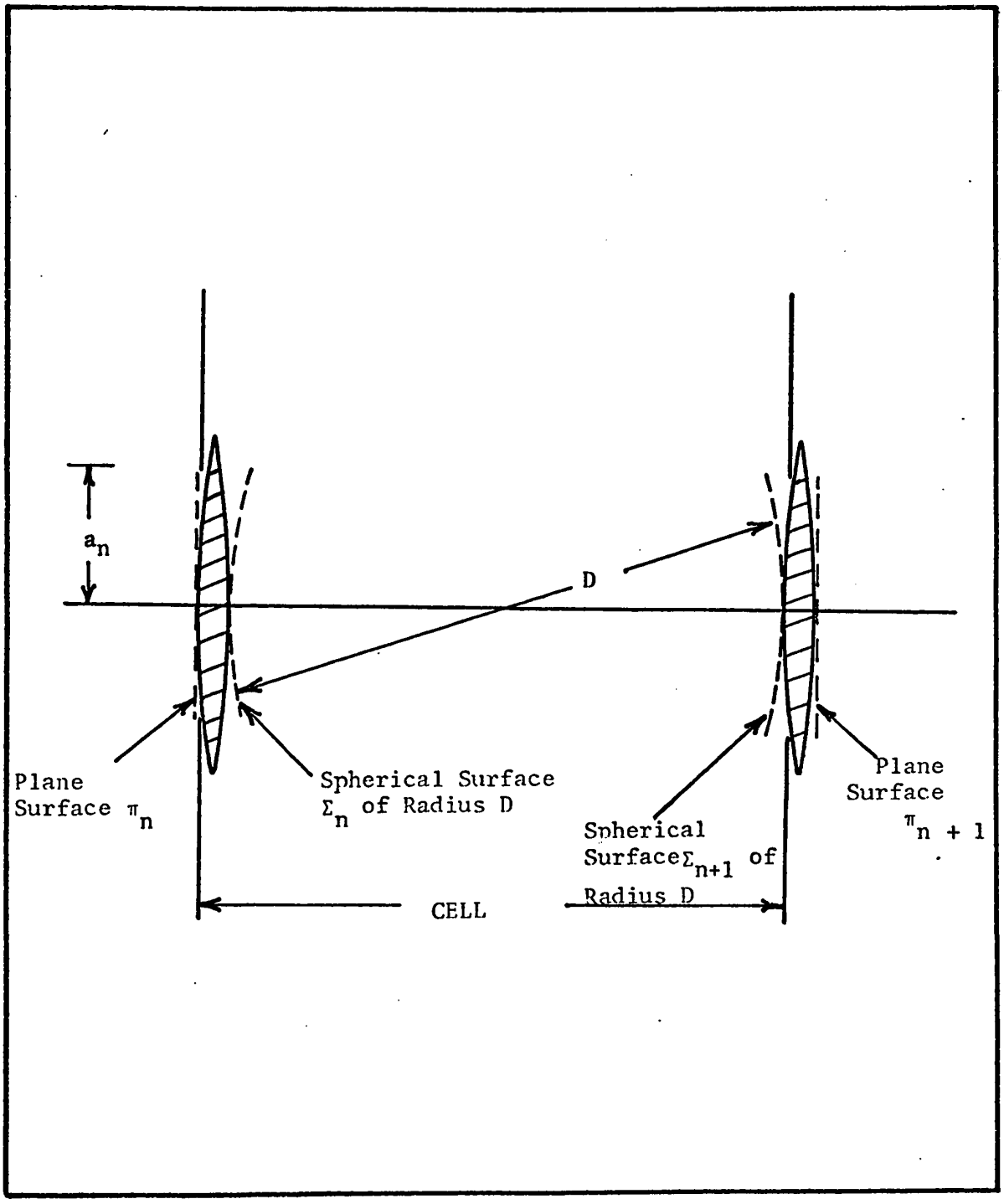

figure 1.4 Plane and confocal spherical surfaces for calculating iterated diffraction patterns.

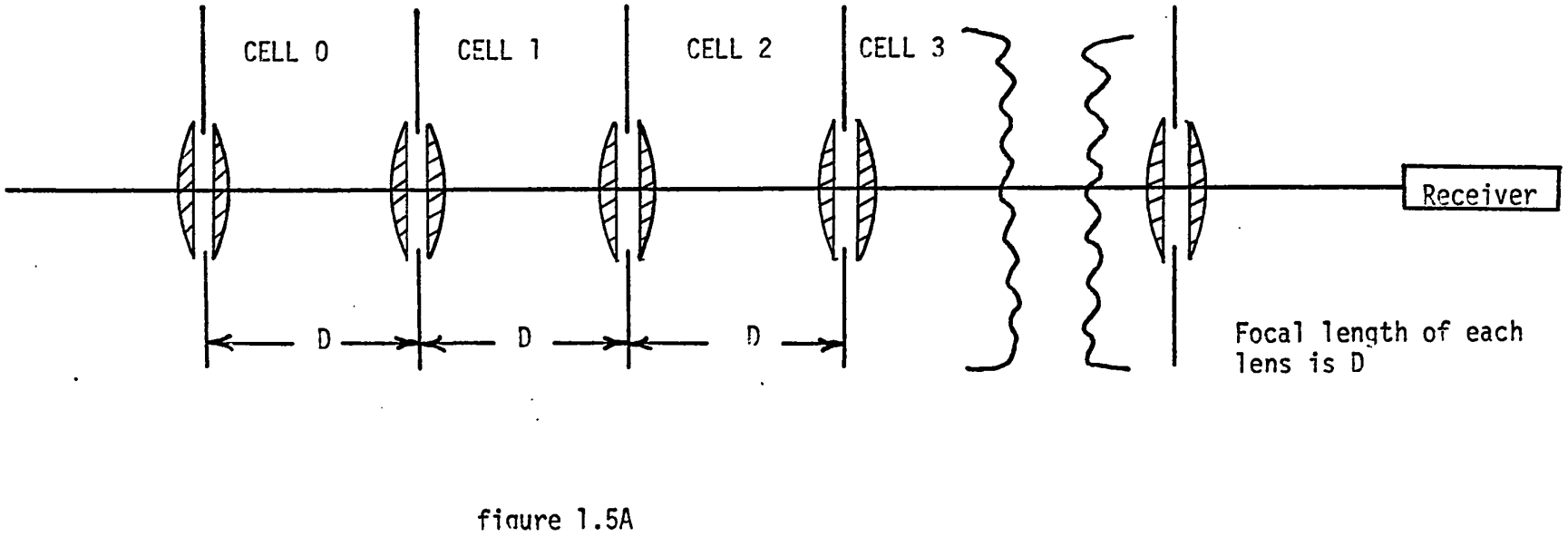

figure 1.5A

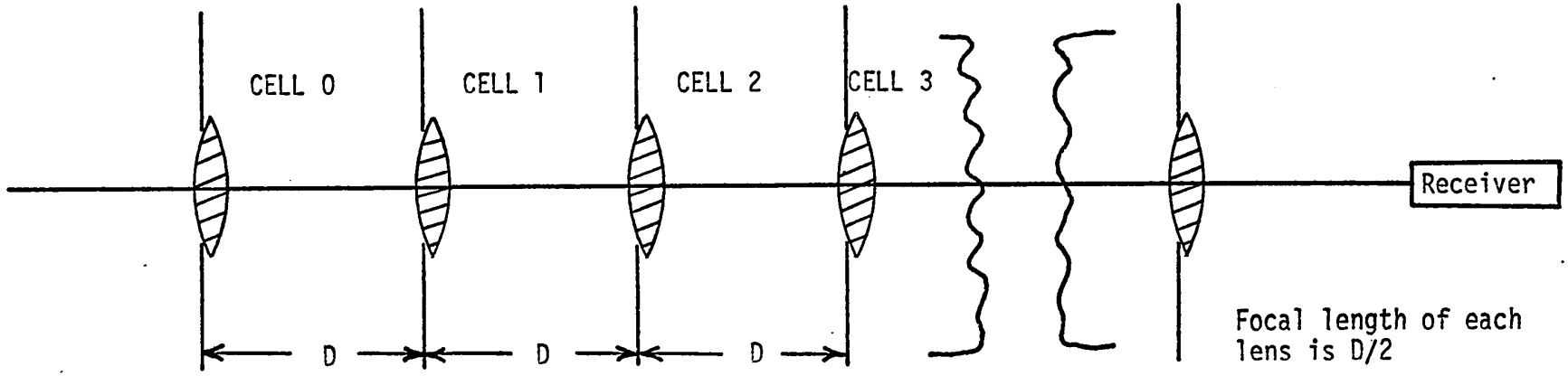

figure 1.5B

For convenience, the complex amplitude distributions will be expressed in terms of the independent variable W on the even planes and the independent variable X on the odd planes. This ensures that the results of one calculation can be immediately applied to the next calculation without a change of variable.

Thus we have,

$$g_{n+1}(W, \theta, S) = \frac{1}{2\pi} \int_0^{2\pi} \int_0^{A_n} g_n(X, \phi, S) e^{iWX \cos(\phi - \theta)} \, X dX d\phi \qquad n \text{ even} \qquad 1.3$$

$$g_{n+1}(X, \phi, S) = \frac{1}{2\pi} \int_0^{2\pi} \int_0^{A_n} g_n(W, \theta, S) e^{iWX \cos(\phi - \theta)} \, W dW d\theta \qquad n \text{ odd}$$

Corresponding to each of these functions, it is useful to define a normalized function given by,

$$G_n(W, \theta, S) = \frac{g_n(W, \theta, S)}{g_n(0, 0, 0)} \qquad n \text{ odd}$$

$$G_n(X, \phi, S) = \frac{g_n(X, \phi, S)}{g_n(0, 0, 0)} \qquad n \text{ even}$$

In the course of the research work, it was found necessary to modify the original concept of diffraction channels having only central diaphrams to diffraction channels with annuli. Diffraction channels with up to two annuli were studied. The notation chosen for the parameters and radii of these annuli are:

$A_n = a_n \sqrt{\frac{2\pi}{D\lambda}}$ where a_n is the outer radius of the largest annulus.

$B_n = b_n \sqrt{\frac{2\pi}{D\lambda}}$ where b_n is the inner radius of the largest annulus.

$C_n = c_n \sqrt{\frac{2\pi}{D\lambda}}$ where c_n is the outer radius of the smallest annulus

$D_n = d_n \sqrt{\frac{2\pi}{D\lambda}}$ where d_n is the inner radius of the smallest annulus.

When only one annulus was studied, the notation for the largest annulus was chosen.

CHAPTER 2.

PROPERTIES OF ITERATED DIFFRACTION PATTERNS.

Several mathematical expressions have been found which show explicitly certain properties of iterated diffraction patterns, thereby providing greater insight into the study of diffraction channels. We were obliged to derive most of these expressions since it was not possible to find them in the literature.

2.1 Calculation of Diffraction Patterns for the special case of Axial Symmetry and Identical Diaphrams.

A diffraction channel with identical radii and with the point source on the axis has special significance because of its simplicity and similarity with other systems (i.e. the beam waveguide, and the confocal resonator which is essential to certain types of CW lasers). Since the point source is on the axis, $g_n(X, \phi)$ of equation 1.1 is independent of ϕ. The equation then becomes.

$$g_{n+1}(W) = \frac{1}{2\pi} \int_0^{2\pi} \int_0^{A_n} g_n(X)\, e^{iWX \cos(\phi-\theta)} X\, dX\, d\phi \qquad 2.1$$

It is well known that,

$$\int_0^{2\pi} e^{iWX \cos(\phi-\theta)} d\phi = 2\pi J_o(WX) \qquad 2.2$$

where $J_o(WX)$ is a Bessel Function of the first kind and of zero order.

Thus, equation 2.1 simplifies to,

$$g_{n+1}(W) = \int_0^{A_n} g_n(X)\ J_o(WX)\ XdX \qquad 2.3$$

This equation, which reduces considerably the time needed to calculate a diffraction pattern having axial symmetry, has been used in this investigation to calculate iterated diffraction patterns.

In the special case where $n = 0$, $A_o = 1$, $g_o(X) = 1$ for $0 \leq X \leq 1$ this becomes,

$$g_1(W) = \int_0^1 J_o(WX)\ XdX = \frac{J_1(W)}{W} \qquad 2.4$$

This function represents the well known Airy pattern and has been used as an input distribution to the Diffraction Channel in this study. A picture of this pattern is shown in figure 2.1

2.2 Modes.

A diffraction channel with identical diaphrams has the same amplitude distributions as both the Beam Waveguide and the Confocal Resonator. The Beam Waveguide* is identical to a diffraction channel having identical diaphrams and is used for transmitting with low loss, high frequency electromagnetic radiation from one point in space to another point in space. The confocal resonator (which is sometimes used in lasers) consists of two confocal mirrors similar to the surfaces Σ_n and Σ_{n+1} in figure 1.3. Suppose a point source at 0 on the surface Σ_n illuminates the surface Σ_{n+1}. Then Σ_{n+1} can be considered as

* (Goubau and Schwering, 1961 and Christian and Goubau, 1961)

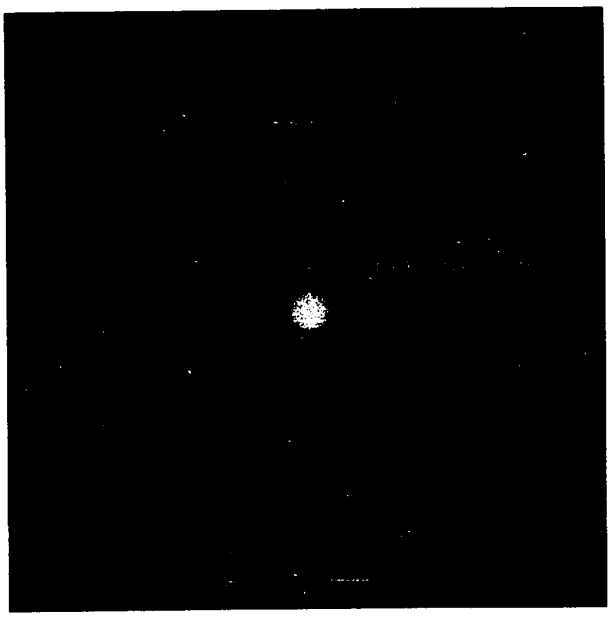

Figure 2.1 Photograph of Airy pattern.

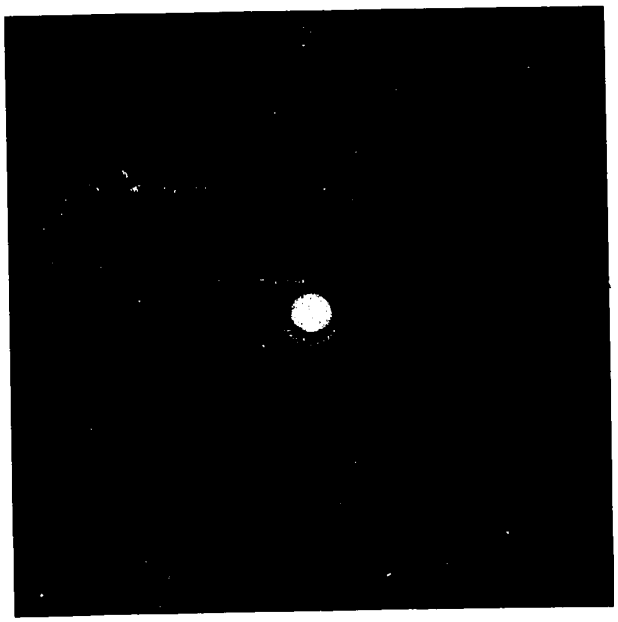

Figure 2.1 Photograph of Airy pattern.

an extended coherent source for Σ_n. The surface Σ_n in turn serves as a source for Σ_{n+1} and so on. Thus, the complex amplitude associated with each reflection may be calculated from repeated use of equation 1.1; they are therefore identical to those in a diffraction channel having identical diaphrams. Hence, any theoretical or experimental work performed on one system can be applied to the other system.

Much experimental and theoretical work has been performed on the Beam Waveguide and Confocal Resonator because of their important applications. One important characteristic found by several authors is that certain amplitude distributions on Σ_n will give identical distributions on Σ_{n+1}. If $f_{p,q}(X,\phi)$ is such a distribution, it must satisfy the relation,

$$K_{p,q}\, f_{p,q}(W,\theta) = \frac{1}{2\pi} \int_0^{2\pi} \int_0^{A} f_{p,q}(X,\phi)\, e^{iWX\cos(\phi-\theta)} X\,dX\,d\phi \qquad 2.5$$

There exist many distributions which will satisfy this equation and which will therefore be identical on the planes Σ_n and Σ_{n+1}. Each particular amplitude distribution is usually referred to as a mode, is designated by two mode numbers (p,q) and has its characteristic eigenvalue $K_{p,q}$ giving its associated diffraction loss. The mode having the lowest loss, the (0,0) mode is called the dominant mode; it is the only one which will exist after many iterations, the others becoming damped at a much higher rate.

2.3 Homothetic Hyperresolving Systems.

Consider a circular pupil of radius a_n with complex amplitude distribution $g_n(X,\phi)$. The amplitude distribution of the corresponding diffraction pattern is given by,

$$g_{n+1}(W,\theta) = \frac{1}{2\pi} \int_0^{2\pi} \int_0^{A_n} g_n(X,\phi) e^{iWX \cos(\phi-\theta)} X dX d\phi \qquad 2.6$$

where

$$A_n = \sqrt{\frac{2\pi}{D\lambda}}\, a_n$$

Suppose that the pupil undergoes the transformation $X' = kX$, $a_n' = k\, a_n$ giving a new pupil having a radius a_n' and complex amplitude distribution given by $g_n'(X',\phi) = g_n(kX,\phi)$. This transformation is called a homothetic transformation and the constant k is called the ratio of similitude. If k is less than one, the transformation contracts the pupil; if it is greater than one, the transformation expands the pupil. The corresponding new diffraction pattern is given by,

$$g_{n+1}'(W',\theta) = \frac{1}{2\pi} \int_0^{2\pi} \int_0^{A_n'} g_n'(X',\phi) e^{iWX' \cos(\phi-\theta)} X' dX' d\phi$$

$$= \frac{1}{k^2}\, g_{n+1}\left(\frac{W}{k},\theta\right) \qquad 2.7$$

where

$$A_n' = \sqrt{\frac{2\pi}{D\lambda}}\, a_n'$$

Thus, apart from a constant factor $1/k^2$, a homothetic transformation of the pupil results in an "inverse" homothetic transformation of the corresponding diffraction pattern. If the pupil is contracted by a factor k, the corresponding diffraction pattern is expanded by the same factor k, and vice versa.

This result can be applied to a hyperresolving system. An expansion of the input function, g_o, results in a contraction of the function g_1 which in turn results in an expansion of g_2 and so on. Of course the expansion of the input function g_o by the ratio of similitude, corresponds to the transformation of S given by $S' = S/k$ with k less than one. The consequence of this for hyperresolving systems is that experimental or theoretical results obtained for a particular system may be applied to an infinite set of homothetic systems.

For the special case of a point source on the axis of a hyperresolving system having identical diaphrams of radii a, a homothetic system is obtained by performing a homothetic transformation on the diaphrams in the even planes and an inverse homothetic transformation on the diaphrams in the odd planes. Thus, a system having diaphrams with identical radii $a_e = ka$ in the even planes and identical radii $a_o = a/k$ in the odd planes is homothetic to a system having all identical diaphrams of radii $a = \sqrt{a_e a_o}$.

2.4 Symmetry of the Amplitude Functions.

An analysis was made of the symmetry of the functions $g_n(X,\phi)$ and $g_{n+1}(W,\theta)$. Any symmetry depends on the symmetry of the complex amplitude

$$\text{i.e.} \quad g_o(X,\phi,S) = e^{i\,SX\cos\phi} \tag{2.8}$$

The definitions for these variables are given in equation 1.2. $g_o(X,\phi,S)$ may be expressed explicitly in its real and imaginary forms:

$$g_o(X,\phi,S) = g_{oe}(X,\phi,S) + i\,g_{oo}(X,\phi,S) \tag{2.9}$$

where

$$g_{oe} = \cos\,(SX\cos\,\phi)$$

$$g_{oo} = \sin\,(SX\cos\,\phi)$$

The first subscript refers to the cell number and the second subscript is e or o (even or odd) depending on whether or not the function changes sign under the transformation $\phi \to \pi - \phi$. This latter subscript indicates the state of symmetry about the $\phi = 90^0$ axis. Another property of these two functions is that they are both even about the axis $\phi = 0$ since the

transformation $\phi \rightarrow -\phi$ does not change the sign or value. It will be shown next that the output function of cell 0 (or equivalently the input function of cell 1) $g_1(X,\phi,S)$ can also be expressed in terms of functions having the same symmetry properties.

By expressing the exponential term $e^{iWX\cos(\phi-\theta)}$ of equation 1.1 in its real and imaginary parts, $g_1(W,\theta,S)$ becomes,

$$g_1(W,\theta,S) = I1 + I2 + I3 + I4 + i\,(I5 + I6 + I7 + I8) \qquad 2.10$$

where

$$I1 = \frac{1}{2\pi}\int_0^{2\pi}\int_0^{A_1} g_{oe}(X,\phi,S)\ [\cos(WX\cos\phi\cos\theta)]\ [\cos(WX\sin\phi\sin\theta)]XdXd\phi$$

$$I2 = -\frac{1}{2\pi}\int_0^{2\pi}\int_0^{A_1} g_{oe}(X,\phi,S)\ [\sin(WX\cos\phi\cos\theta)]\ [\sin(WX\sin\phi\sin\theta)]XdXd\phi$$

$$I3 = -\frac{1}{2\pi}\int_0^{2\pi}\int_0^{A_1} g_{oo}(X,\phi,S)\ [\sin(WX\cos\phi\cos\theta)]\ [\cos(WX\sin\phi\sin\theta)]XdXd\phi$$

$$I4 = -\frac{1}{2\pi}\int_0^{2\pi}\int_0^{A_1} g_{oo}(X,\phi,S)\ [\cos(WX\cos\phi\cos\theta)]\ [\sin(WX\sin\phi\sin\theta)]XdXd\phi$$

$$I5 = \frac{1}{2\pi}\int_0^{2\pi}\int_0^{A_1} g_{oe}(X,\phi,S)\ [\sin(WX\cos\phi\cos\theta)]\ [\cos(WX\sin\phi\sin\theta)]XdXd\phi$$

$$I6 = \frac{1}{2\pi} \int_0^{2\pi} \int_0^{A_1} g_{oe}(X,\phi,S) \quad [\cos(WX \cos\phi \cos\theta)][\sin(WX \sin\phi \sin\theta)]XdXd\phi$$

$$I7 = \frac{1}{2\pi} \int_0^{2\pi} \int_0^{A_1} g_{oo}(X,\phi,S) \quad [\cos(WX \cos\phi \cos\theta)][\cos(WX \sin\phi \sin\theta)]XdXd\phi$$

$$I8 = -\frac{1}{2\pi} \int_0^{2\pi} \int_0^{A_1} g_{oo}(X,\phi,S) \quad [\sin(WX \cos\phi \cos\theta)][\sin(WX \sin\phi \sin\theta)]XdXd\phi$$

Some of these integrals are equal to zero:

(1) $I2 = 0$ $I4 = 0$ $I6 = 0$ $I8 = 0$ — These have integrands which are odd about the axis $\phi = 0$ i.e. the integrands change sign under the transformation $\phi \rightarrow -\phi$.

(2) $I5 = 0$ $I7 = 0$ — These have integrands odd about the axis $\phi = \pi/2$ i.e. the integrands change sign under the transformation $\phi \rightarrow \pi - \phi$.

The remaining integrals, I1 and 13, have integrands which are even about both the axis $\phi = o$ and $\phi = \pi/2$.

$g_1(W,\theta,S)$ is thus given by

$$g_1(W,\theta,S) = g_{1e}(W,\theta,S) - g_{1o}(W,\theta,S) \qquad 2.11$$

where,

$$g_{1e}(W,\theta,S) = \frac{1}{2\pi}\int_0^{2\pi}\int_0^{A_1} g_{oe}(X,\phi,S)\ [\cos(WX\ \cos\phi\ \cos\theta)][\cos(WX\ \sin\phi\ \sin\theta)]$$

$$XdXd\phi$$

$$g_{1o}(W,\theta,S) = \frac{1}{2\pi}\int_0^{2\pi}\int_0^{A_1} g_{oo}(X,\phi,S)\ [\sin(WX\ \cos\phi\ \cos\theta)][\cos(WX\ \sin\phi\ \sin\theta)]$$

$$XdXd\phi$$

The functions $g_{1e}(W,\theta,S)$ and $g_{1o}(W,\theta,S)$ have identical symmetry properties to the functions $g_{oe}(X,\phi,S)$ and $g_{oo}(X,\phi,S)$. That is, an even function transforms into another even function and an odd function transforms into another odd function. The process of transforming the input functions into output functions may be shown as follows:

$$g_{oe}(X,\phi,S) \rightarrow g_{1e}(W,\theta,S)$$

$$i\ g_{oo}(X,\phi,S) \rightarrow -g_{1o}(W,\theta,S)$$

This transformation process may be repeated for successive iterations. It is thus clear that,

(1) For any even value of $n \geq 0$

$$g_{n+1}(W,\theta,S) = g_{n+1e}(W,\theta,S) + i^{n+2} g_{n+1o}(W,\theta,S) \qquad 2.12$$

where

$$g_{n+1e}(W,\theta,S) = \frac{1}{2\pi} \int_o^{2\pi} \int_o^{A_n} g_{ne}(X,\phi,S) \; [\cos(WX \cos \phi \cos \theta)]$$

$$[\cos(WX \sin \phi \sin \theta)] \; X dX d\phi$$

$$g_{n+1o}(W,\theta,S) = \frac{1}{2\pi} \int_o^{2\pi} \int_o^{A_n} g_{no}(X,\phi,S) \; [\sin(WX \cos \phi \cos \theta)]$$

$$[\cos(WX \sin \phi \sin \theta)] \; X dX d\phi$$

$g_{oe}(X,\phi,S)$ and $g_{oo}(X,\phi,S)$ are defined by equation 2.9

(2) For any odd value of n >0

$$g_{n+1}(X,\phi,S) = g_{n+1e}(X,\phi,S) + i^{n+2} g_{n+1o}(X,\phi,S) \qquad 2.13$$

where

$$g_{n+1e}(X,\phi,S) = \frac{1}{2\pi} \int_o^{2\pi} \int_o^{A_n} g_{ne}(W,\theta,S) \; [\cos(WX \cos \phi \cos \theta)]$$

$$[\cos(WX \sin \phi \sin\theta)] \; W dW d\theta$$

$$g_{n+1o}(X,\phi,S) = \frac{1}{2\pi} \int_o^{2\pi} \int_o^{A_n} g_{no}(W,\theta,S) \; [\sin(WX \cos \phi \cos \theta)]$$

$$[\cos(WX \sin \phi \sin \theta)] \; W dW d\theta$$

2.5 Generation of Even and Odd Functions

The even function defined in section 2.4 can be expressed as two components:

$$g_{oe}(X,\phi,S) = \cos(SX\cos\phi)$$

$$= \frac{1}{2}(e^{iSX\cos\phi} + e^{-iSX\cos\phi})$$

$$= \frac{1}{2}[g_o(X,\phi,S) + g_o(X,\phi,-S)]$$

$$g_{1e}(W,\theta,S) = \frac{1}{2\pi}\int_0^{2\pi}\int_{B_1}^{A_1} g_{oe}(X,\phi,S)\, e^{iWX\cos(\phi-\theta)} X\,dX\,d\phi$$

$$= \frac{1}{4\pi}\int_0^{2\pi}\int_{B_1}^{A_1} g_o(X,\phi,S)\, e^{iWX\cos(\phi-\theta)} X\,dX\,d\phi$$

$$+ \frac{1}{4\pi}\int_0^{2\pi}\int_{B_1}^{A_1} g_o(X,\phi,-S)\, e^{iWX\cos(\phi-\theta)} X\,dX\,d\phi$$

$$= \frac{1}{2}[g_1(W,\theta,S) + g_1(W,\theta,-S)]$$

Similarly,

for n even $\quad g_{n+1,e}(W,\theta,S) = \frac{1}{2}[g_{n+1}(W,\theta,S) + g_{n+1}(W,\theta,-S)]$

for n odd $\quad g_{n+1,e}(X,\phi,S) = \frac{1}{2}[g_{n+1}(X,\phi,S) + g_{n+1}(X,\phi,-S)]$

Thus, the even function can be generated at each plane by using as input to the hyperresolving system, two point sources coherent with each other and situated equal distances S on opposite sides of the optical axis.

In a similar way, by setting

$$g_{oo}(X,\phi,S) = \sin(SX\cos\phi) = -\frac{1}{2}i\left(e^{iSX\cos\phi} - e^{-iSX\cos\phi}\right)$$

$$= -\frac{1}{2}i\left[g_o(X,\phi,S) - g_o(X,\phi,-S)\right]$$

we can show that the odd function, apart from a constant phase factor $-i$, can be generated at each plane by using as input to the hyperresolving system two point sources, coherent with each other, out of phase with each other by π, and situated equal distances S on opposite sides of the optical axis.

2.6 Symmetry of the Function of Luminous Intensity I_n.

The symmetry of the intensity function I_n can be obtained from the symmetry properties of the even and odd functions. The amplitude function given by equations 2.12 and 2.13 may be rewritten as:

$$g_n(W,\theta,S) = g_{ne}(W,\theta,S) + (-1)^{\frac{n+1}{2}} g_{no}(W,\theta,S) \quad n \text{ odd} \qquad 2.14$$

$$g_n(X,\phi,S) = g_{ne}(X,\phi,S) + (-1)^{\frac{n}{2}}\, i\, g_{no}(X,\phi,S) \quad n \text{ even}$$

where the even and odd functions satisfy the following symmetry relations:

$$\begin{aligned} g_{ne}(W,\theta,S) &= g_{ne}(W,-\theta,S) = g_{ne}(W,\pi-\theta,S) \\ g_{no}(W,\theta,S) &= g_{no}(W,-\theta,S) = -g_{no}(W,\pi-\theta,S) \end{aligned} \quad \text{n odd} \qquad 2.15$$

$$\begin{aligned} g_{ne}(X,\phi,S) &= g_{ne}(X,-\phi,S) = g_{ne}(X,\pi-\phi,S) \\ g_{no}(X,\phi,S) &= g_{no}(X,-\phi,S) = -g_{no}(X,\pi-\phi,S) \end{aligned} \quad \text{n even}$$

The equations 2.14 show explicitly that the amplitude is always real in the odd planes and always complex in the even planes. This is associated with the symmetry of the intensity function I_n defined as,

$$\begin{aligned} I_n(W,\theta,S) &= |g_n(W,\theta,S)|^2 \\ &= g_{ne}^2(W,\theta,S) + g_{no}^2(W,\theta,S) + 2(-1)^{\frac{n+1}{2}} g_{ne}(W,\theta,S)\, g_{no}(W,\theta,S) \quad \text{n odd} \end{aligned}$$

$$\begin{aligned} I_n(X,\phi,S) &= |g_n(X,\phi,S)|^2 \\ &= g_{ne}^2(X,\phi,S) + g_{no}^2(X,\phi,S) \quad \text{n even} \end{aligned} \qquad 2.16$$

Applying the symmetry relations of the even and odd functions (equations 2.15), we easily obtain,

$$I_n(W,\theta,S) = I_n(W,-\theta,S) \neq I_n(W,\pi-\theta,S) \quad \text{n odd}$$

$$\text{unless } g_{ne}(W,\theta,S) \equiv 0 \quad \text{or} \quad g_{no}(W,\theta,S) \equiv 0 \qquad 2.17$$

$$I_n(X,\phi,S) = I_n(X,-\phi,S) = I_n(X,\pi-\phi,S) \quad \text{n even}$$

Thus, the intensity function is symmetrical about the axis $\phi = 0$ for n even and $\theta = 0$ for n odd. Although it is also symmetrical about the axis $\phi = \frac{\pi}{2}$ for n even, it is not symmetrical in general about the axis $\theta = \frac{\pi}{2}$ for n odd. As a result, the intensity function has a center of symmetry about the origin for the even planes only.

2.7 Effect of Point Source Displacement S on the Airy pattern.

$$g_1(W,\theta,S) = \frac{1}{2\pi}\int_0^{2\pi}\int_0^1 e^{iSX\cos\phi}\, e^{iWX\cos(\phi-\theta)}\, X\,dX\,d\phi$$

$$= \frac{1}{2\pi}\int_0^{2\pi}\int_0^1 e^{iX[(W\cos\theta + S)\cos\phi + W\sin\phi\sin\theta]}\, X\,dX\,d\phi$$

$$= \frac{1}{2\pi}\int_0^{2\pi}\int_0^1 e^{iW' X\cos(\phi-\theta')}\, X\,dX\,d\phi$$

$$= \frac{J_1(W')}{W'} \qquad 2.18$$

where W' and θ' satisfy the relations,

$$W\cos\theta + S = W'\cos\theta'$$

$$W\sin\theta = W'\sin\theta'$$

Consequently,

$$W' = \sqrt{W^2 + 2WS\cos\theta + S^2} \qquad 2.19$$

$$\cos\theta' = \frac{W\cos\theta + S}{\sqrt{W^2 + 2WS\cos\theta + S^2}}$$

Using the law of cosines for a plane triangle, we may interpret W' as a radial coordinate with center at $W = -S$, $\theta = 0$. As a result, $g_1(W,\theta,S)$ is an Airy pattern with center at $W = -S, \theta = 0$. Thus, moving the point

source by S, simply moves the Airy pattern by an equal and opposite amount, - S.

2.8 Amplitude in Plane 2 for large S.

We were able to derive a mathematical expression for the amplitude $g_2(X,\phi,S)$ in the case when S is large:

$$g_2(X,\phi,S) = \frac{1}{2\pi}\int_0^{2\pi}\int_0^{A_1} g_1(W,\theta,S)\, e^{iWX\cos(\phi-\theta)} W dW d\theta \qquad 2.20$$

We have shown in section 2.7 that,

$$g_1(W,\theta,S) = \frac{J_1(W')}{W'} \quad \text{with} \quad W' = \sqrt{W^2 + 2WS\cos\theta + S^2} \qquad 2.21$$

Since for large S, W' is large, the Bessel function may be expressed in its asymptotic form,

$$\frac{J_1(W')}{W'} \sim \frac{1}{(W')^{3/2}}\sqrt{\frac{2}{\pi}}\cos\left(W' - \frac{3\pi}{4}\right) \qquad 2.22$$

Now $W' = S\left(1 + \frac{2W}{S}\cos\theta + \frac{W^2}{S^2}\right)^{1/2}$

$$\approx S + W\cos\theta + \frac{1}{2}\frac{W^2}{S}$$

$$W' \approx S + W\cos\theta \qquad 2.23$$

Similarly,

$$\frac{1}{(W')^{3/2}} \approx \frac{1}{S^{3/2}} - \frac{3}{2}\frac{W}{S^{5/2}} \cos\theta \qquad 2.24$$

Since W cos θ is the x coordinate of a rectangular coordinate system, the contours of equal amplitude of the function $g_1(W, ,S)$ are straight lines perpendicular to the direction of movement of the point source. In the photographs these will appear vertical since the point source was moved horizontally.

From equations 2.21, 2.22, 2.23 and 2.24,

$$g_1(W,\theta,S) = \sqrt{\frac{2}{\pi}}\left(\frac{1}{S^{3/2}} - \frac{3}{2}\frac{W\cos\theta}{S^{5/2}}\right)\cos\left(S + W\cos\theta - \frac{3\pi}{4}\right)$$

$$= \frac{1}{\sqrt{2\pi}}\left(\frac{1}{S^{3/2}} - \frac{3}{2}\frac{W\cos\theta}{S^{5/2}}\right)\left[e^{i(S+W\cos\theta - \frac{3\pi}{4})} + e^{-i(S+W\cos\theta - \frac{3\pi}{4})}\right] \qquad 2.25$$

Substituting 2.25 in 2.20,

$$g_2(X,\phi,S) = \frac{1}{\sqrt{2\pi}}\frac{1}{2\pi S^{3/2}} e^{i(S-\frac{3\pi}{4})}\int_0^{2\pi}\int_0^{A_1} e^{iW\cos\theta}\, e^{iWX\cos(\phi-\theta)}\, W\,dW\,d\theta \qquad 2.26$$

$$+ \frac{1}{\sqrt{2\pi}}\frac{1}{2\pi S^{3/2}} e^{-i(S-\frac{3\pi}{4})}\int_0^{2\pi}\int_0^{A_1} e^{-iW\cos\theta}\, e^{iWX\cos(\phi-\theta)}\, W\,dW\,d\theta$$

$$-\frac{1}{\sqrt{2\pi}}\ \frac{3}{4\pi S^{5/2}}\ e^{i(S-\frac{3\pi}{4})}\int_0^{2\pi}\int_0^{A_1} W\cos\theta\ e^{iW\cos\theta}\ e^{iWX\cos(\phi-\theta)}WdWd\theta$$

$$-\frac{1}{\sqrt{2\pi}}\ \frac{3}{4\pi S^{5/2}}\ e^{-i(S-\frac{3\pi}{4})}\int_0^{2\pi}\int_0^{A_1} W\cos\theta\ e^{-iW\cos\theta}\ e^{iWX\cos(\phi-\theta)}WdWd\theta$$

Consider the exponential terms in these integrands:

$$e^{i[W\cos\theta + WX\cos(\phi-\theta)]} = e^{iW[(X\cos\phi+1)\cos\theta + X\sin\phi\sin\theta]}$$

$$= e^{iWX_1'\cos(\phi_1'-\theta)}$$

where

$$X\cos\phi + 1 = X_1'\cos\phi_1'$$

$$X\sin\phi = X_1'\sin\phi_1'$$

Consequently,

$$X_1' = \sqrt{X^2 + 2X\cos\phi + 1}$$

$$\cos\phi_1' = \frac{X\cos\phi + 1}{\sqrt{X^2 + 2X\cos\phi + 1}}$$

Similarly,

$$e^{i[-W\cos\theta + WX\cos(\phi-\theta)]} = e^{iWX_2'\cos(\phi_2'-\theta)}$$

with $$X_2' = \sqrt{X^2 - 2X\cos\phi + 1}$$

$$\cos\phi_2' = \frac{X\cos\phi + 1}{\sqrt{X^2 - 2X\cos\phi + 1}}$$

Therefore equation 2.26 becomes

$$g_2(X,\phi,S) = \frac{1}{\sqrt{2\pi}}\frac{1}{2\pi S^{3/2}} e^{i(S-\frac{3\pi}{4})}\int_0^{2\pi}\int_0^{A_1} e^{iWX_1'\cos(\phi_1'-\theta)}WdWd\theta$$

$$+ \frac{1}{\sqrt{2\pi}}\frac{1}{2\pi S^{3/2}} e^{-i(S-\frac{3\pi}{4})}\int_0^{2\pi}\int_0^{A_1} e^{iWX_2'\cos(\phi_2'-\theta)}WdWd\theta$$

$$- \frac{1}{\sqrt{2\pi}}\frac{3}{4\pi S^{5/2}} e^{i(S-\frac{3\pi}{4})}\int_0^{2\pi}\int_0^{A_1} W\cos\theta\, e^{iWX_1'\cos(\phi_1'-\theta)}dWd\theta$$

$$- \frac{1}{\sqrt{2\pi}}\frac{3}{4\pi S^{5/2}} e^{-i(S-\frac{3\pi}{4})}\int_0^{2\pi}\int_0^{A_1} W\cos\theta\, e^{iWX_2'\cos(\phi_2'-\theta)}dWd\theta$$

2.27

The integrals may now be integrated with the use of equations A3 and A5 of appendix A to give,

$$g_2(X,\phi,S) = \frac{1}{\sqrt{2\pi}} \frac{A_1^2}{S^{3/2}} e^{i(S-\frac{3\pi}{4})} \frac{J_1(A_1X_1')}{A_1 X_1'}$$

$$+ \frac{1}{\sqrt{2\pi}} \frac{A_1^2}{S^{3/2}} e^{-i(S-\frac{3\pi}{4})} \frac{J_1(A_1 X_2')}{A_1 X_2'}$$

$$- \frac{3i}{2\sqrt{2\pi}} \frac{A_1^3}{S^{5/2}} e^{i(S-\frac{3\pi}{4})} \frac{J_2(A_1X_1')}{A_1 X_1'} \cos\phi_1'$$

$$- \frac{3i}{2\sqrt{2\pi}} \frac{A_1^3}{S^{5/2}} e^{-i(S-\frac{3\pi}{4})} \frac{J_2(A_1X_2')}{A_1 X_2'} \cos\phi_2' \qquad 2.28$$

where,

$$X_1' = \sqrt{X^2 + 2X\cos\phi + 1} \qquad \cos\phi_1' = \frac{X\cos\phi + 1}{\sqrt{X^2 + 2X\cos\phi + 1}}$$

$$X_2' = \sqrt{X^2 - 2X\cos\phi + 1} \qquad \cos\phi_2' = \frac{X\cos\phi + 1}{\sqrt{X^2 - 2X\cos\phi + 1}}$$

Using the law of cosines for a plane triangle, we may interpret X_1' and X_2' as radial coordinates with centers at ($X = -1$, $\phi = 0$) and ($X = +1$, $\phi = 0$) respectively. Therefore, the first two terms, which are the dominant terms for large S, are Airy patterns with these centers. The last two terms also have these centers but are not symmetrical. The resultant pattern therefore consists of the superposition of two

Airy patterns separated by $\Delta X = 2$, each Airy pattern being perturbed by an asymmetrical pattern.

2.9 Intensity in the far region of the diffraction pattern.

It is known that the intensity in the far region of a Fraunhofer diffraction pattern essentially depends on the luminous amplitude of the light in the close vicinity of the diffracting edge. The greater the amplitude at the diffracting edge, the greater the intensity of the strongly diffracted light irrespective of the distribution far from the diffracting edge.

a) In the special case where $S = 0$, we have derived a mathematical expression illustrating this principle. We use for convenience, the notation with n odd. From equations 2.1 and 2.2,

$$g_{n+1}(X) = \frac{1}{2\pi} \int_0^{2\pi} \int_{B_n}^{A_n} g_n(W)\, e^{iWX \cos(\phi-\theta)} W dW d\theta$$

$$= \int_{B_n}^{A_n} g_n(W)\, J_o(WX) W dW$$

This may be integrated by parts using equation A10 of appendix A

$$g_n(X) = \frac{1}{X} \int_{B_n}^{A_n} g_n(W) \frac{d}{dW} [W J_1(WX)]\, dW$$

$$= \frac{1}{X} \left[A_n g_n(A_n) J_1(A_n X) - B_n g_n(B_n) J_1(B_n X) - \int_{B_n}^{A_n} g_n'(W) J_1(WX) W dW \right]$$

By repeated integration by parts, the following expansion may be obtained for $g_{n+1}(X)$,

$$g_{n+1}(X) = \sum_{k=0}^{\infty} (-1)^k \frac{A_n^{k+1} g_n^k(A_n) J_{k+1}(A_n X) - B_n^{k+1} g_n^k(B_n) J_{k+1}(B_n X)}{X^{k+1}} \qquad 2.29$$

It is clear from this expression that as $X \to \infty$,

$$g_{n+1}(X) \to \frac{1}{X} [A_n g_n(A_n) J_1(A_n X) - B_n g_n(B_n) J_1(B_n X)] \qquad 2.30$$

provided $g_n(A_n)$ and $g_n(B_n)$ are both not zero.

$$g_{n+1}(X) \to \frac{1}{X^2} [A_n^2 g_n'(A_n) J_2(A_n X) - B_n^2 g_n'(B_n) J_2(B_n X)]$$

if $g_n(A_n) = g_n(B_n) = 0$ and provided that $g_n'(A_n)$ and $g_n'(B_n)$ are both not zero.

In the case of a central diaphram of radius A_n, $g_{n+1}(X)$ becomes:

$$g_{n+1}(X) = A_n^2 g_n(A_n) \frac{J_1(A_n X)}{A_n X} \qquad 2.31$$

In this case the strongly diffracted light varies as an Airy pattern, the amplitude of which depends directly on $g_n(A_n)$ at the circular diffracting edge.

b) A similar result can be derived for the case where g_n depends on cos 2θ.

If $g_n(W,\theta,S) = g_n(W,S) \cos 2\theta$,

$$g_{n+1}(X,\phi,S) = \frac{1}{2\pi} \int_0^{2\pi} \int_{B_n}^{A_n} g_n(W,S) \cos 2\theta \; e^{iWX \cos(\phi-\theta)} W dW d\theta$$

Using equation A3 of appendix A to integrate over the angle θ,

$$g_{n+1}(X,\phi,S) = - \cos 2\phi \int_{B_n}^{A_n} g_n(W,S) \; J_2(WX) W dW$$

Integrating by parts,

$$g_{n+1}(X,\phi,S) = \frac{\cos 2\phi}{X} \int_{B_n}^{A_n} \frac{g_n(W,S)}{W^2} \frac{d}{dW} [W^3 J_3(WX)] dW$$

$$= \frac{\cos 2\phi}{X} [A_n g_n(A_n,S) J_3(A_n X) - B_n g_n(B_n,S) J_3(B_n X)]$$

$$- \frac{\cos 2\phi}{X} \int_{B_n}^{A_n} [W g_n'(W,S) - 2 g_n(W,S)] J_3(WX) \, dW$$

By repeating the integration by parts, it can be shown that the last integral varies as X^{-1}. Therefore, as $X \to \infty$,

$$g_{n+1}(X,\theta,S) \to \frac{\cos 2\phi}{X} \left[A_n g_n(A_n,S) J_3(A_n X) - B_n g_n(B_n,S) J_3(B_n X) \right] \qquad 2.32$$

In this case, the strongly diffracted light still depends on the amplitude at the circular diffracting edge and it retains its cosine dependency on the angular coordinate.

2.10 Analytical Approach to Iterated Diffraction

An attempt was made to solve the problem of iterated diffraction by performing each successive iteration analytically.
From equation A9 of appendix A, the input function $e^{iSX \cos\phi}$ can be expressed as,

$$e^{iSX \cos \phi} = J_o(SX) + 2 \sum_{n=1}^{\infty} i^n J_n(SX) \cos n \phi$$

Therefore,

$$g_1(W,\theta,S) = \frac{1}{2\pi} \int_o^{2\pi} \int_o^1 e^{iSX \cos\phi} \; e^{iWX \cos (\phi-\theta)} X dX d\phi$$

$$= \frac{1}{2\pi} \int_o^{2\pi} \int_o^1 \left[J_o(SX) + 2 \sum_{n=1}^{\infty} i^n J_n(SX) \cos n \phi \right] e^{iWX \cos (\phi-\theta)} X dX d\phi$$

By equation A3 of appendix A, this becomes,

$$g_1(W,\theta',S) = \int_o^1 J_o(SX)\ J_o(WX)\ XdX + 2\ \sum_{n=1}^{\infty}(-1)^n \cos\ n\ \theta \int_o^1 J_n(SX) J_n(WX)\ XdX$$

From equation A7 of appendix A,

$$g_1(W,\theta,S) = \frac{1}{S^2-W^2}\ [SJ_o(W)\ J_1(S) - WJ_o(S)J_1(W)]$$

$$+ \frac{2}{S^2-W^2}\ [\ \sum_{n=1}^{\infty}\ (-1)^n \cos\ n\theta\ [SJ_n(W)J_{n+1}(S) - WJ_n(S)J_{n+1}(W)]] \quad W \neq S$$

$$= \frac{1}{2}\ [J_o^2(W) + J_1^2(W)] + \sum_{n=1}^{\infty}\ (-1)^n\ \cos\ n\ \theta [J_n^2(W) - J_{n-1}(W)J_{n+1}(W)] \quad S=W$$

Unfortunately, these expressions are very complicated and no process has been found to calculate another iteration.

2.11 Fourier Transform Inverse Theorem.

The Fourier transform has a well known property, the inverse theorem, which will not be proved here but simply stated in terms of the Fourier transform notation of equations 1.3 with n even:

If
$$g_{n+1}(W,\theta,S) = \frac{1}{2\pi} \int_o^{2\pi} \int_o^{\infty} g_n(X,\phi,S)\ e^{iWX \cos\ (\phi-\theta)} XdXd\phi \qquad 2.33$$

Then

$$g_n(X,\phi,S) = \frac{1}{2\pi} \int_0^{2\pi} \int_0^{\infty} g_{n+1}(W,\theta,S)\, e^{-iWX \cos(\phi-\theta)}\, W dW d\theta \qquad 2.34$$

Since

$$g_{n+2}(X,\phi,S) = \frac{1}{2\pi} \int_0^{2\pi} \int_{B_{n+1}}^{A_{n+1}} g_{n+1}(W,\theta,S)\, e^{iWX \cos(\phi-\theta)}\, W dW d\theta$$

this theorem has the consequence that,

$$g_{n+2}(X,\phi,S) = g_n(-X,\phi,S) = g_n(X,\phi,-S) \text{ if } A_{n+1} \to \infty \text{ and } B_{n+1} = 0$$

Example

Consider the case where n = 0:

(1) $g_o(X,\phi,S) = e^{iXS \cos \phi}$ $\quad X \leq 1$

$= 0$ $\quad X > 1$

(2) Equation 2.33 becomes,

$$g_1(W,\theta,S) = \frac{1}{2\pi} \int_0^{2\pi} \int_0^{1} e^{iXS \cos \phi}\, e^{iWX \cos(\phi-\theta)}\, X dX d\phi$$

(3) If $A_1 \to \infty$ and $B_1 = 0$,

$g_2(X,\phi,S) = e^{-iXS \cos \phi}$ $\quad X \leq 1$

$= 0$ $\quad X > 0$

$= g_o(X,\phi,-S)$

These equations may be interpreted as follows:

(1) The point source with displacement S from the axis illuminates in plane 0 a lens limited by a diaphram or radius given by $A_o = 1$. Consequently the amplitude distribution in plane 0 is the function $g_o(X,\phi,S)$ stated above.

(2) The Airy pattern with displacement - S from the axis is formed in plane 1 where there is a lens of large radius a_1. The large radius of this lens satisfies the condition that $g_1(W,\theta,S)$ be integrated from zero to infinity.

(3) In plane 2, a pattern in practice identical to that in plane 0 is formed. For $X \leq 1$, the amplitude is a constant equal to 1 and the phase is $e^{-iSX\cos\phi}$. For $X > 1$, the amplitude is zero.

2.12 A Process Reducing the Normalized Even Energy Values.

Many types of objects to be resolved must be illuminated by an external light source. The light from the source may be collimated and then focussed by a lens in the plane of the object. We suppose that the focussing lens is aberration free and correctly focussed. As a result, the object is not uniformly illuminated as assumed previously in this thesis but illuminated by a diffraction pattern centered on the optical axis. Consequently, the signal transmitted through the hyperesolving system from a point of the object off axis, is not as intense as if the

object were uniformly illuminated. Moreover, we can assume that the focussing lens has the same numerical aperture as the primary lens of the hyperresolving system. In this case, the normalized even energy values associated with a point S of the object must be multiplied by $\left[\frac{J_1(S)}{S} \right]^2$. It has the effect of reducing substantially the normalized even energy values for intermediate and large values of S. The effective distribution of luminous intensity in the object plane produced by this particular type of illumination will be called the "Effective Object Distribution". It is the product of the distribution of luminous intensity in the object plane when it is uniformly illuminated by the function $\left[\frac{J_1(S)}{S}\right]^2$ which will be called in this thesis the modulation function (MF).

CHAPTER 3

Computational Procedure

A major difficulty that had to be overcome was to find a suitable method for integrating the equations 1.3. The method chosen must be very accurate since errors may accumulate upon successive calculations and furthermore, the method must be fast enough so that the calculations may be performed within a reasonable length of time using the IBM 360 (Model 40 or 65). The fact that the amplitude of diffraction patterns sometimes fluctuates very rapidly places severe limitations on the accuracy which can be achieved in a reasonable period of computation time. Nevertheless, in order to carry out a study of iterated diffraction, it is important that the computation time be as short as possible.

The first important step was to develop equations 1.3 analytically into a more efficient form for calculation. For this purpose, the special case $S = 0$ used in the study of mode formation was calculated separately with the equation 2.3 which is a simplified form of equation 1.3. For $S \neq 0$. the symmetry properties of the even and odd functions were used in calculating the amplitude function from equations 2.12 and 2.13

A complete description of all the numerical processes attempted to evaluate the integrals was given in the report presented for transferal from the M. Sc. status to the Ph.D. status. Only those numerical processes which were used are presented here.

3.1 Distribution of Integration Points.

One question was that of the most suitable distribution of points of integration. It might at first seem reasonable to choose the distribution such that the density of points per unit area is a constant, for example, the distribution $X_i = \sqrt{\frac{i}{N}}$, where i = 1, 2... N. However, the distribution which gives the most accurate results must depend on the function g_n since in regions where the function varies greatly, the density of points should be high and vice versa. But because the function g_n is not known in general, it was decided to choose the simplest possible distribution of points, namely equidistant points.

3.2 Integration Formulas.

The Newton Cotes formulas of integration were chosen for the integration procedure because the distribution of points of integration may be chosen to be equidistant. The table below gives the Newton Cotes coefficients for the form:

$$\int_o^{Nh} f(x)dx = Ah\,[B_o f(o) + B_1 f(h) + \ldots\ldots B_N f(Nh)] + k_N \qquad 3.1$$

where h = the interval.

N = number of intervals

k_N = error term

B_n = integration coefficient.

The coefficients B_n are symmetric and hence only part of the table need be given:

N	A	B_o	B_1	B_2	B_3	B_4	B_5	k_N
1	1/2	1	1					$-(\frac{1}{2})h^3f^{ii}$
2	1/3	1	4	1				$-1/90h^5f^{iv}$
3	3/8	1	3	3	1			$-3/80h^5f^{iv}$
4	2/45	7	32	12	32	7		$-8/945h^7f^{vi}$
5	5/288	19	75	50	50	75	19	$-275/12096h^7f^{vi}$
6	4/140	41	216	27	272	27	216	$-9/1400h^9f^{viii}$
7	7/17,280	751	3,577	1,323	2,989	2,989	1,325	$-8183/518400h^9f^{viii}$
8	4/14,175	989	5,888	-928	10,496	-4,540	10,496	
9	9/89,600	2,857	15,741	1,080	19,344	5,778	5,778	
10	5/299376	16,067	106,300	-48,525	272,400	-260,500	427,368	

3.3 Number of Integration Points.

The region of integration was divided into 10 equal parts, each part consisting of 11 points of integration. The integration formula was applied successively to these 10 parts. Two factors were involved in the choice of N as 10:

(1) The error term for most functions is lower for higher values of N. Moreover, it will be noticed that the order of the error term, k_N, jumps by 2 in going from an odd value of N to the next even value of N, which tends to favor the even order formulas. On this basis, it would appear reasonable to choose N to be highest for which the Newton Cotes coefficients are readily available, namely N = 10.

(2) Errors due to roundoff in calculation must also be considered. According to Hamming (Numerical Methods for Scientists and Engineers, pg. 54), "Minimum roundoff occurs when $\sum_{i=1}^{I} w_i^2$ is a minimum". (w_i is the weight given to point i). Hence it is obvious that smaller roundoff errors occur for small values of N where the weights are small.

The question of errors is a very complicated one and it is seldom worth the effort to attempt a thorough analysis, especially if the results can be checked for particular cases.

3.4 Integration Procedure for S = 0

For the special case S = 0, g_{n+1} may be calculated from the simplified equation 2.3

$$g_{n+1}(W) = \int_o^{A_n} g_n(X) J_o(WX) X dX. \qquad 3.2$$

For simplicity A_n was normalized so that $A_n=1$, but calculations for any value of A_n may be obtained by similar processes.

This equation may be integrated numerically using the Newton Cotes equation 3.1 by dividing the region of integration into 10 equal sections, each section consisting of 11 points of integration. Applying equation 3.1 we obtain

$$\int_o^1 g_n(X) J_o(WX) X dX = \int_o^{0.1} g_n(X) J_o(WX) X dX + \ldots\ldots\ldots + \int_{0.9}^{1.0} g_n(X) J_o(WX) X dX \qquad 3.3$$

$$= Ah[B_o g_n(X_o)J_o(WX_o)X_o + B_1 g_n(X_1)J_o(WX_1)X_1 + \ldots\ldots + B_{10} g_n(X_{10})J_o(WX_{10})X_{10}]$$

$$+ Ah[B_o g_n(X_{10})J_o(WX_{10})X_{10} + B_1 g_n(X_{11})J_o(WX_{11})X_{11} + \ldots + B_{20} g_n(X_{20})J_o(WX_{20})X_{20}]$$

$$+ Ah[B_o g_n(X_{90})J_o(WX_{90})X_{90} + B_1 g_n(X_{91})J_o(WX_{91})X_{91} + \ldots\ldots B_{100} g_n(X_{100})J_o(WX_{100})X_{100}]$$

$$= \sum_{i=o}^{100} D_i g_n(X_i)J_o(WX_i)X_i$$

where the coefficients D_i satisfy the relations,

$$D_{10} = 2AhB_{10}$$

$$D_i = AhB_i \qquad i = 0,1,2,\ldots.9$$

$$D_{i+10} = D_i \qquad i = 1,2,\ldots.90$$

Equation 3.3 may thus be expressed as,

$$g_{n+1}(W) = \sum_{i=o}^{100} g_n(X_i)C_i(W) \qquad 3.4$$

where

$$C_i(W) = D_i J_o(WX_i) \approx D_i \sum_{k=o}^{\infty} \frac{(-1)^k \left(\frac{W}{2}\right)^{2k} X_i^{2k+1}}{(k!)^2}$$

Tables of values of $C_i(W)$ may be calculated and stored for subsequent use.

The method was tested on the IBM 360 models 40 and 65 computers for the special case $g_n(X) = 1$ in the range $0 \leq x \leq 1$. The values of $g_{n+1}(W)$ agreed to between 12 and 16 digits with the known values of the Airy pattern for values of W ranging from 0 to 10 in steps of 0.01. The accuracy decreased progressively for larger values of W. Since this method was accurate and efficient, it was used for the studies described in Chapter 4.

3.5 Integration Procedure for $S \neq 0$

As in section 3.4, this method involves the immediate application of the Newton-Cotes formula of integration. Consider first the integration of any function $f(X,\phi)$.

$$\int_0^{\phi m} \int_0^{Xm} f(X,\phi)\, dX d\phi = \sum_{i=o}^{I} \sum_{j=o}^{J} f(X_i \phi_j) D_i D_j \qquad 3.5$$

where

$$D_{10} = 2AhB_{10}$$

$$D_i = AhB_i \qquad i = 0,1.....9$$

$$D_{i+10} = D_i \qquad i = 1,2.....90$$

A, h, B_i are defined by equation 3.1

If this is applied to equation 1.3, $f(X,\phi) = \frac{1}{2\pi} g_n(X,\phi)\, e^{iWX \cos(\phi-\theta)X}$.

This function must be evaluated at many points throughout the region of integration. As in the special case of axial symmetry, the distribution of integration points was chosen for simplicity to be linear. i.e.

$$X_i = \frac{i}{I}, \quad i = 1, 2....I, \quad \phi_j = \frac{j}{J}, \quad j = 1, 2.....J.$$

Before any calculations were attempted, a very rough estimate was made on the computer time which would be required for these calculations. In the special case of axial symmetry, the time taken to calculate each iteration was approximately 2 seconds on the IBM 360, model 65 computer and 60 seconds on the IBM 360 model 40 computer. In this case each iteration involved the calculation of 101 integrals each of which involves 101 terms. That is to say, each iteration involved roughly 10^4 terms. If for the case of non-axial symmetry it is assumed that I = 50 and J = 200, (corresponding to 10,000 points), each iteration involves 10^8 terms. That is, the case of non-axial symmetry requires the evaluation of 10^4 times more terms than for the case of axial symmetry. Assuming that the time required to process each term is the same for both cases, one iteration for non-axial symmetry would require approximately 5 hours on the IBM 360 model 65 and 170 hours on the IBM 360 model 40. Although these estimates are very rough, they do illustrate the difficulties involved in obtaining accurate results in a reasonable period of time. It should be emphasized that although reducing the values of I and J may reduce the computation time significantly, it may also reduce the accuracy significantly.

Since diffraction pattern quite often have rapid fluctuations, it is essential that the number of points of integration be high.

Fortunately, it was possible to reduce the computation time to 6.5 minutes on the IBM 360, model 65 without any decrease in accuracy by using the symmetry properties of equations 2.12 and 2.13. The special techniques for this are described in the following section.

3.5.1 Numerical Methods to Evaluate Equations 2.12 and 2.13.

In evaluating the integrals of equations 2.12 and 2.13, every possible use was made of the symmetry properties. To understand the method, it is first necessary to study two concepts which are now presented:

(1) Consider the particular case of equation 2.12 where $\theta = o$. The integrals simplify to:

$$g_{n+1e}(W,O,S) = \frac{1}{2\pi}\int_o^{2\pi}\int_o^{A_n} g_{ne}(X,\phi,S)\ [\cos(WX\cos\phi)]\ XdXd\phi \qquad 3.6$$

$$g_{n+1o}(W,O,S) = \frac{1}{2\pi}\int_o^{2\pi}\int_o^{A_n} g_{no}(X,\phi,S)\ [\sin(WX\cos\phi)]\ XdXd\phi$$

These functions may be calculated numerically according to equation 3.5 to obtain,

$$g_{n+1e}(W,O,S) = \sum_{i=0}^{I} \sum_{j=0}^{J} g_{ne}(X_i,\phi_j,S)\ C_{eij}(W) \qquad 3.7$$

$$g_{n+1o}(W,O,S) = \sum_{i=0}^{I} \sum_{j=0}^{J} g_{no}(X_i,\phi_j,S)\ C_{oij}(W)$$

where

$$C_{eij}(W) = [\cos(WX_i \cos \phi_j)]\ X_i D_i D_j$$

$$C_{oij}(W) = [\sin(WX_i \cos \phi_j)]\ X_i D_i D_j$$

The relationship between the values of $g_{ne}(X_i,\phi_j,S)$ and $g_{n+1}(W,O,S)$ depends on the coefficients $C_{eij}(W)$ which in turn are determined entirely by the geometric relationship between the points (W,O) on the surface n+1 and the point (X_i,ϕ_j) on the surface n. A similar statement can be made of the functions $g_{no}(X_i,\phi_j,S)$, $g_{n+1o}(W,O,S)$, and $C_{oij}(W)$.

(2). If the funtion $g_n(X,\phi,S)$ is rotated through an angle $\Delta\theta$, then the function $g_{n+1}(W,\theta,S)$ will be rotated through the same angle.

The new function $g'_{n+1}(W,\theta,S)$ is given by,

$$g'_{n+1}(W,\theta,S) = \frac{1}{2\pi}\int_0^{2\pi}\int_0^{A_n} g_n(X,\phi+\Delta\theta,S)e^{iWX\cos(\phi-\theta)}XdXd\phi$$

$$= \frac{1}{2\pi}\int_0^{2\pi}\int_0^{A_n} g_n(X,\phi',S)e^{iWX\cos(\phi'-\theta-\Delta\theta)}XdXd\phi'$$

$$= g_{n+1}(W,\theta+\Delta\theta,S) \qquad 3.8$$

It readily follows that the new even and odd functions are given by,

$$g'_{n+1e}(W,\theta,S) = g_{n+1e}(W,\theta+\Delta\theta,S)$$

$$g'_{n+1o}(W,\theta,S) = g_{n+1o}(W,\theta+\Delta\theta,S) \qquad 3.9$$

By rotating the functions $g_{ne}(X_i,\phi_j,S)$ and $g_{no}(X_i,\phi_j,S)$ through an angle ϕ_k, equations 3.7 become,

$$g_{n+1e}(W,\theta_k,S) = \sum_{i=0}^{I}\sum_{j=0}^{J} g_{ne}(X_i,\phi_{j+k},S)\, C_{eij}(W) \qquad 3.10$$

$$g_{n+1o}(W,\theta_k,S) = \sum_{i=0}^{I}\sum_{j=0}^{J} g_{no}(X_i,\phi_{j+k},S)\, C_{oij}(W)$$

Hence it becomes clear that the coefficients $C_{eij}(W)$ and $C_{oij}(W)$ may be used to calculate the functions $g_{n+1}(W,\theta,S)$ and $g_{n+1o}(W,\theta,S)$ not only for $\theta = 0$, but for any angle θ_k. The method therefore represents a considerable saving in computer time.

Furthermore, because of the symmetry properties of the functions $C_{eij}(W)$, $C_{oij}(W)$, $g_{ne}(X,\phi,S)$, $g_{no}(X,\phi,S)$, $g_{n+1e}(W,\theta,S)$ and $g_{n+1o}(W,\theta,S)$ about the axis $\phi = 0^o$ and $\phi = \pi/2$, calculations need only be performed over one quadrant - representing a further reduction in computer time.

The evaluation of the coefficients $C_{eij}(W)$ and $C_{oij}(W)$ involves the calculation of cos (WX cos ϕ) and sin (WX cos ϕ) for many values of W, X, and ϕ (assuming S is constant) Since the evaluation of each of these sine and cosine functions requires approximately 600μ seconds on the IBM 360, model 65, it would require in the order of 3 minutes to evaluate all the coefficients. This computation time may be reduced by the use of an iterative procedure: For constant ϕ and W, the argument of the sine and cosine functions increases by a constant amount as X changes from X_i to X_{i+1}.

Let $\Delta X = X_{i+1} - X_i$

$A = \cos(W\Delta X \cos\phi)$

$B = \sin(W\Delta X \cos\phi)$

Then $\cos(WX_{i+1} \cos\phi) = A \cos(WX_i \cos\phi) - B \sin(WX_i \cos\phi)$ 3.11

$$\sin(WX_{i+1} \cos \phi) = A \sin(WX_i \cos \phi) - B \cos(WX_i \cos \phi)$$

That is, the sine and cosine functions at the point X_{i+1} may be calculated in terms of the sine and cosine at the point X_i. For constant ϕ and W these functions need be evaluated only once - to obtain A and B. All other values may be obtained by repeated use of the equations 3.11.

3.6 Calculations Performed by the Computer Program

Using the equations 3.10, a computer program was developed to calculate the following functions which give detailed information for the design of channels.

(1) the normalized even function

For n even, $G_{ne}(X,\phi,S) = g_{ne}(X,\phi,S)/g_{ne}(0,0,0)$

For n odd, $G_{ne}(W,\theta,S) = g_{ne}(W,\theta,S)/g_{ne}(0,0,0)$

(2) the normalized odd function

for n even, $G_{ne}(X,\phi,S) = g_{no}(X,\phi,S)/g_{no}(0,0,0)$

For n odd, $G_{no}(W,\theta,S) = g_{no}(W,\theta,S)/g_{no}(0,0,0)$

(3) the phase

For n even, $\psi_n = \tan^{-1} [g_{no}(X,\phi,S)/g_{ne}(X,\phi,S)]$

(4) the normalized amplitude

For n even, $$|G_n(X,\phi,S)| = \sqrt{[G_{ne}(X,\phi,S)]^2 + [G_{no}(X,\phi,S)]^2}$$

For n odd, $$G_n(W,\theta,S) = G_{ne}(W,\theta,S) + i^{n+1} G_{no}(W,\theta,S)$$

(5) the even energy E_{ne} within a circle of radius W or X

For n even, $$E_{ne}(X,S) = \frac{1}{2\pi} \int_0^{2\pi} \int_0^X g_{ne}^2 (X,\phi,S)\, X dX d\phi$$

For n odd, $$E_{ne}(W,S) = \frac{1}{2\pi} \int_0^{2\pi} \int_0^W g_{ne}^2(W,\theta,S)\, W dW d\theta$$

(6) the odd energy E_{oe} within a circle of radius W or X

For n even, $$E_{no}(X,S) = \frac{1}{2\pi} \int_0^{2\pi} \int_0^X g_{no}{}^2(X,\phi,S)\, X dX d\phi$$

For n odd, $$E_{no}(W,S) = \frac{1}{2\pi} \int_0^{2\pi} \int_0^W g_{no}{}^2(W,\theta,S)\, W dW d\theta$$

(7) the total energy E_t within a circle of radius W or X

For n even, $$E_{nt}(X,S) = E_{no}(X,S) + E_{ne}(X,S)$$

For n odd, $$E_{nt}(W,S) = E_{no}(W,S) + E_{ne}(W,S)$$

(8) the normalized even energy e_i within a circle of radius W or X

For n even, $$e_{ne}(X,S) = \frac{E_{ne}(X,S)}{E_{nt}(0,0)}$$

For n odd, $$e_{ne}(W,S) = \frac{E_{ne}(W,S)}{E_{nt}(0,0)}$$

(9) the normalized odd energy e_o within a circle of radius W or X

For n even, $$e_{no}(X,S) = \frac{E_{no}(X,S)}{E_{nt}(0,0)}$$

For n odd, $$e_{no}(W,S) = \frac{E_{no}(W,S)}{E_{nt}(0,0)}$$

(10) the normalized total energy e_t within a circle of radius W or X

For n even, $$e_{nt}(X,S) = \frac{E_{nt}(X,S)}{E_{nt}(0,0)}$$

For n odd, $$e_{nt}(W,S) = \frac{E_{nt}(W,S)}{E_{nt}(0,0)}$$

(11) the average angular even amplitude $\overline{G}_e$ at radius W or X

For n even, $$\overline{G}_{ne}(X,S) = \frac{1}{2\pi} \int_0^{2\pi} G_{ne}(X,\phi,S)\, d\phi$$

For n odd, $$\overline{G}_{ne}(W,S) = \frac{1}{2\pi} \int_0^{2\pi} G_{ne}(W,\theta,S)\, d\theta$$

(12) the even function integral values EFI on the axis

For n even, $$EFI(X,S) = \frac{1}{2\pi} \int_0^{2\pi} \int_0^{X} g_{ne}(X,\phi,S)\, X dX d\phi$$

For n odd, $$EFI(W,S) = \frac{1}{2\pi} \int_0^{2\pi} \int_0^{W} g_{ne}(W,\theta,S)\, W dW d\theta$$

For convenience in analysis, a plot of each one dimensional distribution was made by the computer. The two dimensional functions G G_e, G_o, ψ are evaluated at the points of a polar system having 51 equally spaced points on each of 51 radial lines which divide the quadrant into 50 equal angles. To aid in the analysis of these functions, it was decided to have the computer represent the calculations in three different ways:

(1) the values for each radial line are tabulated with 16 digit accuracy.

(2) plots of the distribution are made along every 10 radial line.

(3) contour maps are constructed of each function as follows: The values are calculated for the points of a polar coordinate system and are normalized so that $g_n(0,0,0) = 100$. Each value is then approximated by the nearest integer. Thus for example, the Airy pattern would be presented by positive or negative integers ranging from 0 to 100. An approximate map of the values is then constructed by placing the appropriate integer at each point of a scaled coordinate system. This map then provides a display of the distribution. Since the values can not be placed by the computer on a polar coordinate system, they are placed on the closest corresponding points of a rectangular coordinate system. Each contour map is symmetrical about the axis $\theta = 0$ or $\phi = 0$. Therefore, only the half of each map from 0 to π is presented.

3.7 Accuracy check for the Computer Program.

In order to check the program for accuracy, we used a function which could be integrated analytically. From equation A6 of appendix A,

$$\frac{1}{2\pi} \int_0^{2\pi} \int_0^1 g_o(X,\phi)\, e^{iWX \cos(\phi-\theta)} X\,dX\,d\phi = g_1(W,\theta) \qquad 3.12$$

where

$$g_o(X,\phi) = X^k \cos\ k\,\phi$$

$$g_1(W,\theta) = i^k \cos\ k\,\theta\ \frac{J_{k+1}}{W}\ (W)$$

The function $g_o(X,\phi)$ has the following symmetry properties:

$$\begin{aligned} g_o(X,\phi) &= g_o(X,-\phi) \\ g_o(X,\phi) &= g_o(X,\pi-\phi) \qquad k \text{ even} \\ g_o(X,\phi) &= -g_o(X,\pi-\phi) \qquad k \text{ odd} \end{aligned} \tag{3.13}$$

Hence, by choosing k to be even or odd, functions which satisfy the same symmetry relations as the even and odd functions may be obtained. We have

$$g_o(X,\phi) = g_{oe}(X,\phi) + g_{oo}(X,\phi) \tag{3.14}$$

where

$$g_{oe}(X,\phi) = X^m \cos\ m\,\phi \qquad m \text{ even}$$

$$g_{oo}(X,\phi) = X^n \cos\ n\,\phi \qquad n \text{ odd}$$

The result is a function $g_1(W,\theta)$ given by,

$$g_1(W,\theta) = g_{1e}(W,\theta) + g_{1o}(W,\theta) \tag{3.15}$$

where

$$g_{1e}(W,\theta) = \frac{i^m \cos\ m\theta\ J_{m+1}(W)}{W} \qquad m \text{ even}$$

$$g_{1o}(W,\theta) = \frac{i^n \cos\ n\theta\ J_{n+1}(W)}{W} \qquad n \text{ odd}$$

The general program was checked for the cases (m = 2, n = 1), (m = 4, n = 3), (m = 6, n = 5) by comparing the results with values given by equation 3.15. The values of the Bessel functions of orders 1 and 2 were available to an accuracy greater than 16 digits from published tables but since the accuracy for orders higher than 2 was only 10 digits at most, a recursion relation was used for these orders:

$$J_{k+1}(W) = \frac{2k}{W} J_k(W) - J_{k-1}(W) \qquad 3.16$$

For the case n = 2, n = 1, agreement between the two sets of results was found to vary from 9 digits at W = 10 to 14 digits at W = 0. For m = 4, n = 3 and for m = 6, n = 5 agreement varied from 2 digits at W = 10 to 4 digits at W = 0. The accuracy then appears to depend on how rapidly the input function varies with X and ϕ.

LEAF 60 OMITTED IN PAGE NUMBERING.

Chapter 4

Mode Formation in a Diffraction Channel having Identical Circular Diaphrams.

It was stated in section 2.2 that there exist functions known as modes which have identical distributions on the reference surfaces Σ_n and Σ_{n+1} (figure 1.3) or equivalently on the planes n and n + 1 in a diffraction channel having identical diaphrams. If an input function to a diffraction channel is iterated, there may be convergence to one of these modes. The transition of input functions to this steady state condition has been studied, iteration by iteration, in this investigation. Some insight is thus gained into the stability of the modes and the characteristics of the channel.

Although the study was performed on a hyperresolving system having identical diaphrams of radii defined by $A_n = 1$ for n even, and $A_n = W_m$ for n odd, the results may be readily applied to the homothetic channel with all identical diaphrams of radii defined by $A_n = \sqrt{W_m}$ as explained in section 2.3. This particular choice enables easy comparison of the final modes with those calculated by Lansraux; it has the disadvantage that iterated modes are alternately contracted and expanded so that the amplitude distributions in the odd planes must be defined by a new variable $w = W_m W$ to enable direct comparison of successive iterations.

Four different input distributions to the hyperresolving system were iterated - the uniform amplitude distribution of a point source on

the axis, the mode (0, 1), the mode (0, 2) and several sets of pseudo-random numbers. The modes (0, 1) and (0, 2), calculated by Lansraux are tabulated in figures 4.1 for W_m = 1.0 and are somewhat similar for other values of W_m.

With values of W_m ranging from .05 to 5 in steps of 0.5, each distribution was iterated until the amplitudes for two successive iterations agreed to 16 digits. The results of these calculations are described below:

4.1 Uniform Amplitude Input Function

For each value of W_m there was convergence toward the mode (0, 0) (dominant mode). The amplitude values of the final pattern agreed to within 12 digits of those calculated by Lansraux using a different process. As W_m was increased, more iterations were required for convergence to the dominant mode e.g. only 10 were required at W_m = 0.5 whereas 100 were required at W_m = 5.0. Sample patterns for several values of W_m are shown in figures 4.2 and 4.3.

In addition to calculating all the cases from W_m = 0.05 to W_m = 5 in steps of 0.5, the case W_m = 10 was attempted. However, the convergence is very slow for this case and after 40,000 iterations two successive iterations agreed to within only 2 digits. Because of the prohibitively high number of iterations required and the consequent long

computer time, no further iterations were performed for this case. An interesting feature of this case is that for the first few hundred iterations, each alternate diffraction pattern is almost identical and this situation is remarkably stable. Iterations 414, 415, 416, 417 in figure 4.4 illustrate this stability.

4.2 Mode (0, 1) Input Distribution

With the (0, 1) mode as input, the successive distributions were reasonably stable in the first few iterations, changing very little from iteration to iteration but progressively deviating from the (0, 1) mode. However, in a few further iterations there were rather spectacular changes in the distributions. For each value of W_m, the distributions changed dramatically from a distribution resembling the (0, 1) mode (which has positive and negative regions as shown in figures 4.1) to a distribution resembling the (0, 0) mode (which is always positive as shown in figures 4.1). This was followed by a gradual approach to the mode (0, 0). As W_m was increased the changes were slower. Figures 4.5 and 4.6 show the distributions for several cases. The conclusions obtained are that the mode (0, 1) is unstable for small values of W_m but that the stability increases with W_m.

4.3 Mode (0, 2) Input Distribution

The changes for this input distribution can be described in the same way as those for the mode (0, 1) above, except that they occur more rapidly. It is interesting to note that there was not convergence to the mode (0, 1) before convergence to the dominant mode. Figures 4.7 and 4.8 show that distributions for various cases.

4.4 Arbitrary Input Distributions

It was decided to check that several arbitrary distributions would also converge to the dominant mode. If a set of random numbers is iterated once by the computer program, the result is an arbitrary distribution suitable for further iterations since it has no discontinuities or rapid fluctuation. 5 different sets of pseudo-random numbers generated by an IBM subroutine (RANDU) were iterated once to give 5 different arbitrary distributions which were then iterated. There was convergence toward the dominant mode for each of these distributions.

4.5 Effect of Errors.

Some idea of the effect of errors on the calculations was obtained from two minor mistakes:

(a) Many of the calculations were first performed with "single

precision" (8 digits). The calculations were then repeated with "double precision" (16 digits) and the two sets of amplitudes compared iteration by iteration. It was found that as the number of iterations increased, the difference between two corresponding amplitudes increased to a maximum and then decreased continuously as the distribution gradually converged to the dominant mode. In many cases the maximum difference was so great that none of the digits agreed. It was also found that for a given iteration the difference increased with W.

(b) For many of the calculations, each amplitude distribution was normalized to 1 at W = 0 and this normalized distribution was then printed and used as input for the next iteration. However, a process involving fewer operations and therefore more accuracy is to print values normalized to 1 at W = 0 but to use the unnormalized values as input for the next iteration. The calculations were repeated using this latter method and the two sets of amplitudes were compared iteration by iteration. The amplitudes showed the same type of changes as in (a).

4.6 Analysis of Calculations

All the distributions iterated converged to the dominant mode. It can be shown theoretically that any input distribution will in practice converge to the dominant mode. If we assume the set of modes $f_{pq}(X, \phi)$ is complete, any arbitrary input distribution can be expressed as a linear combination of these modes,

$$g_o(X, \phi) = \sum_p \sum_q C_{pq} f_{pq}(X, \phi) \qquad 4.1$$

Substituting this into the right hand side of equation 1.1, the amplitude distribution after one iteration is obtained

$$g_1(W, \theta) = \frac{1}{2\pi} \sum_p \sum_q C_{pq} \int_o^1 \int_o^{2\pi} f_{pq}(X, \phi)\, e^{iWX \cos(\phi - \theta)} X dX d\phi \qquad 4.2$$

By equation 2.5,

$$g_1(W, \theta) = \sum_p \sum_q C_{pq} K_{pq} f_{pq}(W, \theta) \qquad 4.3$$

Using this distribution in the right hand side of 1.1 and repeating this iterative procedure, the distribution after I iterations can be obtained as,

$$g_I(W, \theta) = \sum_p \sum_q C_{pq} (K_{pq})^I f_{pq}(W, \theta) \qquad 4.4$$

In the limit of large I, only the term belonging to the eigenvalue of largest magnitude will remain this being the dominant mode (0, 0). This then explains why each input function converges to the dominant mode. In the case where the input function is one of the higher modes, for example, the (0, 1) mode it may be expected that $C_{pq} = 0$ for $p \neq 0$, $q \neq 1$ and that this mode would remain stable since,

$$g_I(W, \theta) = C_{01} \ (K_{01})^I \ f_{01}(W, \theta) \qquad 4.5$$

However, the condition that $C_{pq} = 0$ for $p \neq 0$, $q \neq 1$ can never be rigorously attained in practice since the calculations cannot be performed with perfect accuracy, the precision being limited by the number of digits available for each number (in the IBM 360, the number of digits is 16). Thus higher order modes will in practice converge to the dominant mode. This result has also been demonstrated by Lansraux using a different approach (unpublished work).

Mode (0, 1) WITH W_m = 1.0

W	Amplitude
0.0	0.9999999999999986D 00
0.010	0.9997673453352095D 00
0.020	0.9991403967987288D 00
0.030	0.9980862011980660D 00
0.040	0.9965978363647880D 00
0.050	0.9946844113091959D 00
0.060	0.9923460661523109D 00
0.070	0.9895929721463905D 00
0.080	0.9863953316467062D 00
0.090	0.9827833780996972D 00
0.100	0.9787473760255376D 00
0.110	0.9742876209985331D 00
0.120	0.9694044396251606D 00
0.130	0.9640981895199097D 00
0.140	0.9583692592782175D 00
0.150	0.9522180684486074D 00
0.160	0.9456450675005292D 00
0.170	0.9386507377913972D 00
0.180	0.9312355915307426D 00
0.190	0.9234001717421653D 00
0.200	0.9151450522230080D 00
0.210	0.9064708375017342D 00
0.220	0.8973781627930343D 00
0.230	0.8878676939506442D 00
0.240	0.8779401274178970D 00
0.250	0.8675961901759760D 00
0.260	0.8568366396900264D 00
0.270	0.8456622638527011D 00
0.280	0.8340739809258465D 00
0.290	0.8220723394796380D 00
0.300	0.8096585183295814D 00
0.310	0.7968333264712509D 00
0.320	0.7835977030127882D 00
0.330	0.7699526171051662D 00
0.340	0.7558590578702217D 00
0.350	0.7414380843264660D 00
0.360	0.7265707253126791D 00
0.370	0.7112580794092842D 00
0.380	0.6956212648575259D 00
0.390	0.6795414294764403D 00
0.400	0.6630597505770345D 00
0.410	0.6461774348778805D 00
0.420	0.6288957184095242D 00
0.430	0.6112159864287265D 00
0.440	0.5931391733215323D 00
0.450	0.5743069625077846D 00
0.460	0.5558005863428871D 00
0.470	0.5365414260174172D 00
0.480	0.5168906914546090D 00
0.490	0.4968504212057063D 00
0.500	0.4764214823431922D 00
0.510	0.4556055703519119D 00
0.520	0.4344042090180872D 00
0.530	0.4128189503162400D 00
0.540	0.3908513742940284D 00
0.550	0.3685030889550049D 00
0.560	0.3457757301393107D 00
0.570	0.3226709614023057D 00
0.580	0.2991904738911563D 00
0.590	0.2753359862193800D 00
0.600	0.2511092443393603D 00
0.610	0.2265120214126470D 00
0.620	0.2015461176794426D 00
0.630	0.1762133603230948D 00
0.640	0.1505156033365963D 00
0.650	0.1244547273841118D 00
0.660	0.9803263966173810D-01
0.670	0.7125127375610590D-01
0.680	0.4411258950104346D-01
0.690	0.1661857283230174D-01
0.700	-0.1122876435963358D-01
0.710	-0.3942738437864732D-01
0.720	-0.6797522387398940D-01
0.730	-0.9687019349315810D-01
0.740	-0.1261110180536654D 00
0.750	-0.1556930441145964D 00
0.760	-0.1856166203051803D 00
0.770	-0.2158787198149747D 00
0.780	-0.2466477128641039D 00
0.790	-0.2774096082348491D 00
0.800	-0.3086738756680092D 00
0.810	-0.3402677037997598D 00
0.820	-0.3721887214462402D 00
0.830	-0.4044346135515102D 00
0.840	-0.4370030213603082D 00
0.850	-0.4698915025925374D 00
0.860	-0.5030978316194560D 00
0.870	-0.5366019399641581D 00
0.880	-0.5704538140682360D 00
0.890	-0.6045586026988114D 00
0.900	-0.6390512659056430D 00
0.910	-0.6738092848135361D 00
0.920	-0.7088701175109124D 00
0.930	-0.7442311994375561D 00
0.940	-0.7798394463739519D 00
0.950	-0.8156437491071985D 00
0.960	-0.8520397712848700D 00
0.970	-0.8886259860770140D 00
0.980	-0.9254490934357077D 00
0.990	-0.9625965239730653D 00
1.000	-0.9995433474460771D 00

FIGURE-4-1A

Mode (0, 2) WITH W_m = 1.0

W	Amplitude
0.0	0.99999999999999550 00
0.010	0.99938743390829330 00
0.020	0.99765050189050130 00
0.030	0.99449150262178370 00
0.040	0.99021426690478300 00
0.050	0.98472415718574760 00
0.060	0.97802806687724930 00
0.070	0.97013441948761040 00
0.080	0.96105316755723600 00
0.090	0.95079579140205390 00
0.100	0.93937529766431740 00
0.110	0.92680621767104770 00
0.120	0.91310460560044560 00
0.130	0.89828803645673580 00
0.140	0.88237560385361810 00
0.150	0.86538791760704660 00
0.160	0.84734710113763410 00
0.170	0.82827678868327090 00
0.180	0.80820212232251970 00
0.190	0.78714974880936880 00
0.200	0.76514781622000040 00
0.210	0.74222597041224000 00
0.220	0.71841535129839970 00
0.230	0.69374858932293600 00
0.240	0.66825979941118820 00
0.250	0.64198458059353770 00
0.260	0.61496000763337870 00
0.270	0.58722462833228370 00
0.280	0.55881845830982630 00
0.290	0.52978297599354480 00
0.300	0.50016111742943550 00
0.310	0.46995727091403560 00
0.320	0.43933727144918670 00
0.330	0.40822839502065840 00
0.340	0.37671935270176620 00
0.350	0.34486028458323840 00
0.360	0.31270275353057550 00
0.370	0.28029973877019790 00
0.380	0.24770562940572650 00
0.390	0.21497621716576560 00
0.400	0.18216869048459040 00
0.410	0.14934162641722490 00
0.420	0.11655498389035560 00
0.430	0.83870096190644400-01
0.440	0.51349663391997350-01
0.450	0.19057744623390800-01
0.460	-0.12940249821082570-01
0.470	-0.44577566528289700-01
0.480	-0.75786117166507900-01
0.490	-0.10649648683849670 00
0.500	-0.13663794258539620 00
0.510	-0.16613844203960630 00
0.520	-0.19492464222477050 00
0.530	-0.22292190850694590 00
0.540	-0.25005432365301300 00
0.550	-0.27624469712031050 00
0.560	-0.30141457436548790 00
0.570	-0.32548424638049070 00
0.580	-0.34837275932756470 00
0.590	-0.36999792431313480 00
0.600	-0.39027632729237990 00
0.610	-0.40912333910225970 00
0.620	-0.42645312562074080 00
0.630	-0.44217865804991110 00
0.640	-0.45621172332065260 00
0.650	-0.46846293461647560 00
0.660	-0.47884174201409600 00
0.670	-0.48725644323831280 00
0.680	-0.49361419452867160 00
0.690	-0.49782102161538220 00
0.700	-0.49978183080192280 00
0.710	-0.49940042015170540 00
0.720	-0.49657949077616000 00
0.730	-0.49122065822153960 00
0.740	-0.48322446395172040 00
0.750	-0.47249038692423220 00
0.760	-0.45891685525669840 00
0.770	-0.44240125798085670 00
0.780	-0.42283995688125950 00
0.790	-0.40012829841574670 00
0.800	-0.37416062571471450 00
0.810	-0.34483029065615150 00
0.820	-0.31202596660136712D 00
0.830	-0.27565015767362890 00
0.840	-0.23558221691961190 00
0.850	-0.19171535277973210 00
0.860	-0.14393814443438250 00
0.870	-0.92138253680924000-01
0.880	-0.36202437492110130-01
0.890	0.23983439615119060-01
0.900	0.88534392563768200-01
0.910	0.15756630345726360 00
0.920	0.23119590867969170 00
0.930	0.30954078619926560 00
0.940	0.39271934279852220 00
0.950	0.48085040127480510 00
0.960	0.57405518761458200 00
0.970	0.67245318145268D 00
0.980	0.77016678666816160 00
0.990	0.86531795157623C3D 00
1.000	0.10000295229604560 01

FIGURE 4.1 B

ITERATION 0 WITH W_m = 1.0, UNIFORM AMPLITUDE INPUT FUNCTION

W	Amplitude
0.0	0.9999999999999980D 00
0.010	0.9999875000052083CD 00
0.020	0.9999500008333261D 00
0.030	0.9998875042186705D 00
0.040	0.9998000013332888D 00
0.050	0.9996875325503879D 00
0.060	0.9995500674949373D 00
0.070	0.9993876250393176D 00
0.080	0.9992002133048907D 00
0.090	0.9989878416610906D 00
0.100	0.9987505207248390D 00
0.110	0.9984882623598856D 00
0.120	0.9982010796760580D 00
0.130	0.9978889870284513D 00
0.140	0.9975520000165260D 00
0.150	0.9971901354831351D 00
0.160	0.9968034119134705D 00
0.170	0.9963918474339352D 00
0.180	0.9959554638109317D 00
0.190	0.9954942824495807D 00
0.200	0.9950083263923594D 00
0.210	0.9944976199176584D 00
0.220	0.9939621885382683D 00
0.230	0.9934020589977773D 00
0.240	0.9928172592789225D 00
0.250	0.9922078818381852D 00
0.260	0.9915737674213380 00
0.270	0.9909151372192195D 00
0.280	0.9902319610960974D 00
0.290	0.9895242730774242D 00
0.300	0.9887921084873594D 00
0.310	0.9880355038673567D 00
0.320	0.9872544969738920D 00
0.330	0.9864491267760895D 00
0.340	0.9856194334533066D 00
0.350	0.9847654583926155D 00
0.360	0.9838872441862247D 00
0.370	0.9829848346280174D 00
0.380	0.9820582747148238D 00
0.390	0.9811076106356089D 00
0.400	0.9801328897765932D 00
0.410	0.9791341607142951D 00
0.420	0.9781114732133022D 00
0.430	0.9770648782316780 00
0.440	0.9759944278752303D 00
0.450	0.9749001754793673D 00
0.460	0.9737821755206688D 00
0.470	0.9726404836560384D 00
0.480	0.9714751567107309D 00
0.490	0.9702862526748003D 00
0.500	0.9690738306994952D 00
0.510	0.9678379510935672D 00
0.520	0.9665786753319515D 00
0.530	0.9652960659875800 00
0.540	0.9639901868627296D 00
0.550	0.9626611028389122D 00
0.560	0.9613088799567950D 00
0.570	0.9599335853875890 00
0.580	0.9585352874368970D 00
0.590	0.9571140555287638D 00
0.600	0.9556699602130522D 00
0.610	0.9542030731552031D 00
0.620	0.9527134671329504D 00
0.630	0.9512012160317879D 00
0.640	0.9496663958403758D 00
0.650	0.9481090796458919D 00
0.660	0.9465293476292619D 00
0.670	0.9449272770664057D 00
0.680	0.9433029472933449D 00
0.690	0.9416564387612817D 00
0.700	0.9399878329715964D 00
0.710	0.9382972125007882D 00
0.720	0.9365846609893406D 00
0.730	0.9348502631365336D 00
0.740	0.9330941046951783D 00
0.750	0.9313162724662986D 00
0.760	0.9295168542937404D 00
0.770	0.9276959390587213D 00
0.780	0.9258536166743183D 00
0.790	0.9239899780798874D 00
0.800	0.9221051152354246D 00
0.810	0.9201991211158673D 00
0.820	0.9182720970332510 00
0.830	0.9163241159912593D 00
0.840	0.9143552959859600D 00
0.850	0.9123657265837774D 00
0.860	0.9103555058287597D 00
0.870	0.9083247326349437D 00
0.880	0.9062733069170481D 00
0.890	0.9042012955693230D 00
0.900	0.9021101023973463D 00
0.910	0.8999981823563170D 00
0.920	0.8978661108173697D 00
0.930	0.8957124154827997D 00
0.940	0.8935423658961434D 00
0.950	0.8913508056749490 00
0.960	0.8891397163178151D 00
0.970	0.8869096071536503D 00
0.980	0.8846590255218791D 00
0.990	0.8823896384743931D 00
1.000	0.8800101171489866D 00

FIGURE 4.2A

ITERATION 1 WITH W_m = 1.0 AND UNIFORM AMPLITUDE INPUT FUNCTION

W	Amplitude
0.0	0.99999999999999800 00
0.010	0.99998776008992070 00
0.020	0.99995104096436770 00
0.030	0.99989844443735600 00
0.040	0.99983041735321201D 00
0.050	0.99969403248092510 00
0.060	0.99955942672480550 00
0.070	0.99940036291322640 00
0.080	0.99921684890367250 00
0.090	0.99900089376115980 00
0.100	0.99877650775767440 00
0.110	0.99851970231153460 00
0.120	0.99823849028668010 00
0.130	0.99793288539188490 00
0.140	0.99760290277989620 00
0.150	0.99724855874649910 00
0.160	0.99686987078950600 00
0.170	0.99646685760767130 00
0.180	0.99603953909953330 00
0.190	0.99558793536217950 00
0.200	0.99511207168993950 00
0.210	0.99461196857300250 00
0.220	0.99408765169596240 00
0.230	0.99353914693628660 00
0.240	0.99296648136271230 00
0.250	0.99236968323357040 00
0.260	0.99174878199503210 00
0.270	0.99110380827928620 00
0.280	0.99043479390264000 00
0.290	0.98974177186354850 00
0.300	0.98902477634056970 00
0.310	0.98828384269024710 00
0.320	0.98751900744492020 00
0.330	0.98673030831046120 00
0.340	0.98591778416394010 00
0.350	0.98509147505121620 00
0.360	0.98422142218445890 00
0.370	0.98333766793959660 00
0.380	0.98243025585366100 00
0.390	0.98149923062224380 00
0.400	0.98054463809642930 00
0.410	0.97956652528025610 00
0.420	0.97856494032765770 00
0.430	0.97753993253751390 00
0.440	0.97649155236059900 00
0.450	0.97541985137646110 00
0.460	0.97432488231023080 00
0.470	0.97320669901936060 00
0.480	0.97206535649229250 00
0.490	0.97090091084505900 00
0.500	0.96971341931781180 00
0.510	0.96850294027128380 00
0.520	0.96726953318318080 00
0.530	0.96601329864450550 00
0.540	0.96473417835581270 00
0.550	0.96343235512339600 00
0.560	0.96210785285540870 00
0.570	0.96076073655791400 00
0.580	0.95939107233087090 00
0.590	0.95799892736405180 00
0.600	0.95658436993289350 00
0.610	0.95514746939428090 00
0.620	0.95368829618226740 00
0.630	0.95220692180372630 00
0.640	0.95070341883393780 00
0.650	0.94917786091211260 00
0.660	0.94763032273684740 00
0.670	0.94606088006151840 00
0.680	0.94446960968960920 00
0.690	0.94285658946997560 00
0.700	0.94122189829204590 00
0.710	0.93956561608095880 00
0.720	0.93788782379263820 00
0.730	0.93618860340890440 00
0.740	0.93446803793192450 00
0.750	0.93272621138010000 00
0.760	0.93096320878189350 00
0.770	0.92917911617109290 00
0.780	0.92737402058141690 00
0.790	0.92554801004115850 00
0.800	0.92370117356776780 00
0.810	0.92183360116237770 00
0.820	0.91994538380426700 00
0.830	0.91803661344526810 00
0.840	0.91610738300411210 00
0.850	0.91415778636071950 00
0.860	0.91218791835043080 00
0.870	0.91019787475818090 00
0.880	0.90818775231261530 00
0.890	0.90615764868015120 00
0.900	0.90410766245898180 00
0.910	0.90203789317302390 00
0.920	0.89994844126581220 00
0.930	0.89783940809433760 00
0.940	0.89571089592282960 00
0.950	0.89356300791648800 00
0.960	0.89139584813515760 00
0.970	0.88920952152695220 00
0.980	0.88700413392182410 00
0.990	0.88477979202508300 00
1.000	0.88253660341086120 00

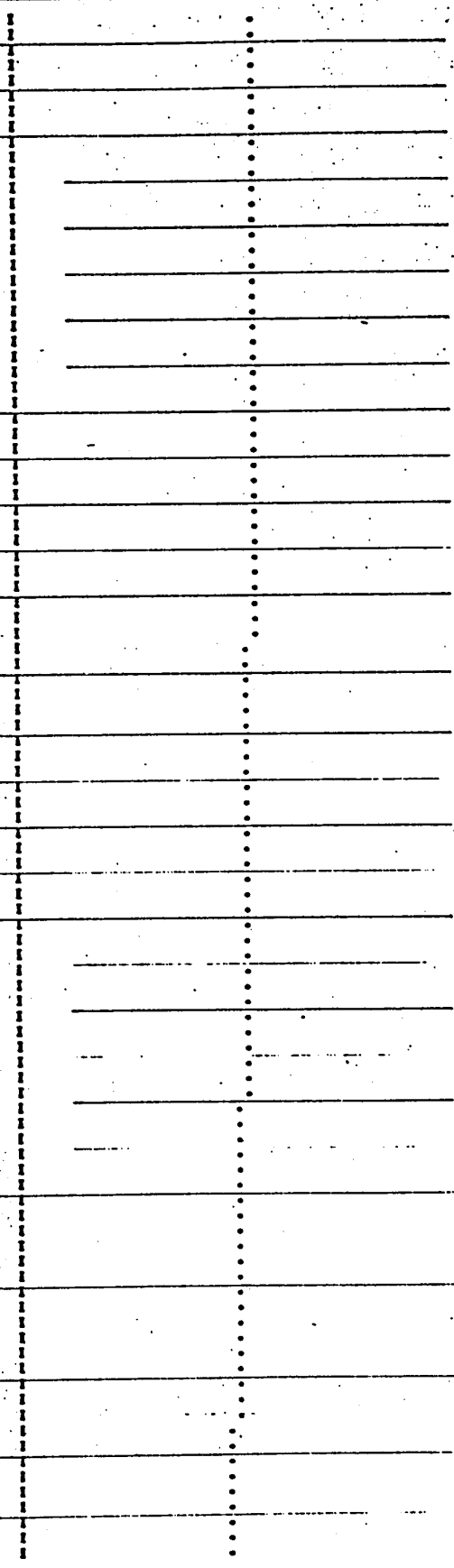

FIGURE 4.2B

ITERATION 29 WITH W_m = 1.0, UNIFORM AMPLITUDE INPUT FUNCTION

W	Amplitude
0.0	0.9999999999999980D 00
0.010	0.9999877602189923D 00
0.020	0.9999510414815038D 00
0.030	0.9998898456041036D 00
0.040	0.9998041756142801D 00
0.050	0.9996940357502530D 00
0.060	0.9995594314607116D 00
0.070	0.9994003694044783D 00
0.080	0.9992168574500848D 00
0.090	0.9990089046753010D 00
0.100	0.9987765213665558D 00
0.110	0.9985197190183052D 00
0.120	0.9982385103323170D 00
0.130	0.9979329092168835D 00
0.140	0.9976029307859557D 00
0.150	0.9972485913582071D 00
0.160	0.9968699084560190D 00
0.170	0.9964669008043933D 00
0.180	0.9960395883297894D 00
0.190	0.9955879921588674D 00
0.200	0.9951121346172775D 00
0.210	0.9946120392280730D 00
0.220	0.9940877307104505D 00
0.230	0.9935392349781149D 00
0.240	0.9929665791376933D 00
0.250	0.9923697914870490D 00
0.260	0.9917489015135301D 00
0.270	0.9911039398921343D 00
0.280	0.9904349384836110D 00
0.290	0.9897419303324801D 00
0.300	0.9890249496649831D 00
0.310	0.9882840318869607D 00
0.320	0.9875192135816566D 00
0.330	0.9867305325074462D 00
0.340	0.9859180275954968D 00
0.350	0.9850817389473520D 00
0.360	0.9842217078324446D 00
0.370	0.9833379766855401D 00
0.380	0.9824305891041014D 00
0.390	0.9814995498455895D 00
0.400	0.9805450248246869D 00
0.410	0.9795669411104534D 00
0.420	0.9785653800923406D 00
0.430	0.9775404116325350D 00
0.440	0.9764920657522380D 00
0.450	0.9754204305391959D 00
0.460	0.9743254659891754D 00
0.470	0.9732073268337464D 00
0.480	0.9720660265369540D 00
0.490	0.9709016252919027D 00
0.500	0.9697141804172770D 00
0.510	0.9685037503537938D 00
0.520	0.9672703946605840D 00
0.530	0.9660141740115042D 00
0.540	0.9647351501913847D 00
0.550	0.9634333860922037D 00
0.560	0.9621089457091966D 00
0.570	0.9607618941368464D 00
0.580	0.9593922475651081D 00
0.590	0.9580002232748150D 00
0.600	0.9565857396340164D 00
0.610	0.9551489160935035D 00
0.620	0.9536898231825621D 00
0.630	0.9522085325046178D 00
0.640	0.9507051167328066D 00
0.650	0.9491796496054880D 00
0.660	0.9476322059216861D 00
0.670	0.9460628615364732D 00
0.680	0.9444716933562810D 00
0.690	0.9428587793341560D 00
0.700	0.9412241984649431D 00
0.710	0.9395680307804128D 00
0.720	0.9378903573443195D 00
0.730	0.9361912602474020D 00
0.740	0.9344708226023170D 00
0.750	0.9327291285385155D 00
0.760	0.9309662631970514D 00
0.770	0.9291823127253366D 00
0.780	0.9273773642718263D 00
0.790	0.9255515059806500D 00
0.800	0.9237046269861807D 00
0.810	0.9218374174075445D 00
0.820	0.9199493583430691D 00
0.830	0.9180407714646099D 00
0.840	0.9161117210121933D 00
0.850	0.9141623097876769D 00
0.860	0.9121926331445786D 00
0.870	0.9102027873006916D 00
0.880	0.9081928682133877D 00
0.890	0.9061629745614032D 00
0.900	0.9041132047760776D 00
0.910	0.9020436585091615D 00
0.920	0.8999544363324172D 00
0.930	0.8978456347339415D 00
0.940	0.8957173711069314D 00
0.950	0.8935694733746397D 00
0.960	0.8914020318503237D 00
0.970	0.8892167704437705D 00
0.980	0.8870116556424314D 00
0.990	0.8847575341301302D 00
1.000	0.8825446093064272D 00

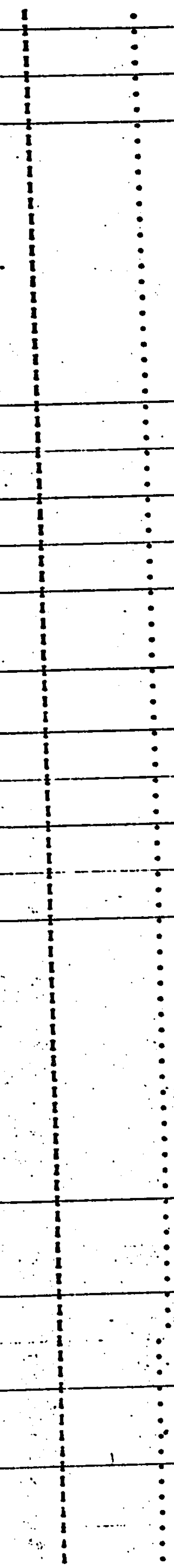

FIGURE 4.2C

ITERATION O WITH W_m = 5.0, UNIFORM AMPLITUDE INPUT FUNCTION

W	Amplitude
0.0	0.999995599995995800 CO
0.050	0.999687532550387900 00
0.100	0.998750520724839000 CO
0.150	0.997190135483135100 00
0.200	0.995008326392359400 OC
0.250	0.992207818581815200 CO
0.300	0.988792108487359400 00
0.350	0.984765452397615200 CC
0.400	0.980132889776593200 00
0.450	0.974900175479367300 00
0.500	0.969073830699494800 00
0.550	0.962661102838912000 00
0.600	0.955669960213052200 CO
0.650	0.948109070964595170 00
0.700	0.939987832971596400 00
0.750	0.931316272466296860 CO
0.800	0.922105115235424600 00
0.850	0.912365726583777400 00
0.900	0.902110102397346500 OC
0.950	0.891350850567494900 CC
1.000	0.880101171485866900 00
1.050	0.868374837671868500 CO
1.100	0.856186172484168800 00
1.150	0.843550028093072900 CC
1.200	0.830481762612025300 00
1.250	0.816996721651120840 00
1.300	0.803112688330246300 00
1.350	0.788844906723387300 00
1.400	0.774211019901220400 OC
1.450	0.759228539491954600 00
1.500	0.743915343880132400 CC
1.550	0.728285636063568400 OC
1.600	0.712369919067710020 00
1.650	0.696174968029018100 CO
1.700	0.679723801798850700 OC
1.750	0.663035654444562700 OC
1.800	0.646129946367961400 00
1.850	0.629026255287356600 00
1.900	0.611744287066773000 00
1.950	0.594303846451132300 00
2.000	0.576724807756873800 00
2.050	0.559027085567437900 CC
2.100	0.541236606543284480 OC
2.150	0.523355274972795600 CC
2.200	0.505420954380968600 00
2.250	0.487447428130632600 CO
2.300	0.469454376177665000 00
2.350	0.451461345759310300 CO
2.400	0.433487723482494300 OC
2.450	0.415535270781475580 OC
2.500	0.397675281971420400 CO
2.550	0.379874187328840200 CO
2.600	0.362167897321215600 CO
2.650	0.344574591914310100 00
2.700	0.327112132680188800 OC
2.750	0.309798038514839300 00
2.800	0.292649462037350700 OC
2.850	0.275683166707677080 00
2.900	0.258915504698687500 00
2.950	0.242362395556834300 CO
3.000	0.226039305683958200 CC
3.050	0.209961228671548400 CC
3.100	0.194142666516811700 00
3.150	0.178597611748347000 OC
3.200	0.163339530487816200 00
3.250	0.148381346447085530 CO
3.300	0.133735428051662300 OC
3.350	0.119413564209367800 OC
3.400	0.105426971577357800 CC
3.450	0.917862625106355000-01
3.500	0.785014442076444000-01
3.550	0.655819068950051000-01
3.600	0.530364150588206800-01
3.650	0.408730999905366300-01
3.700	0.290994528353854400-01
3.750	0.177223195358299200-01
3.800	0.674789627722771600-02
3.850	-0.381827372385315300-02
3.900	-0.139713023696303700-01
3.950	-0.237069577323653200-01
4.000	-0.330216640117742100-01
4.050	-0.419125000405458570-01
4.100	-0.503771989011405600-01
4.150	-0.584141410013839700-01
4.200	-0.660223533933554000-01
4.250	-0.732015025784360000-01
4.300	-0.799518884751344000-01
4.350	-0.862744370215317000-01
4.400	-0.921706917032212000-01
4.450	-0.976428046018833000-01
4.500	-0.102693525295276200 00
4.550	-0.107326190463985700 CC
4.600	-0.111544711346714200 00
4.650	-0.115353556091770770 CO
4.700	-0.118757759933334700 OC
4.750	-0.121762862588257100 00
4.800	-0.124374940874816200 OC
4.850	-0.126600562859256320 OC
4.900	-0.128446804495996300 00
4.950	-0.129921174797632000 00
5.000	-0.131031655036587000 CO

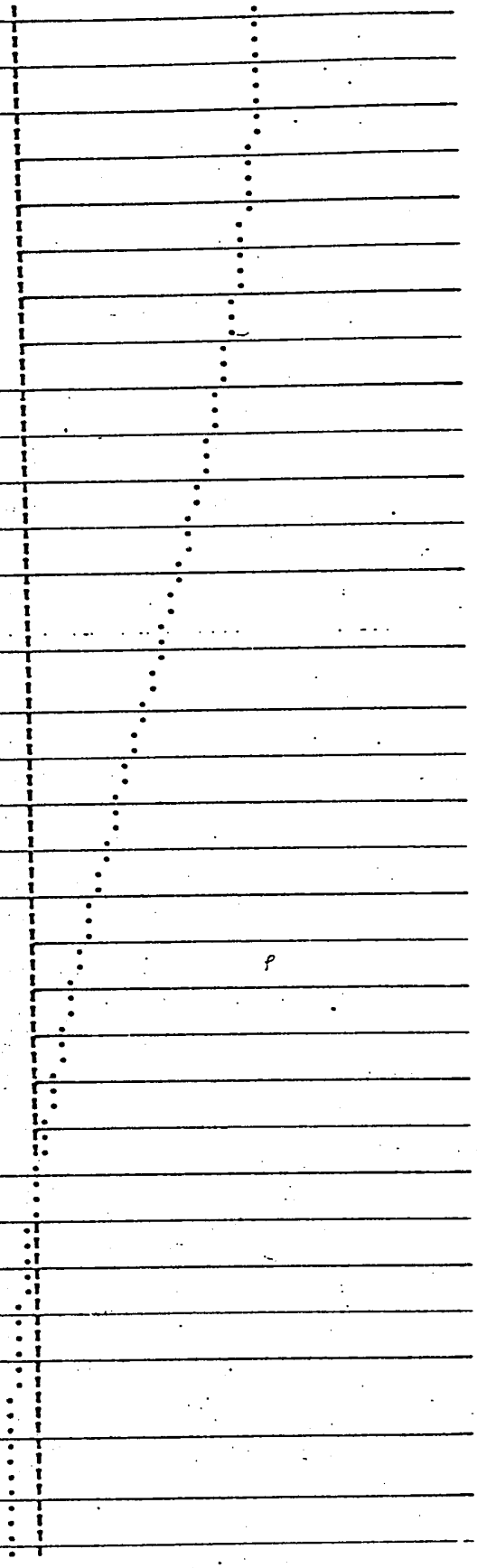

FIGURE 4.3A

ITERATION 1 WITH W_m = 5.0, UNIFORM AMPLITUDE INPUT FUNCTION

W	Amplitude
0.0	0.9999999999999980D 00
0.050	0.9999752776999619D 00
0.100	0.9999010119567770D 00
0.150	0.9997769C54901074D 00
0.200	0.9996024603284396D 00
0.250	0.9993776C9C508224D 00
0.300	0.9990996465216268D 00
0.350	0.9987693071146670D 00
0.400	0.9983847284219897D 00
0.450	0.9979444624416022D 00
0.500	0.9974468792374198D 00
0.550	0.9968901710636939D 00
0.600	0.9962723569452160D 00
0.650	0.9955912877096177D 00
0.700	0.9948446514191462D 00
0.750	0.9940299793163813D 00
0.800	0.9931446520614452D 00
0.850	0.9921859064574014D 00
0.900	0.9911508425236781D 00
0.950	0.9900364309445519D 00
1.000	0.9888395208709263D 00
1.050	0.9875568480589038D 00
1.100	0.9861850433279204D 00
1.150	0.9847206413205302D 00
1.200	0.9831601089452914D 00
1.250	0.9814997576839450D 00
1.300	0.9797359471466656D 00
1.350	0.9778649C082C59900 00
1.400	0.9758828131044960D 00
1.450	0.9737858406107104D 00
1.500	0.9715710951551102D 00
1.550	0.9692317320122529D 00
1.600	0.9667668108868359D 00
1.650	0.9641714531869023D 00
1.700	0.9614441780362093D 00
1.750	0.9585739390524485D 00
1.800	0.9555641119019457D 00
1.850	0.9524065283740866D 00
1.900	0.9491034755464207D 00
1.950	0.9456453C8286091400
2.000	0.9420304628071265D 00
2.050	0.9382554615153046D 00
2.100	0.9343165292366324D 00
2.150	0.9302116006881058D 00
2.200	0.9259363312357514D 00
2.250	0.9214881064222153D 00
2.300	0.9166640542330843D 00
2.350	0.9120614497207C37D 00
2.400	0.9070777293246936D 00
2.450	0.9C1910457452829BD 00
2.500	0.8965575357744945D 00
2.550	0.8910168117114420D 00
2.600	0.8852664866072509D 00
2.650	0.8793649235574438D 00
2.700	0.8732506594882951?D 00
2.750	0.8669425892303119D 00
2.800	0.8604395182827134D 00
2.850	0.8537410230668111D 00
2.900	0.8468462274841004?D 00
2.950	0.8397551055517560D 00
3.000	0.8324674628453440D 00
3.050	0.8249835646233784D 00
3.100	0.8173038781312939D 00
3.150	0.8094291285699761D 00
3.200	0.8013603022216658D 00
3.250	0.7930986490822040D 00
3.300	0.7846456849927128D 00
3.350	0.7760031932648296D 00
3.400	0.7671732257945667D 00
3.450	0.7581581036609530D 00
3.500	0.7489600417206627D 00
3.550	0.7395830255985566D 00
3.600	0.7300290558684148D 00
3.650	0.7203019014320817D 00
3.700	0.7104052200910215D 00
3.750	0.7003429315165205D 00
3.800	0.6901192142210572D 00
3.850	0.6797385C2C2098690 00
3.900	0.6692054799960433D 00
3.950	0.6585250799521793D 00
4.000	0.6477024753951889D 00
4.050	0.6367430760236103D 00
4.100	0.6256525217503288D 00
4.150	0.6144366762632502D 00
4.200	0.6031016201363423D 00
4.250	0.5916533435032446D 00
4.300	0.5800992383065215D 00
4.350	0.5684450901364688D 00
4.400	0.5566992069867422?3D 00
4.450	0.5448652237547C15D 00
4.500	0.5329537866566615D 00
4.550	0.5209710674998899D 00
4.600	0.5089245461782343D 00
4.650	0.4968221571618393D 00
4.700	0.4846713818725396D 00
4.750	0.4724830217241006?D 00
4.800	0.4602566460271320 00
4.850	0.4480068818362323?D 00
4.900	0.4357448544475654D 00
4.950	0.4234730185740418D 00
5.000	0.4112016143428320D 00

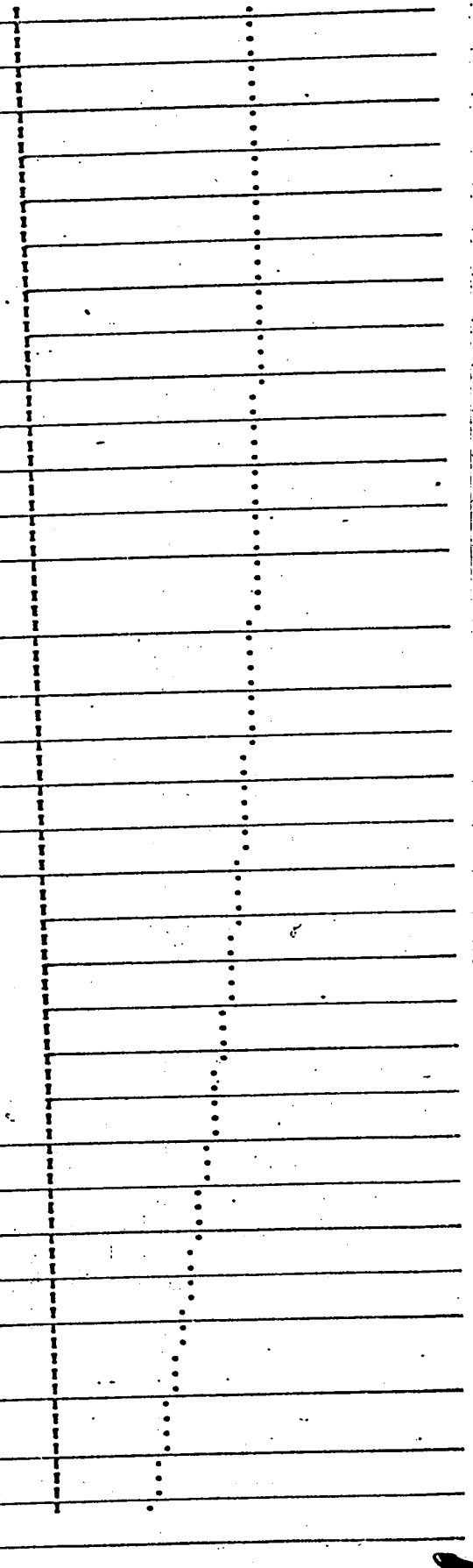

FIGURE 4.3B

ITERATION 2 WITH W_m = 5.0, UNIFORM AMPLITUDE INPUT FUNCTION

W	Amplitude
C.C	0.99999999999999800 00
C.C5C	0.99973168133620510 00
C.1CC	0.99892703184120310 00
C.15C	0.99758697055278510 CO
C.2CC	0.99571302769684820 CO
C.250	C.99330734243441400 00
C.3CC	0.99037265971274970 0C
C.35C	0.98691232622587540 CC
C.400	C.98293028545122690 00
C.45C	0.97843107205075360 00
C.5CC	0.97341580480614460 00
C.55C	0.96790217949937840 0C
C.6CC	0.96188446035118110 00
C.65C	0.95537347087140630 00
C.7CC	0.94837658385671550 CC
C.75C	0.94090171059229520 CC
C.8C0	0.93295728927566540 C0
C.850	0.92455227268193320 C0
C.9C0	0.91569611509107470 0C
C.95C	C.90639875849908CC0 00
1.0C0	0.89667061813593250 CC
1.C50	0.88652256731456330 C0
1.1C0	0.87596592163595380 CC
1.15C	0.86501242257693200 00
1.2C0	0.85367422048708C10 00
1.25C	0.84196385702437500 CC
1.3CC	0.82989424705726010 0C
1.35C	0.81747866006395580 CC
1.4CC	0.80473070105946680 C0
1.45C	0.79166429108182140 00
1.5C0	0.77829364726969920 C0
1.55C	0.76463326256424440 CC
1.6CC	0.75069788506840330 0C
1.65C	0.73650249709765830 00
1.7CC	0.72206229395644440 C0
1.750	0.70739266247493780 C0
1.8CC	0.69250915934121110 CC
1.85C	0.67742748926402880 C0
1.9CC	0.66216348300172150 C0
1.950	0.64673307529274490 0C
2.CCC	0.63115278272356580 CC
2.C5C	C.61543718156955560 C0
2.1CC	0.59960388564449070 0C
2.150	0.58366852419410460 C0
2.2CC	0.56764721986917680 CC
2.25C	0.55155606681290660 0C
2.3CC	0.53541110889765420 CC
2.35C	0.51922831814525100 C0
2.4C0	0.50302357336491040 00
2.45C	C.48681263904221580 00
2.5CC	C.47061114451213280 00
2.55C	C.45443456344839190 00
2.6CC	0.43829815370C88360 C0
2.65C	C.42221713751222300 0C
2.7CC	0.40620628214339510 CC
2.75C	C.39028028C93823C40 CC
2.8C0	0.37445353485499350 CC
2.85C	C.35874017449291570 0C
2.9CC	0.34315404264021640 00
2.95C	0.32770867736937260 00
3.CC0	0.31241729570425520 CC
3.C5C	0.29729277788270160 0C
3.1CC	0.28234765223695340 CC
3.15C	C.26759408071324970 CC
3.2CC	0.25304384505067800 00
3.250	0.23870833363814010 CC
3.3CC	0.22459852906707750 CC
3.35C	C.21072499639628870 CC
3.4CC	0.19709787214389800 0C
3.450	0.18372685402018860 C0
3.5CC	C.17062119141370300 CC
3.55C	0.15778967664161640 00
3.6CC	0.14524063697405750 C0
3.650	0.13298192744063450 0C
3.7CC	0.12102092442604820 CC
3.75C	0.10936452006028460 00
3.8CC	C.98019117407445100-C1
3.85C	0.86990626455910100-01
3.9CC	C.76284460911098400-01
3.95C	0.65905535790697200-01
4.CCC	0.55858265820860880-C1
4.C5C	0.46146564630471010-01
4.1CC	0.36773844739196800-01
4.150	0.27743018333733490-C1
4.2CC	C.19056498825265600-01
4.25C	C.10716203179867230-01
4.3CC	0.27235550122701800-C2
4.35C	-0.49205115678556670-02
4.4CC	-0.12215547369201050-01
4.45C	-C.19161582805072200-01
4.5CC	-0.25759121866756170-01
4.55C	-0.32009135400698870-01
4.6CC	-0.37913053704550930-01
4.65C	-C.43472758461691820-C1
4.7C0	-0.48690574032085140-C1
4.75C	-C.53569258119776370-C1
4.8CC	-0.58111991837834840-C1
4.85C	-0.62322369142571140-C1
4.9C0	-0.66204386009716900-C1
4.95C	-C.69762428326076400-01
5.CCC	-C.73001260270956200-01

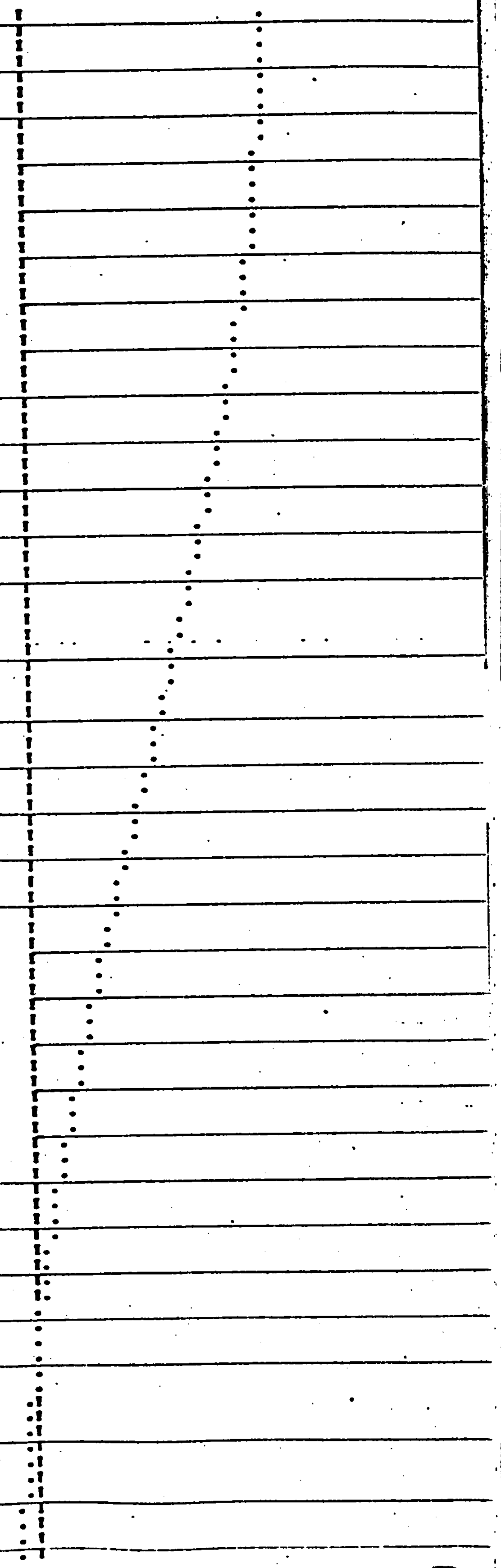

FIGURE 4.3C

ITERATION 3 WITH W_m = 5.0, UNIFORM AMPLITUDE INPUT FUNCTION

W	Amplitude
0.0	0.9999999999999980D 00
0.050	0.9998885265412935D 00
0.100	0.9995541498902866D 00
0.150	0.9989970012271440D 00
0.200	0.9982172992014761D 00
0.250	0.9972153499560598D 00
0.300	0.9959915471594797D 00
0.350	0.9945463720471228D 00
0.400	0.9928803934698009D 00
0.450	0.9909942679491243D 00
0.500	0.9888887397385821D 00
0.550	0.9865646408891495D 00
0.600	0.9840228913180866D 00
0.650	0.9812644928794445D 00
0.700	0.9782905594346700D 00
0.750	0.9751022569215459D 00
0.800	0.9717008634196011D 00
0.850	0.9680877392099660D 00
0.900	0.9642643328275666D 00
0.950	0.9602321811034142D 00
1.000	0.9559929091946543D 00
1.050	0.9515482305999385D 00
1.100	0.9468999471575898D 00
1.150	0.9420499490239559D 00
1.200	0.9370002146292610D 00
1.250	0.9317528106082080D 00
1.300	0.9263098917025216D 00
1.350	0.9206737006325744D 00
1.400	0.9148465675351917D 00
1.450	0.9088309117647124D 00
1.500	0.9026292376543436D 00
1.550	0.8962441382348491D 00
1.600	0.8896782929075992D 00
1.650	0.8829344674690151D 00
1.700	0.8760155136834628D 00
1.750	0.8689243688016692D 00
1.800	0.8616640550217735D 00
1.850	0.8542376788901655D 00
1.900	0.8466484306393220D 00
1.950	0.8388995834599126D 00
2.000	0.8309944927045178D 00
2.050	0.8229365950203875D 00
2.100	0.8147294074087545D 00
2.150	0.8063765262083328D 00
2.200	0.7978816260070746D 00
2.250	0.7892484584354686D 00
2.300	0.7804808505730993D 00
2.350	0.7715827055436339D 00
2.400	0.7625579971194331D 00
2.450	0.7534107722040990D 00
2.500	0.7441451472102886D 00
2.550	0.7347653068026045D 00
2.600	0.7252755020753467D 00
2.650	0.7156800486932990D 00
2.700	0.7059833249173406D 00
2.750	0.6961857695401417D 00
2.800	0.6863038797278850D 00
2.850	0.6763302087678548D 00
2.900	0.6662733637219137D 00
2.950	0.6561380029861263D 00
3.000	0.6459288337569606D 00
3.050	0.6356506094047504D 00
3.100	0.6253081267552862D 00
3.150	0.6149062232806256D 00
3.200	0.6044497742004573D 00
3.250	0.5939436894955218D 00
3.300	0.5833929108348674D 00
3.350	0.5728024084188591D 00
3.400	0.5621771777404120D 00
3.450	0.5515222362660143D 00
3.500	0.5408426200405675D 00
3.550	0.5301433802174757D 00
3.600	0.5194295795178676D 00
3.650	0.5087062886219255D 00
3.700	0.4979785824958215D 00
3.750	0.4872515366579082D 00
3.800	0.4765302233880153D 00
3.850	0.4658197078389740D 00
3.900	0.4551250443690371D 00
3.950	0.4444512721562183D 00
4.000	0.4338034116714246D 00
4.050	0.4231864604427966D 00
4.100	0.4126053890555367D 00
4.150	0.4020651371057834D 00
4.200	0.3915706090746431D 00
4.250	0.3811266702676556D 00
4.300	0.3707381426851410D 00
4.350	0.3604098009129403D 00
4.400	0.3501463680111931D 00
4.450	0.3399525114108754D 00
4.500	0.3298328388239028D 00
4.550	0.3197918941726709D 00
4.600	0.3098341535449733D 00
4.650	0.2999640211802745D 00
4.700	0.2901858254933542D 00
4.750	0.2805038151413710D 00
4.800	0.2709221551403986D 00
4.850	0.2614449230374846D 00
4.900	0.2520761051442901D 00
4.950	0.2429155978393200D 00
5.000	0.2336751789377416D 00

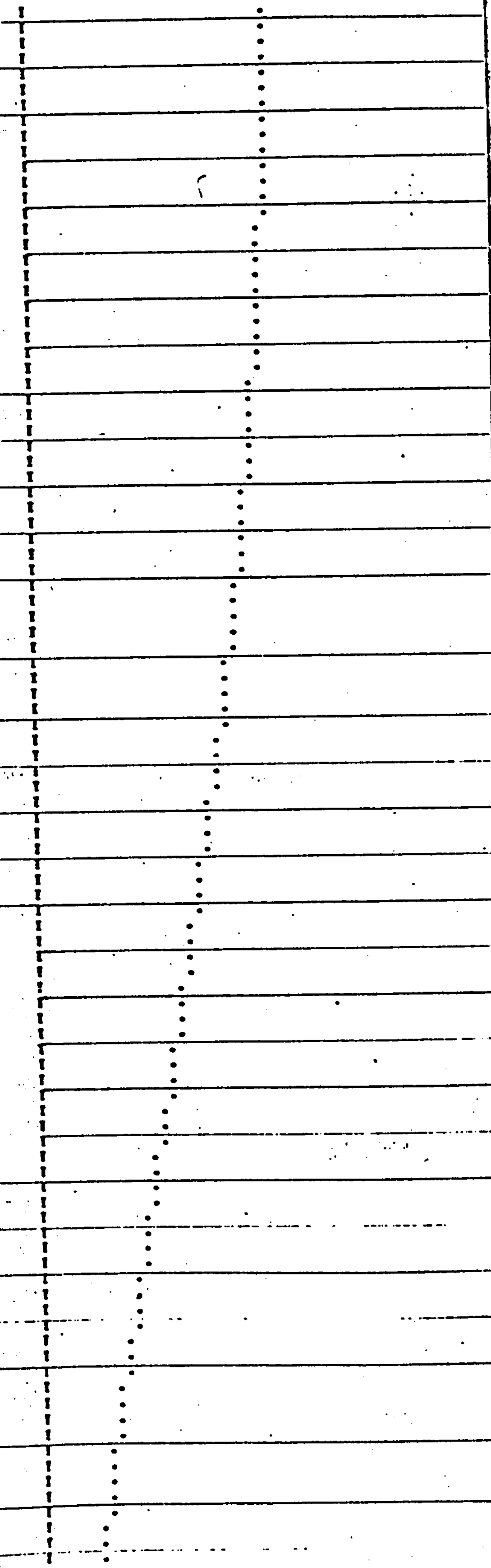

FIGURE 4.3D

ITERATION 4 WITH W_m = 5.0, UNIFORM AMPLITUDE INPUT FUNCTION

W	Amplitude
0.0	0.9999999999999980D 00
0.050	0.9997582911480016D 00
0.100	0.9990334263479521D 00
0.150	0.9978261904942027D 00
0.200	0.9961378904996749D 00
0.250	0.9939703534315111D 00
0.300	0.9913259235052782D 00
0.350	0.9882074607420088D 00
0.400	0.9846183328935682D 00
0.450	0.9805624146430513D 00
0.500	0.9760440800880807D 00
0.550	0.9710681969160728D 00
0.600	0.9656401194916848D 00
0.650	0.9597658811577999D 00
0.700	0.9534511862525232D 00
0.750	0.9467034006657659D 00
0.800	0.9395255427008200D 00
0.850	0.9319372726413781D 00
0.900	0.9239346819663434D 00
0.950	0.9155302819141610D 00
1.000	0.9067329914812494D 00
1.050	0.8975521248585880D 00
1.100	0.8879973783321009D 00
1.150	0.8780788166674331D 00
1.200	0.8678068590012550D 00
1.250	0.8571922642620137D 00
1.300	0.8462461161437859D 00
1.350	0.8349798076575778D 00
1.400	0.8234050252850624D 00
1.450	0.8115337327603648D 00
1.500	0.7993781545060454D 00
1.550	0.7865507527459677D 00
1.600	0.7742642403501840D 00
1.650	0.7613315033554051D 00
1.700	0.7481656433289882D 00
1.750	0.7347759294646886D 00
1.800	0.7211877865227111D 00
1.850	0.7074027766148007D 00
1.900	0.6934385808672942D 00
1.950	0.6793085809911760D 00
2.000	0.6650278407882430D 00
2.050	0.6506090876225129D 00
2.100	0.6360666933859715D 00
2.150	0.6214146584876911D 00
2.200	0.6066665883951811D 00
2.250	0.5918376802567046D 00
2.300	0.5769407021330161D 00
2.350	0.5619899753667301D 00
2.400	0.5469993566171775D 00
2.450	0.5315826200882511D 00
2.500	0.5169534395763084D 00
2.550	0.5019253731647357D 00
2.600	0.4869118421912621D 00
2.650	0.4719261185135894D 00
2.700	0.4569813060981673D 00
2.750	0.4420903253565968D 00
2.800	0.4272658974530862D 00
2.850	0.4125205290059676D 00
2.900	0.3978664972053786D 00
2.950	0.3833158353684546D 00
3.000	0.3688803189525517D 00
3.050	0.3545714520461635D 00
3.100	0.3404004543562899D 00
3.150	0.3263782487101045D 00
3.200	0.3125159445087825D 00
3.250	0.2988223492027373D 00
3.300	0.2853089116431652D 00
3.350	0.2719847575905394D 00
3.400	0.2588591571261740D 00
3.450	0.2459410201387059D 00
3.500	0.2332388878428910D 00
3.550	0.2207609249153897D 00
3.600	0.2085149122840947D 00
3.650	0.1965082404944284D 00
3.700	0.1847479037989183D 00
3.750	0.1732404948352379D 00
3.800	0.1619921999807705D 00
3.850	0.1510087953586205D 00
3.900	0.1402956435008699D 00
3.950	0.1298576906697397D 00
4.000	0.1196994648362101D 00
4.050	0.1098250743145212D 00
4.100	0.1002382070498643D 00
4.150	0.9094213055549150D-01
4.200	0.8193969249437420D-01
4.250	0.7323332189946510D-01
4.300	0.6482503102557660D-01
4.350	0.5671641782483787D-01
4.400	0.4890866903668531D-01
4.450	0.4140256388233629D-01
4.500	0.3419847835273019D-01
4.550	0.2729639007797941D-01
4.600	0.2069568376543083D-01
4.650	0.1439615715256578D-01
4.700	0.8396027740136753D-02
4.750	0.2693939449959348D-02
4.800	-0.2712029408739260D-02
4.850	-0.7824158281605098D-02
4.900	-0.1264507579775153D-01
4.950	-0.1717775078313896D-01
5.000	-0.2142548283785141D-01

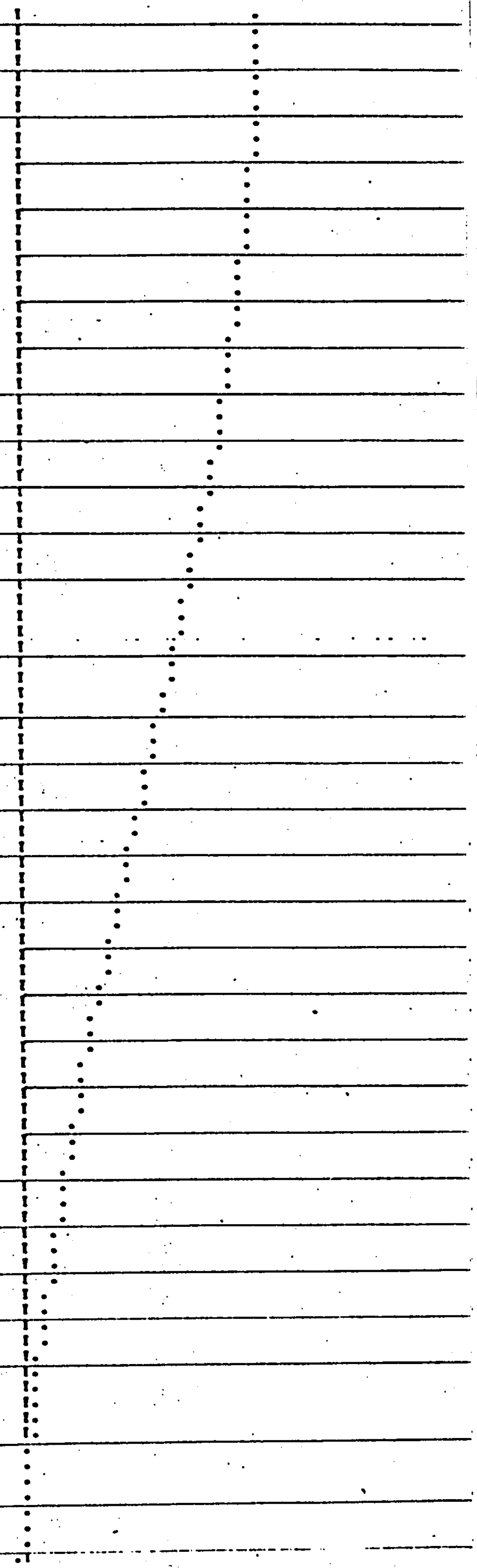

FIGURE 4.3E

ITERATION 5 WITH W_m = 5.0, UNIFORM AMPLITUDE INPUT FUNCTION

w	Amplitude
0.0	0.99999999999999980D 00
0.050	0.99984888664697670D 00
0.100	0.99939565664931600D 00
0.150	0.99864064008099900D 00
0.200	0.99758438669798070D 00
0.250	0.99622766538762290D 00
0.300	0.99457146339881180D 00
0.350	0.99261698535366610D 00
0.400	0.99036565204200760D 00
0.450	0.98781509900000430D 00
0.500	0.98497917487467780D 00
0.550	0.98184793957619450D 00
0.600	0.97842766222011350D 00
0.650	0.97472081836203330D 00
0.700	0.97073009002728570D 00
0.750	0.96645835803859920D 00
0.800	0.96190870414487010D 00
0.850	0.95708440545442600D 00
0.900	0.95198893167636960D 00
0.950	0.94662594167386060D 00
1.000	0.94099927983334590D 00
1.050	0.93511297225403380D 00
1.100	0.92897122276205650D 00
1.150	0.92257840875399160D 00
1.200	0.91593907687462910D 00
1.250	0.90905793853400780D 00
1.300	0.90193986526898450D 00
1.350	0.89458588395473670D 00
1.400	0.88701317187179080D 00
1.450	0.87921505163431170D 00
1.500	0.87120098598556670D 00
1.550	0.86297657246660110D 00
1.600	0.85454753756432190D 00
1.650	0.84591973314529890D 00
1.700	0.83709912678173780D 00
1.750	0.82809179997616560D 00
1.800	0.81890394029152030D 00
1.850	0.80954183579337180D 00
1.900	0.80001186901116030D 00
1.950	0.79032051082536140D 00
2.000	0.78047431428759890D 00
2.050	0.77047590838076450D 00
2.100	0.76034399172626900D 00
2.150	0.75007332624560250D 00
2.200	0.73967473078338920D 00
2.250	0.72915907469918320D 00
2.300	0.71852127143525240D 00
2.350	0.70778027206760130D 00
2.400	0.69693905884748900D 00
2.450	0.68600463874070390D 00
2.500	0.67498403697180540D 00
2.550	0.66388429058054440D 00
2.600	0.65271244199762480D 00
2.650	0.64147553264692300D 00
2.700	0.63018059658123100D 00
2.750	0.61883465415851560D 00
2.800	0.60744470576563750D 00
2.850	0.59601772559636360D 00
2.900	0.58456065549043630D 00
2.950	0.57308039884034250D 00
3.000	0.56158301457247270D 00
3.050	0.55007771120870250D 00
3.100	0.53856884101540500D 00
3.150	0.52706389424539040D 00
3.200	0.51556949347925730D 00
3.250	0.50409218807190690D 00
3.300	0.49263844871002080D 00
3.350	0.48121466208609460D 00
3.400	0.46982712569446680D 00
3.450	0.45848204275461010D 00
3.500	0.44718551726678220D 00
3.550	0.43594354920493500D 00
3.600	0.42476202985160810D 00
3.650	0.41364673727932970D 00
3.700	0.40260333198285360D 00
3.750	0.39163735266635320D 00
3.800	0.38075421218948770D 00
3.850	0.36995919367604820D 00
3.900	0.35925744678865710D 00
3.950	0.34865398417280220D 00
4.000	0.33815367807323450D 00
4.050	0.32776125712555210D 00
4.100	0.31748130332555740D 00
4.150	0.30731824917873420D 00
4.200	0.29727637503197860D 00
4.250	0.28735980658945350D 00
4.300	0.27757251261423030D 00
4.350	0.26791830281711630D 00
4.400	0.25840082593384320D 00
4.450	0.24902356799155020D 00
4.500	0.23978985076525130D 00
4.550	0.23070283042473730D 00
4.600	0.22176549637213240D 00
4.650	0.21298067027007290D 00
4.700	0.20435100526025320D 00
4.750	0.19587898537183720D 00
4.800	0.18756692511900610D 00
4.850	0.17941696928667370D 00
4.900	0.17143109290321160D 00
4.950	0.16361110139866180D 00
5.000	0.15595863094696620D 00

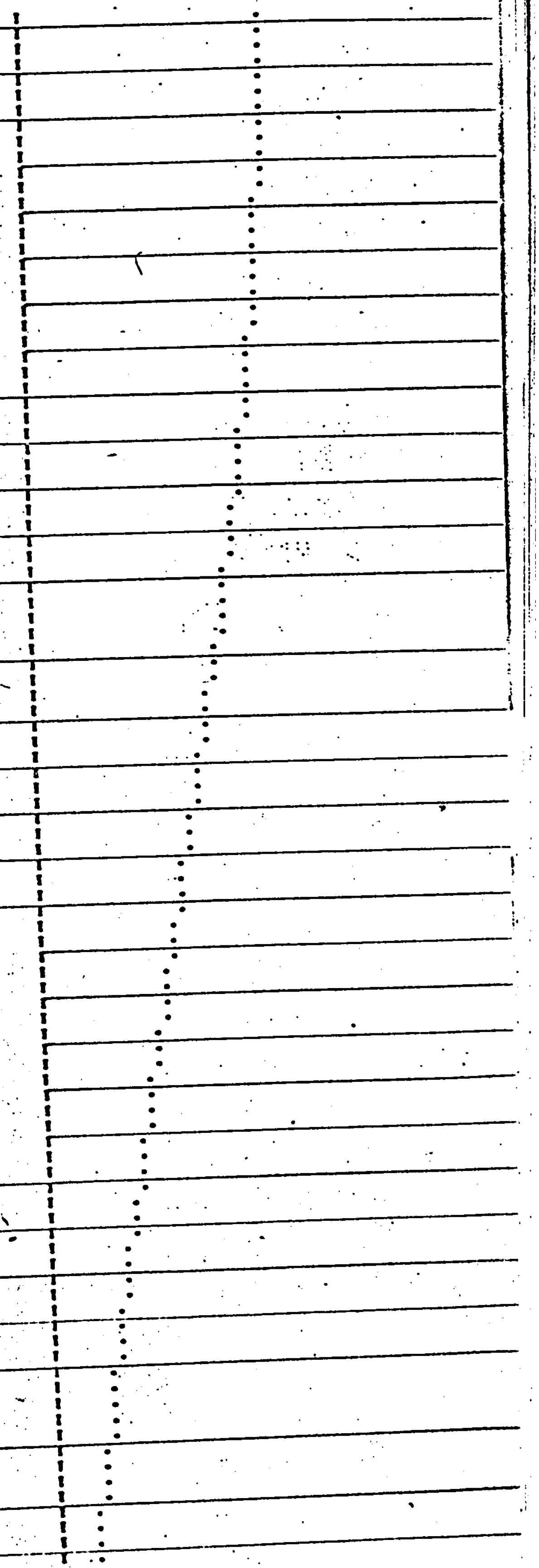

FIGURE 4.3F

ITERATION 121 WITH W_m = 5.0, UNIFORM AMPLITUDE INPUT FUNCTION

w	Amplitude
0.0	0.599999999999999800 00
0.050	0.999804049243465900 00
0.100	0.999216554997418500 00
0.150	0.998237942492129200 00
0.200	0.996869179084377270 00
0.250	0.995111556854297600 00
0.300	0.992966734173835000 00
0.350	0.990436733548210400 00
0.400	0.987523938994873900 00
0.450	0.984231092951271400 00
0.500	0.980561292720400900 00
0.550	0.976517986459031400 00
0.600	0.972104968714666700 00
0.650	0.967326375518200800 00
0.700	0.962186679039721000 00
0.750	0.956694688185551300 00
0.800	0.950843510555610900 00
0.850	0.944650609540289500 00
0.900	0.938117733617083600 00
0.950	0.931250940800763760 00
1.000	0.924056584536455800 00
1.050	0.916541305493130100 00
1.100	0.908712023140467900 00
1.150	0.900575926881413300 00
1.200	0.892140466898181100 00
1.250	0.883413344677482100 00
1.300	0.874402503236186600 00
1.350	0.865116117062197400 00
1.400	0.855562581725716400 00
1.450	0.845750503596463400 00
1.500	0.835688688422769200 00
1.550	0.825386130888786600 00
1.600	0.814852003066370800 00
1.650	0.804095643038444700 00
1.700	0.793126543290922600 00
1.750	0.781954338550472300 00
1.800	0.770588795E8559320 00
1.850	0.759039798688863700 00
1.900	0.747317338556543000 00
1.950	0.735431501088130400 00
2.000	0.723392454015915500 00
2.050	0.711210434890398600 00
2.100	0.698895738734825100 00
2.150	0.686458705688391000 00
2.200	0.673905706865581120 00
2.250	0.661255914098110860 00
2.300	0.648517404163354500 00
2.350	0.635694895631985600 00
2.400	0.622801956659513330 00
2.450	0.609846064000622290 00
2.500	0.596846398581895000 00
2.550	0.583804273028023700 00
2.600	0.570732880350373900 00
2.650	0.557642342350059300 00
2.700	0.544542694292005500 00
2.750	0.531443873765170900 00
2.800	0.518355709750677900 00
2.850	0.505287911912552300 00
2.900	0.492250060124069700 00
2.950	0.479251559424555700 00
3.000	0.466301804165814000 00
3.050	0.453406982012060600 00
3.100	0.440584603300587900 00
3.150	0.427834936760650200 00
3.200	0.415169416642103800 00
3.250	0.402596443718538500 00
3.300	0.390124215275671800 00
3.350	0.377760717334886400 00
3.400	0.365513717225566800 00
3.450	0.353390756542731600 00
3.500	0.341399144413855900 00
3.550	0.329545951222109400 00
3.600	0.317838002652643900 00
3.650	0.306281874151874000 00
3.700	0.294883885777068700 00
3.750	0.283650097444858300 00
3.800	0.272586326458252370 00
3.850	0.261698034187347100 00
3.900	0.250996054128967400 00
3.950	0.240468805834250100 00
4.000	0.230137529968404400 00
4.050	0.220001135743249800 00
4.100	0.210063763232698800 00
4.150	0.200329269057425800 00
4.200	0.190801225325159800 00
4.250	0.181482918977619000 00
4.300	0.172377351543639000 00
4.350	0.163487239295961100 00
4.400	0.154815013806054900 00
4.450	0.146362822896456100 00
4.500	0.138132531975791100 00
4.550	0.130125725766559350 00
4.600	0.122343710403895750 00
4.650	0.114787515502723480 00
4.700	0.107457899015521700 00
4.750	0.100355346377375000 00
4.800	0.934800760884400800-01
4.850	0.868320515668725000-01
4.900	0.804109657574882000-01
4.950	0.742162656548537000-01
5.000	0.682471471349581000-01

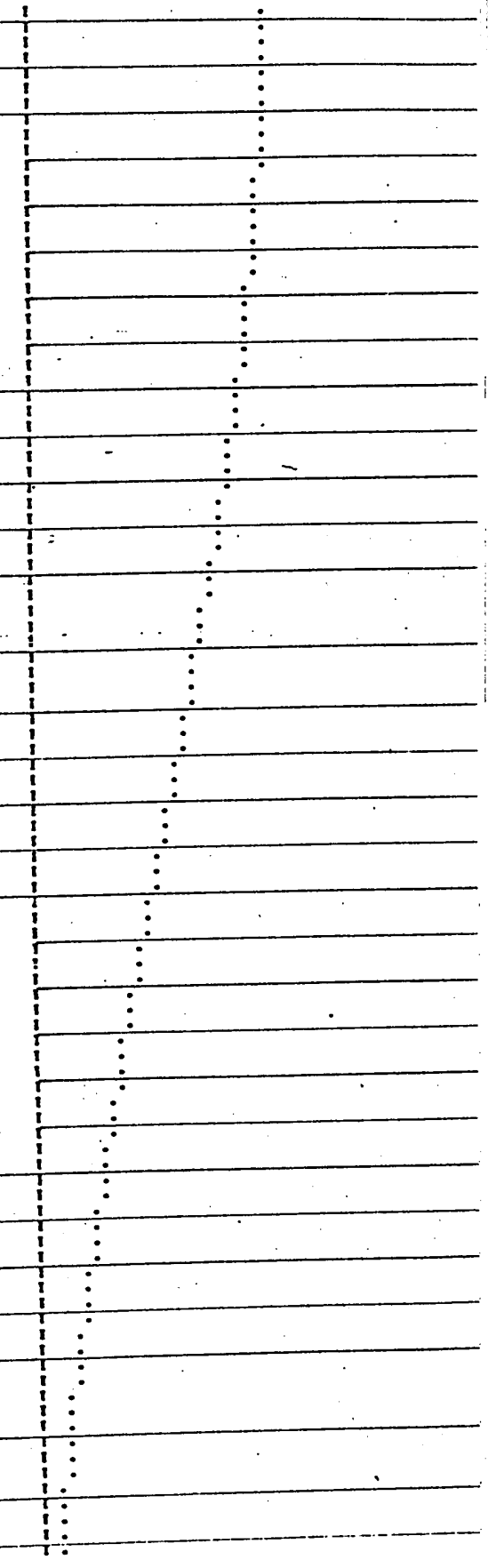

FIGURE 4.3G

ITERATION 122 WITH W_m = 5.0, UNIFORM AMPLITUDE INPUT FUNCTION

W	Amplitude
0.0	0.9999999999999998D 00
0.050	0.9998040924834659D 00
0.100	0.9992165549974185D 00
0.150	0.9982379424921292D 00
0.200	0.9968691790837727D 00
0.250	0.9951115568542976D 00
0.300	0.9929667341738350D 00
0.350	0.9904367335482104D 00
0.400	0.9875239389948739D 00
0.450	0.9842310929512714D 00
0.500	0.9805612927204039D 00
0.550	0.9765179864590314D 00
0.600	0.9721049687146667D 00
0.650	0.9673263755182086D 00
0.700	0.9621866790397210D 00
0.750	0.9566906818155513D 00
0.800	0.9508435105556109D 00
0.850	0.9446506095402895D 00
0.900	0.9381177336170836D 00
0.950	0.9312509408076376D 00
1.000	0.9240565845364558D 00
1.050	0.9165413054931301D 00
1.100	0.9087120231404679D 00
1.150	0.9005759268814133D 00
1.200	0.8921404668981811D 00
1.250	0.8834133446774821D 00
1.300	0.8744025032361866D 00
1.350	0.8651161170621974D 00
1.400	0.8555623817857164D 00
1.450	0.8457505035964634D 00
1.500	0.8356886884227692D 00
1.550	0.8253861309887860D 00
1.600	0.8148520030663708D 00
1.650	0.8040956430384447D 00
1.700	0.7931265432909226D 00
1.750	0.7819543385504723D 00
1.800	0.7705887958559932D 00
1.850	0.7590397986986379D 00
1.900	0.7473173385565430D 00
1.950	0.7354315010881304D 00
2.000	0.7233924540159155D 00
2.050	0.7112104348903986D 00
2.100	0.6988957387348251D 00
2.150	0.6864587056883910D 00
2.200	0.6739097086558112D 00
2.250	0.6612591409811086D 00
2.300	0.6485174041633545D 00
2.350	0.6356948956319856D 00
2.400	0.6228019965991333D 00
2.450	0.6098459060062229D 00
2.500	0.5968463985818950D 00
2.550	0.5838042730280237D 00
2.600	0.5707328803503739D 00
2.650	0.5576423423500993D 00
2.700	0.5445426942920055D 00
2.750	0.5314438737651079D 00
2.800	0.5183557097506779D 00
2.850	0.5052879119125523D 00
2.900	0.4922500601240697D 00
2.950	0.4792515942455557D 00
3.000	0.4663018041658140D 00
3.050	0.4534098201206066D 00
3.100	0.4405846033005879D 00
3.150	0.4278345367606502D 00
3.200	0.4151694166421038D 00
3.250	0.4025964437185385D 00
3.300	0.3901242152756718D 00
3.350	0.3777607173348864D 00
3.400	0.3655137172255668D 00
3.450	0.3533907565427316D 00
3.500	0.3413991444138559D 00
3.550	0.3295459512221094D 00
3.600	0.3178380026526439D 00
3.650	0.3062818741518740D 00
3.700	0.2948838857770687D 00
3.750	0.2836509744489583D 00
3.800	0.2725863045829237D 00
3.850	0.2616980341873471D 00
3.900	0.2509905412896704D 00
3.950	0.2404688058342501D 00
4.000	0.2301375299680494D 00
4.050	0.2200011357432498D 00
4.100	0.2100637632326838D 00
4.150	0.2003292690574258D 00
4.200	0.1908012253251998D 00
4.250	0.1814829189776190D 00
4.300	0.1723773515436390D 00
4.350	0.1634872392959611D 00
4.400	0.1548150138065049D 00
4.450	0.1463628228964561D 00
4.500	0.1381325319757911D 00
4.550	0.1301257257665935D 00
4.600	0.1223437104038975D 00
4.650	0.1147875155072348D 00
4.700	0.1074578990155217D 00
4.750	0.1003553463773725D 00
4.800	0.9348007808844080D-01
4.850	0.8683205156687250D-01
4.900	0.8041096575748820D-01
4.950	0.7421626565485320D-01
5.000	0.6824714713495810D-01

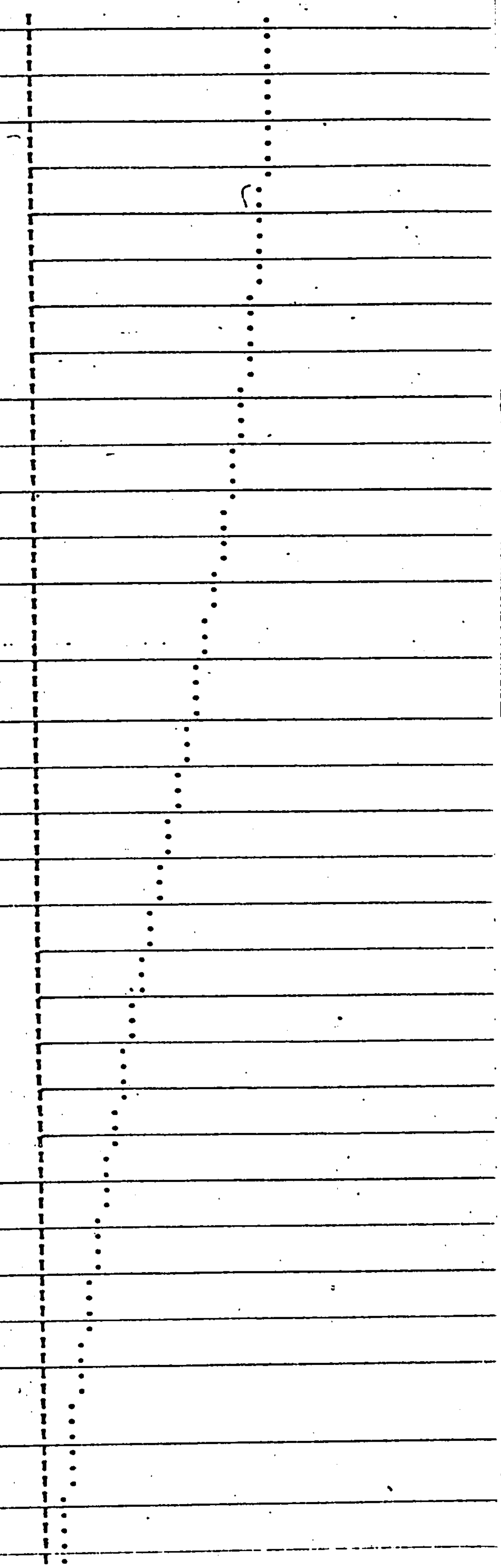

FIGURE 4.3H

ITERATION 414 WITH W_m = 10.0, UNIFORM AMPLITUDE INPUT FUNCTION

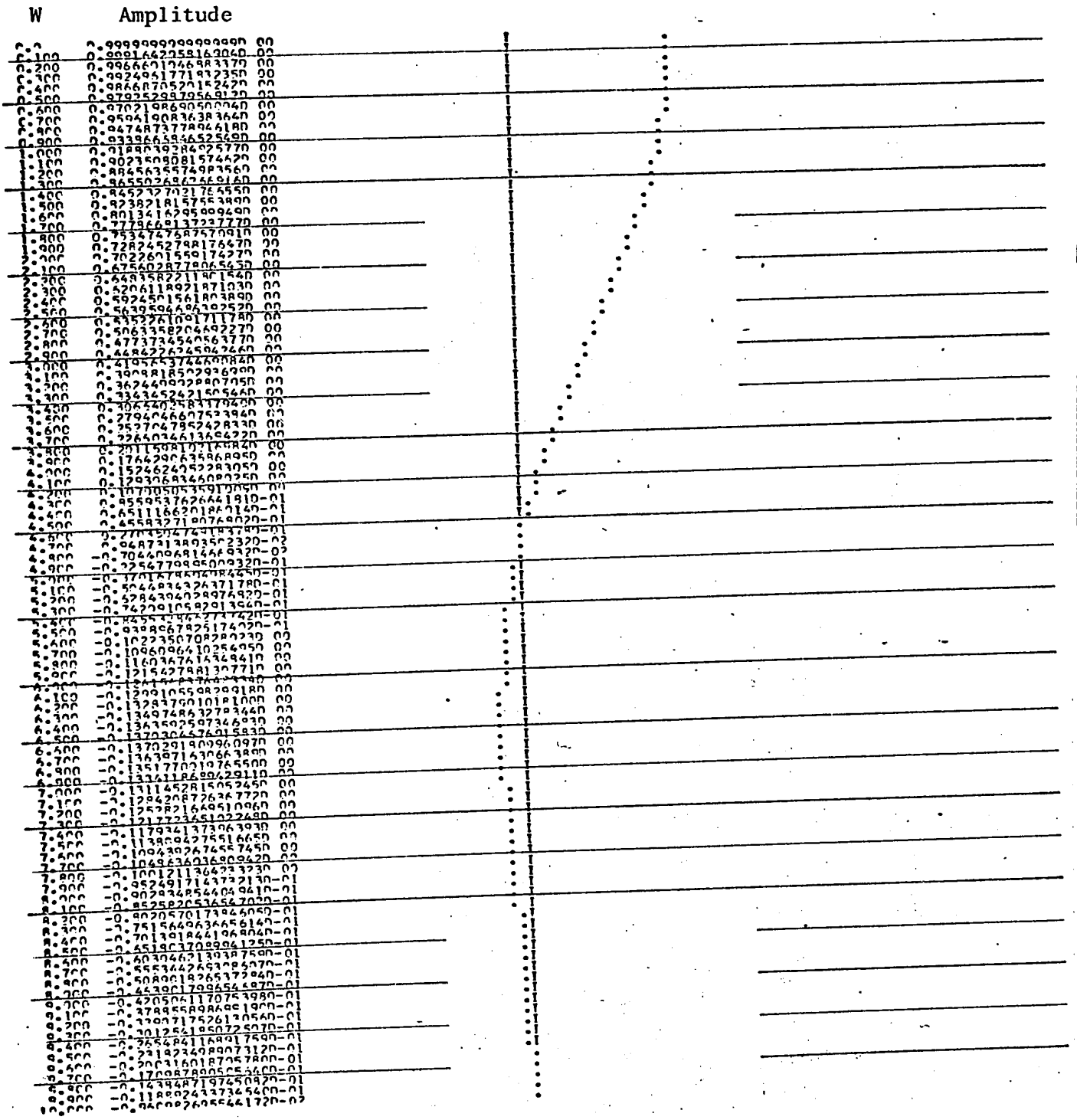

FIGURE 4.4A

ITERATION 415 WITH W_m = 10.0, UNIFORM AMPLITUDE INPUT FUNCTION

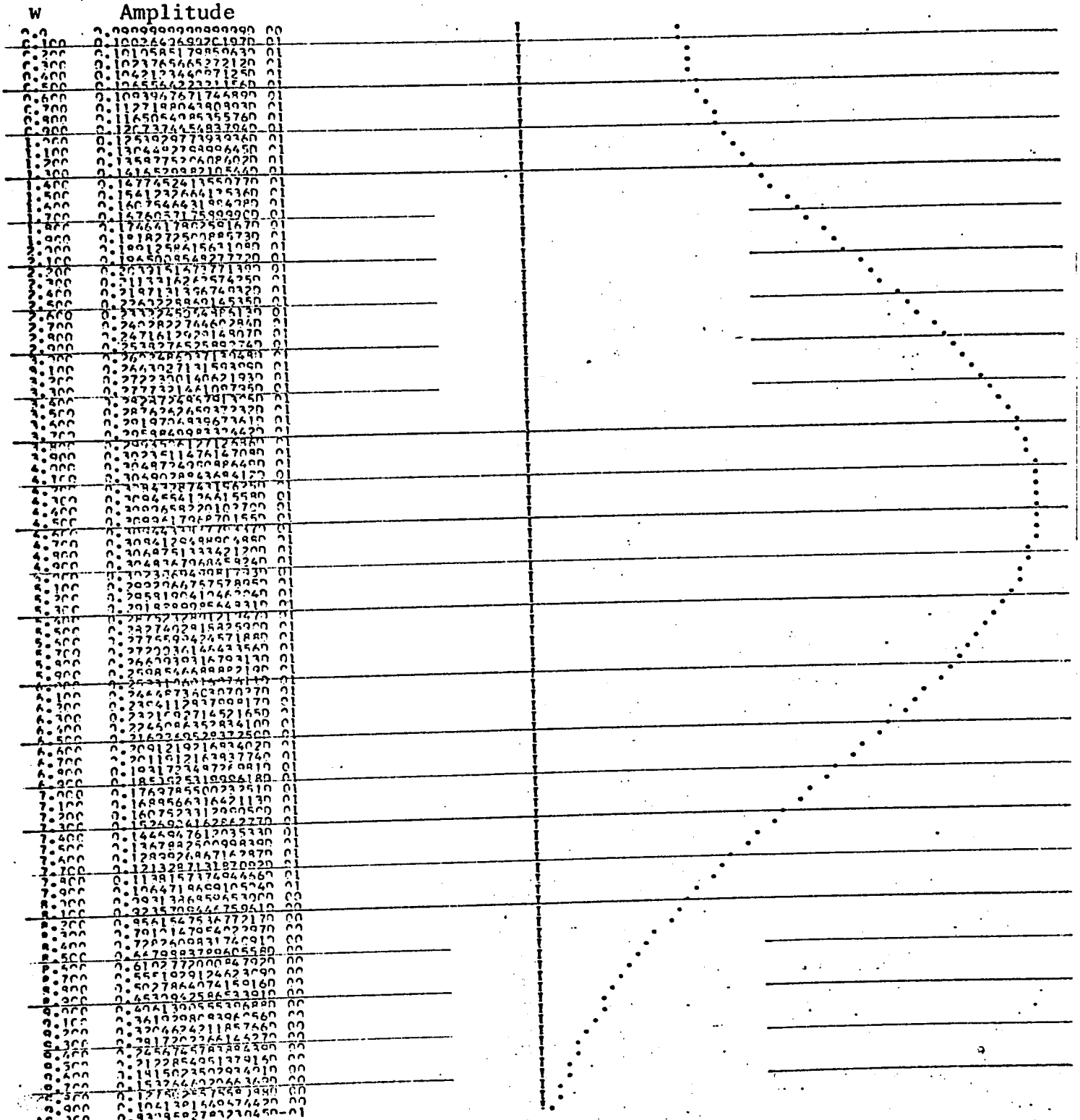

FIGURE 4.4B

ITERATION 416 WITH W_m = 10.0, UNIFORM AMPLITUDE INPUT FUNCTION

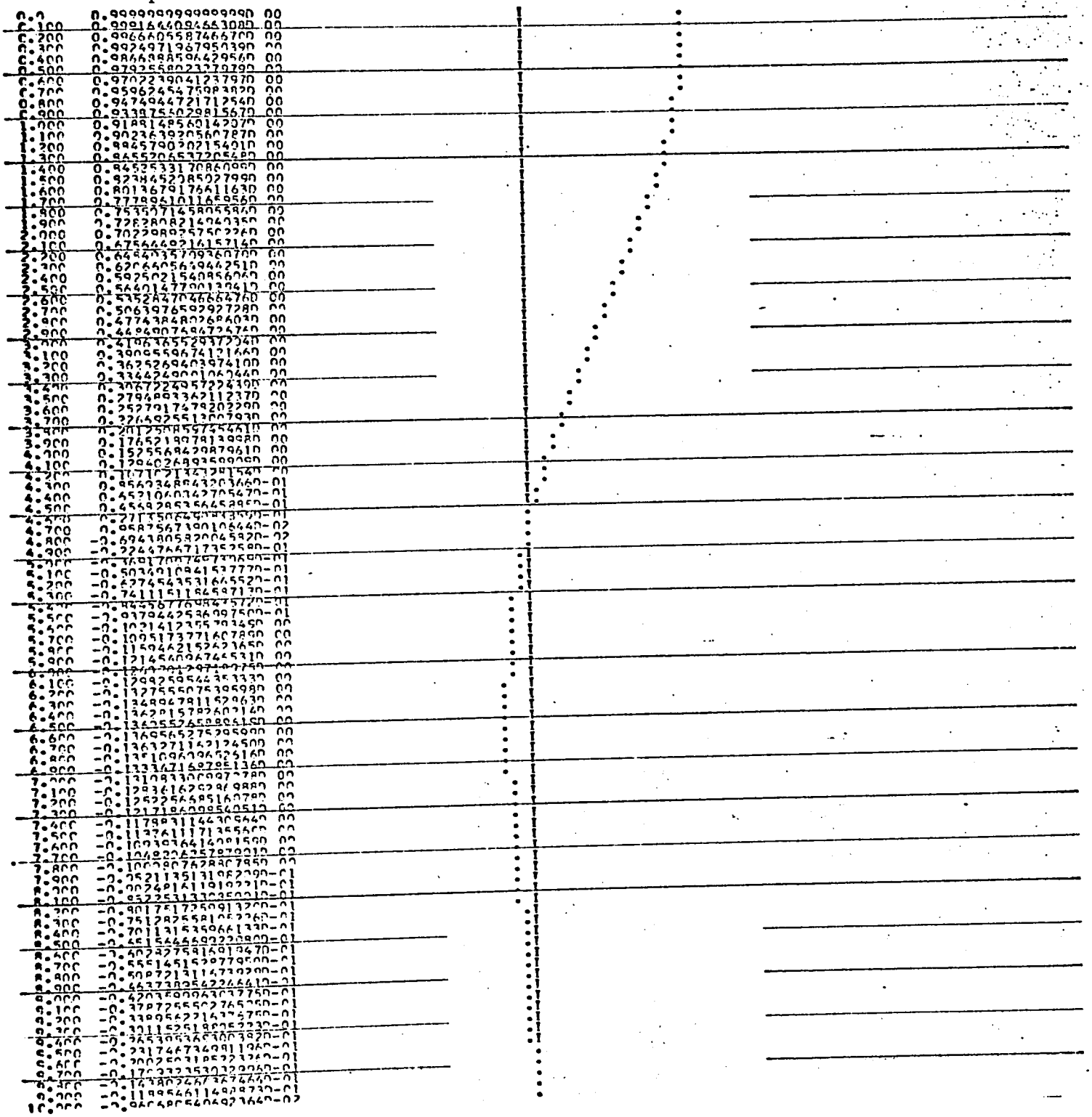

FIGURE 4.4C

ITERATION 417 WITH W_m = 10.0, UNIFORM AMPLITUDE INPUT FUNCTION

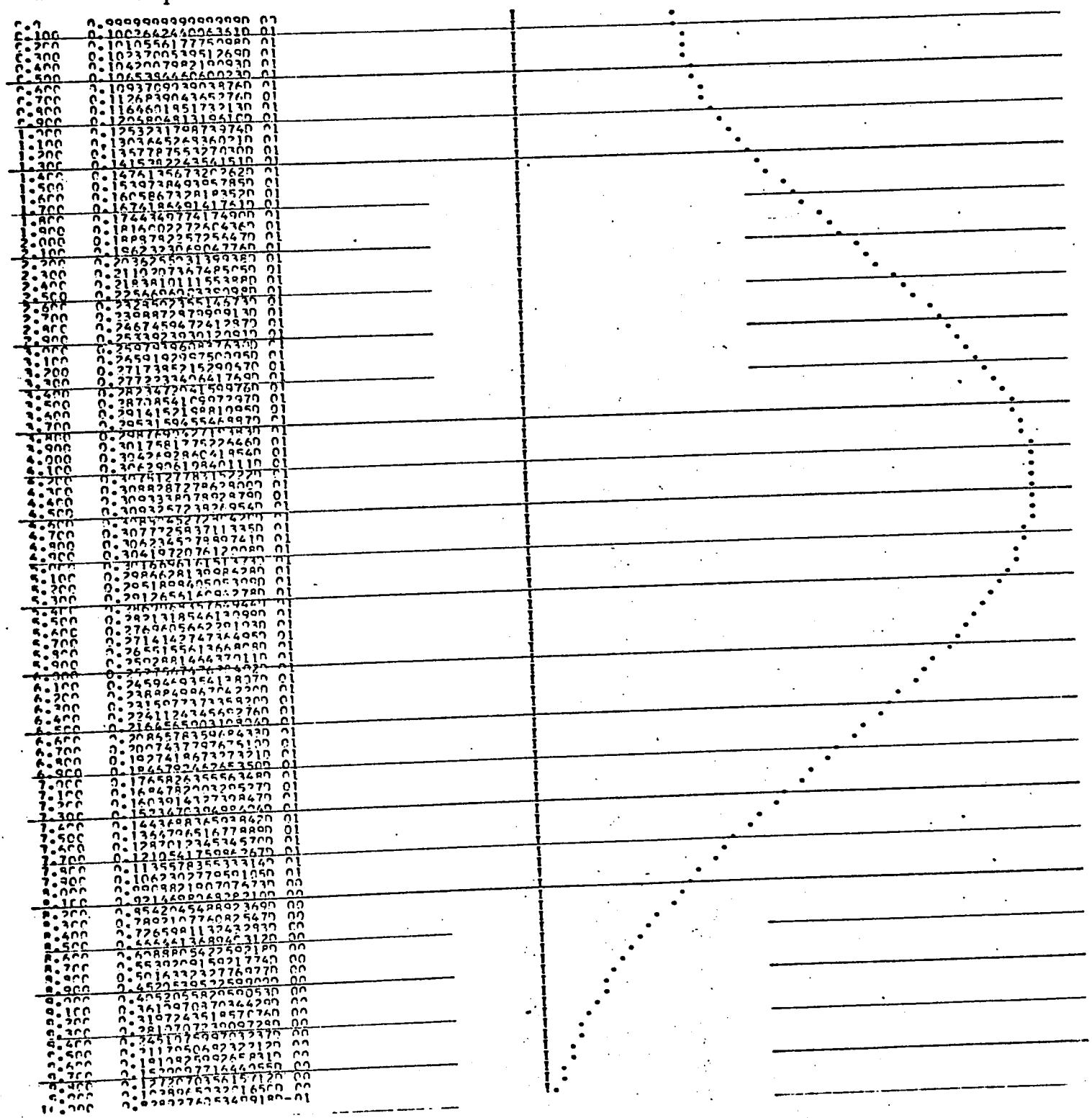

FIGURE 4.4D

ITERATION O WITH W_m = 1.0 AND (0, 1) MODE AS INPUT FUNCTION

W	Amplitude
0.0	0.9999999999999800D 00
0.010	0.9997873453019190D 00
0.020	0.9991493967815930D 00
0.030	0.9980862011596509D 00
0.040	0.9965978362999443D 00
0.050	0.9946844112037618D 00
0.060	0.9923460660017473D 00
0.070	0.9895829719434707D 00
0.080	0.9863953313846938D 00
0.090	0.9827833777723751D 00
0.100	0.9787473756272997D 00
0.110	0.9742876205244175D 00
0.120	0.9694044390709068D 00
0.130	0.9640981888190370D 00
0.140	0.9583692585539189D 00
0.150	0.9522180676359859D 00
0.160	0.9456450659848210D 00
0.170	0.9386507367996692D 00
0.180	0.9312355904499314D 00
0.190	0.9234001705737260D 00
0.200	0.9151450509692471D 00
0.210	0.9064708361657880D 00
0.220	0.8973781613788476D 00
0.230	0.8878676924629569D 00
0.240	0.8779401258621819D 00
0.250	0.8675961835584293D 00
0.260	0.8568366380174450D 00
0.270	0.8456622621325246D 00
0.280	0.8340738791660269D 00
0.290	0.8220723768859120 00
0.300	0.8096585165160983D 00
0.310	0.7968333264464301D 00
0.320	0.7835977011819565D 00
0.330	0.7699526152797717D 00
0.340	0.7558990660597568D 00
0.350	0.7414380825403707D 00
0.360	0.7265707235602518D 00
0.370	0.7112980776995842D 00
0.380	0.6956212631992768D 00
0.390	0.6795414278779474D 00
0.400	0.6630597490466736D 00
0.410	0.6461774334216521D 00
0.420	0.6288957170345355D 00
0.430	0.6112158651407191D 00
0.440	0.5931391721254255D 00
0.450	0.5746669614076087D 00
0.460	0.5558005853413724D 00
0.470	0.5365414251173583D 00
0.480	0.5168908906567251D 00
0.490	0.4968504205100232D 00
0.500	0.4764214817486764D 00
0.510	0.4556055698564592D 00
0.520	0.4344042286185670D 00
0.530	0.4128189500085064D 00
0.540	0.3908513740729622D 00
0.550	0.3685030888145770D 00
0.560	0.3457757300726564D 00
0.570	0.3226709614018061D 00
0.580	0.2991904739435560D 00
0.590	0.2753359863258917D 00
0.600	0.2511092444858114D 00
0.610	0.2265120215898090D 00
0.620	0.2015461178774131D 00
0.630	0.1762133605326472D 00
0.640	0.1505156035685819D 00
0.650	0.1244547275898293D 00
0.660	0.9803263985314120D-01
0.670	0.7125127392600380D-01
0.680	0.4411258964328470D-01
0.690	0.1661857294200670D-01
0.700	-0.1122876428592802D-01
0.710	-0.3942738434275050D-01
0.720	-0.6797522387594830D-01
0.730	-0.9687019403106320D-01
0.740	-0.1261101806065500D 00
0.750	-0.1556930442103621D 00
0.760	-0.1856166206185156D 00
0.770	-0.2158787199353579D 00
0.780	-0.2464771287558029D 00
0.790	-0.2774096983292809D 00
0.800	-0.3086738957255470D 00
0.810	-0.3402677039022441D 00
0.820	-0.3721887213742940D 00
0.830	-0.4044346133849989D 00
0.840	-0.4370030210789317D 00
0.850	-0.4698915621765513D 00
0.860	-0.5030978310505484D 00
0.870	-0.5366193989038949D 00
0.880	-0.5704538139696013D 00
0.890	-0.6045986015921402D 00
0.900	-0.6390512646105810D 00
0.910	-0.6738092833433266D 00
0.920	-0.7088701158745222D 00
0.930	-0.7442311982221112D 00
0.940	-0.7798899445274322D 00
0.950	-0.8158437472465298D 00
0.960	-0.8520899773429053D 00
0.970	-0.8884255944819861D 00
0.980	-0.9254490972270099D 00
0.990	-0.9625566232365680D 00
1.000	-0.9999458496357620D 00

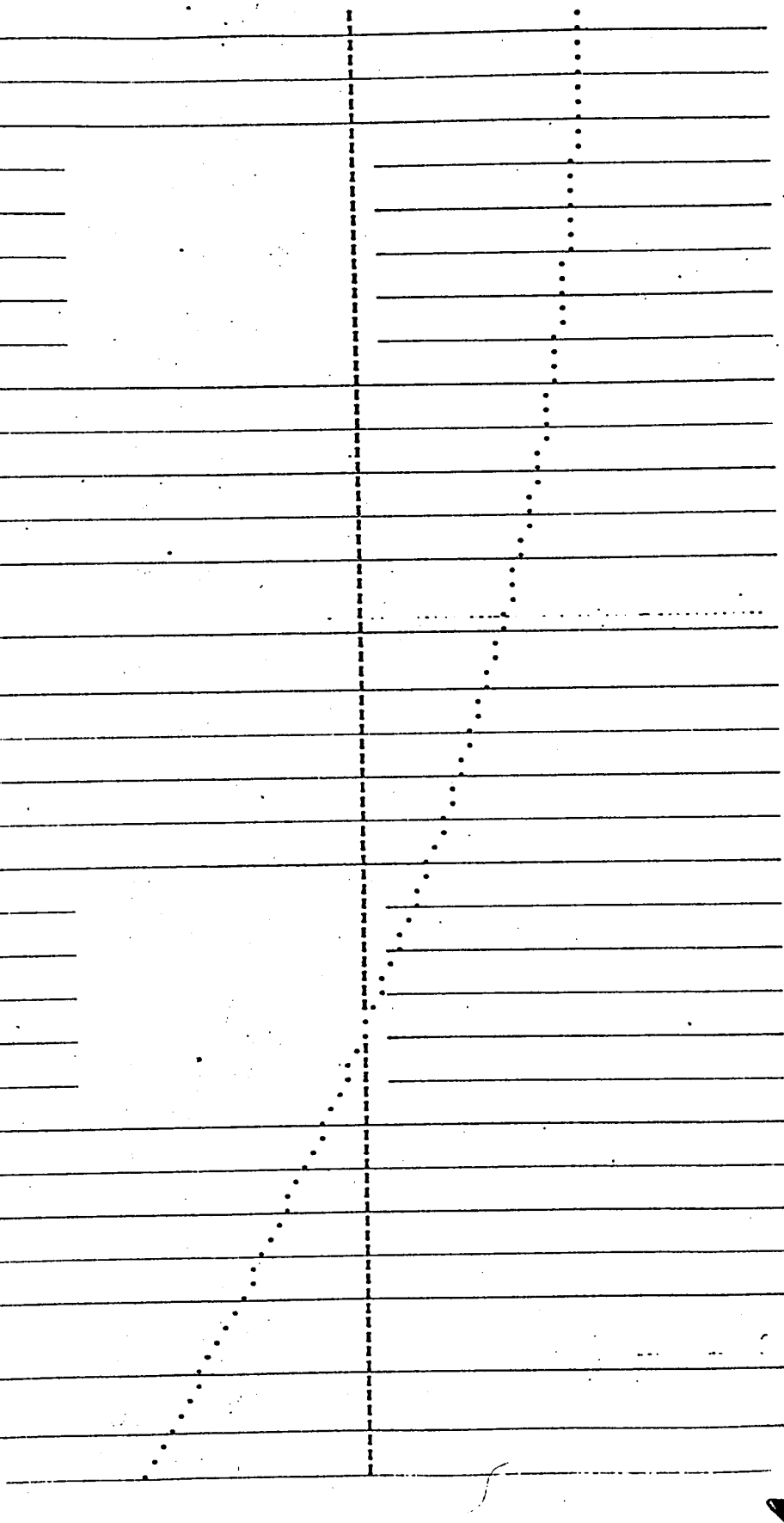

FIGURE 4.5A

ITERATION 1 WITH W_m = 1.0 and (0, 1) MODE AS INPUT FUNCTION

w	Amplitude
0.0	0.99999999999999800 00
0.010	0.99978734530191680 00
0.020	0.99914939678158870 00
0.030	0.99808620115954870 00
0.040	0.99659783620999650 00
0.050	0.99468441120376380 00
0.060	0.99234606600174880 00
0.070	0.98958297194347070 00
0.080	0.98639533136469400 00
0.090	0.98279337777237660 00
0.100	0.97878737562730150 00
0.110	0.97428762052442300 00
0.120	0.96940443907091530 00
0.130	0.96409818888191420 00
0.140	0.95836925855392760 00
0.150	0.95221806763599850 00
0.160	0.94564506659849430 00
0.170	0.93865073679968810 00
0.180	0.93123559044995200 00
0.190	0.92340017057375020 00
0.200	0.91514505096926840 00
0.210	0.90647083616531550 00
0.220	0.89737816137887870 00
0.230	0.88786769246299200 00
0.240	0.87794012586221940 00
0.250	0.86759618855846900 00
0.260	0.85683663801749070 00
0.270	0.84566226213257530 00
0.280	0.83407387916607880 00
0.290	0.82207233768664650 00
0.300	0.80965851651616180 00
0.310	0.79683332444469890 00
0.320	0.78359770118202830 00
0.330	0.76995261527984570 00
0.340	0.75589906605983120 00
0.350	0.74143808254045760 00
0.360	0.72657072356034220 00
0.370	0.71129807769967460 00
0.380	0.69562126319937410 00
0.390	0.67954142787804490 00
0.400	0.66305974904578990 00
0.410	0.64617743342177200 00
0.420	0.62889571703445870 00
0.430	0.61121586514084560 00
0.440	0.59313917212555920 00
0.450	0.57466696140774700 00
0.460	0.55580058534187030 00
0.470	0.53654142511751330 00
0.480	0.51689089065688710 00
0.490	0.49685042051019020 00
0.500	0.47642148174884720 00
0.510	0.45560556985664450 00
0.520	0.43440620861875730 00
0.530	0.41281895000870000 00
0.540	0.39085137407316710 00
0.550	0.36850308881478800 00
0.560	0.34577573007287090 00
0.570	0.32267096140203310 00
0.580	0.29919047394878710 00
0.590	0.27533598632613020 00
0.600	0.25110924446605920 00
0.610	0.22651202159007040 00
0.620	0.20154611787767980 00
0.630	0.17621336053292270 00
0.640	0.15051540154886660 00
0.650	0.12445472759012220 00
0.660	0.98032639853440700-01
0.670	0.71251273926312400-01
0.680	0.44112509643608280-01
0.690	0.16618572942334770-01
0.700	-0.11228764285585670-01
0.710	-0.39427384342406310-01
0.720	-0.67975223875590300-01
0.730	-0.96870194030699000-01
0.740	-0.12611018060617170 00
0.750	-0.15569304420997840 00
0.760	-0.18561662041811710 00
0.770	-0.21587871993495380 00
0.780	-0.24647712875538860 00
0.790	-0.27740950832885810 00
0.800	-0.30867389572510980 00
0.810	-0.34026770380179730 00
0.820	-0.37218872213738360 00
0.830	-0.40443461384533900 00
0.840	-0.43700302107845250 00
0.850	-0.46989156217606280 00
0.860	-0.50309733105004710 00
0.870	-0.53661939890338270 00
0.880	-0.57045381394907550 00
0.890	-0.60459860159160050 00
0.900	-0.63905126461002920 00
0.910	-0.67380928334276890 00
0.920	-0.70887011587395490 00
0.930	-0.74423119922152740 00
0.940	-0.77988994452683850 00
0.950	-0.81584374724592560 00
0.960	-0.85208997134228580 00
0.970	-0.88862594448135570 00
0.980	-0.92544909722636690 00
0.990	-0.96255662323591320 00
1.000	-0.99994584946290760 00

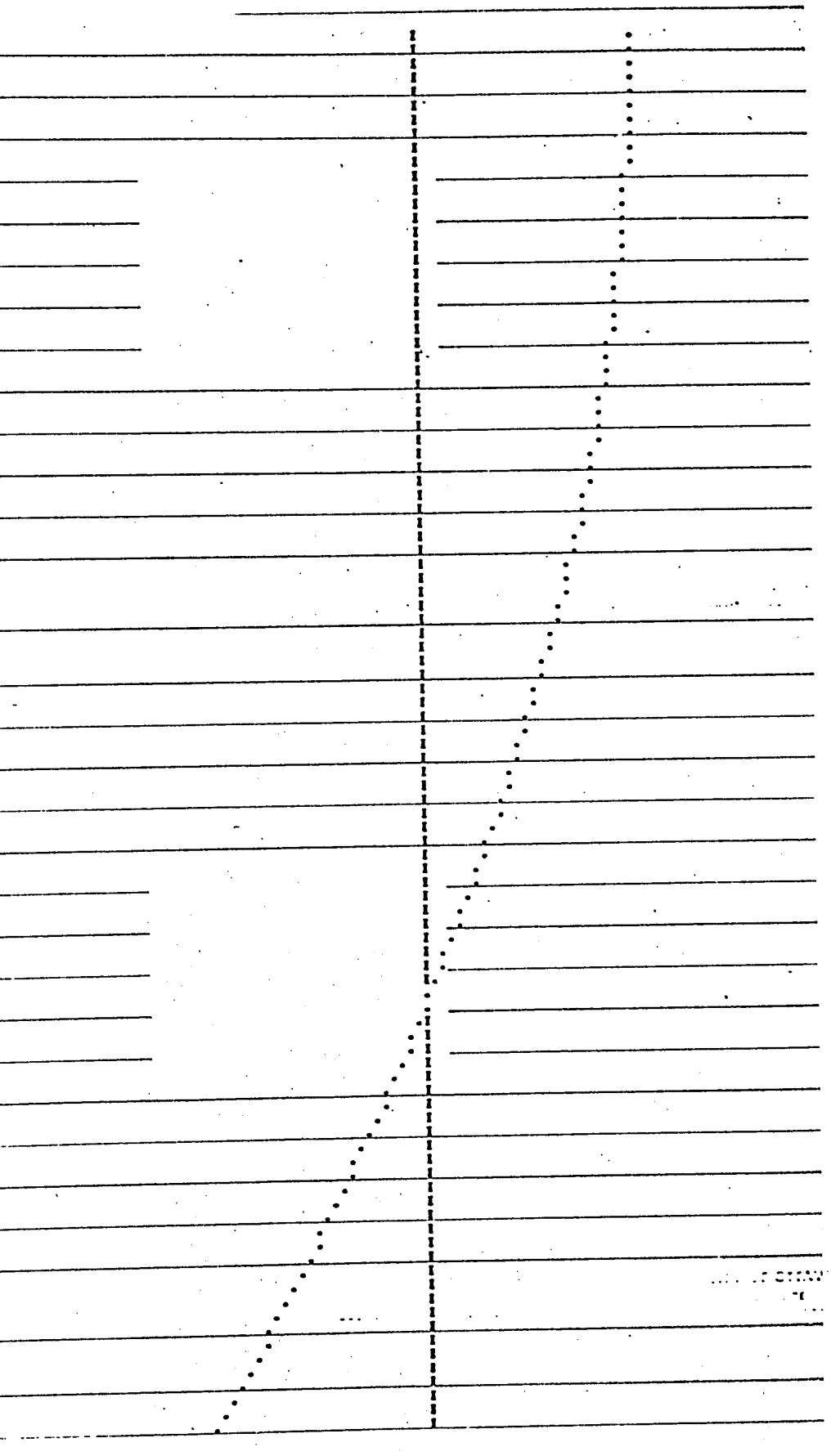

FIGURE 4.5B

ITERATION 2 WITH W_m = 1.0 AND (0, 1) MODE AS INPUT FUNCTION

W	Amplitude
0.0	0.999999979999980D 00
0.010	0.999787931928540D 00
0.020	0.999151743245870D 00
0.030	0.998091480539981 1D 00
0.040	0.996607221456068 6D 00
0.050	0.994699074688786 2D 00
0.060	0.992367179974539 2D 00
0.070	0.989611708081136 3D 00
0.080	0.986432860795069 6D 00
0.090	0.982830870906548 0D 00
0.100	0.978806002192198 9D 00
0.110	0.974358549395449 1D 00
0.120	0.969488038204655 3D 00
0.130	0.964197225228904 3D 00
0.140	0.958484097971507 6D 00
0.150	0.952349874801201 7D 00
0.160	0.945795004921108 3D 00
0.170	0.938819968335329 9D 00
0.180	0.931425275813304 1D 00
0.190	0.923611468851866 6D 00
0.200	0.915379119635007 8D 00
0.210	0.906728830991387 8D 00
0.220	0.897661236349539 5D 00
0.230	0.888176999690845 0D 00
0.240	0.878276915500186 0D 00
0.250	0.867961408714373 6D 00
0.260	0.857231534668308 1D 00
0.270	0.846087979038864 0D 00
0.280	0.834531557786557 7D 00
0.290	0.822563117094929 2D 00
0.300	0.810183533307694 3D 00
0.310	0.797393712863679 4D 00
0.320	0.784194592229507 9D 00
0.330	0.770587137830023 5D 00
0.340	0.756572345976577 6D 00
0.350	0.742151242793008 3D 00
0.360	0.727324884139454 1D 00
0.370	0.712094355533982 4D 00
0.380	0.696460772071937 7D 00
0.390	0.680425278343214 3D 00
0.400	0.663989048347231 4D 00
0.410	0.647153285405607 2D 00
0.420	0.629919222071804 3D 00
0.430	0.612288120047646 6D 00
0.440	0.594261270071667 6D 00
0.450	0.575839991842290 2D 00
0.460	0.557025439100884 5D 00
0.470	0.537819573579663 5D 00
0.480	0.518223216807494 7D 00
0.490	0.498237998097525 3D 00
0.500	0.477865380394740 3D 00
0.510	0.457106854976605 9D 00
0.520	0.435963941342440 5D 00
0.530	0.414438187100608 4D 00
0.540	0.392531167853757 9D 00
0.550	0.370244487081896 1D 00
0.560	0.347579776023437 1D 00
0.570	0.324538693554194 9D 00
0.580	0.301122926064353 7D 00
0.590	0.277334187333342 1D 00
0.600	0.253174218402762 5D 00
0.610	0.228644787447254 1D 00
0.620	0.203747689643357 4D 00
0.630	0.178484747036415 9D 00
0.640	0.152857809405456 1D 00
0.650	0.126868749126106 8D 00
0.660	0.100519471031573 3D 00
0.670	0.738119D2271646 50D-01
0.680	0.467479971697564 6D-01
0.690	0.193297360781108 7D-01
0.700	-0.844087476907706 0D-02
0.710	-0.365618034042609 8D-01
0.720	-0.650309922772058 0D-01
0.730	-0.938463584073858 0D-01
0.740	-0.123005793583672 0D 00
0.750	-0.152507164293994 5D 00
0.760	-0.182348312336466 8D 00
0.770	-0.212527054526193 9D 00
0.780	-0.243041183083516 8D 00
0.790	-0.273888465752250 6D 00
0.800	-0.305066645964977 5D 00
0.810	-0.336573443010170 7D 00
0.820	-0.368406552201088 6D 00
0.830	-0.400563645046380 9D 00
0.840	-0.433042369422520 7D 00
0.850	-0.465840349747898 8D 00
0.860	-0.498955187158669 6D 00
0.870	-0.532384459686327 1D 00
0.880	-0.566125722436898 7D 00
0.890	-0.600176507771932 9D 00
0.900	-0.634534325491031 1D 00
0.910	-0.669196630161249 0D 00
0.920	-0.704160985577320 7D 00
0.930	-0.739424736400438 0D 00
0.940	-0.774985336896083 5D 00
0.950	-0.810840136853065 1D 00
0.960	-0.846986666171886 0D 00
0.970	-0.883422127412081 9D 00
0.980	-0.920143911007595 7D 00
0.990	-0.957149330930236 5D 00
1.000	-0.994435681658906 8D 00

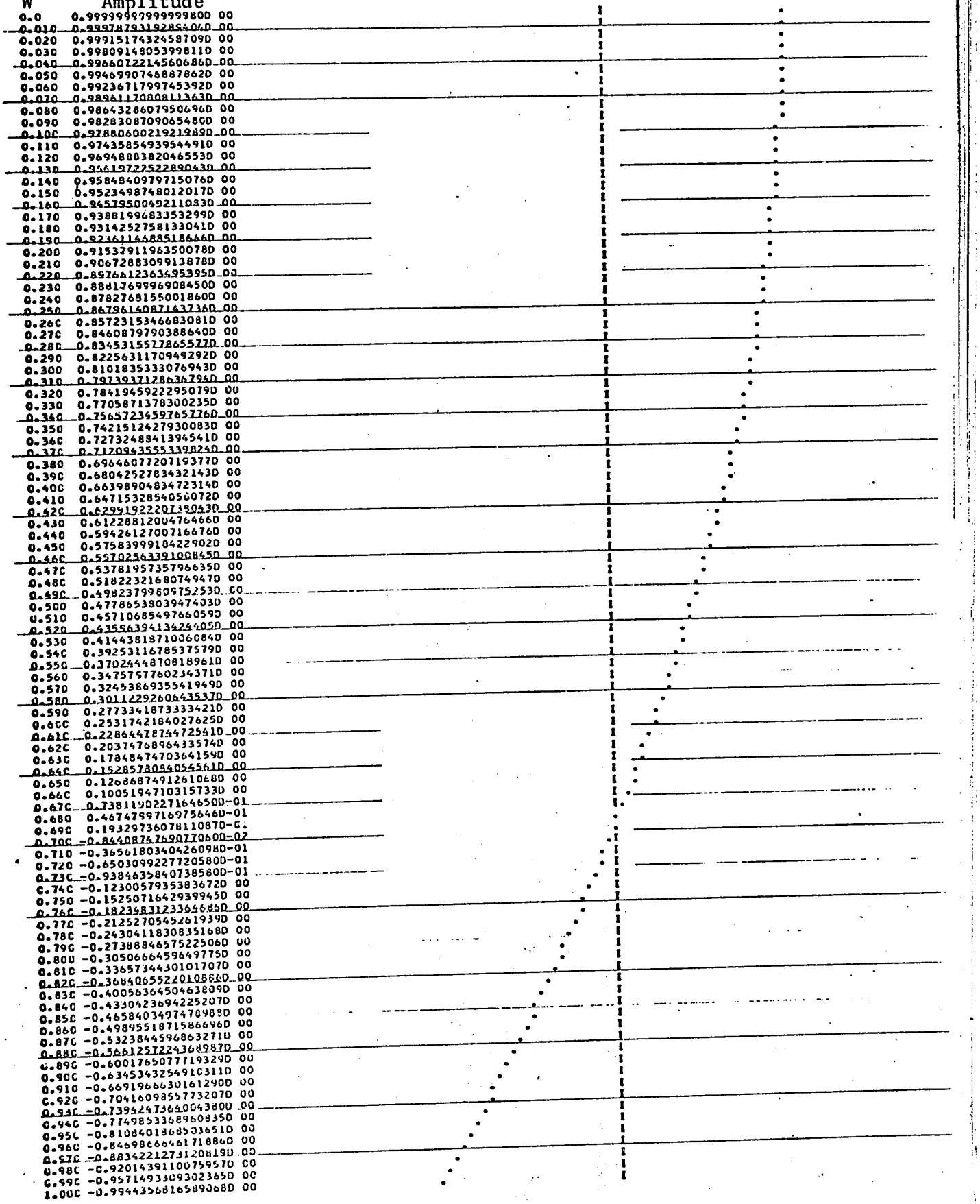

FIGURE 4.5C

ITERATION 8 WITH W_m = 1.0 and (0, 1) MODE AS INPUT FUNCTION

W	Amplitude
0.0	0.9999999999999980D 00
0.010	0.9997564557247174D 00
0.020	0.9990267967619870D 00
0.030	0.9978103596993701D 00
0.040	0.9961074728473586D 00
0.050	0.9939182612277539D 00
0.060	0.9912428855693557D 00
0.070	0.9880815422935191D 00
0.080	0.9844344635000408D 00
0.090	0.9803019169499111D 00
0.100	0.9756842040453920D 00
0.110	0.9705816698074731D 00
0.120	0.9649946828506405D 00
0.130	0.9589238455350457D 00
0.140	0.9523690330359755D 00
0.150	0.9453312971107447D 00
0.160	0.9378109642629011D 00
0.170	0.9298085866038063D 00
0.180	0.9213247516315834D 00
0.190	0.9123600021874459D 00
0.200	0.9029152364093777D 00
0.210	0.8929909076832103D 00
0.220	0.8825878245910707D 00
0.230	0.8717067509572311D 00
0.240	0.8603484852912810D 00
0.250	0.8485138617288006D 00
0.260	0.8362037489693538D 00
0.270	0.8234190507118699D 00
0.280	0.8101607054875272D 00
0.290	0.7964296865899340D 00
0.300	0.7822270020028141D 00
0.310	0.7675536943250713D 00
0.320	0.7524108406932938D 00
0.330	0.7367995527016997D 00
0.340	0.7207209763195139D 00
0.350	0.7041762918058138D 00
0.360	0.6871667136217949D 00
0.370	0.6696934903405269D 00
0.380	0.6517579045541690D 00
0.390	0.6333612727786666D 00
0.400	0.6145049453559065D 00
0.410	0.5951903063533998D 00
0.420	0.5754187734614346D 00
0.430	0.5551917978877300D 00
0.440	0.5345108642496518D 00
0.450	0.5133774904638814D 00
0.460	0.4917932276336813D 00
0.470	0.4697596599336488D 00
0.480	0.4472784044920570D 00
0.490	0.4243511112707163D 00
0.500	0.4009794629424470D 00
0.510	0.3771651747660926D 00
0.520	0.3529099945591409D 00
0.530	0.3282157020679041D 00
0.540	0.3030841098353951D 00
0.550	0.2775170620666700D 00
0.560	0.2515164349919691D 00
0.570	0.2250841366273705D 00
0.580	0.1982221066331401D 00
0.590	0.1709323161697331D 00
0.600	0.1432167677514764D 00
0.610	0.1150774950978925D 00
0.620	0.8651656298279390D-01
0.630	0.5753606708100682D-01
0.640	0.2813813381282803D-01
0.650	-0.1675079813756317D-02
0.660	-0.3190138636312835D-01
0.670	-0.6253856813438060D-01
0.680	-0.9358437732580800D-01
0.690	-0.1250365362017424D 00
0.700	-0.1568927372614603D 00
0.710	-0.1891506434103777D 00
0.720	-0.2218078881334224D 00
0.730	-0.2548620756705217D 00
0.740	-0.2883107811943104D 00
0.750	-0.3221515509899117D 00
0.760	-0.3563819026369314D 00
0.770	-0.3909993251934828D 00
0.780	-0.4260012793823473D 00
0.790	-0.4613851927792548D 00
0.800	-0.4971404850031466D 00
0.810	-0.5332885179086028D 00
0.820	-0.5698026457802174D 00
0.830	-0.6066881905290537D 00
0.840	-0.6439424468910956D 00
0.850	-0.6815626826276901D 00
0.860	-0.7195461387279786D 00
0.870	-0.7578900296132953D 00
0.880	-0.7965915633434738D 00
0.890	-0.8356478418251915D 00
0.900	-0.8750560610220752D 00
0.910	-0.9148133111668612D 00
0.920	-0.9549166769753258D 00
0.930	-0.9953532178621645D 00
0.940	-0.1036149968158663D 01
0.950	-0.1077273937332234D 01
0.960	-0.1118732110207776D 01
0.970	-0.1160521447190805D 01
0.980	-0.1202638804492386D 01
0.990	-0.1245091334355837D 01
1.000	-0.1287845605285189D 01

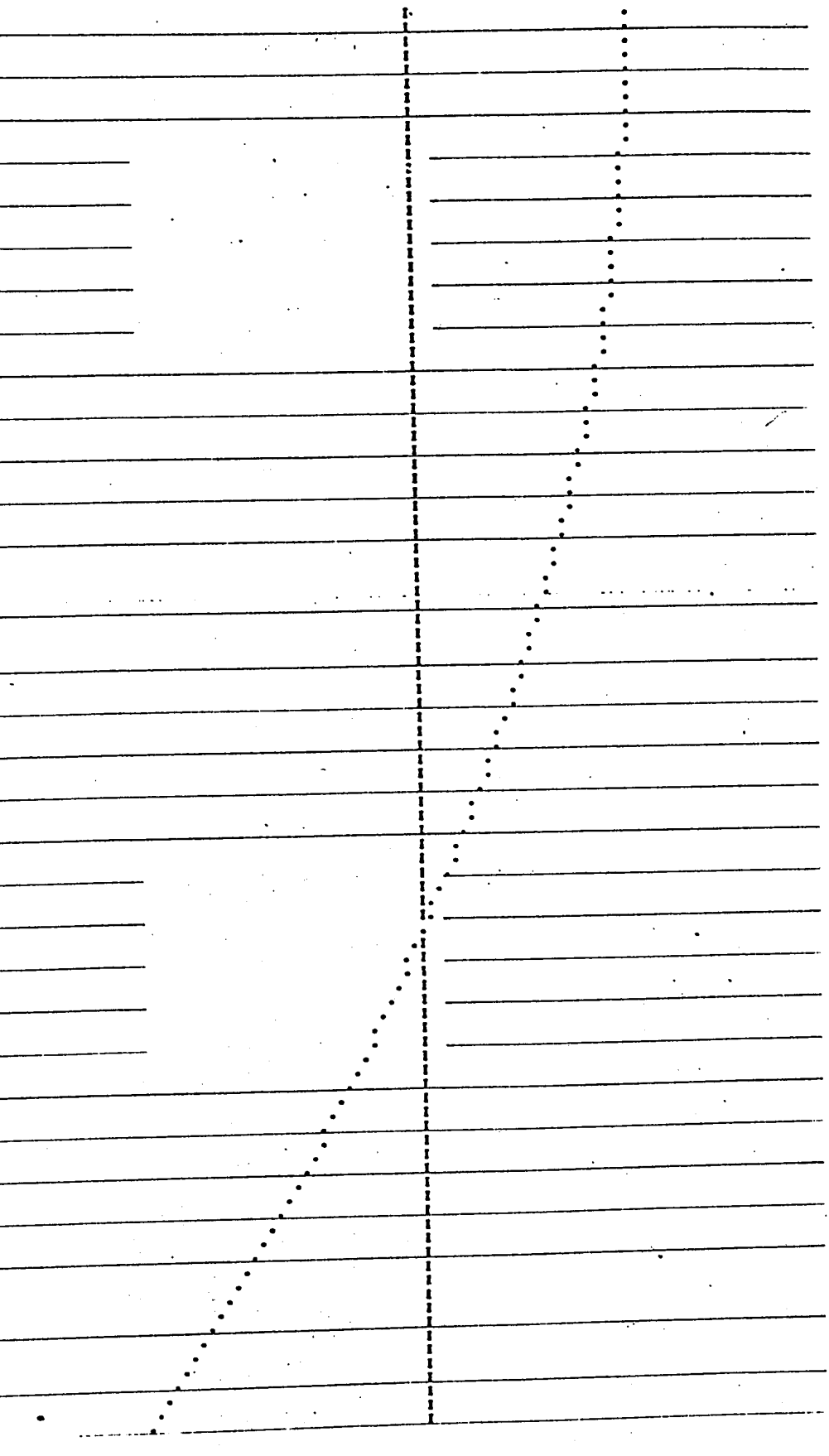

FIGURE 4.5D

ITERATION 9 WITH W_m = 1.0 AND (0, 1) MODE AS INPUT FUNCTION

W	Amplitude
0.0	0.99999999999999800 00
0.010	0.99935910412317090 00
0.020	0.99983641923845810 00
0.030	0.99963195359298330 00
0.040	0.99934572088462850 00
0.050	0.99897774036103730 00
0.060	0.99852803671824450 00
0.070	0.99799664014838840 00
0.080	0.99739358633003840 00
0.090	0.99668891642063110 00
0.100	0.99591267705850140 00
0.110	0.99505492035702770 00
0.120	0.99411570390136050 00
0.130	0.99309506074437620 00
0.140	0.99199314940194290 00
0.150	0.99080995384818200 00
0.160	0.98954558351004300 00
0.170	0.98820012326160950 00
0.180	0.98677366341799590 00
0.190	0.98526629972882970 00
0.200	0.98367813337137590 00
0.210	0.98200927C9432446D 00
0.220	0.98025982445473130 00
0.230	0.97842991320735500 00
0.240	0.97651965435232950 00
0.250	0.97452918174791130 00
0.260	0.97245862708397430 00
0.270	0.97030812930550510 00
0.280	0.96807783271598280 00
0.290	0.96576788696698320 00
0.300	0.96337844704742780 00
0.310	0.96090967327242440 00
0.320	0.95836173127172470 00
0.330	0.95573479197781890 00
0.340	0.95302903151366040 00
0.350	0.95024463167987730 00
0.360	0.94738177894191740 00
0.370	0.94444066654662850 00
0.380	0.94142148835752200 00
0.390	0.93832445024259090 00
0.400	0.93514975875772300 00
0.410	0.93189762678279020 00
0.420	0.92856827237611230 00
0.430	0.92516191875879620 00
0.440	0.92167879429867390 00
0.450	0.91811913249389390 00
0.460	0.91448317195611570 00
0.470	0.91077115639337040 00
0.480	0.90698334592534900 00
0.490	0.90311996040145140 00
0.500	0.89918129271067080 00
0.510	0.89516759543457000 00
0.520	0.89107913749381470 00
0.530	0.88691519279316120 00
0.540	0.88267904020465040 00
0.550	0.87836796354612610 00
0.560	0.87398325156113090 00
0.570	0.86952519789817300 00
0.580	0.86499610108961950 00
0.590	0.86039026453025560 00
0.600	0.85571399545549780 00
0.610	0.85096560991924190 00
0.620	0.84614542277140130 00
0.630	0.84125375763506840 00
0.640	0.83629094188335790 00
0.650	0.83125730761589280 00
0.660	0.82615319163497570 00
0.670	0.82097893542140310 00
0.680	0.81573488510996230 00
0.690	0.81042139146458540 00
0.700	0.80503880986317590 00
0.710	0.79958750022211880 00
0.720	0.79406782707044040 00
0.730	0.78848015952367630 00
0.740	0.78282487080739740 00
0.750	0.77710233922037370 00
0.760	0.77131294710756340 00
0.770	0.76545708133259530 00
0.780	0.75953513315006540 00
0.790	0.75355749817749210 00
0.800	0.74749457636694110 00
0.810	0.74137677197637120 00
0.820	0.73519449354065370 00
0.830	0.72894815384230230 00
0.840	0.72263816988188950 00
0.850	0.71626496284817420 00
0.860	0.70982895808792950 00
0.870	0.70333058507548290 00
0.880	0.69677027739195280 00
0.890	0.69014847264419790 00
0.900	0.68346561253349630 00
0.910	0.67672214272391310 00
0.920	0.66991851286041010 00
0.930	0.66305517452565810 00
0.940	0.65613259121258370 00
0.950	0.64915121828163580 00
0.960	0.64211152293777360 00
0.970	0.63501397419219840 00
0.980	0.62785904482981490 00
0.990	0.62064721137540570 00
1.000	0.61337895405958240 00

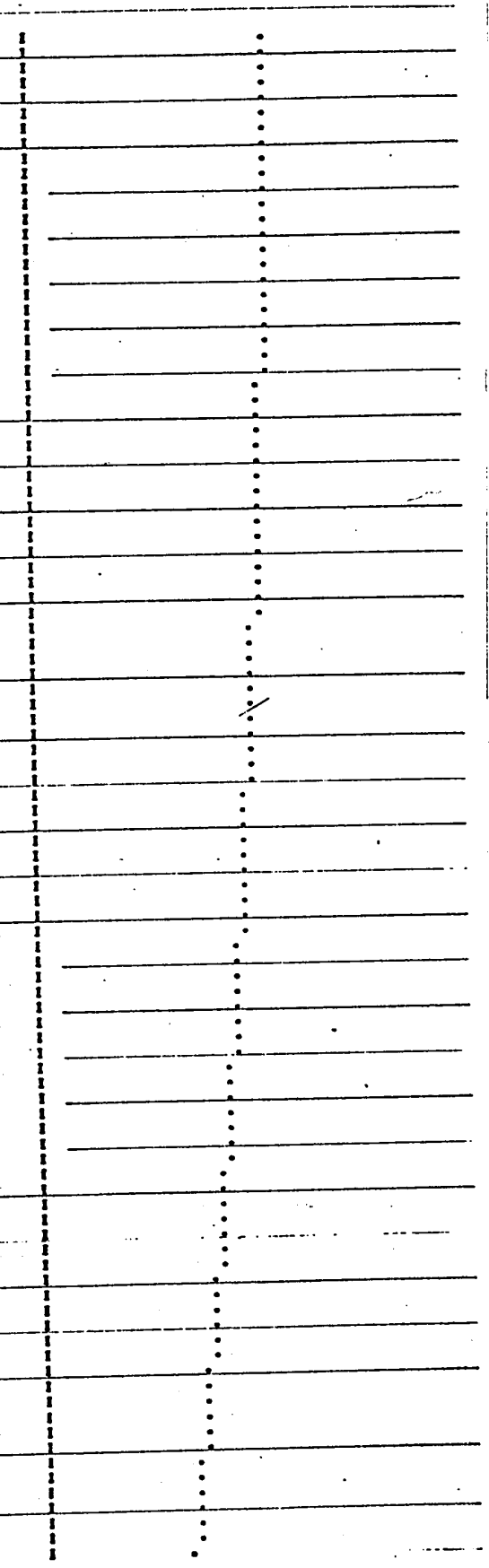

FIGURE 4.5E

ITERATION 10 WITH W_m = 1.0 AND (0, 1) MODE AS INPUT FUNCTION

W	Amplitude
0.0	0.99999999999999980D 00
0.010	0.99999185029577157D 00
0.020	0.99995401238092580D 00
0.030	0.99989652991978340D 00
0.040	0.99981605832443300D 00
0.050	0.99971260144484270D 00
0.060	0.99958616423057010D 00
0.070	0.99943675273064030D 00
0.080	0.99926437409227990D 00
0.090	0.99906903656228090D 00
0.100	0.99885074948469980D 00
0.110	0.99860952330118360D 00
0.120	0.99834536955018040D 00
0.130	0.99805830085618760D 00
0.140	0.99774833097903330D 00
0.150	0.99741547471301720D 00
0.160	0.99705974798601280D 00
0.170	0.99668116780850030D 00
0.180	0.99627975228253340D 00
0.190	0.99585552060063630D 00
0.200	0.99540849304463820D 00
0.210	0.99493869098444040D 00
0.220	0.99444613687671720D 00
0.230	0.99393085426354980D 00
0.240	0.99339286777099660D 00
0.250	0.99283220310759510D 00
0.260	0.99224088706280070D 00
0.270	0.99164294750535710D 00
0.280	0.99101441338160470D 00
0.290	0.99036331471371890D 00
0.300	0.98968968259788840D 00
0.310	0.98899354920242510D 00
0.320	0.98827494776580850D 00
0.330	0.98753391259456870D 00
0.340	0.98677047906170060D 00
0.350	0.98598468360351730D 00
0.360	0.98517656371843480D 00
0.370	0.98434615796419760D 00
0.380	0.98349350595563480D 00
0.390	0.98261864836225710D 00
0.400	0.98172162690578600D 00
0.410	0.98080248435762280D 00
0.420	0.97986126453625090D 00
0.430	0.97889801230457730D 00
0.440	0.97791277356721030D 00
0.450	0.97690559526767370D 00
0.460	0.97587652538555920D 00
0.470	0.97482561293361480D 00
0.480	0.97375290795477330D 00
0.490	0.97265846151911620D 00
0.500	0.97154232572077800D 00
0.510	0.97040455367478590D 00
0.520	0.96924519951384110D 00
0.630	0.96806431838503680D 00
0.540	0.96686196644651690D 00
0.550	0.96563820086407070D 00
0.560	0.96439307980767140D 00
0.570	0.96312666244795120D 00
0.580	0.96183900895261710D 00
0.590	0.96053018048280650D 00
0.600	0.95920023918938520D 00
0.610	0.95784924820918180D 00
0.620	0.95647727166116860D 00
0.630	0.95508437464257940D 00
0.640	0.95367062322497000D 00
0.650	0.95223608445022110D 00
0.660	0.95078082632648200D 00
0.670	0.94930491782405820D 00
0.680	0.94780842887123980D 00
0.690	0.94629143035007400D 00
0.700	0.94475399409207970D 00
0.710	0.94319619287390630D 00
0.720	0.94161810041293640D 00
0.730	0.94001979136283180D 00
0.740	0.93840134130902350D 00
0.750	0.93676282676414830D 00
0.760	0.93510432516342760D 00
0.770	0.93342591485999370D 00
0.780	0.93172767512016010D 00
0.790	0.93000968611864010D 00
0.800	0.92827202893370780D 00
0.810	0.92651478554230850D 00
0.820	0.92473803881511670D 00
0.830	0.92294187251153790D 00
0.840	0.92112637127466130D 00
0.850	0.91929162062615850D 00
0.860	0.91743770696113210D 00
0.870	0.91556471754291020D 00
0.880	0.91367274045779310D 00
0.890	0.91176186480974710D 00
0.900	0.90983218031504920D 00
0.910	0.90788377765687990D 00
0.920	0.90591674847987060D 00
0.930	0.90393118502459650D 00
0.940	0.90192713052202450D 00
0.950	0.89990462896791120D 00
0.960	0.89786422525715310D 00
0.970	0.89580544497308860D 00
0.980	0.89372664400675460D 00
0.990	0.89163360140109250D 00
1.000	0.88952121341511200D 00

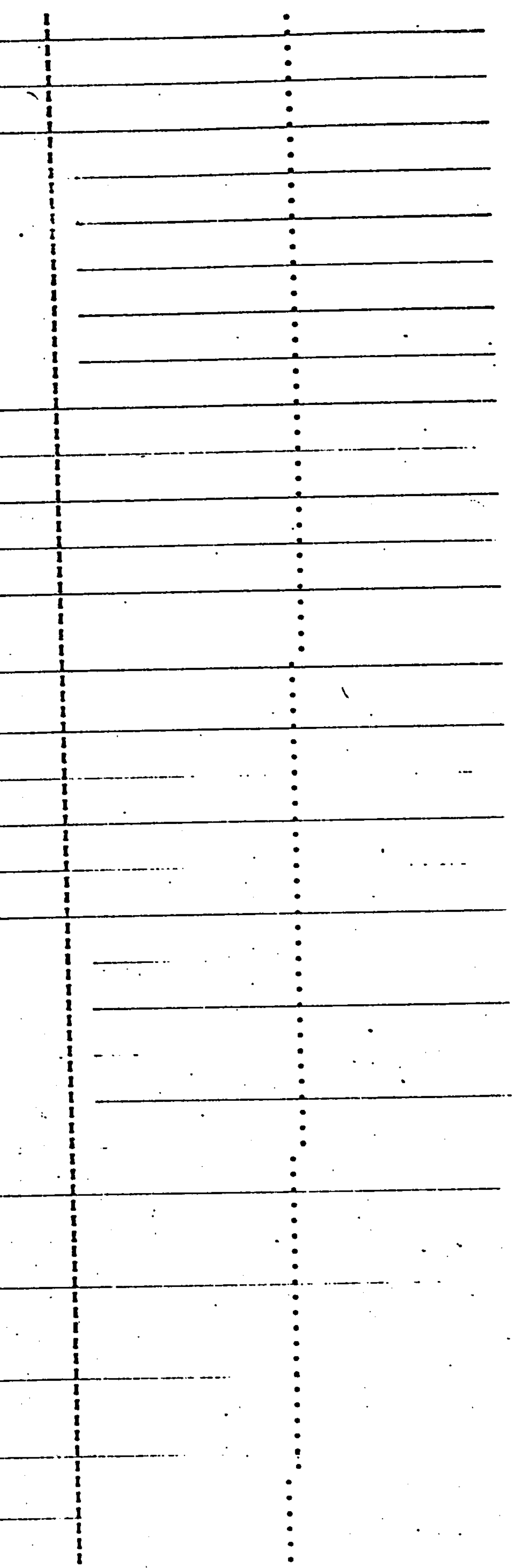

FIGURE 4.5F

ITERATION 33 WITH W_m = 1.0 AND (0, 1) MODE AS INPUT FUNCTION

w	Amplitude
0.0	0.99999999929999800D 00
0.010	0.99998775021899190D 00
0.020	0.99995104148150400D 00
0.030	0.99988984560410360D 00
0.040	0.99980417561428010D 00
0.050	0.99969403575025280D 00
0.060	0.99955943146071140D 00
0.070	0.99940036940447610D 00
0.080	0.99921695745008430D 00
0.090	0.99900890467530100D 00
0.100	0.99877652136655550D 00
0.110	0.99851971901830480D 00
0.120	0.99823851033231700D 00
0.130	0.99793290921688310D 00
0.140	0.99760293078595570D 00
0.150	0.99724859135820710D 00
0.160	0.99686990845601900D 00
0.170	0.99646690080439290D 00
0.180	0.99603958832978920D 00
0.190	0.99558799215884740D 00
0.200	0.99511213461727770D 00
0.210	0.99461203922807300D 00
0.220	0.99408773071044980D 00
0.230	0.99353923497811460D 00
0.240	0.99296657913769310D 00
0.250	0.99236979148704880D 00
0.260	0.99174890151352960D 00
0.270	0.99110393989213430D 00
0.280	0.99043493848361080D 00
0.290	0.98974193033248010D 00
0.300	0.98902494966498250D 00
0.310	0.98828403188669050D 00
0.320	0.98751921358165630D 00
0.330	0.98673053250744620D 00
0.340	0.98591802259549660D 00
0.350	0.98508173894735160D 00
0.360	0.98422170783244460D 00
0.370	0.98333797668554010D 00
0.380	0.98243058910410140D 00
0.390	0.98149958984558930D 00
0.400	0.98054502482468690D 00
0.410	0.97956694111045370D 00
0.420	0.97856538692340570D 00
0.430	0.97754041163253450D 00
0.440	0.97649206575223750D 00
0.450	0.97542040093919710D 00
0.460	0.97432548998917540D 00
0.470	0.97320732683374640D 00
0.480	0.97206602653695380D 00
0.490	0.97090162529192240D 00
0.500	0.96971418041727680D 00
0.510	0.96850375035379360D 00
0.520	0.96727039446059330D 00
0.530	0.96601417401150400D 00
0.540	0.96473515019138470D 00
0.550	0.96343338609220370D 00
0.560	0.96210894570919640D 00
0.570	0.96076189413689640D 00
0.580	0.95939229756510830D 00
0.590	0.95800022327481480D 00
0.600	0.95658573963401640D 00
0.610	0.95514891609350310D 00
0.620	0.95368932318256190D 00
0.630	0.95220853250461740D 00
0.640	0.95070511673280660D 00
0.650	0.94917964960548760D 00
0.660	0.94763220592168590D 00
0.670	0.94606284153647290D 00
0.680	0.94447169335528080D 00
0.690	0.94285877933415600D 00
0.700	0.94122419045549310D 00
0.710	0.93956803078041260D 00
0.720	0.93789035734431910D 00
0.730	0.93619126024740180D 00
0.740	0.93447082260231680D 00
0.750	0.93272912853851480D 00
0.760	0.93096626315705160D 00
0.770	0.92918231272533710D 00
0.780	0.92737736427182630D 00
0.790	0.92555150598054980D 00
0.800	0.92370482698618020D 00
0.810	0.92183741740754450D 00
0.820	0.91995936834306770D 00
0.830	0.91804077186466990D 00
0.840	0.91611172101219330D 00
0.850	0.91416230978767850D 00
0.860	0.91219263314957840D 00
0.870	0.91020278700691620D 00
0.880	0.90819285321338720D 00
0.890	0.90616297456140300D 00
0.900	0.90411320477607750D 00
0.910	0.90204365850916150D 00
0.920	0.89995443633291740D 00
0.930	0.89784563973194130D 00
0.940	0.89571737110693140D 00
0.950	0.89356973374839760D 00
0.960	0.89140283185032450D 00
0.970	0.88921677045377030D 00
0.980	0.88701165564243120D 00
0.990	0.88478759413613000D 00
1.000	0.88254469368427150D 00

FIGURE 4.5G

ITERATION 34 WITH W_m = 1.0 AND (0, 1) MODE AS INPUT FUNCTION

W	Amplitude
0.0	0.9999999999999980D 00
0.010	0.9999877602189921D 00
0.020	0.9999510414915040D 00
0.030	0.9998898456041038D 00
0.040	0.9998041756142759D 00
0.050	0.9996940357502528D 00
0.060	0.9995594314607116D 00
0.070	0.9994003694044766D 00
0.080	0.9992168574500845D 00
0.090	0.9990089046753010D 00
0.100	0.9987765213665558D 00
0.110	0.9985197190183052D 00
0.120	0.9982385103323170D 00
0.130	0.9979329092168833D 00
0.140	0.9976024307859557D 00
0.150	0.9972485913582074D 00
0.160	0.9968679084560190D 00
0.170	0.9964669004043933D 00
0.180	0.9960395863297692D 00
0.190	0.9955879921568874D 00
0.200	0.9951121346172777D 00
0.210	0.9946120392280730D 00
0.220	0.9940877307104505D 00
0.230	0.9935392347811151D 00
0.240	0.9929665791376931D 00
0.250	0.9923697914870492D 00
0.260	0.9917489015135248D 00
0.270	0.9911039398421346D 00
0.280	0.9904349384836112D 00
0.290	0.9897419303324799D 00
0.300	0.9890249496649831D 00
0.310	0.9882840312869610D 00
0.320	0.9875192135816566D 00
0.330	0.9867305325074402D 00
0.340	0.9859180275954966D 00
0.350	0.9850817389473516D 00
0.360	0.9842217378324446D 00
0.370	0.9833379760855401D 00
0.380	0.9824305891641014D 00
0.390	0.9814995898435895D 00
0.400	0.9805450248246671D 00
0.410	0.9795669411104537D 00
0.420	0.9785653369234065D 00
0.430	0.9775404116325347D 00
0.440	0.9764920657522377D 00
0.450	0.9754204009341971D 00
0.460	0.9743254695691754D 00
0.470	0.9732073266337464D 00
0.480	0.9720660265309540D 00
0.490	0.9709016252919027D 00
0.500	0.9697141604172708D 00
0.510	0.9685037503537936D 00
0.520	0.9672703946605833D 00
0.530	0.9660141740115040D 00
0.540	0.9647351501913847D 00
0.550	0.9634333609220370D 00
0.560	0.9621089445709196D 00
0.570	0.9607618941308964D 00
0.580	0.9593422975651083D 00
0.590	0.9580002232746154D 00
0.600	0.9565857396340167D 00
0.610	0.9551489160935033D 00
0.620	0.9536876231625023D 00
0.630	0.9522085325046170D 00
0.640	0.9507051107328006D 00
0.650	0.9491796446054676D 00
0.660	0.9476322959216661D 00
0.670	0.9460628615364724D 00
0.680	0.9444716933562610D 00
0.690	0.9428587793341562D 00
0.700	0.9412241484649434D 00
0.710	0.9395580307604128D 00
0.720	0.9378903573443195D 00
0.730	0.9361912602474016D 00
0.740	0.9344706220023170D 00
0.750	0.9327291205385153D 00
0.760	0.9309652631970516D 00
0.770	0.9291823127253360D 00
0.780	0.9273773542718261D 00
0.790	0.9255515059804980D 00
0.800	0.9237048265861807D 00
0.810	0.9218374174075445D 00
0.820	0.9199443308343067D 00
0.830	0.9180407718046094D 00
0.840	0.9161117210121933D 00
0.850	0.9141625049787675D 00
0.860	0.9121920131475740D 00
0.870	0.9102027147006915D 00
0.880	[illegible]
0.890	[illegible]
0.900	[illegible]
0.910	[illegible]
0.920	[illegible]
0.930	[illegible]
0.940	[illegible]
0.950	[illegible]
0.960	[illegible]
0.970	[illegible]
0.980	[illegible]
0.990	[illegible]
1.000	[illegible]

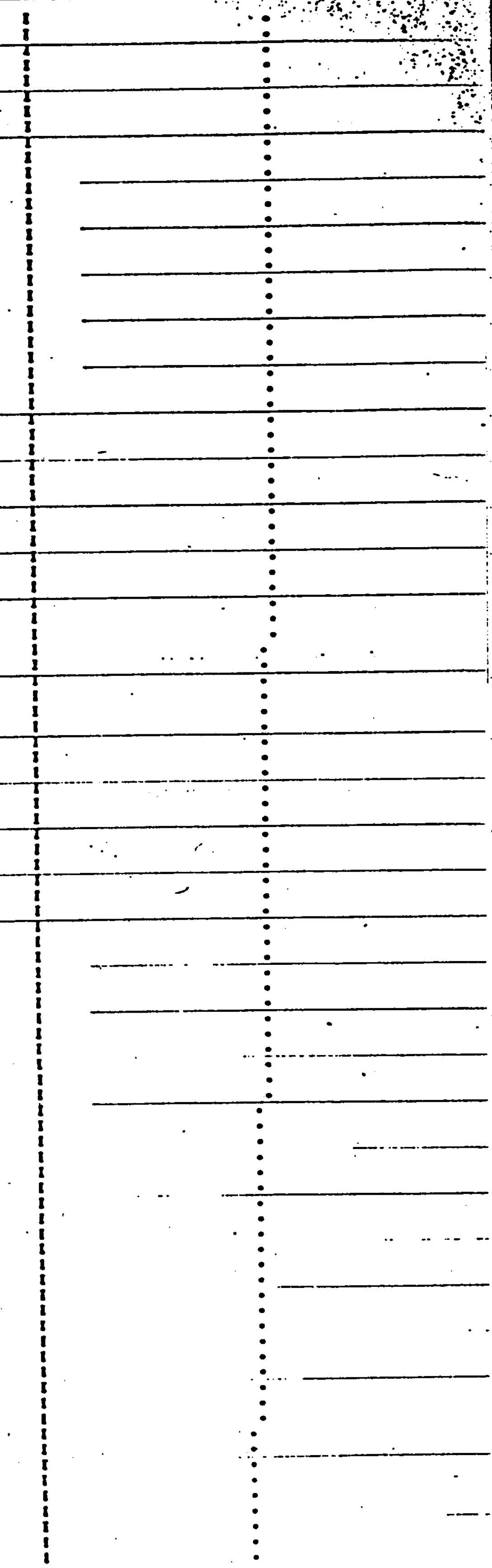

FIGURE 4.5H

ITERATION O WITH W_m = 3.5, (0, 1) MODE AS INPUT FUNCTION

W	Amplitude
0.0	0.9999999929999830D C0
0.035	0.9996270925960786D 00
0.070	0.9985118545535264&0 00
0.105	0.9966527371303379D 00
0.140	0.9940519593599562D 00
0.175	0.9907115065494431D 00
0.210	0.9866339266834205D 00
0.245	0.9818223308617985D 00
0.280	0.9762803992910547D 00
0.315	0.9700123284592978D 00
0.350	0.9630229275656392D 00
0.385	0.9553175144033515D 00
0.420	0.9469019612613438D 00
0.455	0.9377826791644561D 00
0.490	0.9279666132633101D 00
0.525	0.9174612365723122D 00
0.560	0.9062745437449022D 00
0.595	0.8944150443304825D 00
0.630	0.8818917555993321D 00
0.665	0.8687141945419567D 00
0.700	0.8548923718496413D 00
0.735	0.8404367794846358D 00
0.770	0.8253583858437472D 00
0.805	0.8096686245299695D 00
0.840	0.7933793851337020D 00
0.875	0.7765030032363702D 00
0.910	0.7590522500440744D 00
0.945	0.7410403216608616D 00
0.980	0.7224008280111873D 00
1.015	0.7033577814217348D 00
1.050	0.6837755848726985D 00
1.085	0.6636590199292289D 00
1.120	0.6430532343538706D 00
1.155	0.6219737294811289D 00
1.190	0.6004363471555809D 00
1.225	0.5784572565951604D 00
1.260	0.5560529408415803D 00
1.295	0.5332401830198363D 00
1.330	0.5100360523494202D 00
1.365	0.4864576899295028D 00
1.400	0.4625232943110002D 00
1.435	0.4382501060633837D 00
1.470	0.4136563969843422D 00
1.505	0.3887604470505410D 00
1.540	0.3635807373678738D 00
1.575	0.3381359307497371D 00
1.610	0.3124448571919739D 00
1.645	0.2865266982732447D 00
1.680	0.2603999715095667D 00
1.715	0.2340845146076604D 00
1.750	0.2075994896389959D 00
1.785	0.1809642671520947D 00
1.820	0.1541984102336779D 00
1.855	0.1273214583348837D 00
1.890	0.1003530122760245D 00
1.925	0.7331269624401750D-01
1.960	0.4622014379380196D-01
1.995	0.1909498088865955D-01
2.030	-0.8043189869374840D-02
2.065	-0.3517480510004844D-01
2.100	-0.6228035648737715D-01
2.135	-0.8934040652726220D-01
2.170	-0.1163356041873886D 00
2.205	-0.1432467004627713D 00
2.240	-0.1700545538133257D 00
2.275	-0.1967401954700840D 00
2.310	-0.2232847445966818D 00
2.345	-0.2496695232930223D 00
2.380	-0.2758760214280944D 00
2.415	-0.3018859212891458D 00
2.450	-0.3276811203458641D 00
2.485	-0.3532437039331845D 00
2.520	-0.3785560424123861D 00
2.555	-0.4036007217986854D 00
2.590	-0.4283605989133614D 00
2.625	-0.4528188083370239D 00
2.660	-0.4769587654367290D 00
2.695	-0.5007641991096358D 00
2.730	-0.5242191423749990 00
2.765	-0.5473079838415754D 00
2.800	-0.5700153509277345D 00
2.835	-0.5923263800120095D 00
2.870	-0.6142264383169424D 00
2.905	-0.6357013166296578D 00
2.940	-0.6567371798126071D 00
2.975	-0.6773205349583995D 00
3.010	-0.6974384911814725D 00
3.045	-0.7170702690357479D 00
3.080	-0.7362277095557101D 00
3.115	-0.7548750832900885D 00
3.150	-0.7730088966556989D 00
3.185	-0.7906184036098171D 00
3.220	-0.8076931092923251D 00
3.255	-0.8242230289748473D 00
3.290	-0.8401938443059323D 00
3.325	-0.8556109095159713D 00
3.360	-0.8704512571962164D 00
3.395	-0.8847116036477695D 00
3.430	-0.8983843537969842D 00
3.465	-0.9114624056739419D 00
3.500	-0.9239391544512447D 00

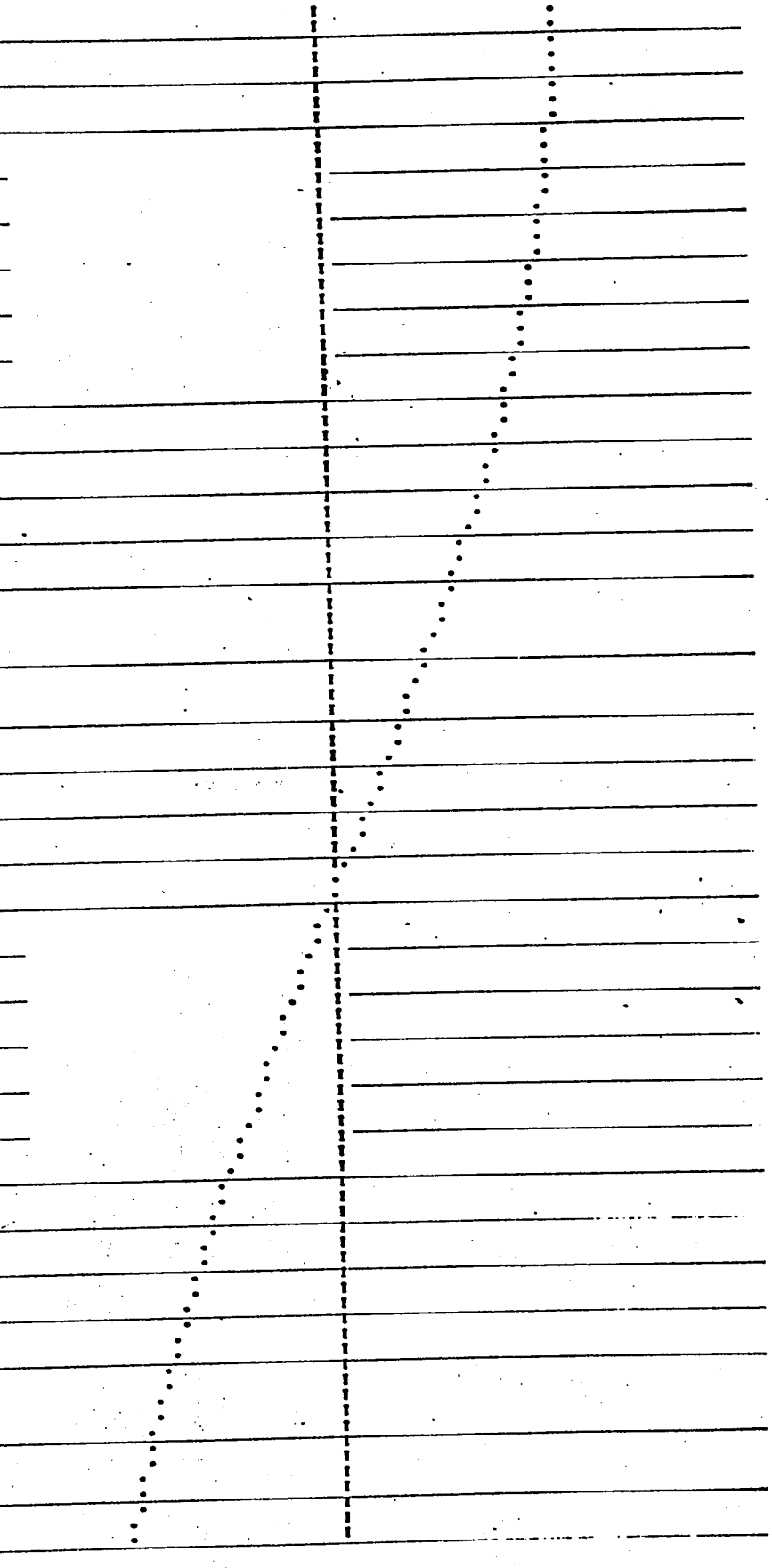

FIGURE 4.6A

ITERATION 1 WITH W_m = 3.5, (0, 1) MODE INPUT FUNCTION

W	Amplitude
0.0	0.9999999999999980D 00
0.035	0.9996278925960792D 00
0.070	0.9985118543852648D 00
0.105	0.9966527371303379D 00
0.140	0.9940519596359560D 00
0.175	0.9907115065494433D 00
0.210	0.9866339266834207D 00
0.245	0.9818223308617970D 00
0.280	0.9762803892910655D 00
0.315	0.9700123284592982D 00
0.350	0.9630229275656394D 00
0.385	0.9553175144835315D 00
0.420	0.9469019612613442D 00
0.455	0.9377826791644561D 00
0.490	0.9279666132633106D 00
0.525	0.9174612365723131D 00
0.560	0.9062745437449024D 00
0.595	0.8944150443304829D 00
0.630	0.8818917555993324D 00
0.665	0.8687141949419674D 00
0.700	0.8548923718498417D 00
0.735	0.8404367794846363D 00
0.770	0.8253583858437474D 00
0.805	0.8096686245299695D 00
0.840	0.7933793851337025D 00
0.875	0.7765030032363708D 00
0.910	0.7590522500440797D 00
0.945	0.7410403216608618D 00
0.980	0.7224808280111876D 00
1.015	0.7033877814217355D 00
1.050	0.6837755848726989D 00
1.085	0.6636590199292293D 00
1.120	0.6430532343638708D 00
1.155	0.6219737294811293D 00
1.190	0.6004363471555813D 00
1.225	0.5784572565951693D 00
1.260	0.5560529408415803D 00
1.295	0.5332401830198365D 00
1.330	0.5100360523494204D 00
1.365	0.4864578899295033D 00
1.400	0.4625232943110004D 00
1.435	0.4382501068683843D 00
1.470	0.4136563969843427D 00
1.505	0.3887604470605414D 00
1.540	0.3635807373678745D 00
1.575	0.3381359307497373D 00
1.610	0.3124448571919746D 00
1.645	0.2865264988273245D 00
1.680	0.2603999715096671D 00
1.715	0.2340845146076608D 00
1.750	0.2075994676389964D 00
1.785	0.1809642671520952D 00
1.820	0.1541984102336786D 00
1.855	0.1273214585348893D 00
1.890	0.1003530122760249D 00
1.925	0.7331269244018400D-01
1.960	0.4622014379680261D-01
1.995	0.1909498088865966D-01
2.030	-0.8043189869374469D-02
2.065	-0.3517485100044460-01
2.100	-0.6228035648737681D-01
2.135	-0.8934040652726200D-01
2.170	-0.1163356041873881D 00
2.205	-0.1432467004627708D 00
2.240	-0.1700545638133250D 00
2.275	-0.1967401954700835D 00
2.310	-0.2232847445966809D 00
2.345	-0.2496695232930217D 00
2.380	-0.2758760214280941D 00
2.415	-0.3018859212891453D 00
2.450	-0.3276811120345839D 00
2.485	-0.3532437039381843D 00
2.520	-0.3785560424123857D 00
2.555	-0.4036007217986852D 00
2.590	-0.4283605989133609D 00
2.625	-0.4528188063370235D 00
2.660	-0.4769587654367290D 00
2.695	-0.5007641991096354D 00
2.730	-0.5242191442374992D 00
2.765	-0.5473079638415751D 00
2.800	-0.5700153589277339D 00
2.835	-0.5923263800120090D 00
2.870	-0.6142264383169422D 00
2.905	-0.6357013166296569D 00
2.940	-0.6567371798126064D 00
2.975	-0.6773205849585392D 00
3.010	-0.6974384911814721D 00
3.045	-0.7170782690357475D 00
3.080	-0.7362277095557094D 00
3.115	-0.7548750329088615D 00
3.150	-0.7730088966556987D 00
3.185	-0.7906184036098162D 00
3.220	-0.8076931092923247D 00
3.255	-0.8242230289748468D 00
3.290	-0.8401908644305931 90
3.325	-0.8556109095159709D 00
3.360	-0.8704512571962157D 00
3.395	-0.8847116036477698D 00
3.430	-0.8983843537969839D 00
3.465	-0.9114624056739415D 00
3.500	-0.9239391544512443D 00

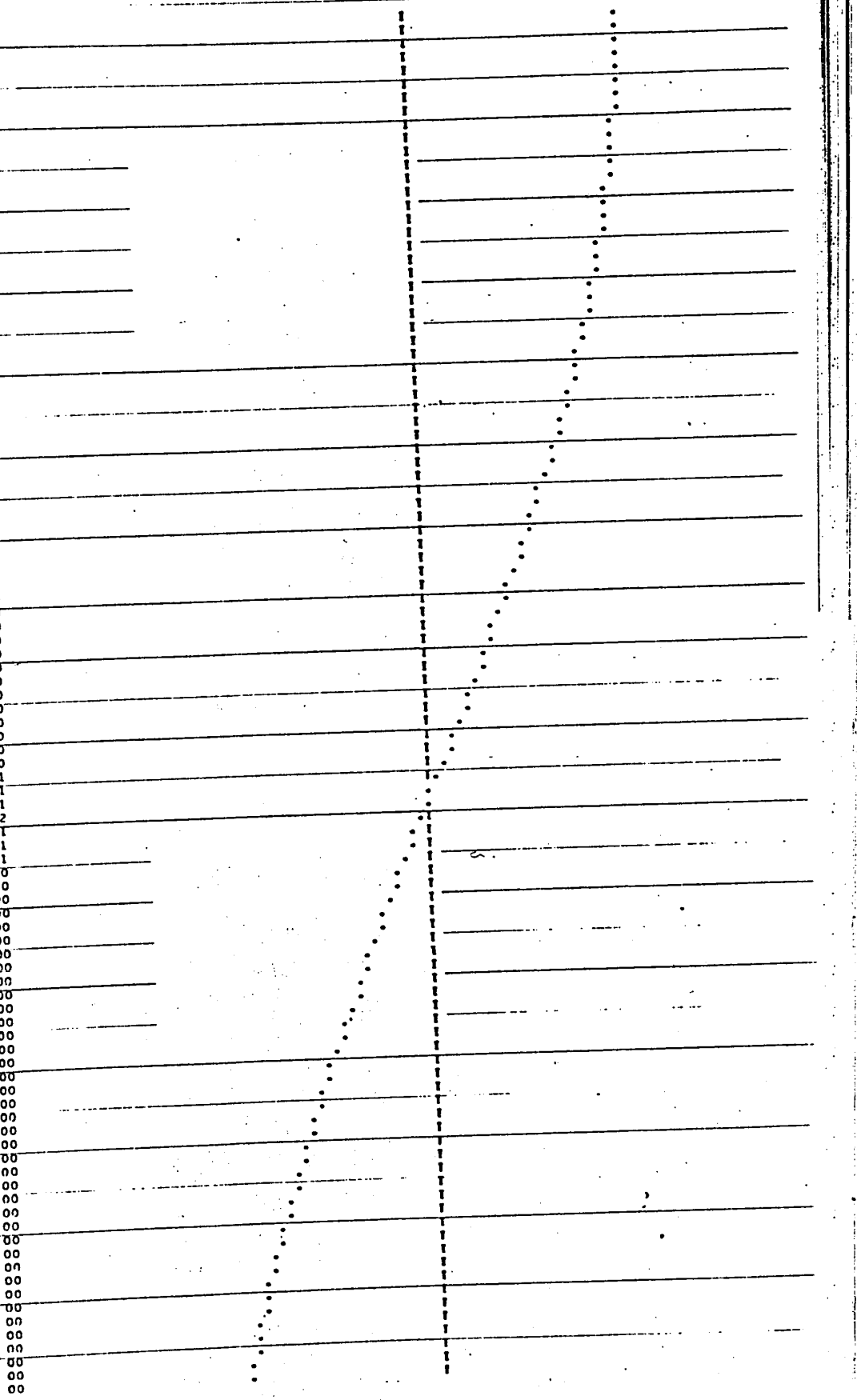

FIGURE 4.6B

ITERATION 36 WITH W_m = 3.5, (0, 1) MODE INPUT FUNCTION

W	Amplitude
0.0	0.9999999999999998D 00
0.035	0.9996078730907482D 00
0.070	0.9984317938092641D 00
0.105	0.9964726662388338D 00
0.140	0.9937319963334167D 00
0.175	0.9902118906411763D 00
0.210	0.9859150545190504D 00
0.245	0.9808447898399759D 00
0.280	0.9750049921948460D 00
0.315	0.9684001475917522D 00
0.350	0.9610353286554875D 00
0.385	0.9529161903307714D 00
0.420	0.9440489650930960D 00
0.455	0.9344404576715230D 00
0.490	0.9240980392882351D 00
0.525	0.9130296414200531D 00
0.560	0.9012437490875773D 00
0.595	0.8887493936780361D 00
0.630	0.8755561453083522D 00
0.665	0.8616741047353293D 00
0.700	0.8471138948203029D 00
0.735	0.8318866515559810D 00
0.770	0.8160040146635879D 00
0.805	0.7994781177688141D 00
0.840	0.7823215781655345D 00
0.875	0.7645474861763990D 00
0.910	0.7461693941200817D 00
0.945	0.7272013048950549D 00
0.980	0.7076576601902380D 00
1.015	0.6875533283331596D 00
1.050	0.6669035917866059D 00
1.085	0.6457241343050334D 00
1.120	0.6240310277623322D 00
1.155	0.6018407186628036D 00
1.190	0.5791700143475233D 00
1.225	0.5560360689084846D 00
1.260	0.5324563688232762D 00
1.295	0.5084487183228445D 00
1.330	0.4840312245065483D 00
1.365	0.4592222822161335D 00
1.400	0.4340405586839504D 00
1.435	0.4085049779681386D 00
1.470	0.3826347051890792D 00
1.505	0.3564491305911951D 00
1.540	0.3299678533743646D 00
1.575	0.3032106655193653D 00
1.610	0.2761975352719101D 00
1.645	0.2489485906499082D 00
1.680	0.2214841027787224D 00
1.715	0.1938244691392745D 00
1.750	0.1659901967338972D 00
1.785	0.1380018851849189D 00
1.820	0.1098802097810027D 00
1.855	0.8164590446862745D-01
1.890	0.5331974492732345D-01
1.925	0.2492253137312188D-01
1.960	-0.3524928277060976D-02
1.995	-0.3200183548273918D-01
2.030	-0.6048741801328789D-01
2.065	-0.8896094688460934D-01
2.100	-0.1174017529968835D 00
2.135	-0.1457892442675041D 00
2.170	-0.1741029218963949D 00
2.205	-0.2023223970972418D 00
2.240	-0.2304274074712904D 00
2.275	-0.2583978332790688D 00
2.310	-0.2862137135572835D 00
2.345	-0.3138552620669285D 00
2.380	-0.3413028830587478D 00
2.415	-0.3685371868424180D 00
2.450	-0.3955390051460021D 00
2.485	-0.4222894062524446D 00
2.520	-0.4487697099001119D 00
2.555	-0.4749615019345820D 00
2.590	-0.5008466486991931D 00
2.625	-0.5264073111520670D 00
2.660	-0.5516259586976377D 00
2.695	-0.5764853827209523D 00
2.730	-0.6009687098133440D 00
2.765	-0.6250594146783749D 00
2.800	-0.6487413327072128D 00
2.835	-0.6719986722130113D 00
2.870	-0.6948160263140639D 00
2.905	-0.7171763344560677D 00
2.940	-0.7390711435638723D 00
2.975	-0.7604801188137213D 00
3.010	-0.7813915540172426D 00
3.045	-0.8017921316087810D 00
3.080	-0.8216689822281166D 00
3.115	-0.8410096933891001D 00
3.150	-0.8598023207402620D 00
3.185	-0.8780353913705873D 00
3.220	-0.8956979167213425D 00
3.255	-0.9127793975292515D 00
3.290	-0.9292763133094350D 00
3.325	-0.9451597190826650D 00
3.360	-0.9604490710865851D 00
3.395	-0.9751024129104160D 00
3.430	-0.9891387403740687D 00
3.465	-0.1002341774235637D 01
3.500	-0.1015304464504786D 01

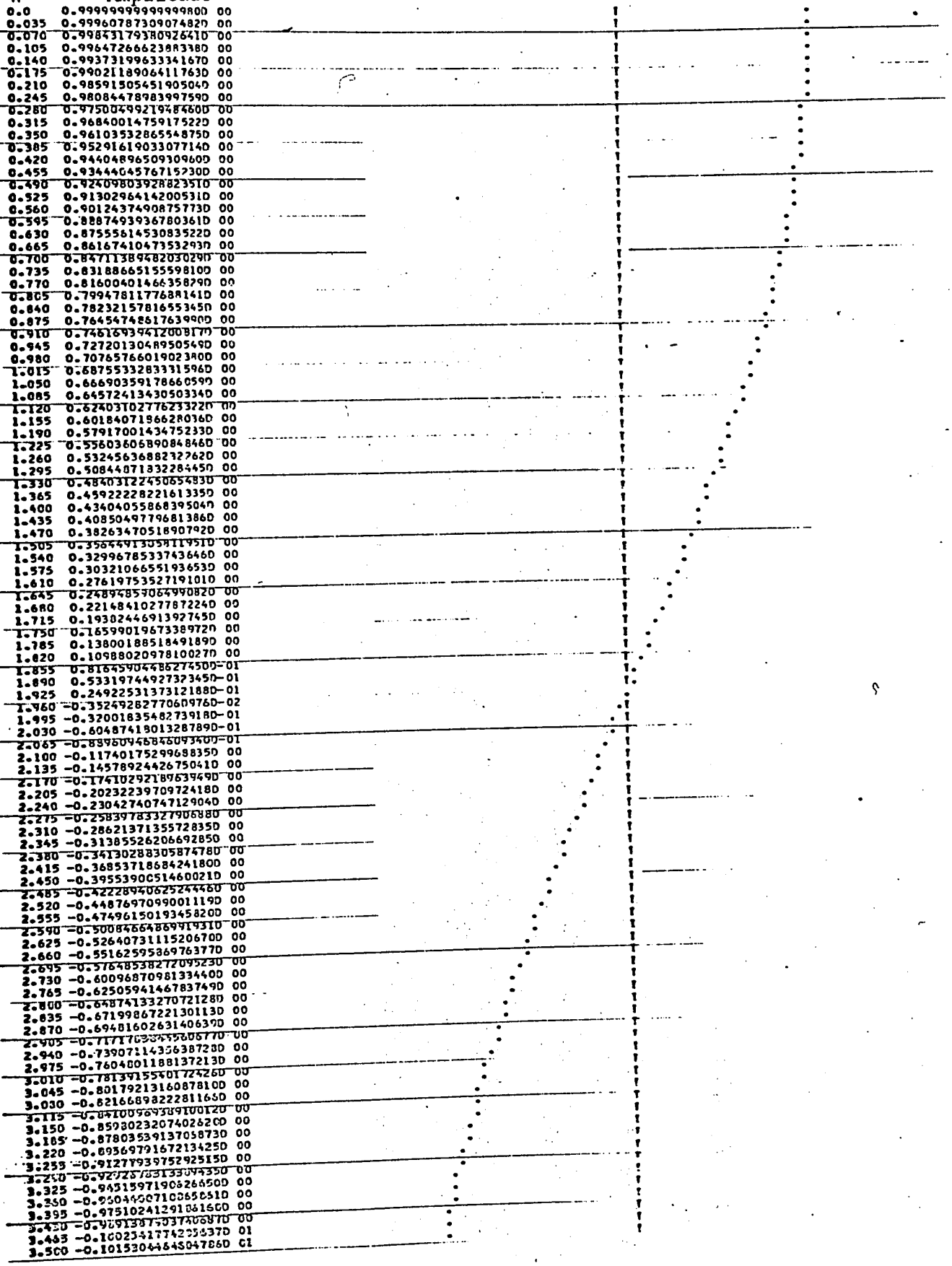

FIGURE 4.6C

ITERATION 37 WITH W_m = 3.5, (0, 1) MODE INPUT FUNCTION

w	Amplitude
0.0	0.999999999999999900 00
0.035	0.999667660105418100 00
0.070	0.998670999768564000 00
0.105	0.997010436820772100 00
0.140	0.994687546950000700 00
0.175	0.991703962655093100 00
0.210	0.988061921783067200 00
0.245	0.983764155650753000 00
0.280	0.978813886752468200 00
0.315	0.973214826055818200 00
0.350	0.966971169889038300 00
0.385	0.960087596415707100 00
0.420	0.952569261721001700 00
0.455	0.944421795478029800 00
0.490	0.935651296233153700 00
0.525	0.926264326293545200 00
0.560	0.916267906228599600 00
0.595	0.905669508989153700 00
0.630	0.894477053649814100 00
0.665	0.882699898780042100 00
0.700	0.870343835449952600 00
0.735	0.857421079877145500 00
0.770	0.843940265721177800 00
0.805	0.829911436032624200 00
0.840	0.815345034863961200 00
0.875	0.800251898549831900 00
0.910	0.784643246664526700 00
0.945	0.768530677664814200 00
0.980	0.751926134226527700 00
1.015	0.734841943283587200 00
1.050	0.717290755778405800 00
1.085	0.699285561132869100 00
1.120	0.680839671449346000 00
1.155	0.661966710451397500 00
1.190	0.642680602174106900 00
1.225	0.622995559414150200 00
1.260	0.602926071949951600 00
1.295	0.582486894542458100 00
1.330	0.561693034727261000 00
1.365	0.540559740408969200 00
1.400	0.519102487268914900 00
1.435	0.497336965997419200 00
1.470	0.475279069362001000 00
1.505	0.452944879123063000 00
1.540	0.430350652808674800 00
1.575	0.407512810360237600 00
1.610	0.384447920660893700 00
1.645	0.361172687958631200 00
1.680	0.337703938196136100 00
1.715	0.314058605259505100 00
1.750	0.290253717157995900 00
1.785	0.266306382146975500 00
1.820	0.242233774806529200 00
1.855	0.218053122087666500 00
1.890	0.193781689338775300 00
1.925	0.169436766324406200 00
1.960	0.145035653248763100 00
1.995	0.120595646796147900 00
2.030	0.961340262006067000-01
2.065	0.716880393569681000-01
2.100	0.472148898985436800-01
2.135	0.227917188617742800-01
2.170	-0.158439987487144000-02
2.205	-0.258964823246434900-01
2.240	-0.501276433282736400-01
2.275	-0.742611108553774000-01
2.310	-0.982802392680872000-01
2.345	-0.122168522448628300 00
2.380	-0.145909606779499000 00
2.415	-0.169487303965097900 00
2.450	-0.192885603638257000 00
2.485	-0.216088686059802100 00
2.520	-0.239080933943588800 00
2.555	-0.261846944991455000 00
2.590	-0.284371543532926300 00
2.625	-0.306639792216603000 00
2.660	-0.328637003424419900 00
2.695	-0.350348750444739500 00
2.730	-0.371760878394952100 00
2.765	-0.392859514884472800 00
2.800	-0.413631080409754200 00
2.835	-0.434062298469766500 00
2.870	-0.454140205400550500 00
2.905	-0.473852159913912700 00
2.940	-0.493185852333365000 00
2.975	-0.512129313519916700 00
3.010	-0.530670923494543000 00
3.045	-0.548799419718411600 00
3.080	-0.566503905058825100 00
3.115	-0.583773855413652200 00
3.150	-0.600599126995269200 00
3.185	-0.616969963267423700 00
3.220	-0.632877001529779000 00
3.255	-0.648311279145122200 00
3.290	-0.663264239404700100 00
3.325	-0.677727737027364200 00
3.360	-0.691694043288655100 00
3.395	-0.705155850776194700 00
3.430	-0.718106277768179400 00
3.465	-0.730538872232225400 00
3.500	-0.742447615441780200 00

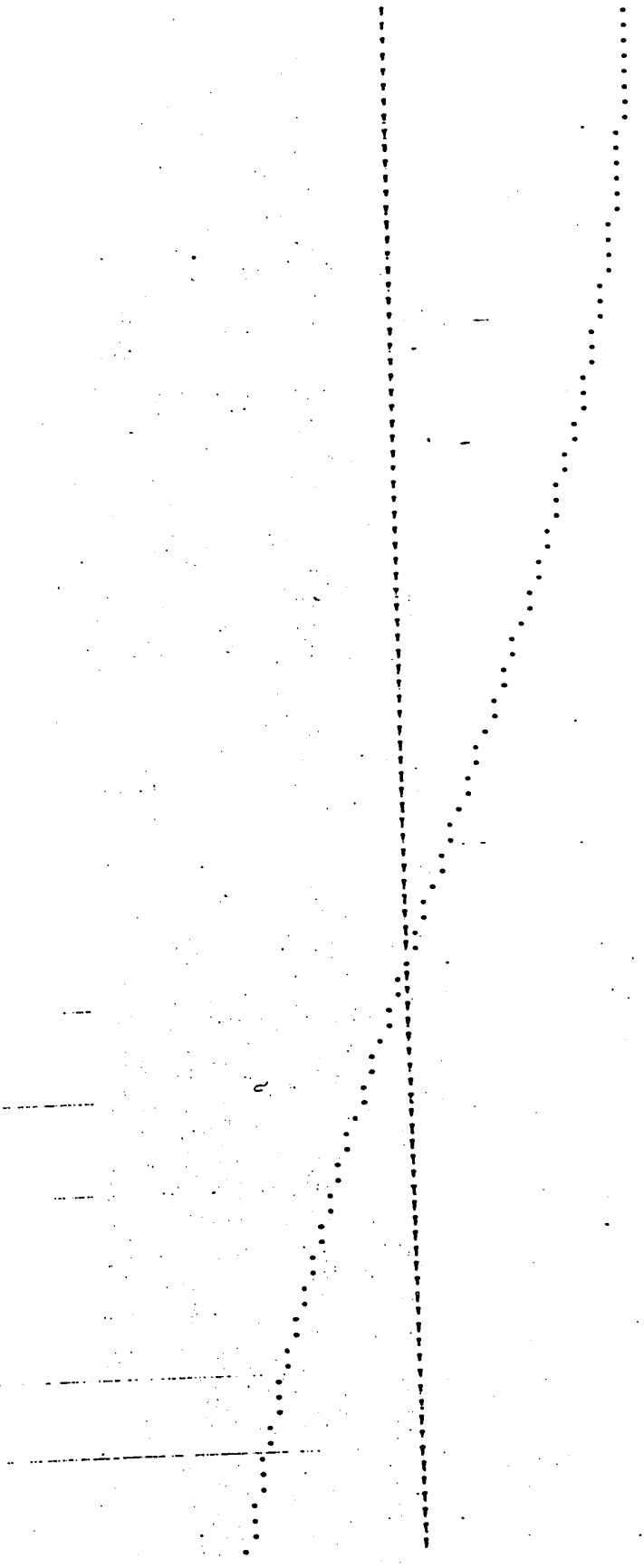

FIGURE 4.6D

ITERATION 38 WITH W_m = 3.5, (0, 1) MODE INPUT FUNCTION

W	Amplitude
0.0	0.9999999999999980D 00
0.035	0.9994007679545333D 00
0.070	0.9976035537471955D 00
0.105	0.9946098027196643D 00
0.140	0.9904219224020063D 00
0.175	0.9850432804269352D 00
0.210	0.9784782016286935D 00
0.245	0.9707319643142597D 00
0.280	0.9618107957139219D 00
0.315	0.9517218656138147D 00
0.350	0.9404732851761996D 00
0.385	0.9280740889529107D 00
0.420	0.9145342420903688D 00
0.455	0.8998646167892947D 00
0.490	0.8840769935897776D 00
0.525	0.8671840476546597D 00
0.560	0.8491993361273306D 00
0.595	0.8301372891638771D 00
0.630	0.8100131961723053D 00
0.665	0.7888431929313333D 00
0.700	0.7666442477164110D 00
0.735	0.7434341457148299D 00
0.770	0.7192314787432316D 00
0.805	0.6940556192815179D 00
0.840	0.6679267133767200 00
0.875	0.6408656606567361D 00
0.910	0.6128940920036798D 00
0.945	0.5840343595945294D 00
0.980	0.5543095074626618D 00
1.015	0.5237432602077218D 00
1.050	0.4923599986871509D 00
1.085	0.4601847399548100D 00
1.120	0.4272431158677114D 00
1.155	0.3935613511802957D 00
1.190	0.3591662411461859D 00
1.225	0.3240851286477894D 00
1.260	0.2883458808745036D 00
1.295	0.2519768655707208D 00
1.330	0.2150069258751668D 00
1.365	0.1774653607735074D 00
1.400	0.1393818901864505D 00
1.435	0.1007866397159273D 00
1.470	0.6171011007220035D-01
1.505	0.2218315220503290D-01
1.540	-0.1776305883768194D-01
1.575	-0.5809705030025153D-01
1.610	-0.9878707833461940D-01
1.645	-0.1398011548169180D 00
1.680	-0.1811070743409905D 00
1.715	-0.2226724413645462D 00
1.750	-0.2644486974835613D 00
1.785	-0.3064511488104080D 00
1.820	-0.3485989934310980D 00
1.855	-0.3908753489170919D 00
1.890	-0.4332472798669422D 00
1.925	-0.4756818254531744D 00
1.960	-0.5181480269497683D 00
1.995	-0.5606069552156549D 00
2.030	-0.6030317381097327D 00
2.065	-0.6453875876129884D 00
2.100	-0.6876418280333920D 00
2.135	-0.7297619210694723D 00
2.170	-0.7717154947084847D 00
2.205	-0.8134703689354494D 00
2.240	-0.8549945824293403D 00
2.275	-0.8962564188231691D 00
2.310	-0.9372244327046992D 00
2.345	-0.9778674753350293D 00
2.380	-0.1018154720062413D 01
2.415	-0.1058055687409096D 01
2.450	-0.1097540269809182D 01
2.485	-0.1136578755976047D 01
2.520	-0.1175141854878034D 01
2.555	-0.1213200719301634D 01
2.590	-0.1250726960981790D 01
2.625	-0.1287692713279300D 01
2.660	-0.1324070573385915D 01
2.695	-0.1359833704037940D 01
2.730	-0.1394955814719880D 01
2.765	-0.1429411190340064D 01
2.800	-0.1463174711360621D 01
2.835	-0.1496221873364928D 01
2.870	-0.1528528806045861D 01
2.905	-0.1560072291599250D 01
2.940	-0.1590029782506870D 01
2.975	-0.1620779418594506D 01
3.010	-0.1649900044050829D 01
3.045	-0.1678171222293593D 01
3.080	-0.1705573252170277D 01
3.115	-0.1732087181980910D 01
3.150	-0.1757694823411535D 01
3.185	-0.1782378764667240D 01
3.220	-0.1806122382894672D 01
3.255	-0.1828909855884281D 01
3.290	-0.1850726173043470D 01
3.325	-0.1871557145532392D 01
3.360	-0.1891389416254944D 01
3.395	-0.1910210467598038D 01
3.430	-0.1928008630413169D 01
3.465	-0.1944773090734765D 01
3.500	-0.1960493896330783D 01

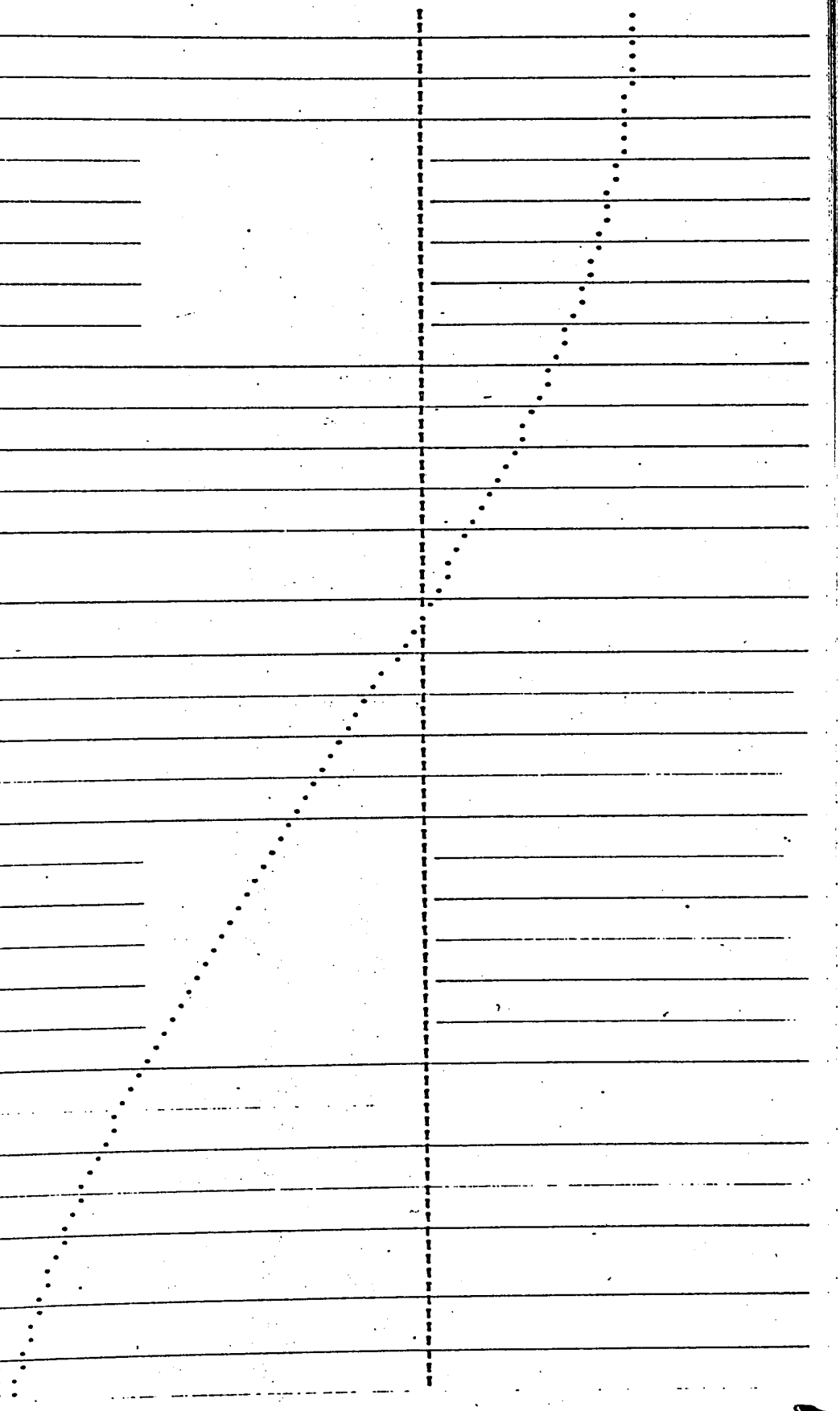

FIGURE 4.6E

ITERATION 39 WITH W_m = 3.5, (0, 1) MODE INPUT FUNCTION

w	Amplitude
0.0	0.999999999999999300 00
0.035	0.999766320879344 3D 00
0.070	0.999065446886565730 00
0.105	0.997897868014671 00D 00
0.140	0.995264400450333 5D 00
0.175	0.994166618593932560 00
0.210	0.991604690843399 7D 00
0.245	0.988581704943884 9D 00
0.280	0.985099339968904 00D 00
0.315	0.981160027971109 4D 00
0.350	0.976766519147955 90 00
0.385	0.971921879802774 60 00
0.420	0.966629489749129 8D 00
0.455	0.960893035580685 8D 00
0.490	0.954716527668900 26D 00
0.525	0.948104256911952 6D 00
0.560	0.941060831235616 1D 00
0.595	0.933591151852777 9D 00
0.630	0.925700413281325 9D 00
0.665	0.917394099126108 0D 00
0.700	0.908677977627938 1D 00
0.735	0.899558096903757 1D 00
0.770	0.890040780442032 4D 00
0.805	0.880132621177787 30 00
0.840	0.869840476951758 6D 00
0.875	0.859171464558436 7D 00
0.910	0.848132954068781 540 00
0.945	0.836732562366378 4D 00
0.980	0.824978149501316 2D 00
1.015	0.812877807335516 50 00
1.050	0.800439853016825 0D 00
1.085	0.787672844768599 6D 00
1.120	0.774585525505706 08D 00
1.155	0.761186865791549 4D 00
1.190	0.747486031613917 1D 00
1.225	0.733492382033382 00 00
1.260	0.719215461663345 4D 00
1.295	0.704666499301675 60D 00
1.330	0.689850868771675 900 00
1.365	0.674783143575463 9D 00
1.400	0.659472026575777 67D 00
1.435	0.643927872679338 60 00
1.470	0.628161174607717 8D 00
1.505	0.612182554465407 35D 00
1.540	0.596002755286610 0D 00
1.575	0.579632632513186 1D 00
1.610	0.563083145368551 6D 00
1.645	0.546365348181696 1D 00
1.680	0.529490381640886 8D 00
1.715	0.512469463994002 5D 00
1.750	0.495313382201803 90 00
1.785	0.478034983051823 5D 00
1.820	0.460644164240586 5D 00
1.855	0.443152665431869 2D 00
1.890	0.425572559298744 2D 00
1.925	0.407914742557138 3D 00
1.960	0.390190926998641 2D 00
1.995	0.372412630530287 0D 00
2.030	0.354591368229011 1D 00
2.065	0.336738643418462 0D 00
2.100	0.318865938775829 0D 00
2.135	0.300984707476269 2D 00
2.170	0.283106364382530 0D 00
2.205	0.265242277287243 3D 00
2.240	0.247403758215386 2D 00
2.275	0.229602054749424 12D 00
2.310	0.211848341698221 3D 00
2.345	0.194153712175749 40 00
2.380	0.176529169665371 40 00
2.415	0.158985619508132 5D 00
2.450	0.141533860763192 3D 00
2.485	0.124184578133513 50 00
2.520	0.106948334008368 1D 00
2.555	0.898355606292853 0D-01
2.590	0.728565523859398 0D-01
2.625	0.560214582483428 1D-01
2.660	0.393402743415679 00D-01
2.695	0.228228366691242 5D-01
2.730	0.647831399090361 3D-02
2.765	-0.968229913849879 0D-02
2.800	-0.256511891654286 7D-01
2.835	-0.414187301613357 6D-01
2.870	-0.569759902700890 30-01
2.905	-0.723142379733827 0D-01
2.940	-0.874249481691695 0D-01
2.975	-0.102299808058390 7D 00
3.010	-0.116930722835394 1D 00
3.045	-0.131309821177588 9D 00
3.080	-0.145429460530130 4D 00
3.115	-0.159282232181606 70 00
3.150	-0.172860966126867 8D 00
3.185	-0.186158735713369 5D 00
3.220	-0.199168862067623 5D 00
3.255	-0.211894911429848 090 00
3.290	-0.224300731347428 12D 00
3.325	-0.236410396371021 5D 00
3.360	-0.248208258988899 33D 00
3.395	-0.259688939835464 4D 00
3.430	-0.270847326971304 0D 00
3.465	-0.281678580819551 4D 00
3.500	-0.292178136734267 0D 00

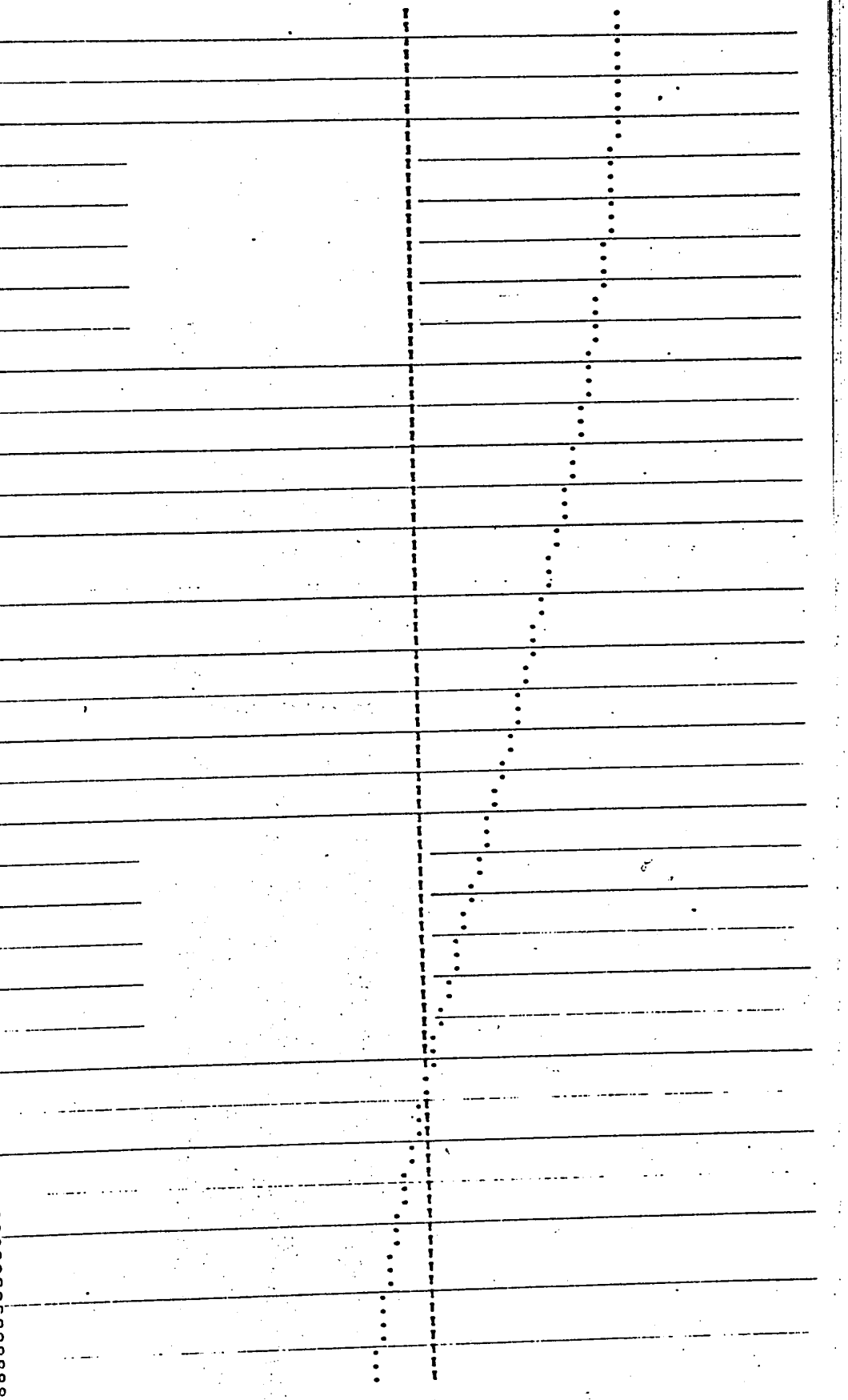

FIGURE 4.6F

ITERATION 40 WITH W_m = 3.5, (0, 1) MODE INPUT FUNCTION

W	Amplitude
0.0	0.999999999999999800 00
0.035	0.100000538176758100 01
0.070	0.100002148212105600 01
0.105	0.100004816626417100 01
0.140	0.100008520970833200 01
0.175	0.100013229853023800 01
0.210	0.100018902973209200 01
0.245	0.100025491170418100 01
0.280	0.100032936478920700 01
0.315	0.100041172194790000 01
0.350	0.100050122952514700 01
0.385	0.100059704811586300 01
0.420	0.100069825352975700 01
0.455	0.100080383785393100 01
0.490	0.100091271061223600 01
0.525	0.100102370002022400 01
0.560	0.100113555433435500 01
0.595	0.100124694329406200 01
0.630	0.100135645965522400 01
0.665	0.100146262081345300 01
0.700	0.100156387051546200 01
0.735	0.100165858065682700 01
0.770	0.100174505316423100 01
0.805	0.100182152196026400 01
0.840	0.100188615500875900 01
0.875	0.100193705643850600 01
0.910	0.100197226874320500 01
0.945	0.100198975077505450 01
0.980	0.100198750149169000 01
1.015	0.100196331956789300 01
1.050	0.100191504867981700 01
1.085	0.100184045864891700 01
1.120	0.100173727232912600 01
1.155	0.100160316827247300 01
1.190	0.100143578345075600 01
1.225	0.100123271607037700 01
1.260	0.100099152819751400 01
1.295	0.100070974903069900 01
1.330	0.100038487741781600 01
1.365	0.100001438501451800 01
1.400	0.999595719240972700 00
1.435	0.999126306313840400 00
1.470	0.998603554310393700 00
1.505	0.998024856261515700 00
1.540	0.997387593270433000 00
1.575	0.996689137653941000 00
1.610	0.995926856102847700 00
1.645	0.995098112859374600 00
1.680	0.994200272901209800 00
1.715	0.993230705143910700 00
1.750	0.992186785665327900 00
1.785	0.991065900857735500 00
1.820	0.989865450693319700 00
1.855	0.988582851896711400 00
1.890	0.987215541146222200 00
1.925	0.985760978258464400 00
1.960	0.984216649359042200 00
1.995	0.982580070036017600 00
2.030	0.980848788472856700 00
2.065	0.979020388557607400 00
2.100	0.977092492965057000 00
2.135	0.975062766208654500 00
2.170	0.972928917659019800 00
2.205	0.970688704525883400 00
2.240	0.968339934800342200 00
2.275	0.965880470159434750 00
2.310	0.963308228794406700 00
2.345	0.960621188266488650 00
2.380	0.957817388209203300 00
2.415	0.954894933052384300 00
2.450	0.951851994658191500 00
2.485	0.948686814902005100 00
2.520	0.945397708190369700 00
2.555	0.941983063913335700 00
2.590	0.938441348828611100 00
2.625	0.934771109375003000 00
2.660	0.930970973912696000 00
2.695	0.927039654887993500 00
2.730	0.922975950920212400 00
2.765	0.918778748808519400 00
2.800	0.914447025456553700 00
2.835	0.909979849712781300 00
2.870	0.905376384124596300 00
2.905	0.900635886604292000 00
2.940	0.895757712005082100 00
2.975	0.890741313605467500 00
3.010	0.885586244500336400 00
3.045	0.880292158897251100 00
3.080	0.874858813316506200 00
3.115	0.869286067693609800 00
3.150	0.863573886302962700 00
3.185	0.857722339061575700 00
3.220	0.851731601531810800 00
3.255	0.845601956422183000 00
3.290	0.839333793785409400 00
3.325	0.832927611592944900 00
3.360	0.826384016125410500 00
3.395	0.819703722258148000 00
3.430	0.812887553642911800 00
3.465	0.805936442781167700 00
3.500	0.798851430995786100 00

FIGURE 4.6G

ITERATION 41 WITH W_m = 3.5, (0, 1) MODE INPUT FUNCTION

w	Amplitude
0.0	0.99999999999999930D 00
0.035	0.99985265285898480 00
0.070	0.99941069957712530 00
0.105	0.99867440451156310 00
0.140	0.99764420803618370 00
0.175	0.99632072620980950 00
0.210	0.99470475031203960 00
0.245	0.99279724624716280 00
0.280	0.99059935381663770 00
0.315	0.98811238586073990 00
0.350	0.98533782727013310 00
0.385	0.98227733336581829D 00
0.420	0.97893273116496240 00
0.455	0.97530601298400890 00
0.490	0.97139933946299320 00
0.525	0.96721503792958850 00
0.560	0.96275559815377560 00
0.595	0.95802366547848650 00
0.630	0.95302205632945820 00
0.665	0.94775373660669100 00
0.700	0.94222182945886660 00
0.735	0.93642961094274610 00
0.770	0.93038050756951100 00
0.805	0.92407809374011360 00
0.840	0.91752608907180260 00
0.875	0.91072835561807940 00
0.910	0.90368989649844292D 00
0.945	0.89641184534225820 00
0.980	0.88890147834354960 00
1.015	0.88116219593883420 00
1.050	0.87319852710116920 00
1.085	0.86501512445584020 00
1.120	0.85661676083966550 00
1.155	0.84800832572976410 00
1.190	0.83919482164978100 00
1.225	0.83018136045159543D 00
1.260	0.82097315953861840 00
1.295	0.81157553801285700 00
1.330	0.80199391275193390 00
1.365	0.79223379441937570 00
1.400	0.78230078341148140 00
1.435	0.77220056574415720 00
1.470	0.76193890888313910 00
1.505	0.75152165752108340 00
1.540	0.74095472930502730 00
1.575	0.73024411051777140 00
1.610	0.71939585171677150 00
1.645	0.70841605333414020 00
1.680	0.69731091124141610 00
1.715	0.69608661228275280 00
1.750	0.67474942978021810 00
1.785	0.66330566901491520 00
1.820	0.65176167268763380 00
1.855	0.64012381636276560 00
1.890	0.62839850389923070 00
1.925	0.61659216287213930 00
1.960	0.60471123998895580 00
1.995	0.59276219650388640 00
2.030	0.58075150363423910 00
2.065	0.56868563790248050 00
2.100	0.55657107696770760 00
2.135	0.54441429427022760 00
2.170	0.53222175529294110 00
2.205	0.51999991264317060 00
2.240	0.50775520163859640 00
2.275	0.49549403584C87190 00
2.310	0.48322280262053220 00
2.345	0.47094785875670280 00
2.380	0.45867552607514050 00
2.415	0.44641208712804940 00
2.450	0.43416378091910610 00
2.485	0.42193679867705630 00
2.520	0.40973727968121370 00
2.555	0.39757130714212980 00
2.590	0.38544490414066150 00
2.625	0.37336402962852690 00
2.660	0.36133457449364910 00
2.695	0.34936235769298560 00
2.730	0.33745312245615090 00
2.765	0.32561253256252560 00
2.800	0.31384618869475620 00
2.835	0.30215952487138280 00
2.870	0.29055300496129760 00
2.905	0.27904691928259300 00
2.940	0.26763148128838860 00
2.975	0.25631680434200340 00
3.010	0.24510789858390360 00
3.045	0.23400966789264260 00
3.080	0.22302690694201160 00
3.115	0.21216429335647200 00
3.150	0.20142640996690000 00
3.185	0.19081769216852760 00
3.220	0.18034247538291410 00
3.255	0.17000496762567290 00
3.290	0.15980925218156010 00
3.325	0.14975928538847300 00
3.360	0.13985889453177090 00
3.395	0.13011177585026010 00
3.430	0.12052149265505100 00
3.465	0.11109147356243720 00
3.500	0.10182501084178990 00

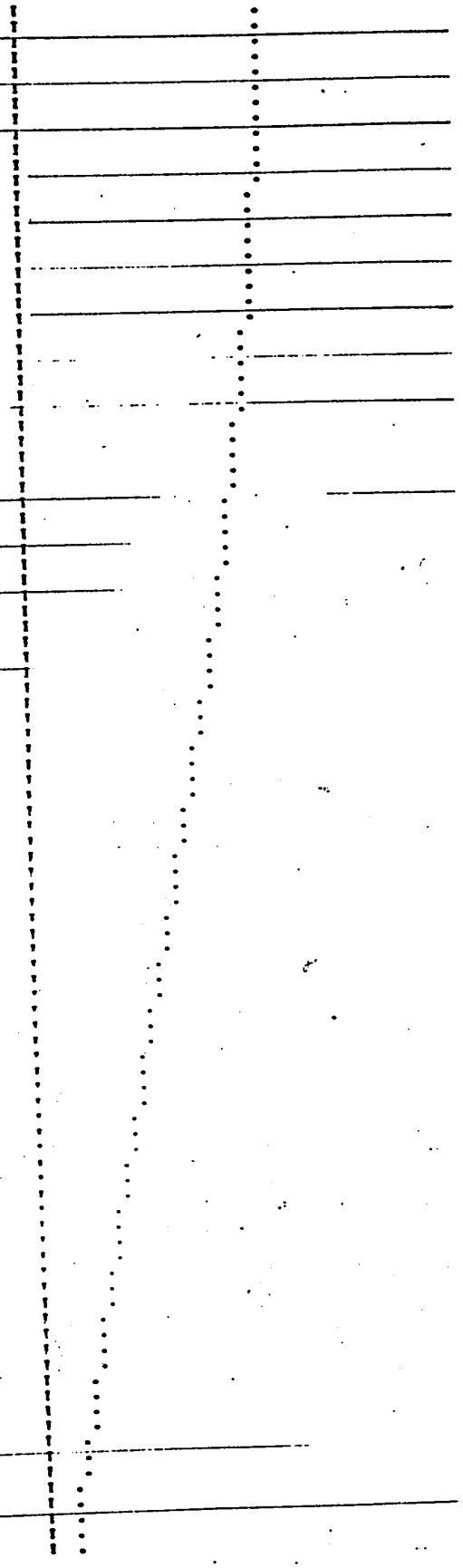

FIGURE 4.6H

ITERATION 86 WITH W_m = 3.5, (0, 1) MODE INPUT FUNCTION

W	Amplitude
0.0	0.9999999999999980D 00
0.035	0.9996816423787490D 00
0.070	0.9990266323942426D 00
0.105	0.9989351586401933D 00
0.140	0.9981075352927461D 00
0.175	0.9970442018905349D 00
0.210	0.9957457230270116D 00
0.245	0.9942127879552982D 00
0.280	0.9924462101058706D 00
0.315	0.9904469265174768D 00
0.350	0.9882159971817301D 00
0.385	0.9857546043019633D 00
0.420	0.9830640514667772D 00
0.455	0.9801457627392273D 00
0.490	0.9770012816621000D 00
0.525	0.9736322701802508D 00
0.560	0.9700405074808147D 00
0.595	0.9662279837522301D 00
0.630	0.9621964238630764D 00
0.665	0.9579482359617854D 00
0.700	0.9534855599983527D 00
0.735	0.9488107411692401D 00
0.770	0.9439262332367155D 00
0.805	0.9388345970739382D 00
0.840	0.9335384983871626D 00
0.875	0.9280437063664808D 00
0.910	0.9223440915165903D 00
0.945	0.9164516237191220D 00
0.980	0.9103663701781221D 00
1.015	0.9040914933003305D 00
1.050	0.8976302405119478D 00
1.085	0.8909859820136420D 00
1.120	0.8841621264755413D 00
1.155	0.8771622086743324D 00
1.190	0.8699898270735117D 00
1.225	0.8626486693501136D 00
1.260	0.8551424998684813D 00
1.295	0.8474751591039370D 00
1.330	0.8396505616181070D 00
1.365	0.8316726903880315D 00
1.400	0.8235456000911740D 00
1.435	0.8152734083484798D 00
1.470	0.8068602959276631D 00
1.505	0.7983105033089339D 00
1.540	0.7896283278153992D 00
1.575	0.7808181207103990D 00
1.610	0.7718842842640660D 00
1.645	0.7628312684791408OD 00
1.680	0.7536635696642419D 00
1.715	0.7443857242993201D 00
1.750	0.7350023091250055D 00
1.785	0.7255179365288639D 00
1.820	0.7159372517885589D 00
1.855	0.7062649249884311D 00
1.890	0.6965056729241700D 00
1.925	0.6866642059979677D 00
1.960	0.6767452751065681D 00
1.995	0.6667536435246139D 00
2.030	0.6566940887856957D 00
2.065	0.6465713995634987D 00
2.100	0.6363903725554575D 00
2.135	0.6261558093712873D 00
2.170	0.6158725134287841D 00
2.205	0.6055452868592583D 00
2.240	0.5951789274249523D 00
2.275	0.5847782254507016D 00
2.310	0.5743479607727273D 00
2.345	0.5638928997051655D 00
2.380	0.5534177920294380D 00
2.415	0.5429273680058981D 00
2.450	0.5324263354116811D 00
2.485	0.5219193766063960D 00
2.520	0.5114111456279190D 00
2.555	0.5009062653204334D 00
2.590	0.4904093244968346D 00
2.625	0.4799248751375746D 00
2.660	0.4694574296279929D 00
2.695	0.4590114580361448D 00
2.730	0.4485913854330902D 00
2.765	0.4382015892575705D 00
2.800	0.4278463967269866D 00
2.835	0.4175300822963669D 00
2.870	0.4072568651675658D 00
2.905	0.3970309068497053D 00
2.940	0.3868563087733010D 00
2.975	0.3767371099592871D 00
3.010	0.3666772847446768D 00
3.045	0.3566807405664049D 00
3.080	0.3467513158048418D 00
3.115	0.3368927176884193D 00
3.150	0.3271088202607663D 00
3.185	0.3174030624116825D 00
3.220	0.3077790459732161D 00
3.255	0.2982402338820826D 00
3.290	0.2887900094095613D 00
3.325	0.2794316694599823D 00
3.360	0.2701684329388379D 00
3.395	0.2610034291914682D 00
3.430	0.2519397015133237D 00
3.465	0.2429802047325057D 00
3.500	0.2341278038655196D 00

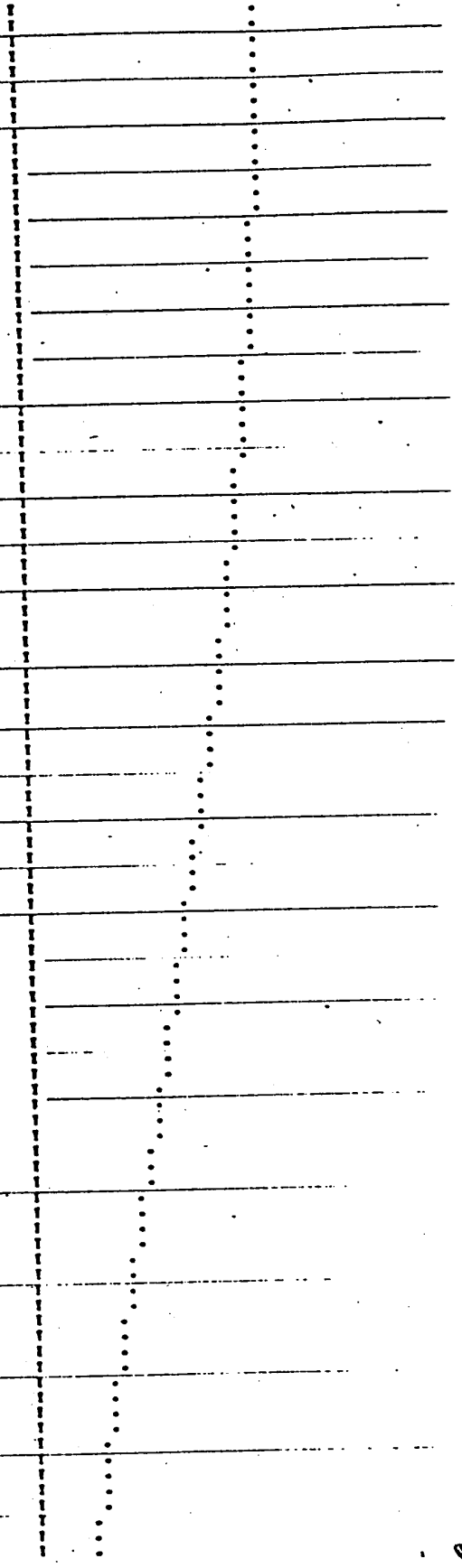

FIGURE 4.6I

ITERATION 87 WITH W_m = 3.5, (0, 1) MODE INPUT FUNCTION

w	Amplitude
0.0	0.99999999999999800 00
0.035	0.99988164237974900 00
0.070	0.99952663239424260 00
0.105	0.99893515864019330 00
0.140	0.99810753529274610 00
0.175	0.99704420189053490 00
0.210	0.99574572302701160 00
0.245	0.99421278795529820 00
0.280	0.99244621016587060 00
0.315	0.99044692651747680 00
0.350	0.98821599718173810 00
0.385	0.98575460430196330 00
0.420	0.98306405146677720 00
0.455	0.98014576273922730 00
0.490	0.97700128166210000 00
0.525	0.97363227018025080 00
0.560	0.97004050748081470 00
0.595	0.96622788875223010 00
0.630	0.96219652386307640 00
0.665	0.95794823596178540 00
0.700	0.95348555999835270 00
0.735	0.94881074116924010 00
0.770	0.94392623328671550 00
0.805	0.93883459707393820 00
0.840	0.93353849838716260 00
0.875	0.92804070636648080 00
0.910	0.92234409151659030 00
0.945	0.91645162371912200 00
0.980	0.91036637017812210 00
1.015	0.90409149330033050 00
1.050	0.89763024851194780 00
1.085	0.89098598201364200 00
1.120	0.88416212847558130 00
1.155	0.87716220857433240 00
1.190	0.86998982707351170 00
1.225	0.86264866935011360 00
1.260	0.85514249986848110 00
1.295	0.84747515910393700 00
1.330	0.83965056101810700 00
1.365	0.83167269038003150 00
1.400	0.82354560009117400 00
1.435	0.81527340834847980 00
1.470	0.80686029592766310 00
1.505	0.79831050330833490 00
1.540	0.78962832781539920 00
1.575	0.78081812071039900 00
1.610	0.77188428426406600 00
1.645	0.76283126879146800 00
1.680	0.75366356966424190 00
1.715	0.74438572429532010 00
1.750	0.73500230912500550 00
1.785	0.72551793652886390 00
1.820	0.71593725178855890 00
1.855	0.70626492988843110 00
1.890	0.69650567292417000 00
1.925	0.68666420599796770 00
1.960	0.67674527510656810 00
1.995	0.66675364352461390 00
2.030	0.65669408878569570 00
2.065	0.64657139495634987C 00
2.100	0.63639037255545750 00
2.135	0.62615580937128730 00
2.170	0.61587251342878410 00
2.205	0.60554528685925930 00
2.240	0.59517892742495230 00
2.275	0.58477822545078160 00
2.310	0.57434796077272730 00
2.345	0.56389289970516550 00
2.380	0.55341779202943800 00
2.415	0.54292736800589810 00
2.450	0.53242633541168110 00
2.485	0.52191937660639600 00
2.520	0.51141114562791900 00
2.555	0.50090626532043340 00
2.590	0.49040932449683460 00
2.625	0.47992487513757460 00
2.660	0.46945742962799290 00
2.695	0.45901145803614480 00
2.730	0.44859138543309020 00
2.765	0.43820158925757050 00
2.800	0.42784639672696630 00
2.835	0.41753008229636690 00
2.870	0.40725686516756500 00
2.905	0.39703090684970530 00
2.940	0.38685630877330100 00
2.975	0.37673710995928710 00
3.010	0.36667728474667680 00
3.045	0.35668074056640490 00
3.080	0.34675131580484180 00
3.115	0.33689277768841930 00
3.150	0.32710882026076630 00
3.185	0.31740306241168250 00
3.220	0.30777904597321610 00
3.255	0.29824023388208260 00
3.290	0.28879000840956130 00
3.325	0.27943166945998230 00
3.360	0.27016843293883290 00
3.395	0.26100342919146920 00
3.430	0.25193970151332370 00
3.465	0.24298020473250570 00
3.500	0.23412780386551960 00

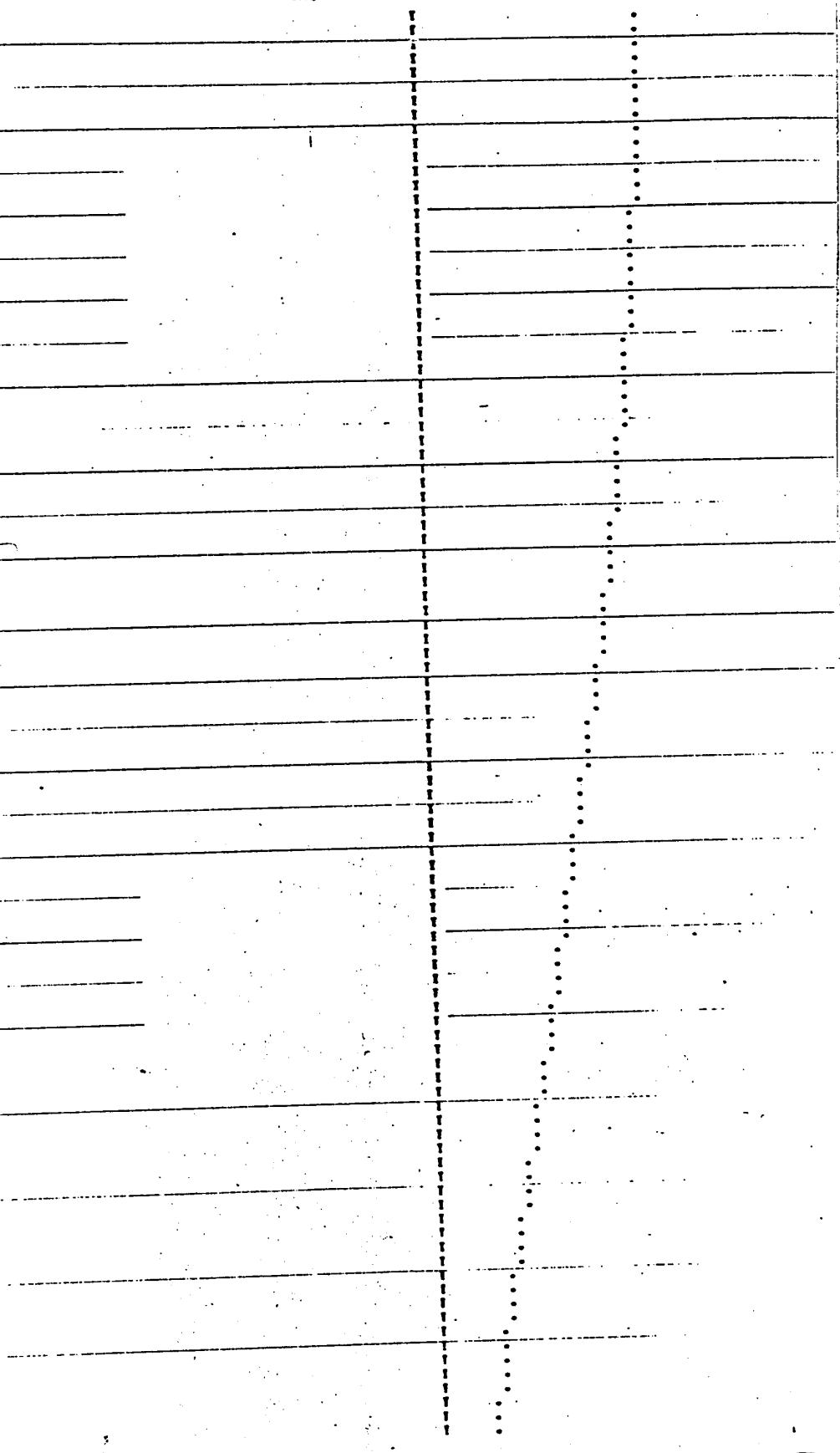

FIGURE 4.6J

ITERATION O WITH W_m = 1.0 AND (0,. 2) MODE AS INPUT FUNCTION

W	Amplitude
0.0	0.999999999999998D 00
0.010	0.999307526574814GD 00
0.020	0.997556718650101D 00
0.038	0.994492332492184SD 00
0.040	0.990215735798210B0 00
0.050	0.934726439482105ID 00
0.060	0.978031330845518BD 00
0.070	0.970133826004246D 00
0.080	0.961058868857481ZD 00
0.090	0.950802929867356BD 00
0.100	0.939304004659357ID 00
0.110	0.926816612487910GD 00
0.120	0.913116794363587ID 00
0.130	0.898038211120208ID 00
0.140	0.882301641631150ZD 00
0.150	0.865405979679212ID 00
0.160	0.847367232261880ID 00
0.170	0.828299016492604GD 00
0.180	0.808226456791373D 00
0.190	0.787171618183831B4D 00
0.200	0.765176321311255GD 00
0.210	0.742256502465512ZD 00
0.220	0.718447846514711GD 00
0.230	0.693782964833484I4D 00
0.240	0.668295954988877GD 00
0.250	0.642022396557770GD 00
0.260	0.614999346880927I8D 00
0.270	0.587265336160727ID 00
0.280	0.558860363487186ZD 00
0.290	0.529825091224672B0 00
0.300	0.500204840316446GD 00
0.310	0.470041589496091420 00
0.320	0.439381947192399GD 00
0.330	0.408273191278194GD 00
0.340	0.376764017942121BD 00
0.350	0.344904558408172GD 00
0.360	0.312746368265619ZD 00
0.370	0.280342421166150ZD 00
0.380	0.247747162330777ID 00
0.390	0.215016201903579ZD 00
0.400	0.182206908112633ID 00
0.410	0.149377800261991BD 00
0.420	0.116558841560935ZD 00
0.430	0.835013711767884ZGD-01
0.440	0.513780996744501GD-01
0.450	0.190830954078636BD-01
0.460	-0.129182174254997ZD-01
0.470	-0.445540697736369GD-01
0.480	-0.757713553303809GD-01
0.490	-0.106485638911803GD 00
0.500	-0.136631164977734GD 00
0.510	-0.166135866336521GD 00
0.520	-0.194926373000866GD 00
0.530	-0.222928072212435CD 00
0.540	-0.250064862667251GD 00
0.550	-0.276259673784742B0 00
0.560	-0.301433965306C608D 00
0.570	-0.325507991915854ZD 00
0.580	-0.348400762C984057D 00
0.590	-0.370033C481C99665D 00
0.600	-0.390312396136232GD 00
0.610	-0.409163136590642GD 00
0.620	-0.426496394577066GD 00
0.630	-0.442225100458207GD 00
0.640	-0.456261000823998GD 00
0.650	-0.468514066900801I7D 00
0.660	-0.478895516555253GD 00
0.670	-0.487311804244798ZD 00
0.680	-0.493670653491610BD 00
0.690	-0.497878057863278GD 00
0.700	-0.499838894743869ZD 00
0.710	-0.499486437136442ID 00
0.720	-0.496634865619657GD 00
0.730	-0.491274280431990ZD 00
0.740	-0.483275713714617GD 00
0.750	-0.472538641888623GD 00
0.760	-0.458961498162975GD 00
0.770	-0.442441685191979ZD 00
0.780	-0.422875587866311I7D 00
0.790	-0.400158586235922ZD 00
0.800	-0.374185068570727ZD 00
0.810	-0.344484844552248GD 00
0.820	-0.312041158602434ZD 00
0.830	-0.275654703327967ZD 00
0.840	-0.235579633116349GD 00
0.850	-0.191705577834570BD 00
0.860	-0.143921256676136GD 00
0.870	-0.921144921183314GD-01
0.880	-0.361722240051657GD-01
0.890	0.240194762400860BD-01
0.900	0.885759128832240D-01
0.910	0.157611143460542GD 00
0.920	0.231243190161452ZD 00
0.930	0.309588759195029GD 00
0.940	0.392765933973253GD 00
0.950	0.480893538602963GD 00
0.960	0.574091172870503BD 00
0.970	0.672479187102526GD 00
0.980	0.776178666932612GD 00
0.990	0.885311417948460GD 00
1.000	0.999999950243003ZD 00

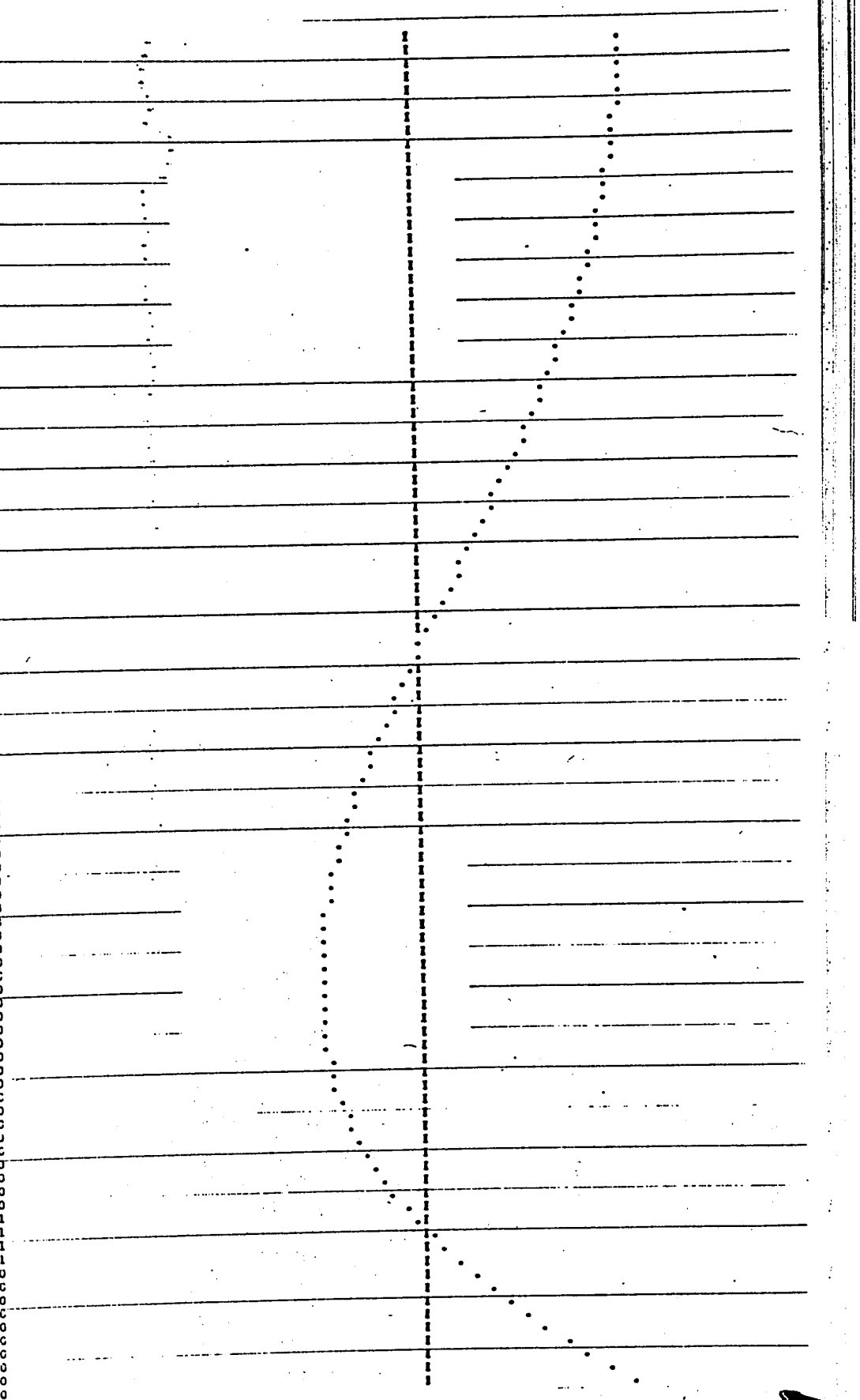

FIGURE 4.7A

ITERATION 1 WITH W_m = 1.0 AND (0, 2) MODE AS INPUT FUNCTION

w	Amplitude
0.00	0.999999999997999300 00
0.010	0.999938752629324490 00
0.020	0.999750037075936880 00
0.030	0.999449232999526220 00
0.040	0.999021573133065340 00
0.050	0.998472643258304060 00
0.060	0.997803132091893210 00
0.070	0.997013381250612690 00
0.080	0.996105385124291960 00
0.090	0.995080290760328440 00
0.100	0.993938397721890960 00
0.110	0.992681657932369260 00
0.120	0.991311675495934130 00
0.130	0.989830206503971950 00
0.140	0.988239158819833590 00
0.150	0.986540591846969930 00
0.160	0.984736716277616620 00
0.170	0.982829893223698740 00
0.180	0.980822636928326870 00
0.190	0.978717608460261850 00
0.200	0.976517621387966510 00
0.210	0.974225638438166560 00
0.220	0.971844771733110270 00
0.230	0.969378282411724580 00
0.240	0.966829580231024290 00
0.250	0.964202223150537930 00
0.260	0.961499916693007130 00
0.270	0.958726514516879710 00
0.280	0.955886015895574200 00
0.290	0.952982567279518700 00
0.300	0.950020460763988670 00
0.310	0.947004133770691870 00
0.320	0.943938168504435250 00
0.330	0.940827291393879060 00
0.340	0.937676372512791810 00
0.350	0.934490424985583720 00
0.360	0.931274604372952990 00
0.370	0.928034208041698070 00
0.380	0.924773667451647261D 00
0.390	0.921501582813214620 00
0.400	0.918220651756978930 00
0.410	0.914937392802489500 00
0.420	0.911658417065599900 00
0.430	0.839009301372766000-01
0.440	0.513776408323090600-01
0.450	0.190826193051978500-01
0.460	-0.129187109122612700-01
0.470	-0.445595804417578700-01
0.480	-0.757718832524334000-01
0.490	-0.106486184030127800 00
0.500	-0.136631727267283600 00
0.510	-0.166136445562477800 00
0.520	-0.194926969077646200 00
0.530	-0.222928633972536000 00
0.540	-0.250065491884000350 00
0.550	-0.276260319226647000 00
0.560	-0.301434626694825500 00
0.570	-0.325508668944662400 00
0.580	-0.348401454418842200 00
0.590	-0.370030735339221200 00
0.600	-0.390313117855722300 00
0.610	-0.409163872339771200 00
0.620	-0.426497143856892500 00
0.630	-0.442225862769826500 00
0.640	-0.456261775507512400 00
0.650	-0.468515455477371800 00
0.660	-0.478896314144843600 00
0.670	-0.487312612241771200 00
0.680	-0.493671471134813300 00
0.690	-0.497878884349863300 00
0.700	-0.499839729218572500 00
0.710	-0.499457778697632300 00
0.720	-0.496635713309912600 00
0.730	-0.491275133247532400 00
0.740	-0.483276570597856000 00
0.750	-0.472539501724733300 00
0.760	-0.458962359784637500 00
0.770	-0.442442547375958800 00
0.780	-0.422876449325615600 00
0.790	-0.400159445631228200 00
0.800	-0.374185924498132000 00
0.810	-0.344849295549101300 00
0.820	-0.312042003138670500 00
0.830	-0.275665539813373300 00
0.840	-0.235580459892681800 00
0.850	-0.191706393174057000 00
0.860	-0.143922058784968500 00
0.870	-0.921152791316506000-01
0.880	-0.361729939879122200-01
0.890	0.240187252978731200-01
0.900	0.885746614706996000-01
0.910	0.157610436929198600 00
0.920	0.231242499152978800 00
0.930	0.309598106026946500 00
0.940	0.392765311042621400 00
0.950	0.480889294839142680 00
0.960	0.574090617941497200 00
0.970	0.672478670105281100 00
0.980	0.776178190605332600 00
0.990	0.885310985117293300 00
1.000	0.999999563822336600 00

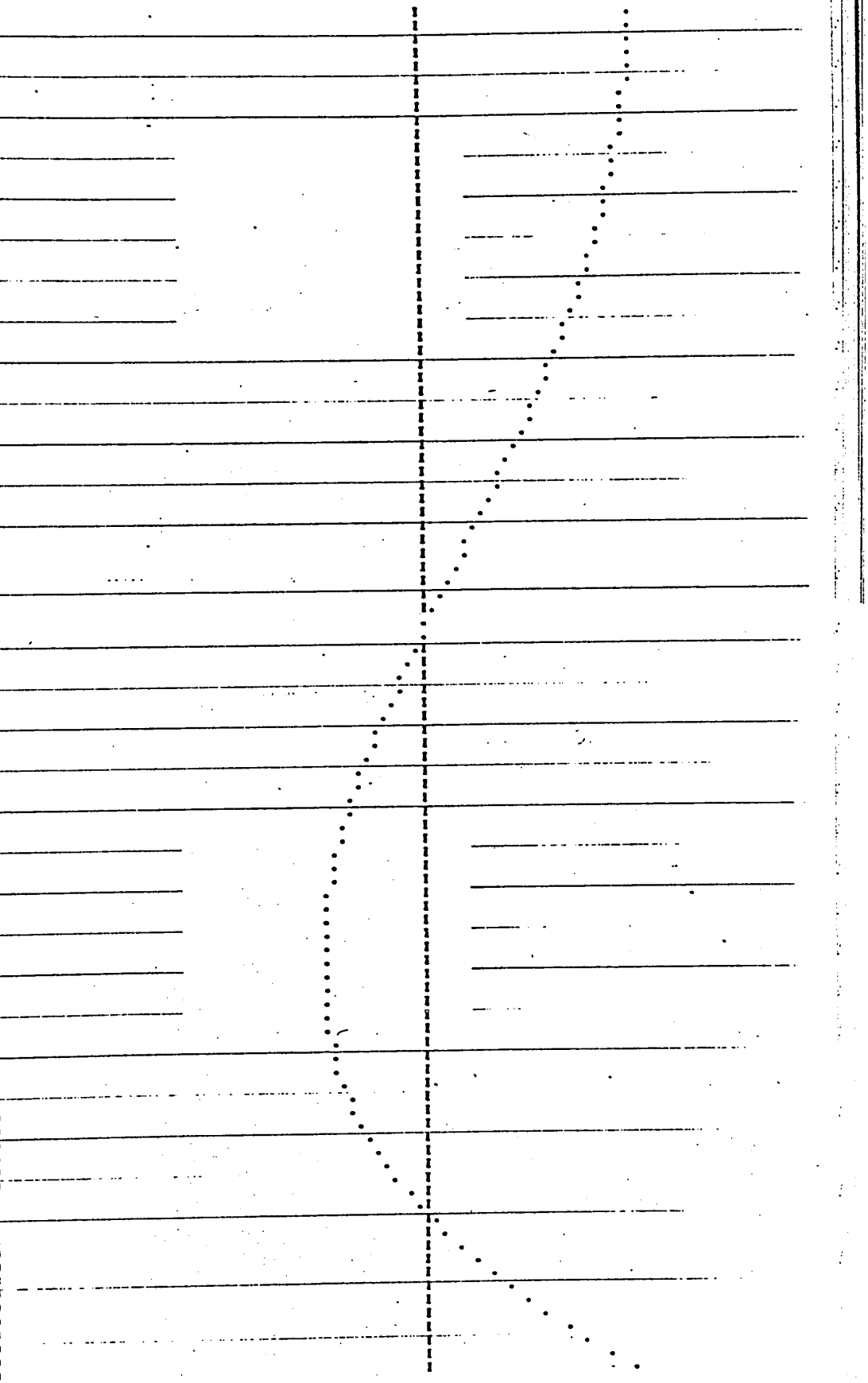

FIGURE 4.7B

ITERATION 2 WITH W_m = 1.0 AND (0, 2) MODE AS INPUT FUNCTION

W	Amplitude
0.0	0.99999999999999800 00
0.010	0.99938319246795250 00
0.020	0.99753354097850770 00
0.030	0.99445335875682870 00
0.040	0.99014650085929680 00
0.050	0.98461836372085740 00
0.060	0.97787588447484380 00
0.070	0.96992754012332470 00
0.080	0.96078334650190910 00
0.090	0.95045485705501570 00
0.100	0.93895516143403160 00
0.110	0.92629888389368960 00
0.120	0.91250218153687180 00
0.130	0.89758274229543940 00
0.140	0.88155978282654110 00
0.150	0.86445404613913290 00
0.160	0.84628779990190770 00
0.170	0.82708482961805170 00
0.180	0.80687044393093680 00
0.190	0.78567146333661260 00
0.200	0.76351622101942500 00
0.210	0.74043455856528000 00
0.220	0.71645782232671480 00
0.230	0.69161885960647580 00
0.240	0.66595201463802660 00
0.250	0.63949312439714260 00
0.260	0.61227951423846950 00
0.270	0.58434999332000530 00
0.280	0.55574484588153160 00
0.290	0.52650584631503350 00
0.300	0.49667621406437890 00
0.310	0.46630064834820500 00
0.320	0.43542530269310940 00
0.330	0.40409778329132390 00
0.340	0.37236714318223190 00
0.350	0.34028387625553430 00
0.360	0.30789991107558060 00
0.370	0.27526860451310910 00
0.380	0.24244473524026320 00
0.390	0.20948449699622610 00
0.400	0.17644549172872990 00
0.410	0.14339367225257565D 00
0.420	0.11038858638860410 00
0.430	0.77452866826406400-01
0.440	0.44702726282224310-01
0.450	0.12182698390622150-01
0.460	-0.20041319950544070-01
0.470	-0.51902076658933340-01
0.480	-0.83330972731761900-01
0.490	-0.11425807066441470 00
0.500	-0.14461210305222760 00
0.510	-0.17432048135090220 00
0.520	-0.20330930479428060 00
0.530	-0.23150336948835990 00
0.540	-0.25882617767596520 00
0.550	-0.28519994714405110 00
0.560	-0.31054562081050610 00
0.570	-0.33478287646783930 00
0.580	-0.35783013667610580 00
0.590	-0.37960457884019220 00
0.600	-0.40002214541674890 00
0.610	-0.41899755429791510 00
0.620	-0.43644430934619670 00
0.630	-0.45227471108168420 00
0.640	-0.46639986752552320 00
0.650	-0.47872970519715720 00
0.660	-0.48917298026591010 00
0.670	-0.49763728984288710 00
0.680	-0.50402908343947380 00
0.690	-0.50825367456098060 00
0.700	-0.51021525245079940 00
0.710	-0.50981689398746000 00
0.720	-0.50696057571564070 00
0.730	-0.50154718603158780 00
0.740	-0.49347653750638960 00
0.750	-0.48264737935179970 00
0.760	-0.46895741002239690 00
0.770	-0.45230328996531120 00
0.780	-0.43258065449856440 00
0.790	-0.40968412683195860 00
0.800	-0.38350733122239260 00
0.810	-0.35394290626129300 00
0.820	-0.32088251828787360 00
0.830	-0.28421687495776400 00
0.840	-0.24383573890712300 00
0.850	-0.19962794157021680 00
0.860	-0.15148139712095650 00
0.870	-0.99283116523149100-01
0.880	-0.42919221735875340-01
0.890	0.17726039993654590-01
0.900	0.82765281688307700-01
0.910	0.15231796209425940 00
0.920	0.22650037100707050 00
0.930	0.30543061448816060 00
0.940	0.38922759995533600 00
0.950	0.47801102117314740 00
0.960	0.57190134312034010 00
0.970	0.67101978675039060 00
0.980	0.77548831363184200 00
0.990	0.88542961050598930 00
1.000	0.10009670737053560 01

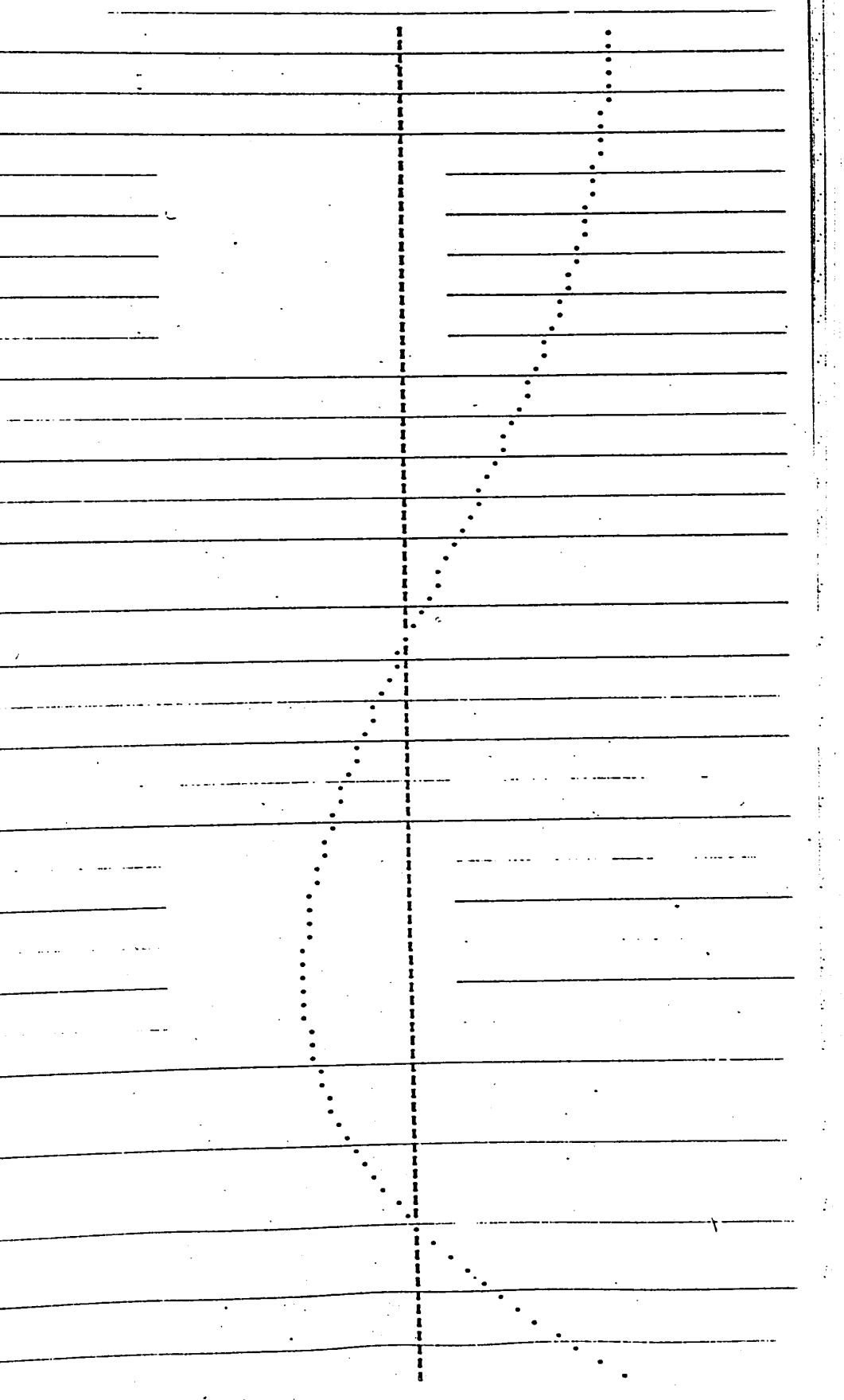

FIGURE 4.7C

ITERATION 3 WITH W_m = 1.0 AND (0, 2) MODE AS INPUT FUNCTION

W	Amplitude
0.0	0.9999999979999998D 00
0.010	0.9999956744034756D 00
0.020	0.9999826381797905D 00
0.030	0.9999610130277509D 00
0.040	0.9999306017825952D 00
0.050	0.9998913864220639D 00
0.060	0.9998432880745522D 00
0.070	0.9997861970298385D 00
0.080	0.9997199927521054D 00
0.090	0.9996445338953687D 00
0.100	0.9995596603211906D 00
0.110	0.9994651931188826D 00
0.120	0.9993609346279139D 00
0.130	0.9992466684628500D 00
0.140	0.9991221595404602D 00
0.150	0.9989871541093921D 00
0.160	0.9988413757819912D 00
0.170	0.9986845456862300D 00
0.180	0.9985163419142364D 00
0.190	0.9983364407373138D 00
0.200	0.9981444954712075D 00
0.210	0.9979401411076833D 00
0.220	0.9977229942429235D 00
0.230	0.9974926531257279D 00
0.240	0.9972486977082091D 00
0.250	0.9969906896985584D 00
0.260	0.9967181726163813D 00
0.270	0.9964306710501079D 00
0.280	0.9961276947168744D 00
0.290	0.9958087305246103D 00
0.300	0.9954732506363805D 00
0.310	0.9951207085371254D 00
0.320	0.9947505399025284D 00
0.330	0.9943621626702789D 00
0.340	0.9939549771134634D 00
0.350	0.9935283659163813D 00
0.360	0.9930816942523516D 00
0.370	0.9926143098640713D 00
0.380	0.9921255431459019D 00
0.390	0.9916147372285492D 00
0.400	0.9910910980659592D 00
0.410	0.9905239945242751D 00
0.420	0.9899426584731274D 00
0.430	0.9893363348791297D 00
0.440	0.9887042519013195D 00
0.450	0.9880456209890613D 00
0.460	0.9873596369818779D 00
0.470	0.9866454782116056D 00
0.480	0.9859023066065237D 00
0.490	0.9851292677976666D 00
0.500	0.9843254912273280D 00
0.510	0.9834900925955209D 00
0.520	0.9826221622928006D 00
0.530	0.9817207888745182D 00
0.540	0.9807850358184404D 00
0.550	0.9798139533224774D 00
0.560	0.9788065760905117D 00
0.570	0.9777619234549155D 00
0.580	0.9766789995014213D 00
0.590	0.9755567931953220D 00
0.600	0.9743942785152139D 00
0.610	0.9731904145739540D 00
0.620	0.9719441457616004D 00
0.630	0.9706544018752907D 00
0.640	0.9693200982569551D 00
0.650	0.9679401359320562D 00
0.660	0.9665134017502996D 00
0.670	0.9650387685280674D 00
0.680	0.9635150951929411D 00
0.690	0.9619412269299321D 00
0.700	0.9603159953296487D 00
0.710	0.9586382185383339D 00
0.720	0.9569068701409629D 00
0.730	0.9551202356582577D 00
0.740	0.9532776000154383D 00
0.750	0.9513775603809250 00
0.760	0.9494188700078442D 00
0.770	0.9474002696117553D 00
0.780	0.9453204875847436D 00
0.790	0.9431782401338115D 00
0.800	0.9409722314518733D 00
0.810	0.9387011538853664D 00
0.820	0.9363636381034664D 00
0.830	0.9339585032694594D 00
0.840	0.9314842572107215D 00
0.850	0.9289395965979110D 00
0.860	0.9263231571156582D 00
0.870	0.9236335636423362D 00
0.880	0.9208694304285147D 00
0.890	0.9180293612772418D 00
0.900	0.9151119497260950D 00
0.910	0.9121157923055030 00
0.920	0.9090394233486860 00
0.930	0.9058814459289219D 00
0.940	0.9026403012951460D 00
0.950	0.8993148344387236D 00
0.960	0.8959032812078195D 00
0.970	0.8924042684984870 00
0.980	0.8888163144547653D 00
0.990	0.8851379286501066D 00
1.000	0.8813676122944460 00

FIGURE 4.7D

ITERATION 4 WITH W_m = 1.0 AND (0, 2) MODE AS INPUT FUNCTION

W	Amplitude
0.0	0.9999999999999980D 00
0.010	0.9999877600899207D 00
0.020	0.9999510409643677D 00
0.030	0.9998830444373560D 00
0.040	0.9998041735321201D 00
0.050	0.9996940324809251D 00
0.060	0.9995594267248055D 00
0.070	0.9994003624132264D 00
0.080	0.9992168489036725D 00
0.090	0.9990088937611598D 00
0.100	0.9987765077576744D 00
0.110	0.9985197023715346D 00
0.120	0.9982384902860801D 00
0.130	0.9979326853918644D 00
0.140	0.9976029027789620D 00
0.150	0.9972485587464991D 00
0.160	0.9968659870769506D 00
0.170	0.9964668576076713D 00
0.180	0.9960395340995333D 00
0.190	0.9955879363621795D 00
0.200	0.9951120710879395D 00
0.210	0.9946119635730025D 00
0.220	0.9940876516959024D 00
0.230	0.9935391469362666D 00
0.240	0.9929064813627123D 00
0.250	0.9923696832335704D 00
0.260	0.9917487313950321D 00
0.270	0.9911038382792862D 00
0.280	0.9904347939026400D 00
0.290	0.9897417718635435D 00
0.300	0.9890247763405647D 00
0.310	0.9882838426902471D 00
0.320	0.9875190074449202D 00
0.330	0.9867305831046120D 00
0.340	0.9859177841639401D 00
0.350	0.9850814750512162D 00
0.360	0.9842214221844585D 00
0.370	0.9833376679345956D 00
0.380	0.9824302555364100D 00
0.390	0.9814992306222439D 00
0.400	0.9805446330964293D 00
0.410	0.9795665252602561D 00
0.420	0.9785649403270577D 00
0.430	0.9775399325395134D 00
0.440	0.9764915523605940D 00
0.450	0.9754196513704611D 00
0.460	0.9743246823102308D 00
0.470	0.9732066940143606D 00
0.480	0.9720653504522425D 00
0.490	0.9709009103450540D 00
0.500	0.9697134193176116D 00
0.510	0.9685029402712638D 00
0.520	0.9672695331831808D 00
0.530	0.9660132586445055D 00
0.540	0.9647341703558127D 00
0.550	0.9634323551233950D 00
0.560	0.9621078528554067D 00
0.570	0.9607607365579140D 00
0.580	0.9593910723303705D 00
0.590	0.9579989273640518D 00
0.600	0.9565843699328435D 00
0.610	0.9551474693442809D 00
0.620	0.9536882901822674D 00
0.630	0.9522069218037263D 00
0.640	0.9507034183339378D 00
0.650	0.9491776604121126D 00
0.660	0.9476303227368474D 00
0.670	0.9460608300615184D 00
0.680	0.9444676096896032D 00
0.690	0.9428505894699756D 00
0.700	0.9412216382920454D 00
0.710	0.9395656160309588D 00
0.720	0.9370078237926382D 00
0.730	0.9361886034088044D 00
0.740	0.9344680379319245D 00
0.750	0.9327262113801300D 00
0.760	0.9309632087818935D 00
0.770	0.9291791161710424D 00
0.780	0.9273740205814169D 00
0.790	0.9255480100411585D 00
0.800	0.9237011735677676D 00
0.810	0.9218336011623777D 00
0.820	0.9199453838042676D 00
0.830	0.9180366134452081D 00
0.840	0.9161073830411210D 00
0.850	0.9141577063607195D 00
0.860	0.9121879103504305D 00
0.870	0.9101976747581804D 00
0.880	0.9081877523120153D 00
0.890	0.9061578486631512D 00
0.900	0.9041076024539810D 00
0.910	0.9020375931173623D 00
0.920	0.8999464412651220D 00
0.930	0.8978374050943376D 00
0.940	0.8957100959228246D 00
0.950	0.8935630074154550D 00
0.960	0.8913945043151576D 00
0.970	0.8892049521520492D 00
0.980	0.8870041334215241D 00
0.990	0.8847757422203030D 00
1.000	0.8825360341040120D 00

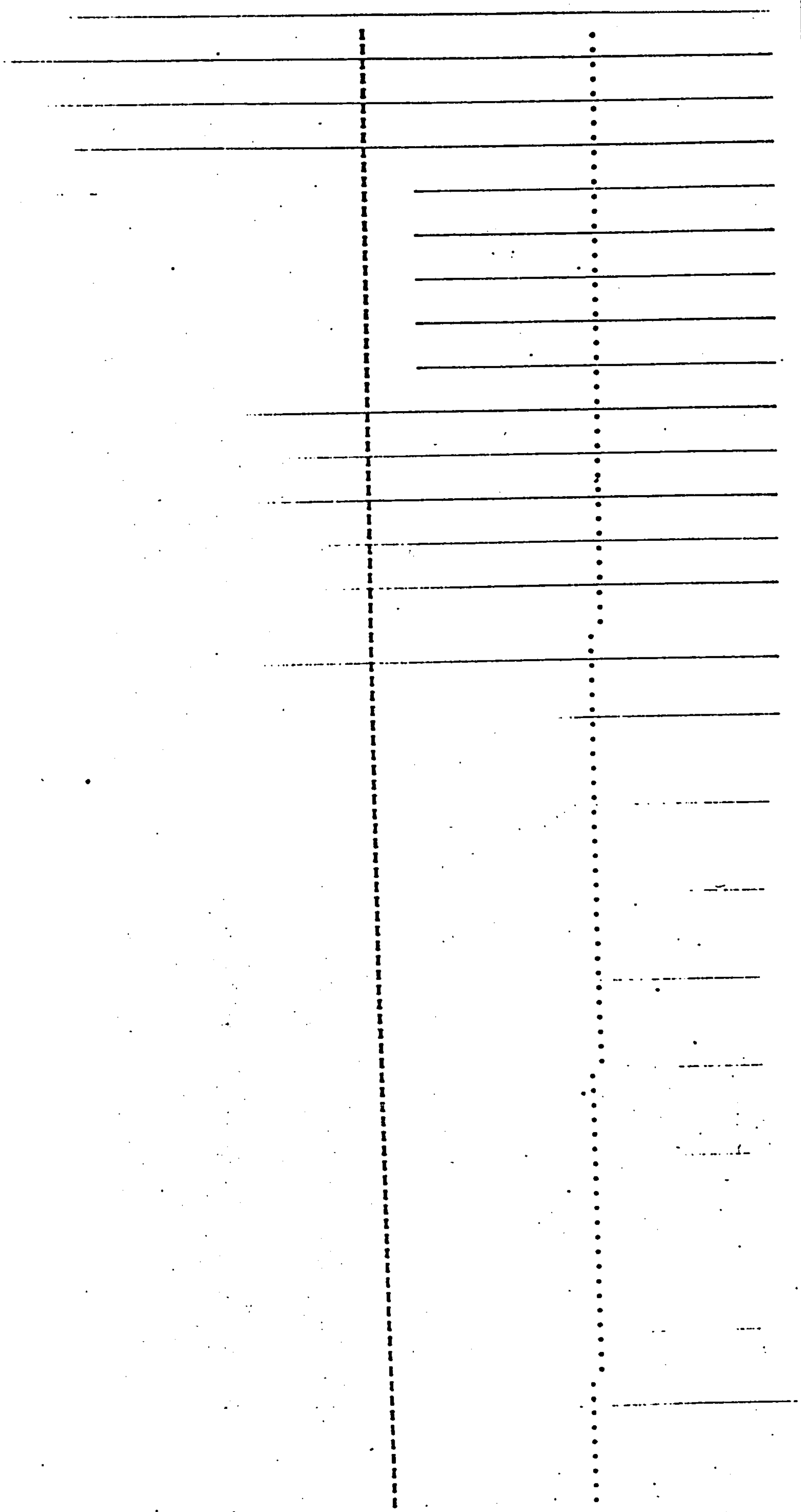

FIGURE 4.7E

ITERATION 18 WITH W_m = 1.0 AND (0, 2) MODE AS INPUT FUNCTION

W	Amplitude
0.0	0.99999999999999980D 00
0.010	0.99998776021899210 00
0.020	0.99995104148150400 00
0.030	0.99988984566410380 00
0.040	0.99980417561427990 00
0.050	0.99969403575025280 00
0.060	0.99955943146071180 00
0.070	0.99940036940447680 00
0.080	0.99921685745008450 00
0.090	0.99900890467530100 00
0.100	0.99877652136655600 00
0.110	0.99851971901830520 00
0.120	0.99823851033231720 00
0.130	0.99793290921698330 00
0.140	0.99760293078595590 00
0.150	0.99724859135820740 00
0.160	0.99686990845601920 00
0.170	0.99646690080439330 00
0.180	0.99603958832978920 00
0.190	0.99558799215888740 00
0.200	0.99511213461727790 00
0.210	0.99461203922807320 00
0.220	0.99408773071045050 00
0.230	0.99353923497811510 00
0.240	0.99296657913769310 00
0.250	0.99236979148704920 00
0.260	0.99174890151352980 00
0.270	0.99110393989213460 00
0.280	0.99043493848361120 00
0.290	0.98974193033247990 00
0.300	0.98902494986498290 00
0.310	0.98828403188696100 00
0.320	0.98751921358165680 00
0.330	0.98673053250744640 00
0.340	0.98591802759549660 00
0.350	0.98508173894735180 00
0.360	0.98422170783244460 00
0.370	0.98333797668554010 00
0.380	0.98243056891041014D 00
0.390	0.98149958984558950 00
0.400	0.98054502482468730 00
0.410	0.97956694111045390 00
0.420	0.97856538692340670 00
0.430	0.97754041163253470 00
0.440	0.97649206575223770 00
0.450	0.97542040093919710 00
0.460	0.97432546998917560 00
0.470	0.97320732683374640 00
0.480	0.97206602653695420 00
0.490	0.97090162529190270 00
0.500	0.96971418041727700 00
0.510	0.96850375035379360 00
0.520	0.96727039466056330 00
0.530	0.96601417401150400 00
0.540	0.96473515019138470 00
0.550	0.96343338609220370 00
0.560	0.96210894570919660 00
0.570	0.96076189413689670 00
0.680	0.95939229756510830 00
0.590	0.95800022327481500 00
0.600	0.95658573963401670 00
0.610	0.95514891609350330 00
0.620	0.95368982318256230 00
0.630	0.95220853250461760 00
0.640	0.95070511673280680 00
0.650	0.94917964960548780 00
0.660	0.94763220592168610 00
0.670	0.94606286153647290 00
0.680	0.94447169335628130 00
0.690	0.94285877933415620 00
0.700	0.94122419846494340 00
0.710	0.93956803078041280 00
0.720	0.93789035734431950 00
0.730	0.93619126024740180 00
0.740	0.93447082260231700 00
0.750	0.93272912853851500 00
0.760	0.93096626316705160 00
0.770	0.92918231272533660 00
0.780	0.92737736427182610 00
0.790	0.92555150598064950 00
0.800	0.92370482698618070 00
0.810	0.92183741740754450 00
0.820	0.91994936834306790 00
0.830	0.91804077186466990 00
0.840	0.91611172101219360 00
0.850	0.91416230978767890 00
0.860	0.91219263314957840 00
0.870	0.91020273700691640 00
0.880	0.90819286821338770 00
0.890	0.90616297456140320 00
0.900	0.90411320477607780 00
0.910	0.90204365850916170 00
0.920	0.89995443633291720 00
0.930	0.89784563973394150 00
0.940	0.89571737110693140 00
0.950	0.89356973374839800 00
0.960	0.89140283185032370 00
0.970	0.88921677704937707D 00
0.980	0.88701165564243140 00
0.990	0.88478759413613040 00
1.000	0.88254469368427200 00

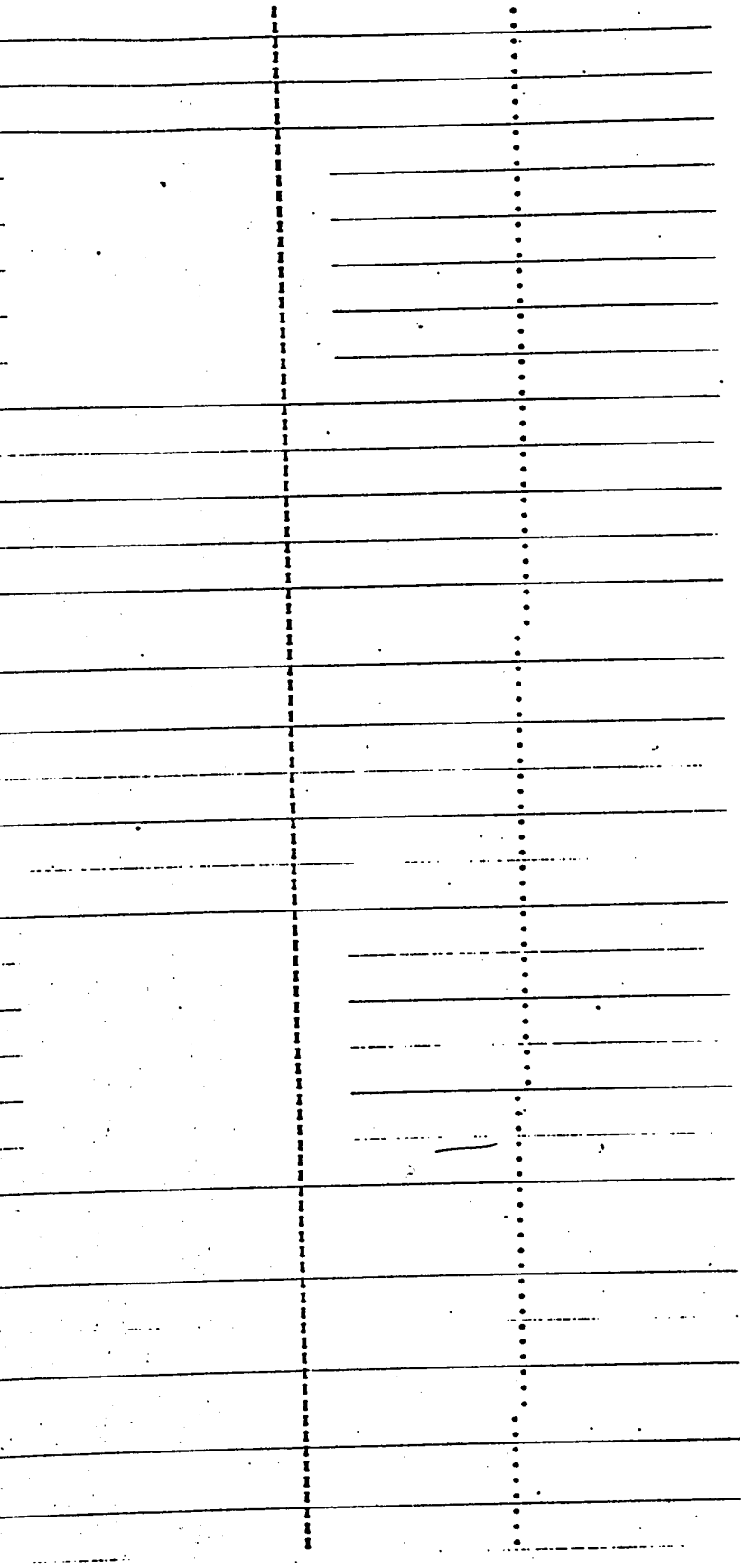

FIGURE 4.7F

ITERATION 19 WITH W_m = 1.0 AND (0. 2) MODE AS INPUT FUNCTION

W	Amplitude
0.0	0.9999999999999980D 00
0.010	0.9999877602189921D 00
0.020	0.9999510414815038D 00
0.030	0.9998898456041038D 00
0.040	0.9998041756162799D 00
0.050	0.9996940357502528D 00
0.060	0.9995594314607116D 00
0.070	0.9994003694044766D 00
0.080	0.9992168574500845D 00
0.090	0.9990089046753007D 00
0.100	0.9987765213665560D 00
0.110	0.9985197190183050D 00
0.120	0.9982385103323170D 00
0.130	0.9979329092168933D 00
0.140	0.9976029078595570 00
0.150	0.9972485913582071D 00
0.160	0.9968699084560192D 00
0.170	0.9964669008043929D 00
0.180	0.9960395883278890 00
0.190	0.9955879221588874D 00
0.200	0.9951121346172777D 00
0.210	0.9946120392280730D 00
0.220	0.9940877307104503D 00
0.230	0.9935392349781151D 00
0.240	0.9929665791376931D 00
0.250	0.9923697914870492D 00
0.260	0.9917489015135298D 00
0.270	0.9911039398921346D 00
0.280	0.9904349384836110D 00
0.290	0.9897419503247990D 00
0.300	0.9890249496649827D 00
0.310	0.9882840318869607D 00
0.320	0.9875192135816568D 00
0.330	0.9867305325074464D 00
0.340	0.9859180275954968D 00
0.350	0.9850817389473516D 00
0.360	0.9842217078324446D 00
0.370	0.9833379766855398D 00
0.380	0.9824305891041014D 00
0.390	0.9814995898455893D 00
0.400	0.9805450248246871D 00
0.410	0.9795669411104534D 00
0.420	0.9785653869214067D 00
0.430	0.9775404116325347D 00
0.440	0.9764920657522375D 00
0.450	0.9754204093919695D 00
0.460	0.9743256699891752D 00
0.470	0.9732073268337464D 00
0.480	0.9720660265369538D 00
0.490	0.9709016252919024D 00
0.500	0.9697141304172769D 00
0.510	0.9685037503537934D 00
0.520	0.9672704946605833D 00
0.530	0.9660141740115042D 00
0.540	0.9647351501913843D 00
0.550	0.9634333960922035D 00
0.560	0.9621089457091966D 00
0.570	0.9607618941368962D 00
0.580	0.9593922975651033D 00
0.590	0.9580002232748150D 00
0.600	0.9565857396340169D 00
0.610	0.9551489160935033D 00
0.620	0.9536898231825623D 00
0.630	0.9522085325046174D 00
0.640	0.9507051167328064D 00
0.650	0.9491796496054878D 00
0.660	0.9476322059216859D 00
0.670	0.9460628615364734D 00
0.680	0.9444716933502808D 00
0.690	0.9428587793341560D 00
0.700	0.9412241984469434D 00
0.710	0.9395680307804126D 00
0.720	0.9378903573443197D 00
0.730	0.9361912602474016D 00
0.740	0.9344708226023170D 00
0.750	0.9327291285385150D 00
0.760	0.9309662631920514D 00
0.770	0.9291823127253366D 00
0.780	0.9273773642718259D 00
0.790	0.9255515059806498D 00
0.800	0.9237048269861807D 00
0.810	0.9218374174075445D 00
0.820	0.9199493683430679D 00
0.830	0.9180407718646699D 00
0.840	0.9161117210121938D 00
0.850	0.9141623097876785D 00
0.860	0.9121926331495784D 00
0.870	0.9102027870059162D 00
0.880	0.9081928682133277D 00
0.890	0.9061629745614032D 00
0.900	0.9041132047760778D 00
0.910	0.9020436585091615D 00
0.920	0.8999544363329172D 00
0.930	0.8978456397339413D 00
0.940	0.8957173711069314D 00
0.950	0.8935697337403978D 00
0.960	0.8914028318503239D 00
0.970	0.8892167704937705D 00
0.980	0.8870116556424316D 00
0.990	0.8847875941361302D 00
1.000	0.8825446936842729D 00

FIGURE 4.7G

ITERATION 0 WITH W_m = 3.5, (0, 2) MODE INPUT FUNCTION

W	Amplitude
0.0	0.99999999999999800 00
0.035	0.99924128922146570 00
0.070	0.99696652063455700 00
0.105	0.99317970383406160 00
0.140	0.98788788930904300 00
0.175	0.98110036019579210 00
0.210	0.97282342074499150 00
0.245	0.96308998151507190 00
0.280	0.95189962131041000 00
0.315	0.93927856503089100 00
0.350	0.92524966341005880 00
0.385	0.90983835681692850 00
0.420	0.89307265290304880 00
0.455	0.87498308837893400 00
0.490	0.85560269280768000 00
0.525	0.83496694850694170 00
0.560	0.81311374745395400 00
0.595	0.79009334524136770 00
0.630	0.76591831213527300 00
0.665	0.74066348128975760 00
0.700	0.71436589417566540 00
0.735	0.68707474328429890 00
0.770	0.65884131216976110 00
0.805	0.62971891289677320 00
0.840	0.59976282096354700 00
0.875	0.56903020777222310 00
0.910	0.53758007072205480 00
0.945	0.50547316100326160 00
0.980	0.47277190917197130 00
1.015	0.43954034858925480 00
1.050	0.40584403680956590 00
1.085	0.37174997500825960 00
1.120	0.33732652552410510 00
1.155	0.30264332765071980 00
1.190	0.26777121170107190 00
1.225	0.23278211151078060 00
1.260	0.19774897543617650 00
1.295	0.16274567596033910 00
1.330	0.12784691800637830 00
1.365	0.93128146060275000-01
1.400	0.58665450207343900-01
1.435	0.24535471187334520-01
1.470	-0.91844954253652980-02
1.505	-0.42417595809275640-01
1.540	-0.75085515142646500-01
1.575	-0.10711057540074010 00
1.610	-0.13841483353366470 00
1.645	-0.16892038033455040 00
1.680	-0.19854943862736670 00
1.715	-0.22722446276329500 00
1.750	-0.25486232721441300 00
1.785	-0.28140397541346360 00
1.820	-0.30675541830628250 00
1.855	-0.33084693257995470 00
1.890	-0.35360360841377410 00
1.925	-0.37495135671261700 00
1.960	-0.39481700564288230 00
1.995	-0.41312839640375590 00
2.030	-0.42981447811131640 00
2.065	-0.44480540168995670 00
2.100	-0.45803261266441670 00
2.135	-0.46942894274724290 00
2.170	-0.47892870011704500 00
2.205	-0.48646775828519280 00
2.240	-0.49198364344893970 00
2.275	-0.49541562023175830 00
2.310	-0.49670477571226280 00
2.345	-0.49579410164540060 00
2.380	-0.49262857478180350 00
2.415	-0.48715523519231160 00
2.450	-0.47932326250762820 00
2.485	-0.46908404998470590 00
2.520	-0.45639127631419810 00
2.555	-0.44120097508517950 00
2.590	-0.42347160182627360 00
2.625	-0.40316409854474570 00
2.660	-0.38024195568769410 00
2.695	-0.35467127145213980 00
2.730	-0.32642080837393940 00
2.765	-0.29546204712818160 00
2.800	-0.26176923747638290 00
2.835	-0.22531944629952910 00
2.870	-0.18609260265812790 00
2.905	-0.14407153982513750 00
2.940	-0.99242034238810900-01
2.975	-0.51342841327571110-01
3.010	-0.11157281618024580-02
3.045	0.52194497109791310-01
3.080	0.10833995907726290 00
3.115	0.16731969217485600 00
3.150	0.22912962110618060 00
3.185	0.29376254461725070 00
3.220	0.36120812264098620 00
3.255	0.43145266663439590 00
3.290	0.50448013452497340 00
3.325	0.58027012600003220 00
3.360	0.65879988570781030 00
3.395	0.74004330569744490 00
3.430	0.82397113409893500 00
3.465	0.91055098584224550 00
3.500	0.99974735729020330 00

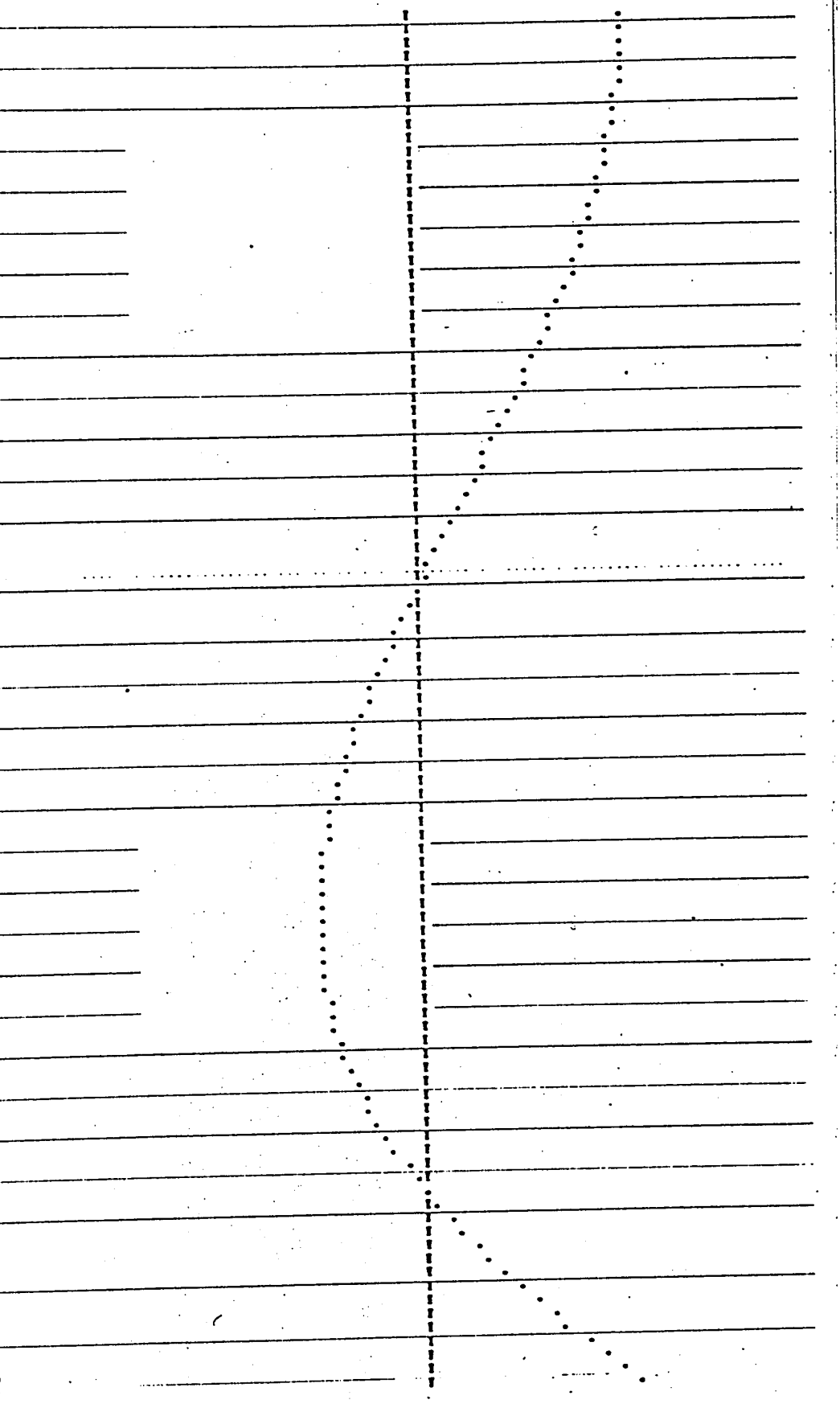

FIGURE 4.8A

ITERATION 1 WITH W_m = 3.5, (0, 2) MODE INPUT FUNCTION

w	Amplitude
0.0	0.9999999999999980D 00
0.035	0.9992412892214461D 00
0.070	0.9969665206345306D 00
0.105	0.9531797838339930D 00
0.140	0.9870378893089253D 00
0.175	0.9811003601955085D 00
0.210	0.9728294207446303D 00
0.245	0.9630899815147151D 00
0.280	0.9518996213059399D 00
0.315	0.9392785658803144D 00
0.350	0.9252496634093523D 00
0.385	0.9098383568160710D 00
0.420	0.8930726529020507D 00
0.455	0.8749830883777551D 00
0.450	0.8556026928063082D 00
0.525	0.8349669485053776D 00
0.560	0.8131137474521900D 00
0.595	0.7900833452394004D 00
C.630	0.7659183121330799D 00
0.665	0.7406634812873373D 00
0.7C0	0.7143658941729970D 00
0.735	0.6870747432813886D 00
0.770	0.6588413121665881D 00
0.8C5	0.6297189128933473D 00
0.840	0.5997628209598579D 00
0.875	0.5690302077682518D 00
C.910	0.5375800707178033D 00
0.945	0.5054731609987270D 00
0.980	0.4727719091671482D 00
1.015	0.4395403485841542D 00
1.050	0.4058440368041724D 00
1.085	0.3717499750005799D 00
1.120	0.3373265255181272D 00
1.155	0.3026433276444662D 00
1.190	0.2677712116945254D 00
1.225	0.2327821115039518D 00
1.260	0.1977489754290653D 00
1.295	0.1627456759529486D 00
1.330	0.1278469179987169D 00
1.365	0.9312814605234490D-01
1.400	0.5866545019915381D-01
1.435	0.2453547117883796D-01
1.47C	-0.9184695434058229D-02
1.5C5	-0.4241759581820105D-01
1.540	-0.7508551515180710D-01
1.575	-0.1C71105754101093D 00
1.610	-0.1384148336032375D 00
1.645	-0.1689203803443159D 00
1.680	-0.1985494385373169D 00
1.715	-0.2272244627734165D 00
1.750	-0.2548682372246919D 00
1.785	-0.2814039754238737D 00
1.820	-0.3067554183198263D 00
1.855	-0.3308469325906157D 00
1.890	-0.3536036084245295D 00
1.925	-0.3749513567234477D 00
1.960	-0.3948170056537754D 00
1.995	-0.4131283964146941D 00
2.030	-0.4298144781222827D 00
2.065	-0.4448054017009301D 00
2.1C0	-0.4580326126753779D 00
2.135	-0.4694289427581763D 00
2.17C	-0.4789287001279323D 00
2.2C5	-0.4864677582960090D 00
2.240	-0.4919836434596751D 00
2.275	-0.4954156202473875D 00
2.310	-0.4967047757227689D 00
2.345	-0.4957941016557580D 00
2.38C	-0.4926285747919993D 00
2.415	-0.4871552352023220D 00
2.450	-0.4793232625174352D 00
2.485	-0.4690940499942922D 00
2.520	-0.4563912763235422D 00
2.555	-0.4412009750942651D 00
2.590	-0.4234716018350799D 00
2.625	-0.4031640985532589D 00
2.660	-0.3802419556958960D 00
2.695	-0.3546712714600073D 00
2.730	-0.3264208083814634D 00
2.765	-0.2954620471353472D 00
2.800	-0.2617697374831694D 00
2.835	-0.2253194463059262D 00
2.870	-0.1960926026641197D 00
2.905	-0.1440715398307170D 00
2.940	-0.9974203474396190D-01
2.975	-0.5159794133227883D-01
3.010	-0.1115728166063476D-02
3.045	0.5219449710559331D-01
3.080	0.1083399590739215D 00
3.115	0.1673196921719985D 00
3.150	0.229129671103797[illegible] 00
3.195	0.293742564461533[illegible] 00
3.220	0.3612041226395526D 00
3.255	0.4314528668334476D 00
3.290	0.5044901345245073D 00
3.325	0.5402701260804930D 00
3.360	0.659799335709[illegible] 00
3.395	0.7409433056994172D 00
3.430	0.8230711341023743D 00
3.465	0.9105509956441450D 00
3.500	0.99474735729[illegible] 00

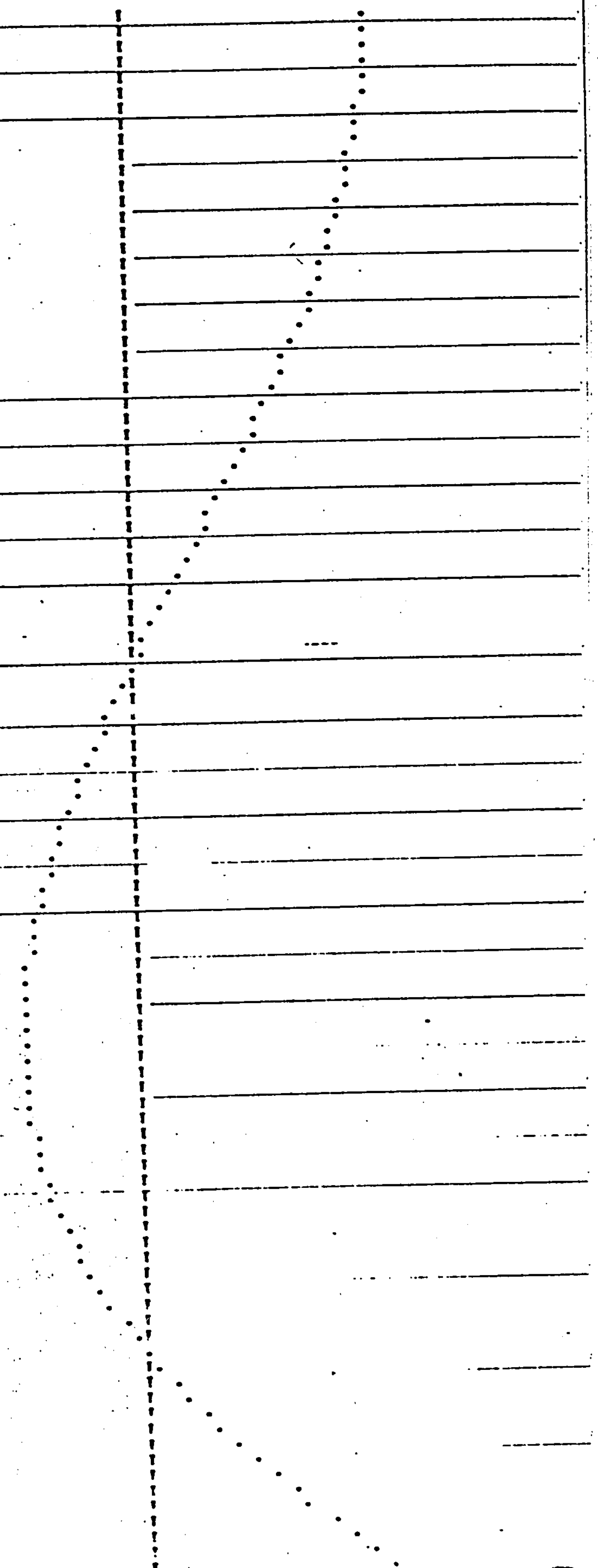

FIGURE 4.8B

ITERATION 6 WITH W_m = 3.5, (0, 2) MODE INPUT FUNCTION

W	Amplitude
0.0	0.99999999999998CD 00
0.035	0.99924022132460009D 00
0.070	0.99695225121711154D 00
0.105	0.99317018577957553D 00
0.140	0.98787084633756440D 00
0.175	0.98107377117972760 00
0.210	0.97279120400616810 00
0.245	0.96303807500917620 00
0.280	0.95183200322617750 00
0.315	0.93919323431567140 00
0.350	0.92514465689508220 00
0.385	0.90971175435276680 00
0.420	0.89292257803388510 00
0.455	0.87480771321174130 00
0.490	0.85540024197121980 00
0.525	0.83473570304571360 00
0.560	0.81285204855211460 00
0.595	0.78978959837198040 00
0.630	0.76559099013003150 00
0.665	0.74030112832478550 00
0.700	0.71396712916859290 00
0.735	0.68663826329849660 00
0.770	0.65836589572117950 00
0.805	0.62920342315929660 00
0.840	0.59920620886878900 00
0.875	0.56843151499968760 00
0.910	0.53693843257595690 00
0.945	0.50478780917216550 00
0.980	0.47204217436769120 00
1.015	0.43876566106161270 00
1.050	0.40502393673362230 00
1.085	0.37088410273888270 00
1.120	0.33641463172684080 00
1.155	0.30168527327615210 00
1.190	0.26676696983978580 00
1.225	0.23173176909656830 00
1.260	0.19665273480694770 00
1.295	0.16160385627255320 00
1.330	0.12665995650089050 00
1.365	0.91896599177718000-01
1.400	0.57389934551259160-01
1.435	0.23216904333560000-01
1.470	-0.10545454274524080-01
1.505	-0.43819505327237060-01
1.540	-0.76527411538219200-01
1.575	-0.10859117223607250 00
1.610	-0.13993272176116230 00
1.645	-0.17047402819331190 00
1.680	-0.20013719229940550 00
1.715	-0.22884454658974210 00
1.750	-0.25651875437160180 00
1.785	-0.28308290869871140 00
1.820	-0.30846063103495680 00
1.855	-0.33257616973127560 00
1.890	-0.35535449785448180 00
1.925	-0.37672141060769080 00
1.960	-0.39660362202210130 00
1.995	-0.41492886088080720 00
2.030	-0.43162596575594240 00
2.065	-0.44662497905178020 00
2.100	-0.45985723994585060 00
2.135	-0.47125547612450150 00
2.170	-0.48075389420631180 00
2.205	-0.48828826875191960 00
2.240	-0.49379602975174900 00
2.275	-0.49721634853420660 00
2.310	-0.49849022186973170 00
2.345	-0.49756055438405080 00
2.380	-0.49437223897651860 00
2.415	-0.48887223527628370 00
2.450	-0.48100964600414850 00
2.485	-0.47073579115787260 00
2.520	-0.45800427993401800 00
2.555	-0.44277108030431360 00
2.590	-0.42499458616358190 00
2.625	-0.40463568197190140 00
2.660	-0.38165780481451640 00
2.695	-0.35602700380634820 00
2.730	-0.32771199677082190 00
2.765	-0.29668422412560290 00
2.800	-0.26291789991045460 00
2.835	-0.22639005989619270 00
2.870	-0.18708060671570510 00
2.905	-0.14497235196295240 00
2.940	-0.10005105520677850 00
2.975	-0.52305459871688520-01
3.010	-0.17273259402830970-02
3.045	0.51688540564983480-01
3.080	0.10794426135879680 00
3.115	0.16703886296372310 00
3.150	0.22896825710613840 00
3.185	0.29372522446549040 00
3.220	0.36129940180053190 00
3.255	0.43167727274737953D 00
3.290	0.50484216039085100 00
3.325	0.58077422736810220 00
3.360	0.65945047393794510 00
3.395	0.74084474359845370 00
3.430	0.82492773050862770 00
3.465	0.91166699062842070 00
3.500	0.10010269562981670 01

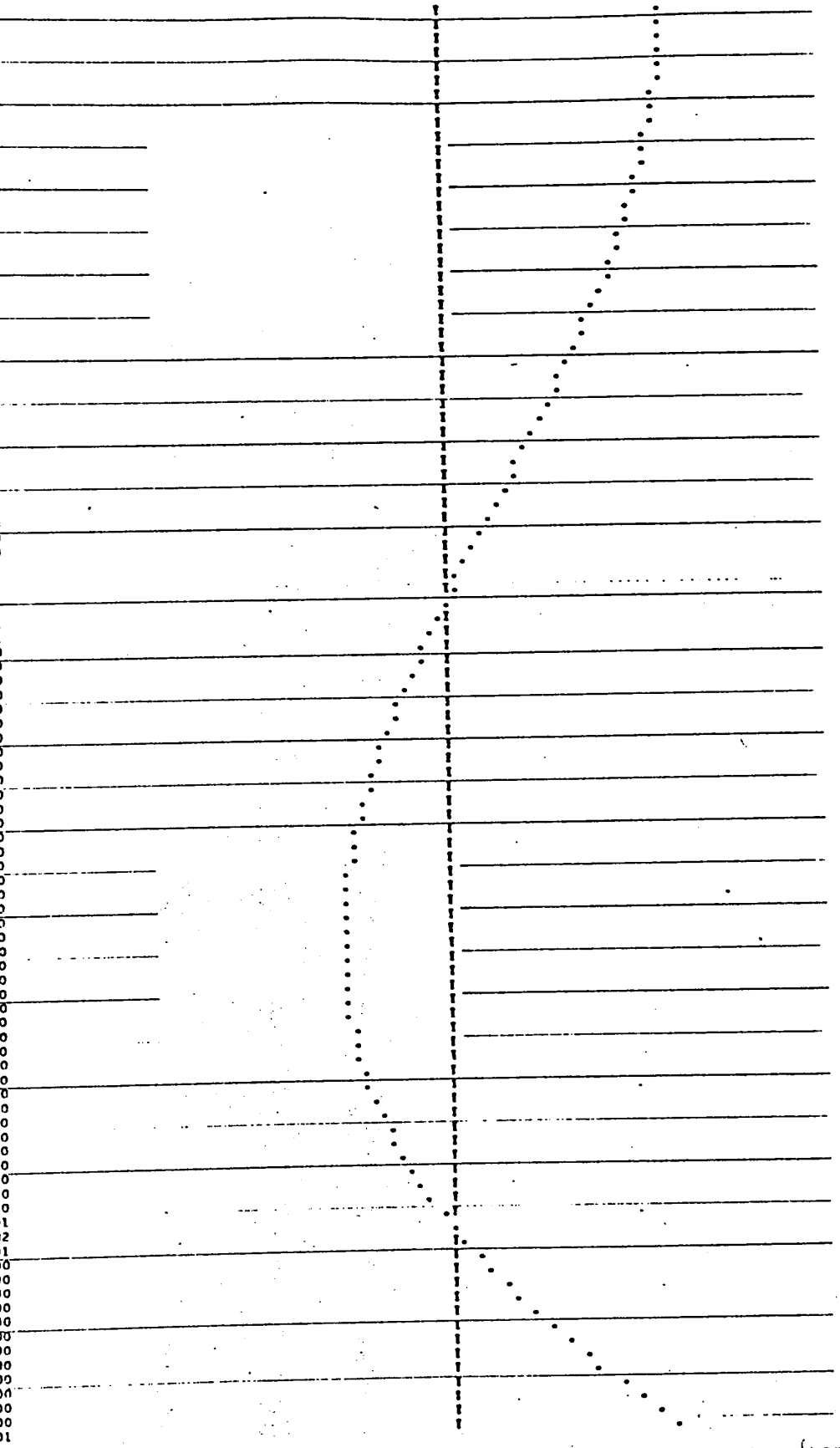

FIGURE 4.8C

ITERATION 7 WITH W_m = 3.5, (0, 2) MODE INPUT FUNCTION.

w	Amplitude
0.0	0.9999999999999980D 00
0.035	0.9991916503806 60 00
0.070	0.9967680661003461D 00
0.105	0.9927336391213621D 00
0.140	0.9870956834615407D 00
0.175	0.9798644263266704D 00
0.210	0.9710529957071978D 00
0.245	0.9606774044551027D 00
0.280	0.9487565308584548D 00
0.315	0.9353120957352376D 00
0.350	0.9203686360718319D 00
0.385	0.9039534752356028D 00
0.420	0.8860966897946045D 00
0.455	0.8668310729813850D 00
0.490	0.8461920948415650D 00
0.525	0.8242178591113933D 00
0.560	0.8009490568723862D 00
0.595	0.7764289170346323D 00
0.630	0.7507031537037365D 00
0.665	0.7238199104901548D 00
0.700	0.6958297018227761D 00
0.735	0.6667853513322330D 00
0.770	0.6367419273724066D 00
0.805	0.6057566757520795D 00
0.840	0.5738889497515691D 00
0.875	0.5412001375024062D 00
0.910	0.5077535868108998D 00
0.945	0.4736145275094793D 00
0.980	0.4388499914223156D 00
1.015	0.4035287300345136D 00
1.050	0.3677211299567519D 00
1.085	0.3314991262795448D 00
1.120	0.2949361139141049D 00
1.155	0.2581068570184741D 00
1.190	0.2210873966103829D 00
1.225	0.1839549564697275D 00
1.260	0.1467878474362522D 00
1.295	0.1096653702089314D 00
1.330	0.7266771675614910D-01
1.365	0.3587587044687534D-01
1.400	-0.6284949855007546D-03
1.435	-0.3676311753335028D-01
1.470	-0.7244524999474774UD-01
1.505	-0.1075917635776313D 00
1.540	-0.1421192529617472D 00
1.575	-0.1759441409510134D 00
1.610	-0.2089827843483011D 00
1.645	-0.2411515798839127D 00
1.680	-0.2723670704287059D 00
1.715	-0.3025460513223565D 00
1.750	-0.3316056766970471D 00
1.785	-0.3594635656769707D 00
1.820	-0.3860379083335119D 00
1.855	-0.4112475712776264D 00
1.890	-0.4350122027684992D 00
1.925	-0.4572523372214520D 00
1.960	-0.4778994989575240D 00
1.995	-0.4968463053452907D 00
2.030	-0.5140465684153119D 00
2.065	-0.5294153961695022D 00
2.100	-0.5428792921327343D 00
2.135	-0.5543662538361742D 00
2.170	-0.5638058698523318D 00
2.205	-0.5711294153098851D 00
2.240	-0.5762694577854690D 00
2.275	-0.5791623894172137D 00
2.310	-0.5797436372794413D 00
2.345	-0.5779526316724177D 00
2.380	-0.5737304524684580D 00
2.415	-0.5670204012687802D 00
2.450	-0.5577680833228998D 00
2.485	-0.5459214871084057D 00
2.520	-0.5314310614790733D 00
2.555	-0.5142497902912104D 00
2.590	-0.4943332644211588D 00
2.625	-0.4716397510897072D 00
2.660	-0.4461302604117622D 00
2.695	-0.4177686090925842D 00
2.730	-0.3865214811952177D 00
2.765	-0.3523584859067252D 00
2.800	-0.3152522122336491D 00
2.835	-0.2751782805612104D 00
2.870	-0.2321153910129141D 00
2.905	-0.1860453685524516D 00
2.940	-0.1369532047708954D 00
2.975	-0.8482709630771200-01
3.010	-0.2965847985750027D-01
3.045	0.2855793628434817D-01
3.080	0.8982414417571650D-01
3.115	0.1541388117212591D 00
3.150	0.2214972617377119D 00
3.185	0.2918914546217019D 00
3.220	0.3653099746452228D 00
3.255	0.4417380199016902D 00
3.290	0.5211573959201631D 00
3.325	0.6035465129624932D 00
3.360	0.6888803870128798D 00
3.395	0.7771306446729440 00
3.430	0.8682655305240625D 00
3.465	0.9622499212744550D 00
3.500	0.1059045339487585D 01

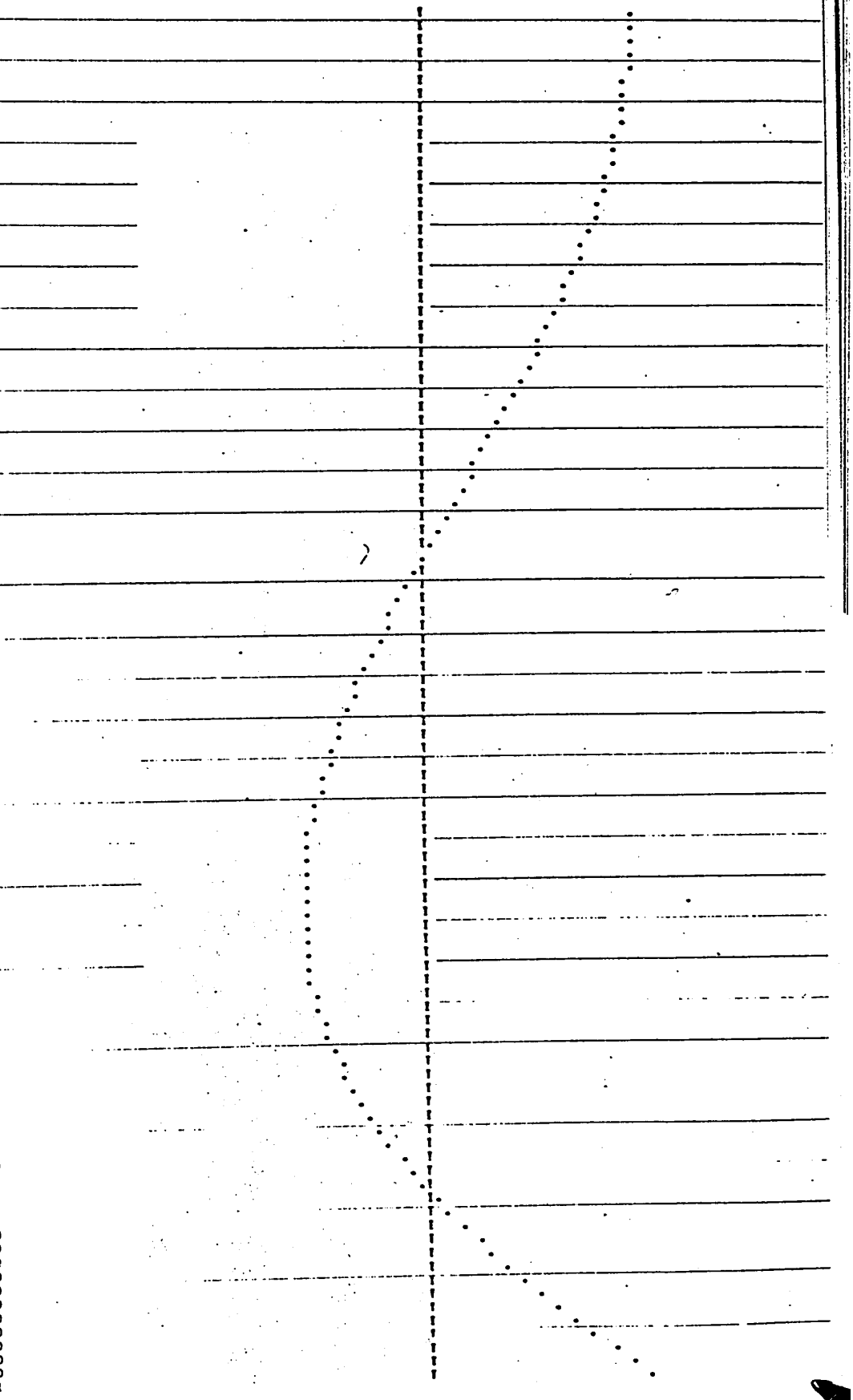

FIGURE 4.8D

ITERATION 8 WITH W_m = 3.5, (0, 2) MODE INPUT FUNCTION

W	Amplitude
0.0	0.9999999999999980D 00
0.035	0.1000184612216239D 01
0.070	0.1000738961876220 01
0.105	0.1001658194598611D 01
0.140	0.1002942747644182D 01
0.175	0.1004587696608345D 01
0.210	0.1006588088682360 01
0.245	0.1008937884318308D 01
0.280	0.1011629963207093D 01
0.315	0.1014656135377736D 01
0.350	0.1018007150901813D 01
0.385	0.1021672712094074D 01
0.420	0.1025641486894739D 01
0.455	0.1029901123603902D 01
0.490	0.1034438266951231D 01
0.525	0.1039238575482832D 01
0.560	0.1044286740245174D 01
0.595	0.1049566504745100D 01
0.630	0.1055060686162778D 01
0.665	0.1060751197793807D 01
0.700	0.1066619072694503D 01
0.735	0.1072644488503600D 01
0.770	0.1078806793411977D 01
0.805	0.1085084533250719D 01
0.840	0.1091455479666574D 01
0.875	0.1097896659352712D 01
0.910	0.1104384384301217D 01
0.945	0.1110894283042849D 01
0.980	0.1117401332838292D 01
1.015	0.1123879892784074D 01
1.050	0.1130303737795237D 01
1.085	0.1136646609342589D 01
1.120	0.1142879671487688D 01
1.155	0.1148976706425466D 01
1.190	0.1154908992408312D 01
1.225	0.1160647921093487D 01
1.260	0.1166164520019872D 01
1.295	0.1171429491586926D 01
1.330	0.1176413752577693D 01
1.365	0.1181085974154447D 01
1.400	0.1185417622361481D 01
1.435	0.1189377993951952D 01
1.470	0.1192936782629543D 01
1.505	0.1196063570574128D 01
1.540	0.1198727920231403D 01
1.575	0.1200899391314276D 01
1.610	0.1202547587967297D 01
1.645	0.1203642201045555D 01
1.680	0.1204153050458962D 01
1.715	0.1204050127532301D 01
1.750	0.1203303637333810D 01
1.785	0.1201884040919807D 01
1.820	0.1199762097449521D 01
1.855	0.1196908906119107D 01
1.890	0.1193295947866566D 01
1.925	0.1188895126798814D 01
1.960	0.1183679811292425D 01
1.995	0.1177619874719872D 01
2.030	0.1170691735753530D 01
2.065	0.1162868398200087D 01
2.100	0.1154124490318364D 01
2.135	0.1144435303574300D 01
2.170	0.1133776830787123D 01
2.205	0.1122125903621729D 01
2.240	0.1109459729382489D 01
2.275	0.1095756927064927D 01
2.310	0.1080996562622109D 01
2.345	0.1065158683403466D 01
2.380	0.1048224251724927D 01
2.415	0.1030175177529677D 01
2.450	0.1010994350102360 01
2.485	0.9906656687832313D 00
2.520	0.9691740726995641D 00
2.555	0.9465055693335202D 00
2.590	0.9226472621755856D 00
2.625	0.8975873770349971D 00
2.660	0.8713152873390701D 00
2.695	0.8438215381776943D 00
2.730	0.8150978691326780D 00
2.765	0.7851372358529373D 00
2.800	0.7539338303477056D 00
2.835	0.7214830999716361D 00
2.870	0.6877817650765889D 00
2.905	0.6528278353070657D 00
2.940	0.6166206245167564D 00
2.975	0.5791607642859728D 00
3.010	0.5404502160209556D 00
3.045	0.5004922816173211D 00
3.080	0.4592916176718917D 00
3.115	0.4168542182284606D 00
3.150	0.3731874710447400D 00
3.185	0.3283011123691089D 00
3.220	0.2822022552178933D 00
3.255	0.2349053861449319D 00
3.290	0.1864223654972940D 00
3.325	0.1367674261522915D 00
3.360	0.8595617073312900D-01
3.395	0.3400556730125732D-01
3.430	-0.1906605647172807D-01
3.465	-0.7373902066500100D-01
3.500	-0.1284923019565429D 00

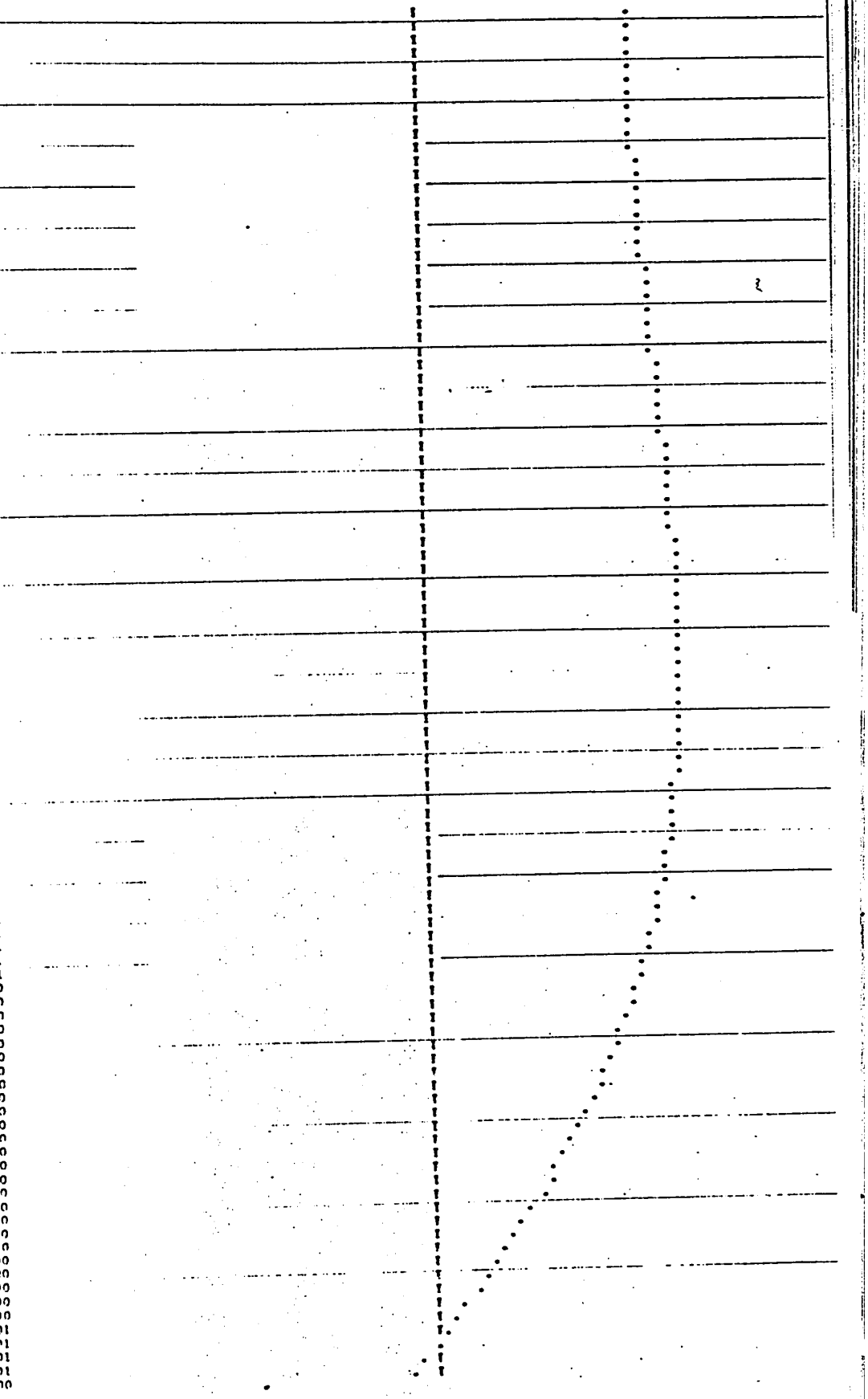

FIGURE 4.8E

ITERATION 9 WITH W_m = 3.5, (0, 2) MODE INPUT FUNCTION

W	Amplitude
0.0	0.999999999999999D 00
0.035	0.999988645265629050 00
0.070	0.999545863793134D 00
0.105	0.998978392732472OD 00
0.140	0.998184304964283 6D 00
0.175	0.997163971936794 8D 00
0.210	0.995917870842910 3D 00
0.245	0.994446584333033 3D 00
0.280	0.992750800164503 7D 00
0.315	0.990831310787786 6D 00
0.350	0.988689012869872 1D 00
0.385	0.986324906755047 0D 00
0.420	0.983740095863501 6D 00
0.455	0.980935786028162 8D 00
0.490	0.977911328477020 7 4D 00
0.525	0.974674000513755 7D 00
0.560	0.971219441740289 9D 00
0.595	0.967551216083367 4D 00
0.630	0.963671029364268 2D 00
0.665	0.959580684589222 7D 00
0.700	0.955282080768931 7D 00
0.735	0.950777211981121 0D 00
0.770	0.946068165976902 5D 00
0.805	0.941157123031775 4D 00
0.840	0.936046354622108 9D 00
0.875	0.930738222068014 0D 00
0.910	0.925235175123518 3D 00
0.945	0.919539750515029 9D 00
0.980	0.913654570429071 9D 00
1.015	0.907582340950331 6D 00
1.050	0.901325850451093 6D 00
1.085	0.894887967933153 1D 00
1.120	0.888271641323344 2D 00
1.155	0.881479895723844 0D 00
1.190	0.874515831618452 6D 00
1.225	0.867382623036063 2D 00
1.260	0.860083515672577 6D 00
1.295	0.852621824972547 0D 00
1.330	0.845000934171838 7D 00
1.365	0.837224292302660 9D 00
1.400	0.829295412162301 2D 00
1.435	0.821217868246952 1D 00
1.470	0.812995294652031 7D 00
1.505	0.804631382940412 1D 00
1.540	0.796129879958000 5D 00
1.575	0.787494585752164 0D 00
1.610	0.778729351132372 7D 00
1.645	0.769838075644740 2D 00
1.680	0.760824705191784 4D 00
1.715	0.751693229761058 3D 00
1.750	0.742447681110139 2D 00
1.785	0.733092130431552 7D 00
1.820	0.723630685999180 7D 00
1.855	0.714067490797740 8D 00
1.890	0.704406720136912 6D 00
1.925	0.694652579251710 6D 00
1.960	0.684809300890699 8D 00
1.995	0.674881142893658 2D 00
2.030	0.664872385760298 0D 00
2.065	0.654787330211654 6D 00
2.100	0.644630294745767 8D 00
2.135	0.634405613184925 6D 00
2.170	0.624117632246411 0D 00
2.205	0.613770709047427 3D 00
2.240	0.603369208697370 0D 00
2.275	0.592917501827493 9D 00
2.310	0.582419962150523 0D 00
2.345	0.571880964021469 9D 00
2.380	0.561304880005609 7D 00
2.415	0.550696078455165 5D 00
2.450	0.540058921096297 8D 00
2.485	0.529397760627942 0D 00
2.520	0.518716938334057 7D 00
2.555	0.508020781710817 3D 00
2.590	0.497313602110261 7D 00
2.625	0.486599692401940 4D 00
2.660	0.475883324653985 5D 00
2.695	0.465168747835170 6D 00
2.730	0.454460185539330 0D 00
2.765	0.443761833733640 6D 00
2.800	0.433077858532124 0D 00
2.835	0.422412393995822 8D 00
2.870	0.411769539960997 9D 00
2.905	0.401153359896679 4D 00
2.940	0.390567878792937 3D 00
2.975	0.380017081081119 6D 00
3.010	0.369504908587438 0D 00
3.045	0.359035258520983 4D 00
3.080	0.348611981497565 2D 00
3.115	0.338238879606045 3D 00
3.150	0.327919704479237 2D 00
3.185	0.317658155487923 1D 00
3.220	0.307457877863362 0D 00
3.255	0.297322460945104 3D 00
3.290	0.287255436437696 2D 00
3.325	0.277260276716437 1D 00
3.360	0.267340393177572 6D 00
3.395	0.257499134633852 6D 00
3.430	0.247739785756362 3D 00
3.465	0.238065565563503 5D 00
3.500	0.228479625957940 2D 00

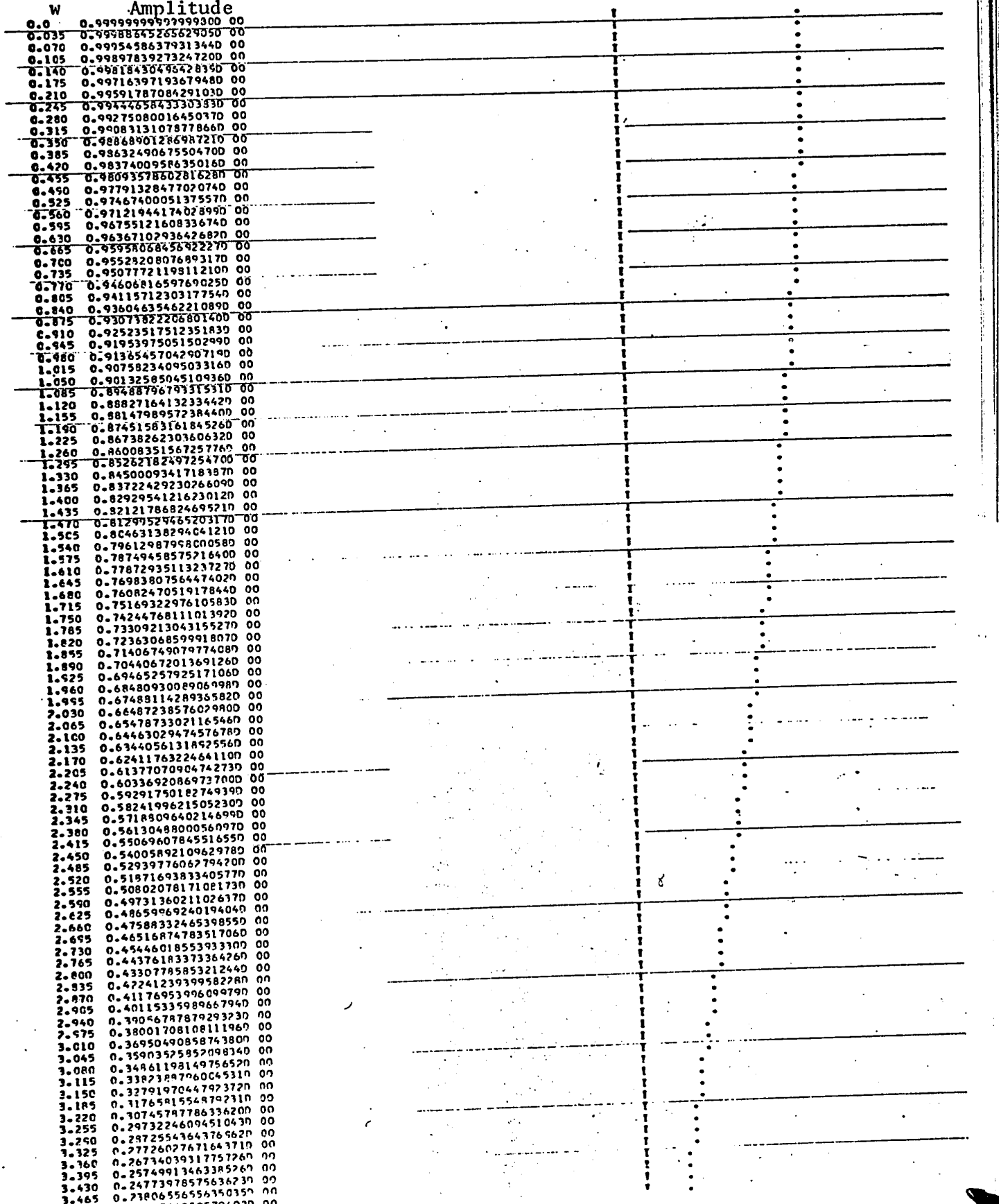

FIGURE 4.8F

ITERATION 39 WITH W_m = 3.5, (0, 2) MODE INPUT FUNCTION

W	Amplitude
0.0	0.9999999999999800 00
0.035	0.9998816423787488D 00
0.070	0.9995266239424240 00
0.105	0.9989351586401933D 00
0.140	0.9981075352927459D 00
0.175	0.9970442018905145D 00
0.210	0.9957457230270116D 00
0.245	0.9942127879552975D 00
0.280	0.9924462101058701D 00
0.315	0.9904469265174746D 00
0.350	0.9882159971817381D 00
0.385	0.9857546043019631D 00
0.420	0.9830640514667767D 00
0.455	0.9801457627392271D 00
0.490	0.9770012816620996D 00
0.525	0.9736322701802506D 00
0.560	0.9700405074808142D 00
0.595	0.9662278887522301D 00
0.630	0.9621964238630766D 00
0.665	0.9579482359617854D 00
0.700	0.9534855599983527D 00
0.735	0.9488107411692401D 00
0.770	0.9439262332967150D 00
0.805	0.9388345970739379D 00
0.840	0.9335384983871623D 00
0.875	0.9280407063664806D 00
0.910	0.9223440915165903D 00
0.945	0.9164516237191215D 00
0.980	0.9103663701781221D 00
1.015	0.9040914933003305D 00
1.050	0.8976302485119478D 00
1.085	0.8909859820136422D 00
1.120	0.8841621284755813D 00
1.155	0.8771622086743324D 00
1.190	0.8699898270735115D 00
1.225	0.8626486693501134D 00
1.260	0.8551424998684811D 00
1.295	0.8474751591039373D 00
1.330	0.8396505610181072D 00
1.365	0.8316726903880311D 00
1.400	0.8235456000911738D 00
1.435	0.8152734083484798D 00
1.470	0.8068602959276631D 00
1.505	0.7983105033089336D 00
1.540	0.7896283278153990D 00
1.575	0.7808181207103997D 00
1.610	0.7718842842640658D 00
1.645	0.7628312687914078D 00
1.680	0.7536635696642415D 00
1.715	0.7443857242993196D 00
1.750	0.7350023091250055D 00
1.785	0.7255179365288637D 00
1.820	0.7159372517885586D 00
1.855	0.7062649299884313D 00
1.890	0.6965056729241700D 00
1.925	0.6866642059979675D 00
1.960	0.6767452751065676D 00
1.995	0.6667536435246141D 00
2.030	0.6566940887856955D 00
2.065	0.6465713995634987D 00
2.100	0.6363903725554575D 00
2.135	0.6261558093712868D 00
2.170	0.6158725134287843D 00
2.205	0.6055452868592583D 00
2.240	0.5951789274249519D 00
2.275	0.5847782254507818D 00
2.310	0.5743479607727270D 00
2.345	0.5638928997051655D 00
2.380	0.5534177920294392D 00
2.415	0.5429273680058978D 00
2.450	0.5324263354116809D 00
2.485	0.5219193766063963D 00
2.520	0.5114111456279190D 00
2.555	0.5009062653204339D 00
2.590	0.4904093244968346D 00
2.625	0.4799248751375748D 00
2.660	0.4694574296279927D 00
2.695	0.4590114580361450D 00
2.730	0.4485913854330905D 00
2.765	0.4382015892575705D 00
2.800	0.4278463967269663D 00
2.835	0.4175300822963672D 00
2.870	0.4072568651675658D 00
2.905	0.3970309068497057D 00
2.940	0.3868563087733012D 00
2.975	0.3767371099592873D 00
3.010	0.3666772847446770D 00
3.045	0.3566807405664051D 00
3.080	0.3467513158048423D 00
3.115	0.3368927776884196D 00
3.150	0.3271088202607663D 00
3.185	0.3174030624116827D 00
3.220	0.3077790459732163D 00
3.255	0.2982402378820828D 00
3.290	0.2887900084095615D 00
3.325	0.2794316694559823D 00
3.360	0.2701684329399331D 00
3.395	0.2610034291914694D 00
3.430	0.2519397015133240D 00
3.465	0.2429802047325060D 00
3.500	0.2341278018655198D 00

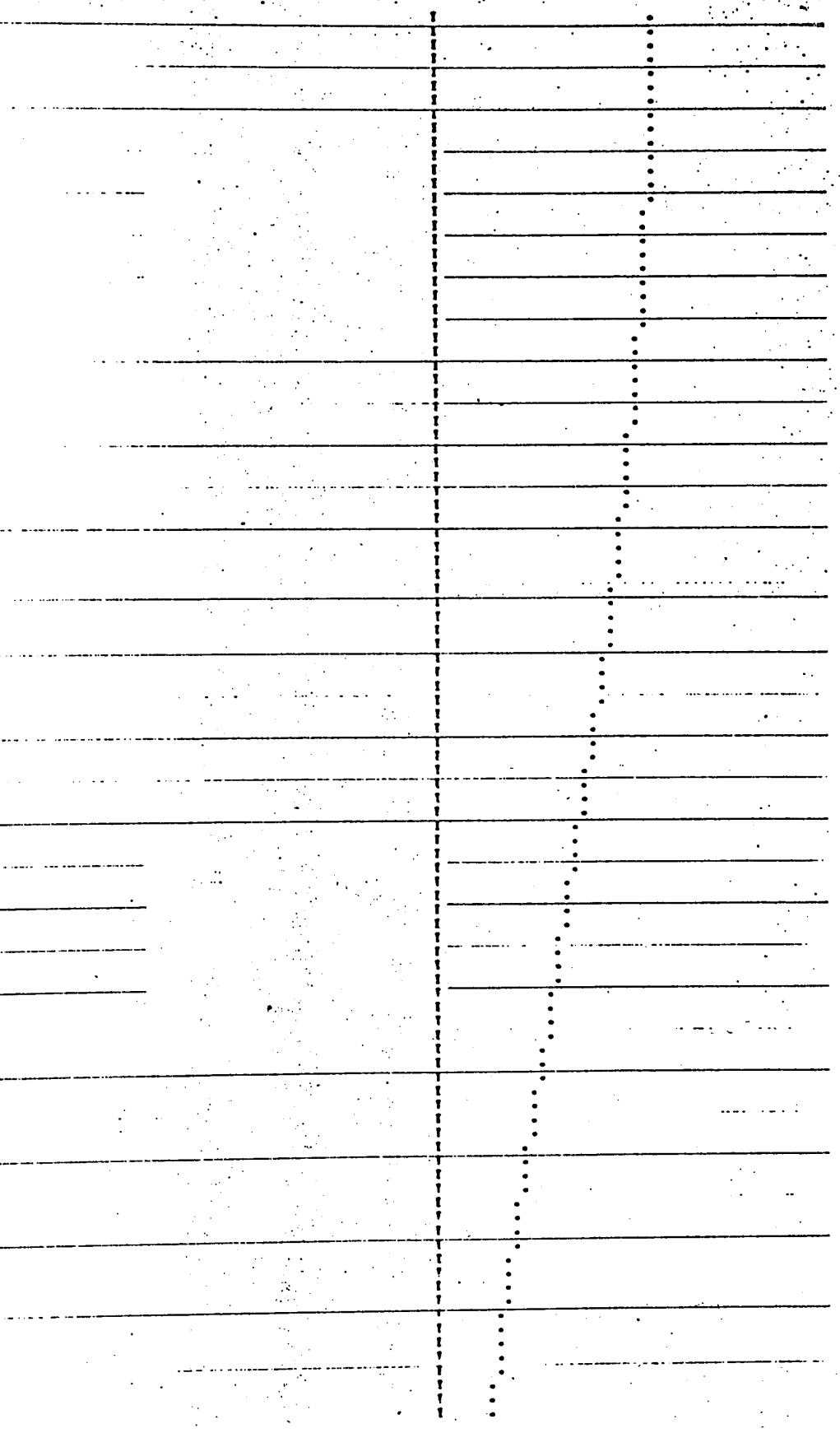

FIGURE 4.8G

ITERATION 40 WITH W_m = 3.5, (0, 2) MODE INPUT FUNCTION

W	Amplitude
0.0	0.99999999999999800 00
0.010	0.99998776021899210 00
0.020	0.99995104148150380 00
0.030	0.99988984560410380 00
0.040	0.99980417561427990 00
0.050	0.99969403575025280 00
0.060	0.99955943146071160 00
0.070	0.99940036940447660 00
0.080	0.99921685745008450 00
0.090	0.99900890467530070 00
0.100	0.99877652136655600 00
0.110	0.99851971901830500 00
0.120	0.99823851033231700 00
0.130	0.99793290921688330 00
0.140	0.99760293078595570 00
0.150	0.99724859135820710 00
0.160	0.99686990845601920 00
0.170	0.99646690080439290 00
0.180	0.99603958832978890 00
0.190	0.99558799215388740 00
0.200	0.99511213461727770 00
0.210	0.99461203922807300 00
0.220	0.99408773071045030 00
0.230	0.99353923497811510 00
0.240	0.99296657913769310 00
0.250	0.99236979148704920 00
0.260	0.99174890151352980 00
0.270	0.99110393989213460 00
0.280	0.99043493848361100 00
0.290	0.98974193033247990 00
0.300	0.98902494966498270 00
0.310	0.98828403188696070 00
0.320	0.98751921358165680 00
0.330	0.98673053250744640 00
0.340	0.98591802759549680 00
0.350	0.98508173894735160 00
0.360	0.98422170783244460 00
0.370	0.98333797668553990 00
0.380	0.98243058910410140 00
0.390	0.98149958984558930 00
0.400	0.98054502482468710 00
0.410	0.97956694111045340 00
0.420	0.97856538692340670 00
0.430	0.97754041163253470 00
0.440	0.97649206575223750 00
0.450	0.97542040093919690 00
0.460	0.97432546998917520 00
0.470	0.97320732683374640 00
0.480	0.97206602653695380 00
0.490	0.97090162529190240 00
0.500	0.96971418041727680 00
0.510	0.96850375035379340 00
0.520	0.96727039466058330 00
0.530	0.96601417401150420 00
0.540	0.96473515019138430 00
0.550	0.96343333609220350 00
0.560	0.96210894570919660 00
0.570	0.96076189413689620 00
0.580	0.95939229756510430 00
0.590	0.95800022327481500 00
0.600	0.95658573963401690 00
0.610	0.95514891609350330 00
0.620	0.95368982318256230 00
0.630	0.95220853250461740 00
0.640	0.95070511673280640 00
0.650	0.94917964960548780 00
0.660	0.94763220592168590 00
0.670	0.94606286153647360 00
0.680	0.94447169335628080 00
0.690	0.94285877933415600 00
0.700	0.94122419846494360 00
0.710	0.93956803078041260 00
0.720	0.93789035734431970 00
0.730	0.93619126024740160 00
0.740	0.93447082260231700 00
0.750	0.93272912853851500 00
0.760	0.93096626319705140 00
0.770	0.92918231272533660 00
0.780	0.92737736427182590 00
0.790	0.92555150598064980 00
0.800	0.92370482698618070 00
0.810	0.92183741740754450 00
0.820	0.91994936836306790 00
0.830	0.91804077186466990 00
0.840	0.91611172101219380 00
0.850	0.91416230978767850 00
0.860	0.91219263314957840 00
0.870	0.91020278700691620 00
0.880	0.90819288821338770 00
0.890	0.90616297456140320 00
0.900	0.90411320477607780 00
0.910	0.90204365850916150 00
0.920	0.89995443633291720 00
0.930	0.89784563973394130 00
0.940	0.89571737110693140 00
0.950	0.89356973374839780 00
0.960	0.89140283185032390 00
0.970	0.88921677049377050 00
0.980	0.88701165564243160 00
0.990	0.88478759413613020 00
1.000	0.88254469368427200 00

FIGURE 4.8H

CHAPTER 5

STUDIES ON THE PROBLEM OF HYPERESOLUTION

Using the computer program mentioned in section 3.6, an investigation has been conducted into the design of hyperresolving channels. The distributions at each plane of the channels were calculated for positions S of the point source ranging from 0 to 10 in steps of 1. These distributions were then analyzed to determine the radius of the annulus or diaphram of the next iteration.

To design a single channel consisting of N lenses, it is necessary to calculate N times 11 distributions. Many different approaches to the problem have been attempted, corresponding to the calculation of more than eight thousand distributions. A picture of some of the computer output is shown in figure 5.1. Obviously, it would be impossible to discuss all of this work within the space of this thesis. Therefore, only two of the most successful cases are illustrated and explained fully in this chapter. First however, some of the principles used to study many of the cases are explained, and a list of some of the more important cases are given.

In order to establish the principle of hyperresolution, it is necessary that the normalized total energy on the axis $e_{nt}(0,S)$ as defined in section 3.6, be negligible for $S \geq S_M$ where $S_M \leq 3.832$ (the Rayleigh limit of resolution). This can be expressed mathematically as $e_{nt}(0,S) \leq e_M$ for $S > S_M$. The smaller the chosen value of S_M within

Figure 5.1 Photograph of portion of the computer output

the Rayleigh limit and the smaller the value of e_M, the better the resolution of the hyperresolving system. We chose $S_M = 2.0$ and $e_M = 0.05$. We consider this a reasonable goal for the definite establishment of hyperresolution. $S_M = 2.0$ corresponds approximately to one half of the Rayleigh limit; the arbitrary choice $e_M = 0.05$, corresponds to a level which although slightly detectable, will not substantially affect the resolution. Furthermore, the diffraction channel was expected to have the characteristic that any additional cells would further improve this energy condition, thus enabling the attainment of any desired degree of resolution. The work reported here is an explanation of the attempts to achieve this goal.

5.1 Comments on Calculated Distributions

After studying many cases, a number of observations were made:

(1) It was soon realized that on the optical axis the normalized total energy is independent of the odd function since the odd function is always zero on the axis. This simplified the problem considerably since the odd function and the phase did not have to be considered. The criterion for hyperresolution simplifies then, to making the normalized even energy, $e_{ne}(0,S) \leq e_M$ for $S \geq S_M$.

(2) After a number of attempts, it was soon realized that it would be much more difficult than originally thought to satisfy the requirements for hyperresolution. It was found quite easy to make $e_{ne}(0,S) \leq 0.05$

for certain chosen domains of S, but to satisfy this condition for all $S \geq 2.0$ seemed very difficult, Indeed, it has not been possible to find a solution using the original concept of a diffraction channel. For the purpose of explanation, the domain of S may be divided arbitrarily into three regions:

$0 \leq S \leq 2.0$	small values of S
$2.0 < S \leq 6.0$	intermediate values of S
$S > 6.0$	large values of S

This division, although arbitrary, is associated with certain practical aspects of hyperresolution. The value S = 2.0, which divides the regions of small and intermediate values of S, represents one half of the Rayleigh limit of resolution. The region from S = 2.0 to S = 6.0 containing the Rayleigh limit of resolution S = 3.832, can be subdivided into two subregions. The subregion from S = 2.0 to S = 3.832 cannot be resolved by conventional optics, while the subregion from S = 3.832 to S = 6.0 can only be resolved by extremely good optical instruments. Thus, any improvement of the resolution in this region of intermediate values of S is especially important. Finally, most optical instruments have good resolution in the region of large value of S, S>6.0.

(3) It was found that in every case, although the addition of the first few cells might give an improvement in the energy characteristic

of the channel, eventually the addition of further cells gave a deterioration of this characteristic.

(4) It was noticed that for small S, low ratios of $e_{ne}(0,S)$ were generally associated with a high degree of asymmetry of the patterns. This seemed to be reasonable because it is known from the theory of modes (section 2.2), that the asymmetrical modes have a much higher diffraction loss than the symmetrical modes.

After a most exhaustive study revealed no change in observation 2, it was decided to find a suitable solution for small values of S only, since the modulation function (MF) explained in section 2.12 may be used to satisfy the required energy condition for other values of S. The theory and concepts used to find this type of solution are now presented.

5.2 Iterated diffraction pattern with small S.

Suppose that for very small S, with n even, $g_{ne}(X,\phi,S)$ may be expressed as,

$$g_{ne}(X,\phi,S) = \Gamma_{ne}(X,S) - \cos 2\phi \ \Gamma'_{ne}(X,S) \qquad 5.1$$

Then

$$g_{n+1,e}(W,\theta,S) = \frac{1}{2\pi} \int_0^{2\pi} \int_{B_n}^{A_n} g_{ne}(X,\phi,S) e^{iWX\cos(\phi-\theta)} X dX d\phi \qquad 5.2$$

$$= \int_{B_n}^{A_n} \Gamma_{ne}(X,S) \left[\frac{1}{2\pi} \int_0^{2\pi} e^{iWX\cos(\phi-\theta)} d\phi\right] X dX \qquad 5.3$$

$$- \int_{B_n}^{A_n} \Gamma'_{ne}(X,S) \left[\frac{1}{2\pi} \int_0^{2\pi} \cos 2\phi \; e^{iWX\cos(\phi-\theta)} d\phi\right] X dX$$

By equations A3 and A4 of appendix A, equation 5.3 becomes,

$$g_{n+1,e}(W,\theta,S) = \Gamma_{n+1,e}(W,S) + \cos 2\theta \; \Gamma'_{n+1,e}(W,S)$$

where $$\Gamma_{n+1,e}(W,S) = \int_{B_n}^{A_n} \Gamma_{ne}(X,S) J_0(WX) X dX \qquad 5.4$$

$$\Gamma'_{n+1,e}(W,S) = \int_{B_n}^{A_n} \Gamma'_{ne}(X,S) J_2(WX) X dX$$

Similarly for n odd,

If $$g_{ne}(W,\theta,S) = \Gamma_{ne}(W,S) + \cos 2\theta \; \Gamma'_{ne}(W,S) \qquad 5.5$$

Then $$g_{n+1,e}(X,\phi,S) = \Gamma_{n+1,e}(X,S) - \cos 2\phi \; \Gamma'_{n+1,e}(X,S)$$

where

$$\Gamma_{n+1,e}(X,S) = \int_{B_n}^{A_n} \Gamma_{ne}(W,S)\, J_o(WX)\, WdW \qquad 5.6$$

$$\Gamma'_{n+1,e}(X,S) = \int_{B_n}^{A_n} \Gamma'_{n+1,e}(W,S)\, J_2(WX)\, WdW$$

In the plane of the lens,

$$g_{oe}(X,S) = \cos(XS\cos\phi) \qquad 5.7$$

For very small S this becomes,

$$g_{oe}(X,\phi,S) = 1 - \frac{X^2S^2\cos^2\phi}{2} = 1 - \left(\frac{S}{2}\right)^2 X^2 - \cos 2\phi \left(\frac{S}{2}\right)^2 X^2 \qquad 5.8$$

Therefore,

$$\Gamma_{oe}(X,S) = 1 - \left(\frac{S}{2}\right)^2 X^2$$

$$\Gamma'_{oe}(X,S) = \left(\frac{S}{2}\right)^2 X^2$$

Thus, upon successive iteration for small S, the even and odd functions retain their same functional form. They always have a cosine of twice the angular coordinate dependency which is separated from the X and S dependency. This form allows easier analysis of the

problem since,

(1) Separation of the X,ϕ, and S variables allows a solution independent of S for small S.

(2) Any process used for hyperresolution in one plane can then be applied to the next plane in a similar way.

The general equations 5.4, 5.5 and 5.6 can be applied to plane 1. Using equations A5 and A11 of appendix A, and B1 of appendix B we obtain,

$$\Gamma_{1e}(W,S) = \int_0^1 [1 - (\frac{S}{2})^2 X^2] J_o(WX) X dX$$

$$\Gamma_{1e}(W,S) = \frac{1}{2} \{L_1(W) - (\frac{S}{2})^2 [L_1(W) - \frac{1}{2} L_2(W)]\} \qquad 5.9$$

$$\Gamma'_{1e}(W,S) = \int_0^1 (\frac{S}{2})^2 X^2 J_2(WX) X dX$$

$$\Gamma'_{1e}(W,S) = -\frac{1}{2} (\frac{S}{2})^2 [L_1(W) - L_2(W)] \qquad 5.10$$

where the function $L_n(W)$ is defined by equation B1 of appendix B.

These equations can also be derived by another process:

$$g_{1e}(W,\theta,S) = \frac{1}{2} [g_1(W,\theta,S) + g_1(W,\theta,-S)] \quad \text{from section 2.5}$$

$$= \frac{1}{2}\left[\frac{J_1(W_1)}{W_1} + \frac{J_1(W_2)}{W_2}\right] \quad \text{from section 2.7}$$

$$= \frac{1}{4}\left[L_1(W_1) + L_1(W_2)\right] \quad \text{from equation B1 of appendix B}$$

where $W_1 = \sqrt{W^2 + S^2 + 2WS\cos\theta}$

$W_2 = \sqrt{W^2 + S^2 - 2WS\cos\theta}$

Using the Taylor expansion, we have,

$$g_{1e}(W,\theta,S) = A_e(W^2 + \Delta(W_i)^2) = \sum_{n=o}^{\infty} \frac{[\Delta(W_i)^2]^n}{n!} \frac{d^n A_e(W^2)}{d(W^2)^n} \qquad 5.11$$

where

$$\Delta(W_1^2) = S^2 + 2WS\cos\theta$$

$$\Delta(W_2^2) = S^2 - 2WS\cos\theta$$

The result is,

$$g_{1e}(W,\theta,S) = \frac{1}{2}L_1(W) - \frac{1}{4}\left[4\cos^2\theta\, L_1(W) - (4\cos^2\theta - 1)\, L_2(W)\right]\left(\frac{S}{2}\right)^2$$

$$+ \frac{1}{24}\left[8\cos^4\theta L_1(W) - 12\cos^2\theta\,(2\cos^2\theta - 1)L_2(W) + (16\cos^4\theta - 12\cos^2\theta + 1)L_3(W)\right]\left(\frac{S}{2}\right)^4$$

$$+ \ldots\ldots \qquad 5.12$$

$$g_{1e}(W,\theta,S) = \frac{1}{2}\{L_1(W) - (\frac{S}{2})^2[L_1(W) - \frac{1}{2}L_2(W)]\} - \frac{1}{2}(\frac{S}{2})^2\cos 2\theta[L_1(W) - L_2(W)]$$

$$+ \frac{1}{24}(\frac{S}{2})^4\{\cos 4\theta[L_1(W) - 3L_2(W) + 2L_3(W) + 2L_3(W)] + \cos 2\theta[4L_1(W) - 6L_2(W) + 2L_3(W)]$$

$$+ 3L_1(W) - 3L_2(W) + L_3(W)\} \qquad 5.13$$

Thus again we obtain,

$$\Gamma_{1e}(W,S) = \frac{1}{2}\{L_1(W) - (\frac{S}{2})^2[L_1(W) - \frac{1}{2}L_2(W)]\}$$

5.14

$$\Gamma'_{1e}(W,S) = -\frac{1}{2}(\frac{S}{2})^2[L_1(W) - L_2(W)]$$

Equations 5.4, 5.5, 5.6, 5.8, 5.13 and 5.14 are the fundamental equations used to search for a solution to the problem of hyperresolution for small S. A few of the various criteria applied to these equations are described in the next section.

5.3 Criteria for the radii of diaphrams or annuli.

Most of the criteria are applied only to $g_{1e}(X,\phi,S)$ and $g_{2e}(W,\theta,S)$, since equations 5.4 and 5.5 permit a given process to be applied to successive iterations. An explanation of the inapplicability of criteria

1, 2 and 3 is given at the beginning of criterion 4. No cases are discussed for criterions 1, 2 and 3 because of this inapplicability.

Criterion 1

Due to observation 4, the asymmetry of the diffraction patterns for small S was considered to be very important. To improve the ratio $e_{ne}(0,S)$ for successive iterations, it is essential that there be at each plane a difference between the diffraction patterns for small S and for S = 0. The degree of asymmetry for small S is a definite indication of this difference since the pattern for S = 0 is symmetrical. Therefore, attempts were made to enhance this symmetry iteration by iteration. In this way, it was hoped that it would become easier, at each successive iteration, to improve the energy characteristic.

A measure of this asymmetry is the difference between the even amplitude for $\theta = 0$, n odd or $\phi = 0$, n even and for $\theta = \frac{\pi}{2}$, n odd or $\phi = \frac{\pi}{2}$ n even:

For small S,

$$\frac{1}{2}\left[g_{ne}(W,0,S) - g_{ne}(W,\tfrac{\pi}{2},S)\right] = \Gamma'_{ne}(W,S) \quad n \text{ odd}$$

$$\frac{1}{2}\left[g_{ne}(X,0,S) - g_{ne}(X,\tfrac{\pi}{2},S)\right] = -\Gamma'_{ne}(X,S) \quad n \text{ even} \qquad 5.15$$

The function Γ'_{ne} may be defined as the variation of angular even amplitude for small S.

As stated in section 2.9, the strongly diffracted light depends on the amplitude at the diffracting edge. The criterion used was based on the maximum variation of angular even amplitude at the circular diffracting edge. The criterion corresponds to the maximum variation of strongly diffracted light and also to angular deformation of the iterated diffraction pattern even at short distances from the optical axis.

$$\Gamma'_{1e}(W,S) = -\frac{1}{2}\left(\frac{S}{2}\right)^2 [L_1(W) - L_2(W)]$$

is a maximum for many values of W, for example, W = 3.611. That is, a diaphram in plane 1 or radius A_1 = 3.611 would give strongly diffracted light having a maximum of variation.

Criterion 2

This condition was based on the variation of even amplitude with S when $\theta = 0$, n odd or $\phi = 0$, n even. The variation is given by the differences,

$$g_{ne}(X,0,0) - g_{ne}(X,0,S) \qquad n \text{ even}$$

$$g_{ne}(W,0,0) - g_{ne}(W,0,S) \qquad n \text{ odd} \qquad 5.16$$

The difference is always proportional to $(\frac{S}{2})^2$ as shown in the following example.

$$g_{1e}(W,0,0) - g_{1e}(W,0,S)=\frac{1}{2}\{L_1(W) - L_1(W) + \frac{1}{2}(\frac{S}{2})^2 [4L_1(W) -3L_2(W)]\}$$

$$= \frac{1}{4}(\frac{S}{2})^2 [4L_1(W) -3L_2(W)]$$

As in criterion 1, attempts were made to make this variation a maximum in order to enhance the difference between the pattern for S = 0 and for small S. There are many values of W which will make this function have a maximum variation and also many values of W which will make the function have zero variation. Two of the maximum variations are given by W = 4.202 and W = 8.157. Two of the zero variations are given by W = 2.300 and W = 6.541

Criterion 3

This criterion, similar to criterion 2, was based on the variation of even amplitude with S when $\theta=\frac{\pi}{2}$, n odd or $\phi=\frac{\pi}{2}$, n even. The variation is given by the difference,

$$g_{ne}(X,\frac{\pi}{2},0) - g_{ne}(X,\frac{\pi}{2},S) \qquad \text{n even}$$

5.17

$$g_{ne}(W,\frac{\pi}{2},0) - g_{ne}(W,\frac{\pi}{2},S) \qquad \text{n odd}$$

For example,

$$g_{1e}(W,\tfrac{\pi}{2},0) - g_{1e}(W,\tfrac{\pi}{2},S) = \tfrac{1}{4}\,(\tfrac{S}{2})^2\, L_2(W)$$

Two of the zero variations are given by W = 5.136 and W = 8.417, one of the maximum variations is given by W = 6.380.

Criterion 4

It was discovered that the angular even amplitude Γ'_n is zero on the axis for all values of n and S since,

$$\Gamma'_{n+1,e}(0,S) = \int_{B_n}^{A_n} \Gamma'_{ne}(X,S)\, J_2(0)\, X dX = 0 \qquad n \text{ even}$$

$$\Gamma'_{n+1,e}(0,S) = \int_{B_n}^{A_n} \Gamma'_{ne}(W,S)\, J_2(0)\, W dW = 0 \qquad n \text{ odd} \qquad 5.18$$

Therefore, the function Γ'_{ne} plays no role in determining the energy characteristic on the axis; the energy characteristic depends entirely on the function Γ_{ne} under the conditions defined. This function is equal to the average angular even amplitude $\bar{g}_{ne}$ as defined by,

$$\begin{aligned} g_{ne}(X,\phi,S) &= \frac{1}{2\pi} \int_0^{2\pi} \bar{g}_{ne}(X,\phi,S)\, d\phi \\ &= \frac{1}{2\pi} \int_0^{2\pi} [\Gamma_{ne}(X,S) - \cos 2\phi\, \Gamma'_{ne}(X,S)]\, d\phi \\ &= \Gamma_{ne}(X,S) \qquad n \text{ even} \end{aligned} \qquad 5.19$$

Similarly,

$$\bar{g}_{ne}(W,\theta,S) = \Gamma_{ne}(W,S) \qquad n \text{ odd.}$$

Thus, although criteria 1,2, and 3 can be useful solutions at points off axis, they cannot be successful solutions under the conditions defined.

One method of obtaining low values of $e_{ne}(0,S)$ is to ensure that the transmitted amplitude is everywhere smaller for small S than for S = 0. That is, the parameters A_n and B_n are chosen such that,

$$g_n(W,S) < g_n(W,0) \qquad \text{for } B_n \leq W \leq A_n \qquad S \text{ small.}$$

The criterion described here optimizes this method. It is optimized when the average angular even amplitude $\bar{g}_n$ on the circular diffracting edge of the diaphram or annulus is a stationary function of S. This may be seen in the following example:In plane 1,

$$g_{1e}(W,S) = \frac{1}{2} L_1(W) - \frac{1}{2} \left(\frac{S}{2}\right)^2 \left[L_1(W) - \frac{1}{2} L_2(W)\right]$$

$$\frac{\partial}{\partial S} \bar{g}_{1e}(W,S) = - \left(\frac{S}{2}\right) \left[L_1(W) - \frac{1}{2} L_2(W)\right] = 0 \qquad 5.20$$

There are many values of W which satisfy this equation: 3.054, 6.706, 9.969.... At these values, $\bar{g}_{1e}(W,S)$ does not change with a small

change in S as illustrated by figure 5.2. It can easily be seen from this figure that,

$$\bar{g}_{1e}(W,S) \leq \bar{g}_{1e}(W,0) \qquad \text{in the domain } o \leq W \leq 3.054$$

$$\bar{g}_{1e}(W,S) \geq \bar{g}_{1e}(W,0) \qquad \text{in the domain } 3.054 \leq W \leq 6.706$$

$$\bar{g}_{1e}(W,S) \leq \bar{g}_{1e}(W,0) \qquad \text{in the domain } 6.706 \leq W \leq 9.969$$

Thus, the stationary points define domains satisfying the conditions $\bar{g}_{1e}(W,S) \leq \bar{g}_{1e}(W,0)$ and $\bar{g}_{1e}(W,S) \geq \bar{g}_{1e}(W,0)$.

This criterion is associated with the maximum gradient of the amplitude on the optical axis for diffraction pattern 2. As indicated in figure 5.2, there are maximum differences between the two functions $g_{2e}(0,S)$ and $g_{2e}(0,0)$ for W = 3.054 and 9.969; there is a minimum difference for W = 6.706. This may be shown mathematically:

$$g_{2e}(0,S) = \frac{1}{2\pi} \int_0^{2\pi} \int_{B_1}^{A_1} g_{1e}(W,\theta,S)\, W dW d\theta = \int_{B_1}^{A_1} \bar{g}_{1e}(W,S)\, W dW$$

$$g_{2e}(0,S) = \frac{1}{2} \int_{B_1}^{A_1} \{L_1(W) - (\frac{S}{2})^2 [L_1(W) - \frac{1}{2} L_2(W)]\} W dW$$

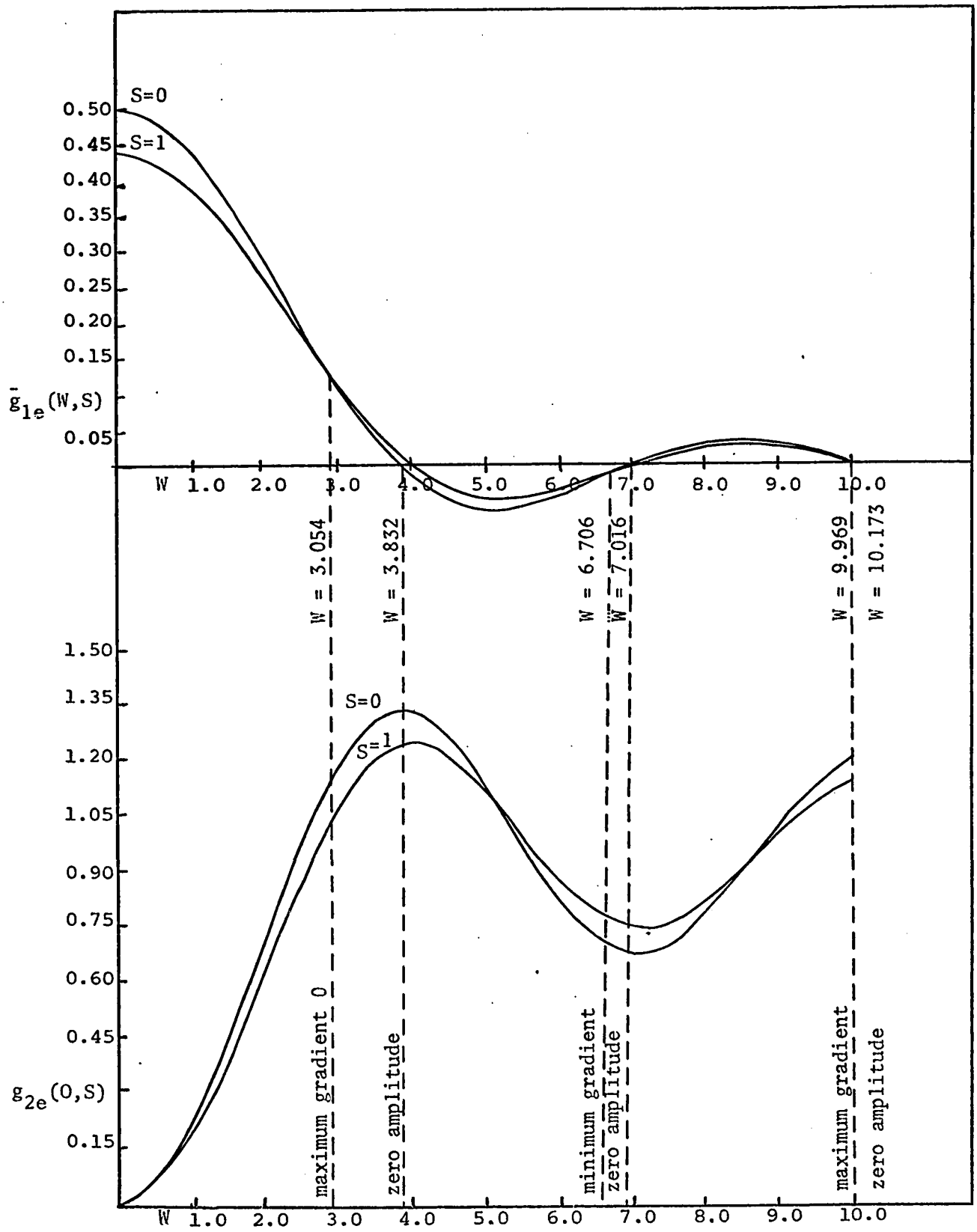

Figure 5.2 Abscissae for extrema of the gradient of $g_{2e}(0,S)$

By equation B4 of appendix B this becomes,

$$g_{2e}(0,S) = \{ - L_o(W) + (\frac{S}{2})^2 [L_o(W) - L_1(W)] \}_{B_1}^{A_1} \qquad 5.22$$

The gradient of $g_{2e}(0,S)$ is given by,

$$\frac{\partial}{\partial S} g_{2e}(0,S) = S [L_o(W) - L_1(W)]_{B_1}^{A_1} \qquad 5.23$$

The maximum gradient is given by the values $W = A_1$ and $W = B_1$ which makes $L_o(W) - L_1(W)$ a stationary function of W.

i.e.

$$\frac{\partial}{\partial W} [L_o(W) - L_1(W)] = 0$$

By equation B3 of appendix B this becomes,

$$-L_1(W) + \frac{1}{2} L_2(W) = 0 \qquad 5.24$$

This equation is identical to equation 5.20 which is the condition that $\bar{g}_{1e}(W,S)$ be a stationary function of S. Thus when $\bar{g}_{1e}(W,S)$ is a stationary function of S, the gradient of $g_{2e}(0,S)$ is an extremum.

It will now be shown for any order n, that the gradient of $g_{n+1e}(0,S)$ is an extremum when $\bar{g}_{ne}$ is a stationary function of S. This theorem will be proved using the notation for n even.

For n even, the gradient of $g_{n+1e}(0,S)$ is given by,

$$\frac{\partial g_{n+1e}(0,S)}{\partial S} = \int_{B_1}^{A_1} \frac{\partial \bar{g}_{ne}(W,S)}{\partial S} \, W dW \qquad 5.25$$

The maximum or minimum gradient is given by,

$$\frac{\partial}{\partial A_1}\left[\frac{\partial\, g_{n+1e}(O,S)}{\partial S}\right] = \frac{\partial}{\partial A_1}\int_{B_1}^{A_1} \frac{\partial\, \bar{g}_{ne}(W,S)}{\partial S}\, WdW = 0$$

$$\frac{\partial}{\partial B_1}\left[\frac{\partial\, g_{n+1e}(OMS)}{\partial S}\right] = \frac{\partial}{\partial B_1}\int_{B_1}^{A_1} \frac{\partial\, \bar{g}_{ne}(W,S)}{\partial S}\, WdW = 0 \qquad 5.26$$

Using Leibniz's formula for differentiating under the integral sign, we obtain the same result for both of equations 5.26,

$$\frac{\partial\, \bar{g}_{ne}(W,S)}{\partial S} = 0 \qquad \text{at } W = A_1 \text{ and } B_1$$

That is, $\bar{g}_{ne}$ is a stationary function of S at the circular diffracting edge.

It is desirable to not only have a process which can be applied repeatedly, but one which will also reduce the ratios $e_{ne}(O,S)$ repeatedly. The criterion: A_n and B_n chosen to maximize $g_{ne}(O,S)$, is not a sufficient condition to ensure that $e_{n+1,e}(O,S) < e_{ne}(O,S)$. Thus it is important to also consider the even energy transmitted through the diaphram or annulus in plane 1.

The criterion: $\bar{g}_{1e}(W,S)$ is a stationary function of S, is associated with the maximum gradient of even energy transmitted through the diaphram

or annulus defined by A_1 and B_1. This is shown as follows:

The even energy $E_{1e}(W,S)$ may be calculated from the function of luminous intensity $I_{1e}(W,S)$ defined by,

$$I_{1e}(W,S) = |g_{1e}(W,S)|^2 = \frac{1}{4} L_1^2(W) - \frac{1}{4} (\frac{S}{2})^2 L_1(W)[L_1(W) - \frac{1}{2} L_2(W)] \qquad 5.27$$

The even energy $E_{1e}(W,S)$ within a circle of radius W is,

$$E_{1e}(W,S) = \frac{1}{4} \int_0^W L_1^2(W)\, W dW - (\frac{S}{2})^2 [L_1^2(W) - \frac{1}{2} L_1(W) L_2(W)]\, W dW.$$

By equation B5 of appendix B this becomes,

$$E_{1e}(W,S) = \frac{1}{4} \{2 - 2L_o^2(W) - \frac{W^2}{2} L_1^2(W) - (\frac{S}{2})^2 [1 - L_o^2(W) - (\frac{W^2}{4} - 1) L_1^2(W)]\} \qquad 5.28$$

This function is shown in figure 5.3 for S = 0 and S = 1, and for W from 0 to 10. The extrema indicated for this function are given by values of W satisfying the equations,

$$L_1(W) = 0 \qquad 5.29$$

$$L_1(W) - \frac{1}{2} L_2(W) = 0 \qquad 5.30$$

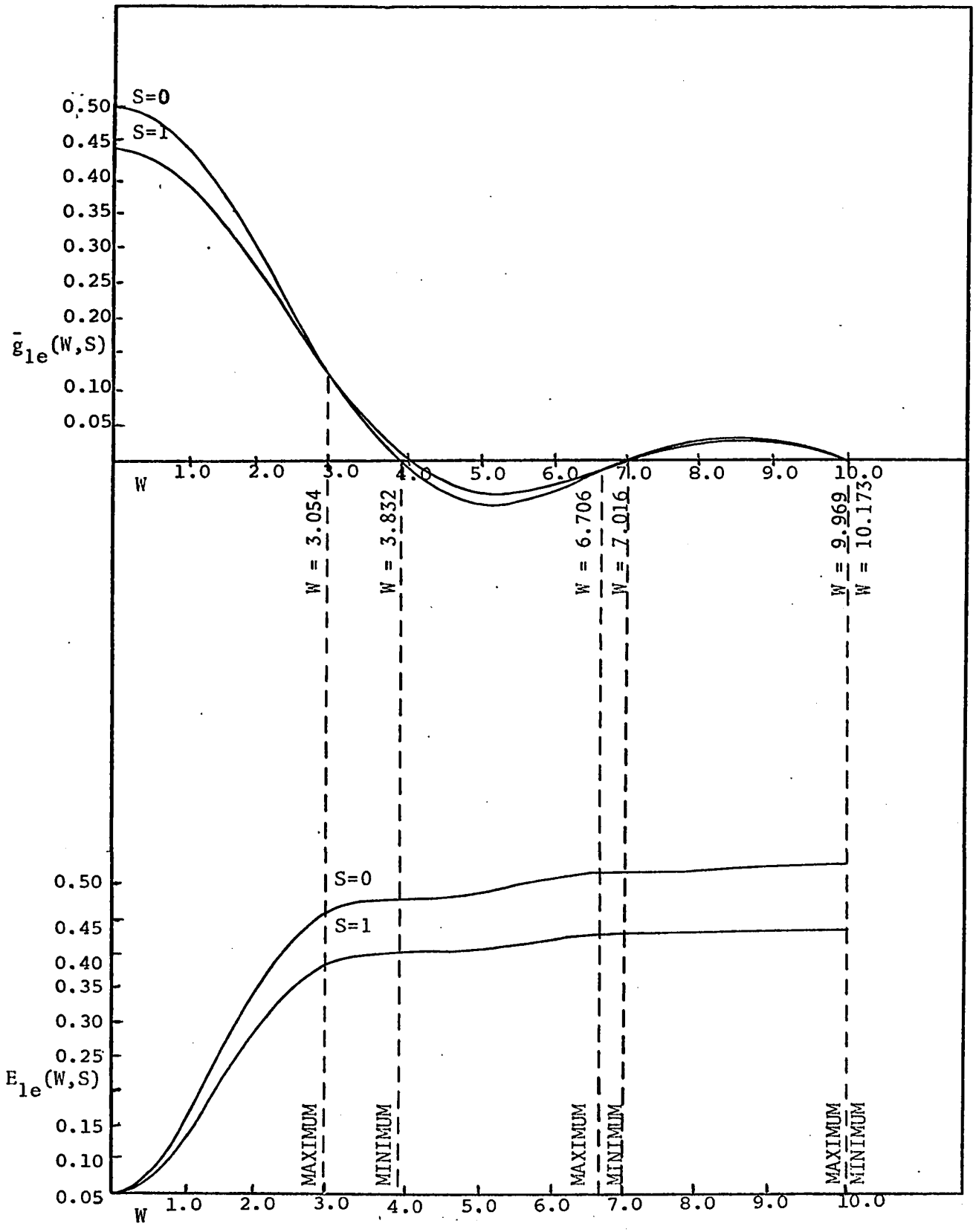

Figure 5.3 Abscissae for extrema of $E_{le}(W,S)$

Equation 5.29 gives the minima; they are the abscissae which give the zeros of the Airy pattern: 3.832, 7.016, 10.173... Equation 5.30 which is identical to equation 5.20, defines the abscissae for the maxima of $E_{1e}(W,S)$. Thus, the criteria for the maximum gradient of $g_{2e}(0,S)$ and for the maximum gradient of even energy transmitted through the diaphram or annulus are associated through this equation. The abscissae satisfying this equation were given previously and are: 3.054, 6.701, 9.969... Maximum energy, $E_{1e}(W,S)$ is transmitted through a diaphram or annulus defined by A_1 and B_1 when two conditions are simultaneously satisfied:

(1) When A_1 is an abscissae which gives a maximum for $E_{1e}(W,S)$

(2) When B_1 is an abscissae which gives a minimum for $E_{1e}(W,S)$

The following combinations of A_1 and B_1 satisfy these two conditions:

A_1	3.054	6.706	6.706	9.969	9.969	9.969
B_1	0.000	3.832	0.000	7.016	3.832	0.000

Strongly diffracted light for criterion 4

As stated in section 2.9, the strongly diffracted light depends essentially on the amplitude of the light in the vicinity of the diffracting edge. Since the average even amplitude $\bar{g}_{1e}(W,S)$ is independent of θ, equation 2.30 gives for the strongly diffracted light,

$$g_{2e}(X,S) = \frac{1}{X}\left[W\,\bar{g}_{1e}(W,S)\,J_1(WX)\right]_{B_1}^{A_1} \qquad 5.31$$

$$= \frac{1}{2X}\left\{W\left[L_1(W) - \left(\frac{S}{2}\right)^2\left(L_1(W) - \frac{1}{2}L_2(W)\right)\right]J_1(WX)\right\}_{B_1}^{A_1}$$

The criterion for the maximum gradient of $g_{2e}(0,S)$ is given by equation 5.20 as,

$$\left[L_1(W) - \frac{1}{2}L_2(W)\right]_{B_1}^{A_1} = 0 \qquad 5.32$$

Applying this criterion to equation 5.31 for the strongly diffracted light,

$$g_{2e}(X,S) = \left[\frac{W}{X}\,L_1(W)\,J_1(WX)\right]_{B_1}^{A_1} \qquad 5.33$$

Thus the amplitude of the strongly diffracted light has a minimum dependency on S ($\propto S^4$) for small S when the amplitude of the light on the axis has a maximum dependency on S.

It is desirable that this strongly diffracted light, with little dependency on S, be eliminated with an appropriate annulus in plane 2.

The criterion of maximum gradient of even energy through the diaphram of an annulus in plane 1 with radii A_1 and B_1 gives the additional condition,

$$\left[L_1(W)\right]_{B_1}^{A_1} = 0 \qquad 5.34$$

Substituting equation 5.34 in equation 5.31, we obtain for the strongly diffracted light,

$$g_{2e}(X,S) = \left[\frac{1}{4X}\left(\frac{S}{2}\right)^2 WL_2(W)J_1(WX)\right]_{B_1}^{A_1} \qquad 5.35$$

In this case, the strongly diffracted light has no component independent of S. There is no strongly diffracted light for S = 0 as expected since there is a zero of amplitude at the circular diffracting edge. Since the strongly diffracted light increases as S^2, it is desirable that it be eliminated in plane 2 with an appropriate annulus.

Criterion 5

This criterion is based on choosing A_1 and B_1 so that the average even amplitude on the axis is zero for S = 0 and an extremum for small S. If the plane 2 contains an annulus with inner radius B_2 of appropriate

size, the central disc will cut out more light for $S \neq 0$ than for $S = 0$.

If

$$g_{2e}'(0,0) = \frac{1}{2} \int_{B_1}^{A_1} L_1(W)\, W dW = - \left[J_o(W) \right]_{B_1}^{A_1} = 0 \qquad 5.36$$

and

$$g_{2e}(0,S) = \frac{1}{2} \int_{B_1}^{A_1} \{ L_1(W) - (\frac{S}{2})^2 [L_1(W) - \frac{1}{2} L_2(W)] \} W dW$$

$$= \frac{1}{4} (\frac{S}{2})^2 \int_{B_1}^{A_1} L_2(W)\, W dW = - (\frac{S}{2})^2 \left[L_1(W) \right]_{B_1}^{A_1} \qquad 5.37$$

Then, B_1 and A_1 are chosen to satisfy two conditions:

$$J_o(A_1) - J_o(B_1) = 0$$

$$L_1(A_1) - L_1(B_1) = \text{an extremum} \qquad 5.38$$

5.4 The investigation for a hyperresolving system when S is small.

The criteria developed for hyperresolving systems when S is small were the optimum conditions for one step of iteration. Unfortunately, using the original concept of a diffraction channel, one step of iteration is not sufficient to meet the goal of hyperresolution stated in the introductory paragraphs of this chapter. Furthermore, repeating the criteria step

by step, does not necessarily give the optimum conditions necessary to meet this goal. For example, the gradient of $g_{n+1}(O,S)$ depends not only on A_n and B_n but also on all the preceding parameters. Since no simple mathematical expression could be developed for $g_{n+1}(O,S)$ in terms of the parameters A_n, $A_{n-1}\ldots A_1$ and B_n, $B_{n-1}\ldots B_1$, the criterion of maximum gradient could not be applied directly to plane n. It could only be applied successively to each plane, a process which is clearly different. Furthermore, contemporary computers are slower than would be necessary to find the parameters by a random trial process.

The problem is a complex one which cannot be easily solved. It was found for example, that if the simple central diaphram in plane 1 is small, the amplitude distribution $g_{2e}(X,\phi,S)$ in plane 2 varies relatively little with small S. This effect can readily be seen in the limiting case where $A_1 \to 0$. In this case, the function $g_{1e}(W,\theta,S) \to \frac{J_1(S)}{S}$ and $g_{2e}(X,\phi,S) \to \frac{J_1(S)}{S} \times \frac{J_1(W)}{W}$.

Consequently $e_{2e}(O,S) \to \left[\frac{J_1(S)}{S}\right]^2$

The result is a distribution with a magnitude dependent on S but with a functional form independent of S. Thus, although the values of $e_{2e}(O,S)$ may be favorable for one step of iteration, they do not satisfy the necessary conditions for hyperesolution, and there is no possibility to improve these values in further steps of iteration. This illustrates that a parameter which gives low values for $e_{2e}(O,S)$ is not necessarily the optimum parameter for several steps of iteration.

Nevertheless, the criteria developed for one step of iteration were the most powerful tools available to study the problem. The parameters generated by these criteria were therefore accepted as fundamentally important in the investigation for a hyperresolving system. For plane 1, these parameters shall be called special points and are given in table 5.1 together with the values of the associated functions. Since these points cover the most significant range of the Airy pattern, namely the range from W = 0 to 10, any study involving all these points is quite comprehensive. Therefore, it was decided to use the computer program mentioned in section 3.6 to calculate $g_{1e}(W,\theta,S)$ with various combinations of the special points for A_1 and B_1. For each calculation, an associated criterion was applied to plane 2 to determine the parameters A_2 and B_2. For calculations which were encouraging, the process was repeated for further steps of iteration. Generally, with the addition of more cells, the system approached the stable condition in which two successive amplitude distributions of even order were almost identical and two successive distributions of odd order were almost identical but with the distributions of even and odd order quite different from each other. To evaluate the improvement in the energy characteristic, it became necessary not to compare two successive iterations but two successive iterations of even order or two successive iterations of odd order. As the stable condition was approached, the improvement in the energy characteristic decreased and became either negligible or worse.

TABLE 5.1 Table of special points and associated functions. Values of associated functions are underlined.

W	$L_1(W)$	$L_2(W)$	$4L_1(W)-3L_2(W)$	$2L_1(W)-L_2(W)$	$L_2(W)-L_1(W)$
0	+1.0000	+1.0000	+1.0000	+1.0000	0.0000
2.300	+0.4695	+0.6260	0.0000	+0.3130	0.1565
3.054	+0.2068	+0.4156	-0.4204	0.0000	0.2088
3.611	+0.0506	+0.2722	-0.6142	-0.1710	0.2216
3.832	+0.0000	+0.2199	-0.6597	-0.2199	+0.2199
4.202	-0.0660	+0.1408	-0.6864	-0.2728	+0.2068
4.613	-0.1131	+0.0667	-0.6525	-0.2929	+0.4798
5.136	-0.1323	0.0000	-0.5292	-0.1323	+0.1323
6.380	-0.0586	-0.0586	-0.0586	-0.0586	0.0000
6.541	-0.0436	-0.0579	0.0000	-0.0293	-0.0143
6.706	-0.0285	-0.0559	+0.0537	0.0000	-0.0274
7.016	0.0000	-0.0487	+0.1460	+0.0486	-0.0487
8.157	+0.0622	-0.0085	+0.2746	+0.1330	-0.0707
8.417	+0.0645	0.0000	+0.2579	+0.1289	-0.0645
9.969	+0.0102	+0.0205	-0.0207	0.0000	+0.0103
10.173	0.0000	+0.0203	-0.0609	-0.0203	+0.0203

5.5 Discussion of calculations and photographs of various systems.

Since it is not possible to present all of the calculated distributions, the following has been selected:

5.5.1 $g_2(X,\phi,S)$ for a central diaphram of radius A_1 equal to abscissae of several special points.

A study of $g_2(X,\phi,S)$ was made with $B_1 = 0$ and A_1 equal to the abscissae of the special points 3.054, 3.832, 5.136, 7.016. Figures 5.4 to 5.7 show the amplitude functions $g_2(X)$ of these diffraction patterns for the special case S = 0. Tables 5.2 to 5.5 show the average even amplitude for integer values of S from 0 to 10 in steps of 1. Photographs of the corresponding diffraction patterns are shown in figures 5.8 to 5.11. For the special point 7.016, the range of S is extended to 23.

These calculations and photographs illustrate the theory of strongly diffracted light presented in section 2.9: when the amplitude near the diffracting edge is low, as in the cases $A_1 = 3.832$ and $A_1 = 7.016$, there is very little strongly diffracted light for S = 0. But when S increases, the amplitude near the diffracting edge increases and causes an increase in the strongly diffracted light. On the contrary, when the amplitude near the diffracting edge is high as in the case $A_1 = 5.136$, the strongly diffracted light is high for small S. When $A_1 = 3.054$, $g_1(W,\theta,S)$ is a stationary function of S, and therefore there is little

change in the strongly diffracted light for small values of S.

For all cases, it can be seen from the photographs that as S becomes large, the diffraction patterns tend toward a steady pattern with two small spots. In section 2.8 we have derived a mathematical expression which approximates this steady pattern. The expression shows that the pattern is a superposition of two Airy patterns and two asymmetrical patterns.

5.5.2.Parameters for various systems

a) Central diaphram for each plane

When this project was initiated, it was considered that each lens of the diffraction channel would have a central diaphram only. Table 5.7 shows a list of the parameters for a few such systems.

b) One annulus for each plane

It was realized that the original concept of a diffraction channel would have to be revised. It was found very advantageous in some cases to block the central region with an annulus of inner radius B_n. Table 5.8 shows a list of parameters for a few such systems.

c) Two annuli for each plane

Since there was greater success with one annulus than with a central diaphram, the case of two annuli at each plane was investigated. The parameters for a few cases are shown in Table 5.9.

X	$g_2(X)$	
0.0	0.1000000000000000D 01	I
0.100	0.9911511235824780 00	I
0.200	0.9649561906324200 00	I
0.300	0.9224519374900840 00	I
0.400	0.8653054000622020 00	I
0.500	0.7957281633156370 00	I
0.600	0.7163613230800040 00	I
0.700	0.6301414833540000 00	I
0.800	0.5401536664080500 00	I
0.900	0.4494804479233310 00	I
1.000	0.3610559018050353D 00	I
1.100	0.2775326225754020 00	I
1.200	0.2011689052280020 00	I
1.300	0.1337421348603120 00	I
1.400	0.7649217351246540-01	I
1.500	0.3099695442503540-01	I .
1.600	-0.5319759916175770-02	.I
1.700	-0.3015043355569220-01	. I
1.800	-0.4523940882331460-01	. I
1.900	-0.5179742665529980-01.	I
2.000	-0.5130136155466160-01.	I
2.100	-0.4539620134699190-01 .	I
2.200	-0.3573633465676360-01 .	I
2.300	-0.2398300992918620-01 .	I
2.400	-0.1161394616791500-01	.I
2.500	0.1000110321154630-03	.
2.600	0.1015772426563970-01	I.
2.700	0.1785820289421550-01	I .
2.800	0.2280839223628020-01	I .
2.900	0.2490953510133600-01	I .
3.000	0.2433249857120649D-01	I .
3.100	0.2143290892255260-01	I .
3.200	0.1676877861252240-01	I .
3.300	0.1096243943239910-01	I.
3.400	0.4674796371635080-02	.
3.500	-0.1461192161855470-02	.
3.600	-0.6891243363646420-02	.I
3.700	-0.1117906656081930-01	.I
3.800	-0.1403227417502650-01	.I
3.900	-0.1531431919226440-01	. I
4.000	-0.1504067544163330-01	. I
4.100	-0.1336690478299240-01	.I
4.200	-0.1056036105914480-01	.I
4.300	-0.6968923302354620-02	.I
4.400	-0.2983738268858720-02	.
4.500	0.9985457300422510-03	.
4.600	0.4611144466691600-02	.
4.700	0.7547311883080790-02	I.
4.800	0.9583148056E75360-02	I.
4.900	0.1059162069337330-01	I.
5.000	0.1054720349462860-01	I.

Figure 5.4 $g_2(X)$ for $A_1 = 3.054$ and $S = 0$

X	$g_2(X)$	
0.0	0.1000000000000000D 01	I
0.100	0.9895052157492600 00	I
0.200	0.9585429854133370 00	I
0.300	0.9086440574114380 00	I
0.400	0.8422438323318320 00	I
0.500	0.7625184221844800 00	I
0.600	0.6731738818795200 00	I
0.700	0.5782053273470650 00	I
0.800	0.4816447463596620 00	I
0.900	0.3873167506136370 00	I
1.000	0.2986203021487300 00	I
1.100	0.2183517201810130 00	I
1.200	0.1485803207182770 00	I
1.300	0.9058325372188540-01	I
1.400	0.4484094126316070-01	I .
1.500	0.1108946623755270-01	I.
1.600	-0.1157823056034580-01	.I
1.700	-0.2457403207060570-01.	I
1.800	-0.2965321073386310-01.	I
1.900	-0.2874482466808430-01.	I
2.000	-0.2378844132969740-01 .	I
2.100	-0.1658996775096670-01 .	I
2.200	-0.8706616870822120-02	.I
2.300	-0.1367582400703620-02	.
2.400	0.4566795510230620-02	.
2.500	0.8608330214171300-02	I.
2.600	0.1061104209815260-01	I.
2.700	0.1071488599601230-01	I.
2.800	0.9271802915998370-02	I.
2.900	0.6763476372488180-02	I.
3.000	0.3719913225037070-02	.
3.100	0.6468285692512940-03	.
3.200	-0.2032013784035280-02	.
3.300	-0.4013620730548840-02	.I
3.400	-0.5134295960549160-02	.I
3.500	-0.5368745166550290-02	.I
3.600	-0.4812616539161630-02	.I
3.700	-0.3652794529999770-02	.
3.800	-0.2130596575793430-02	.
3.900	-0.5031939939066580-03	.
4.000	0.9918651759069960-03	.
4.100	0.2165102333126070-02	.
4.200	0.2893891744431910-02	.
4.300	0.3130613097040310-02	.
4.400	0.2899049781458930-02	.
4.500	0.2284768871067450-02	.
4.600	0.1414962526404360-02	.
4.700	0.4377769854340370-03	.
4.800	-0.4999231928377510-03	.
4.900	-0.1272086001941680-02	.
5.000	-0.1788234871107190-02	.

Figure 5.5 $g_2(X)$ for $A_1 = 3.832$ and $S = 0$

X	$g_2(X)$
0.0	0.1000000000000000D 01
0.100	0.9998740449174480 00
0.200	0.9980323012369300 00
0.300	0.9904290366957630 00
0.400	0.9714012557789980 00
0.500	0.9350479972633540 00
0.600	0.8767323452142100 00
0.700	0.7943873505661850 00
0.800	0.6893468195246850 00
0.900	0.5665195589206740 00
1.000	0.4338603748734610 00
1.100	0.3012345130548820 00
1.200	0.1788944363141850 00
1.300	0.7586384805549110-01
1.400	-0.1461247483314100-02
1.500	-0.5023278408186310-01
1.600	-0.7143033156987620-01
1.700	-0.6946810899488290-01
1.800	-0.5122926594222700-01
1.900	-0.2473472032851270-01
2.000	0.2284709972792330-02
2.100	0.2363939137733150-01
2.200	0.3553218474976650-01
2.300	0.3687980034047830-01
2.400	0.2908787974852590-01
2.500	0.1537370402900610-01
2.600	-0.1857340111933300-03
2.700	-0.1366108356992230-01
2.800	-0.2212123676791260-01
2.900	-0.2416597624643460-01
3.000	-0.2006067803263500-01
3.100	-0.1148509640877640-01
3.200	-0.9904979743742790-03
3.300	0.8685307575597030-02
3.400	0.1527736508593730-01
3.500	0.1748010435929700-01
3.600	0.1516532284114570-01
3.700	0.9305026325280390-02
3.800	0.1642303666555910-02
3.900	-0.5791981889775440-02
4.000	-0.1119083645360120-01
4.100	-0.1338832922400490-01
4.200	-0.1209090082737130-01
4.300	-0.7881810743496400-02
4.400	-0.2014300217370960-02
4.500	0.3941928394790960-02
4.600	0.8505837878900300-02
4.700	0.1064078166576440-01
4.800	0.9978308409053870-02
4.900	0.6864538084415740-02
5.000	0.2229211291224900-02

Figure 5.6 $g_2(X)$ for $A_1 = 5.136$ and $S = 0$

X	$g_2(X)$
0.0	0.1000000000000000D 01
0.100	0.1051416929699110 01
0.200	0.1190126397934620 01
0.300	0.1373880465404710 01
0.400	0.1545547711713330 01
0.500	0.1648881243104240 01
0.600	0.1643632737982040 01
0.700	0.1515742469929930 01
0.800	0.1279948900972750 01
0.900	0.9745110743129060 00
1.000	0.6500578762649440 00
1.100	0.3561486388586810 00
1.200	0.1295058370889100 00
1.300	-0.1297165472689080-01
1.400	-0.7502502811713210-01
1.500	-0.7626364577609810-01
1.600	-0.4396677058146810-01
1.700	-0.4349695712370670-02
1.800	0.2407542836989140-01
1.900	0.3346325160041750-01
2.000	0.2574267894306610-01
2.100	0.8934427136032010-02
2.200	-0.7551963876576090-02
2.300	-0.1686995513581250-01
2.400	-0.1675957760510050-01
2.500	-0.9360977027540220-02
2.600	0.6271282270708240-03
2.700	0.8399074369338550-02
2.800	0.1103540732960370-01
2.900	0.8345795909724590-02
3.000	0.2441936999901850-02
3.100	-0.3559165351656560-02
3.200	-0.7023870643488470-02
3.300	-0.6840153064019980-02
3.400	-0.3649300927493520-02
3.500	0.6991569050402540-03
3.600	0.4123357042982430-02
3.700	0.5241549961209510-02
3.800	0.3872518127503470-02
3.900	0.9508740903847660-03
4.000	-0.2027896201972580-02
4.100	-0.3733110592159810-02
4.200	-0.3561163659068400-02
4.300	-0.1811803335790550-02
4.400	0.5512829250017830-03
4.500	0.2402486951226380-02
4.600	0.2969907299710660-02
4.700	0.2137800631517210-02
4.800	0.4268491368122960-03
4.900	-0.1304465922311390-02
5.000	-0.2276725282426720-02

Figure 5.7 $g_2(X)$ for $A_1 = 7.016$ and $S = 0$

X\S	0	1	2	3	4	5	6	7	8	9	10
0.0	1.000	.908	.670	.376	.128	-.016	-.052	-.025	.012	.025	.013
0.1	.991	.900	.663	.372	.126	-.016	-.052	-.025	.012	.025	.012
0.2	.964	.875	.644	.359	.119	-.018	-.051	-.024	.012	.025	.012
0.3	.922	.836	.613	.339	.109	-.020	-.050	-.022	.013	.024	.011
0.4	.865	.783	.571	.312	.097	-.024	-.049	-.020	.014	.024	.010
0.5	.795	.719	.521	.280	.081	-.028	-.047	-.017	.015	.024	.009
0.6	.716	.645	.463	.243	.064	-.032	-.045	-.015	.016	.023	.009
0.7	.630	.566	.402	.204	.045	-.036	-.042	-.011	.017	.022	.007
0.8	.540	.483	.338	.164	.027	-.039	-.040	-.008	.018	.021	.006
0.9	.449	.400	.273	.124	.009	-.042	-.037	-.005	.018	.020	.005
1.0	.361	.319	.211	.087	-.006	-.044	-.033	-.003	.019	.018	.004
1.1	.277	.242	.154	.053	-.020	-.045	-.029	.000	.019	.017	.003
1.2	.201	.172	.102	.023	-.031	-.044	-.026	.002	.018	.015	.002
1.3	.033	.111	.058	-.001	-.039	-.043	-.022	.004	.017	.014	.001
1.4	.076	.060	.027	-.021	-.043	-.040	-.018	.005	.016	.011	.000
1.5	.030	.019	-.008	-.034	-.045	-.036	-.014	.006	.014	.009	.000
1.6	-.005	-.012	-.028	-.042	-.044	-.031	-.011	.006	.012	.008	-.001
1.7	-.030	-.034	-.041	-.045	-.399	-.025	-.008	.006	.010	.006	-.001
1.8	-.045	-.046	-.047	-.043	-.034	-.020	-.005	.005	.008	.004	-.001
1.9	-.052	-.051	-.046	-.038	-.027	-.013	-.002	.005	.006	.002	-.001
2.0	-.051	-.049	-.042	-.031	-.019	-.008	.000	.004	.003	.001	-.001
2.1	-.045	-.042	-.033	-.022	-.010	-.002	.002	.003	.001	.000	-.001
2.2	-.036	-.032	-.023	-.011	-.003	.002	.003	.002	-.000	-.001	-.001
2.3	-.024	-.026	-.012	-.002	.004	.006	.004	.000	-.002	-.002	-.001
2.4	-.011	-.009	-.001	.006	.010	.009	.004	.000	-.003	-.002	.000
2.5	.010	.002	.008	.013	.014	.011	.004	-.001	-.003	-.002	.000
2.6	.010	.012	.015	.018	.016	.011	.004	-.001	-.004	-.002	.000
2.7	.018	.019	.021	.021	.018	.011	.004	-.002	-.004	-.002	.000
2.8	.023	.023	.023	.021	.017	.010	.003	-.002	-.003	-.002	.000
2.9	.025	.024	.023	.020	.015	.008	.002	-.002	-.003	-.001	.000
3.0	.024	.023	.021	.017	.011	.006	.001	-.002	-.002	.001	.000
3.1	.021	.020	.017	.013	.008	.003	.000	-.001	-.001	.000	.000
3.2	.017	.016	.012	.008	.004	.001	-.001	.000	.000	.000	.000
3.3	.011	.009	.006	.003	.000	-.002	-.001	.000	.000	.000	.000
3.4	.004	.004	.000	-.002	-.004	-.004	-.002	.000	.001	.000	.000
3.5	-.001	-.002	-.005	-.007	-.007	-.005	-.002	.004	.001	.001	.000
3.6	-.007	-.007	-.009	-.010	-.009	-.006	-.002	.000	.002	.001	.000
3.7	-.011	-.012	-.012	-.012	-.010	-.006	-.002	.001	.002	.001	.000
3.8	-.014	-.014	-.014	-.013	-.010	-.006	-.002	.001	.002	.001	.000
3.9	-.015	-.015	-.015	-.013	-.009	-.005	-.001	.001	.002	.001	.000
4.0	-.015	-.015	-.014	-.011	-.008	-.004	.000	.001	.001	.001	.000
4.1	-.013	-.013	-.011	-.009	-.006	-.003	.000	.001	.001	.000	.000
4.2	-.011	-.010	-.008	-.006	-.004	-.001	.000	.001	.000	.000	.000
4.3	-.007	-.006	-.005	-.003	-.001	.000	.000	.000	.000	.000	.000
4.4	-.003	-.002	-.001	.000	.001	.002	.000	.000	.000	.000	.000
4.5	.000	.001	.003	.004	.004	.003	.001	.000	.000	.000	.000
4.6	.005	.005	.006	.006	.006	.004	.001	.000	-.001	.000	.000
4.7	.008	.008	.008	.008	.007	.004	.001	.000	-.001	.000	.000
4.8	.009	.009	.010	.009	.007	.004	.001	.000	-.001	.000	.000
4.9	.011	.011	.010	.009	.007	.004	.001	.000	-.001	.000	.000
5.0	.011	.010	.010	.008	.006	.003	.001	.000	-.001	.000	.000

Table 5.2 Numerical values of the average even amplitude $\overline{g_{1e}(X,S)}$ in iterated diffraction patterns formed in plane 1 for $A_1 = 3.054$ and for different values of X and S. These values are normalized so that $\overline{g_{1e}(0,0)} = 1.000$

X\S	0	1	2	3	4	5	6	7	8	9	10
0.0	.100	.930	.743	.498	.262	.088	-.005	-.030	-.018	.002	.011
0.1	.989	.919	.733	.489	.255	.084	-.006	-.030	-.017	.002	.011
0.2	.958	.889	.705	.464	.237	.074	-.009	-.028	-.014	.004	.010
0.3	.908	.840	.659	.425	.208	.058	-.014	-.026	-.009	.007	.009
0.4	.842	.775	.599	.374	.171	.037	-.021	-.023	-.003	.010	.009
0.5	.762	.697	.527	.315	.128	.013	-.028	-.019	.003	.014	.009
0.6	.673	.610	.449	.251	.084	-.011	-.034	-.015	.009	.017	.008
0.7	.578	.519	.368	.186	.040	-.034	-.040	-.011	.016	.020	.007
0.8	.481	.427	.287	.124	-.000	-.054	-.044	-.007	.021	.023	.006
0.9	.387	.337	.212	.069	-.034	-.068	-.046	-.003	.025	.024	.005
1.0	.298	.254	.145	.023	-.059	-.078	-.046	.000	.027	.025	.004
1.1	.218	.180	.088	-.012	-.075	-.081	-.044	.003	.028	.024	.003
1.2	.148	.117	.042	.036	-.082	-.078	-.039	.005	.027	.022	.002
1.3	.090	.066	.009	.050	-.080	-.070	-.033	.006	.024	.019	.000
1.4	.044	.027	-.013	-.054	-.071	-.058	-.025	.007	.020	.015	.000
1.5	.011	.001	-.025	-.050	-.056	-.043	-.017	.006	.016	.011	-.000
1.6	-.011	-.017	-.029	-.039	-.039	-.027	-.009	.006	.011	.007	-.001
1.7	-.024	-.025	-.026	-.026	-.020	-.011	-.001	.005	.006	.003	-.001
1.8	-.029	-.027	-.020	-.011	-.003	.003	.005	.004	.007	.000	-.001
1.9	-.028	-.023	-.013	-.007	.012	.014	.009	.003	-.002	-.003	-.001
2.0	-.023	-.017	-.002	.013	.022	.021	.012	.002	-.005	-.005	-.001
2.1	-.016	-.010	.005	.021	.028	.024	.013	.000	-.006	-.006	-.001
2.2	-.008	.002	.011	.024	.029	.024	.012	-.000	-.007	-.006	-.000
2.3	-.001	.003	.014	.024	.027	.021	.009	-.001	-.006	-.005	-.000
2.4	-.004	.007	.014	.020	.021	.015	.006	-.001	-.005	-.004	-.000
2.5	-.008	.009	.013	.014	.013	.008	.003	-.002	-.003	-.002	-.000
2.6	-.010	.010	.009	.007	.004	.001	-.000	-.001	-.001	.000	.000
2.7	-.017	.008	.004	-.000	-.004	-.005	-.004	-.001	.000	.001	.000
2.8	-.009	.006	-.000	-.007	-.011	-.010	-.006	-.000	.002	.002	.000
2.9	-.006	.003	-.004	-.012	-.015	-.013	-.007	-.000	.003	.003	.000
3.0	-.003	.004	-.007	-.014	-.017	-.014	-.007	-.000	.004	.003	.000
3.1	-.000	-.002	-.009	-.015	-.017	-.013	-.006	.000	.004	.003	.000
3.2	-.002	-.004	-.009	-.013	-.014	-.011	-.005	.000	.003	.002	.000
3.3	-.004	-.005	-.008	-.009	-.009	-.007	-.003	.000	.002	.001	.000
3.4	-.005	-.004	-.005	-.005	-.004	-.002	-.000	.000	.001	.000	.000
3.5	-.005	-.004	-.003	-.000	.001	.002	.016	.000	.000	.000	.000
3.6	-.004	-.003	.000	.004	.006	.006	.033	.000	-.001	-.001	.000
3.7	-.003	-.001	.003	.008	.010	.008	.044	.000	-.002	-.002	.000
3.8	-.002	.000	.005	.009	.012	.010	.048	.000	-.002	-.002	.000
3.9	.005	.001	.006	.010	.012	.009	.046	.000	-.002	-.002	.000
4.0	.000	.002	.006	.009	.010	.008	.037	.000	-.002	-.002	.000
4.1	.002	.003	.005	.007	.007	.005	.024	.000	-.002	-.001	.000
4.2	.002	.003	.004	.004	.004	.002	.000	.000	.000	.000	.000
4.3	.003	.002	.002	.000	.000	-.000	-.000	.000	.000	.000	.000
4.4	.002	.001	-.000	-.003	-.004	-.004	-.020	.000	.000	.000	.000
4.5	.001	.000	-.002	-.005	-.007	-.006	-.030	.000	.001	.001	.000
4.6	.004	-.000	-.004	-.007	-.009	-.007	-.035	.000	.002	.001	.000
4.7	-.004	-.001	-.004	-.008	-.009	-.007	-.035	.000	.002	.002	.000
4.8	-.001	-.001	-.005	-.007	-.008	-.006	-.029	.000	.002	.001	.000
4.9	-.001	-.002	-.004	-.006	-.006	-.005	-.021	.000	.001	.001	.000
5.0	-.001	-.002	-.003	-.004	-.004	-.002	-.001	.000	.001	.000	.000

Table 5.3 Numerical values of the average even amplitude $\overline{g_{1e}(X,S)}$ in iterated diffraction patterns formed in plane 1 for $A_1 = 3.832$, and for different values of X and S. These values are normalized so that $\overline{g_{1e}(0,0)} = 1.0000$

X\S	0	1	2	3	4	5	6	7	8	9	10
0.0	1.000	.998	.974	.887	.713	.469	.216	.024	-.065	-.061	-.012
0.1	.999	.994	.960	.863	.686	.446	.203	.021	-.062	-.057	-.010
0.2	.998	.980	.918	.795	.608	.381	.166	.013	-.053	-.046	-.007
0.3	.990	.955	.852	.690	.489	.283	.111	.002	-.039	-.030	-.002
0.4	.971	.916	.766	.560	.345	.166	.466	-.010	-.021	-.009	.004
0.5	.935	.861	.666	.418	.194	.045	-.019	-.022	-.002	.011	.009
0.6	.876	.787	.557	.279	.053	-.064	-.076	-.030	.016	.029	.014
0.7	.794	.696	.446	.154	-.063	-.149	-.117	-.034	.031	.044	.016
0.8	.689	.590	.339	.055	-.145	-.201	-.138	-.032	.042	.052	.017
0.9	.566	.473	.242	-.016	-.187	-.218	-.139	-.026	.048	.054	.015
1.0	.433	.355	.158	-.056	-.91	-.203	-.121	-.015	.049	.050	.011
1.1	.301	.240	.090	-.070	-.165	-.163	-.090	-.003	.046	.042	.007
1.2	.178	.138	.039	-.064	-.120	-.109	-.052	.008	.039	.030	.002
1.3	.075	.055	.005	-.044	-.066	-.051	-.015	.018	.029	.018	-.002
1.4	-.001	-.006	-.014	-.020	-.015	-.001	.015	.023	.019	.007	-.006
1.5	-.050	-.043	-.023	.002	.024	.036	.035	.024	.000	-.002	-.007
1.6	-.071	-.057	-.032	.018	.047	.055	.043	.021	.002	-.008	-.007
1.7	-.070	-.054	-.016	.026	.053	.057	.039	.015	-.004	-.010	-.006
1.8	-.051	-.039	-.008	.025	.045	.044	.028	.007	-.007	-.009	-.004
1.9	-.025	-.017	.000	.018	.027	.024	.011	-.011	-.008	-.006	-.001
2.0	.002	.004	.006	.007	.005	.000	-.005	-.008	-.007	-.003	.001
2.1	.002	.020	.009	-.004	-.014	-.019	-.018	-.011	-.005	.001	.003
2.2	.004	.029	.009	-.011	-.027	-.031	-.024	-.012	-.002	.003	.004
2.3	.004	.029	.008	-.016	-.031	-.033	-.024	-.010	.001	.005	.003
2.4	.003	.021	.004	-.015	-.027	-.027	-.018	-.006	.002	.005	.002
2.5	.001	.011	.000	-.011	-.017	-.016	-.009	-.013	.003	.003	.001
2.6	.000	-.001	-.003	-.004	-.004	-.001	.001	.003	.003	.002	.000
2.7	-.001	-.011	-.005	.003	.009	.011	.010	.007	.003	.000	-.001
2.8	-.002	-.017	-.006	.008	.018	.020	.016	.008	.001	-.002	-.002
2.9	-.002	-.019	-.005	.011	.021	.023	.017	.008	.000	-.003	-.002
3.0	-.002	-.015	-.003	.011	.019	.020	.014	.005	-.001	-.003	-.002
3.1	-.001	-.008	-.001	.008	.012	.012	.007	.002	-.002	-.002	-.001
3.2	-.001	.000	.001	.003	.003	.002	.000	-.001	-.002	-.001	.000
3.3	.001	.007	.003	-.002	-.006	-.007	-.007	-.004	-.002	.000	.001
3.4	.015	.012	.004	-.006	-.013	-.014	-.011	-.006	-.001	.001	.002
3.5	.017	.013	.003	-.008	-.016	-.016	-.012	-.006	.000	.002	.002
3.6	.015	.011	.002	-.008	-.014	-.015	-.011	-.004	.000	.002	.001
3.7	.009	.007	.001	-.006	-.009	-.009	-.006	-.002	.001	.002	.001
3.8	.002	.001	-.001	-.002	-.003	-.002	-.001	-.001	.001	.001	.000
3.9	-.006	-.005	-.002	.001	.004	.005	.004	.003	.001	.000	-.001
4.0	-.011	-.009	-.003	.004	.009	.011	.008	.004	.001	-.001	-.001
4.1	-.013	-.010	-.002	.006	.012	.013	.009	.005	.000	-.002	-.001
4.2	-.012	-.009	-.002	.006	.018	.012	.009	.004	.000	-.002	-.001
4.3	-.005	-.006	.001	.005	.008	.008	.006	.002	.000	-.001	-.001
4.4	-.002	-.001	.000	.002	.003	.002	.001	.000	.000	-.001	.001
4.5	.004	.003	.001	-.001	-.003	-.003	-.003	-.002	.000	.000	.000
4.6	.008	.007	.002	-.003	-.007	-.008	-.006	-.003	.000	.001	.001
4.7	.011	.008	.002	-.005	-.009	-.010	-.008	-.004	.000	.001	.001
4.8	.009	.008	.001	-.005	-.009	-.010	-.007	-.003	.000	.001	.001
4.9	.007	.025	.001	-.004	-.007	-.007	-.005	-.002	.000	.001	.001
5.0	.002	.001	.001	-.002	-.003	-.003	-.001	.000	.000	.001	.000

Table 5.4 Numerical values of average even amplitude $\overline{g_{1e}(X,S)}$ in iterated diffraction patterns formed in plane 1 for $A_1 = 5.136$ and for different values of X and S. These values are normalized so that $g_{1e}(0,0) = 1.000$.

X\S	0	1	2	3	4	5	6	7	8	9	10
0.0	1.000	1.101	1.346	1.583	1.658	1.491	1.117	.657	.255	.005	-.008
0.1	1.051	1.138	1.344	1.534	1.572	1.391	1.026	.594	.224	.000	-.073
0.2	1.190	1.235	1.333	1.394	1.331	1.110	.777	.422	.142	-.014	-.054
0.3	1.374	1.359	1.303	1.182	.980	.713	.431	.191	.036	-.028	-.027
0.4	1.545	1.465	1.241	.925	.582	.281	.069	-.040	-.060	-.033	.002
0.5	1.649	1.509	1.137	.654	.205	-.103	-.229	-.209	-.115	-.022	.028
0.6	1.643	1.461	.988	.401	-.097	-.374	-.410	-.284	-.115	.005	.045
0.7	1.515	1.315	.802	.190	-.291	-.504	-.454	-.260	-.063	.043	.050
0.8	1.280	1.086	.598	.036	-.370	-.500	-.383	-.160	.019	.081	.045
0.9	.974	.809	.397	-.057	-.352	-.396	-.241	-.030	.102	.108	.032
1.0	.650	.526	.223	-.094	-.271	-.247	-.086	-.083	.158	.115	.015
1.1	.356	.277	.091	-.090	-.163	-.102	.035	.148	.170	.099	-.002
1.2	.129	.092	.008	-.062	-.064	.003	.095	.152	.138	.066	-.013
1.3	-.013	-.019	-.030	-.026	.004	.053	.095	.104	.076	.025	-.019
1.4	-.075	-.063	-.034	.004	.038	.055	.052	.033	.008	-.011	-.018
1.5	-.076	-.059	-.019	.021	.039	.028	-.003	-.032	-.043	-.034	-.012
1.6	-.044	-.030	.000	.024	.023	-.001	-.044	-.069	-.066	-.038	-.005
1.7	-.004	-.002	.013	.016	.015	-.028	-.057	-.069	-.057	-.028	.002
1.8	-.024	.022	.016	.004	-.014	-.032	-.042	-.040	-.027	-.008	.006
1.9	.033	.027	.011	-.007	-.018	-.019	-.011	-.001	.009	.011	.007
2.0	.026	.018	.001	-.012	-.014	.000	.020	.084	.035	.022	.005
2.1	.009	.004	-.006	-.012	-.004	.016	.037	.048	.042	.023	.002
2.2	-.008	-.009	-.009	-.006	.005	.022	.035	.039	.030	.014	-.002
2.3	-.017	-.014	-.008	-.001	.010	.016	.017	.014	.007	.000	-.004
2.4	-.017	-.012	-.003	.007	.009	.004	-.006	-.014	-.016	-.011	-.004
2.5	-.009	-.005	-.003	.008	.004	-.009	-.023	-.032	-.029	-.017	-.003
2.6	.001	.003	.006	.006	-.001	-.015	-.028	-.033	-.028	-.014	.000
2.7	.008	.008	.006	.002	-.006	-.014	-.020	-.020	-.014	-.006	.001
2.8	.011	.009	.003	-.003	-.006	-.006	-.003	.001	.004	.004	.003
2.9	.008	.005	-.001	-.006	-.004	.003	.013	.019	.018	.011	.002
3.0	.002	.000	-.004	-.006	.000	.010	.022	.027	.023	.013	.001
3.1	-.003	-.004	-.005	-.003	.003	.012	.020	.022	.017	.008	.000
3.2	-.007	-.006	-.004	.000	.004	.008	.009	.007	.004	.001	-.001
3.3	-.007	-.005	-.001	.003	.004	.000	-.005	-.009	-.009	-.006	-.002
3.4	-.004	-.002	-.002	.004	.001	-.007	-.015	-.020	-.017	-.010	-.002
3.5	.001	-.002	.004	.003	-.001	-.010	-.018	-.020	-.017	-.009	-.001
3.6	.004	.004	.003	.001	-.003	-.008	-.012	-.012	-.009	-.004	.001
3.7	.005	.004	.001	-.001	-.003	-.003	-.001	.001	-.002	.002	.001
3.8	.004	.002	-.001	-.003	-.002	.003	-.001	.012	.012	.007	.001
3.9	.001	.000	-.003	-.003	.000	.007	.015	.018	.015	.008	.001
4.0	-.002	-.002	-.003	-.002	.002	.008	.013	.014	.012	.006	.000
4.1	-.004	-.003	-.002	.000	.002	.004	.005	.005	.003	.001	-.001
4.2	-.004	-.002	.000	.002	.002	-.001	-.004	-.006	-.007	-.004	-.001
4.3	-.002	-.001	.002	.003	.000	-.005	-.011	-.014	-.012	-.007	-.001
4.4	.001	.001	.003	.002	-.001	-.007	-.012	-.014	-.012	-.006	-.001
4.5	.002	.002	.002	.001	-.002	-.005	-.008	-.008	-.006	-.003	.000
4.6	.003	.002	.001	-.001	-.002	-.001	.000	.011	.002	.001	.001
4.7	.002	.001	-.001	-.002	-.001	.003	.007	.009	.009	.005	.001
4.8	.000	.000	-.002	-.002	-.000	.006	.010	.013	.011	.006	.000
4.9	.001	-.002	-.002	-.001	.001	.006	.009	.010	.008	.004	.000
5.0	.002	-.002	-.001	.000	.002	.003	.003	.003	.002	.001	.000

Table 5.5 numerical values of average even amplitude $\overline{g_{1e}(X,S)}$ in iterated diffraction patterns formed in plane 1 for $A_1 = 7.016$ and for different values of X and S. These values are normalized so that $g_{1e}(0,0) = 1.000$.

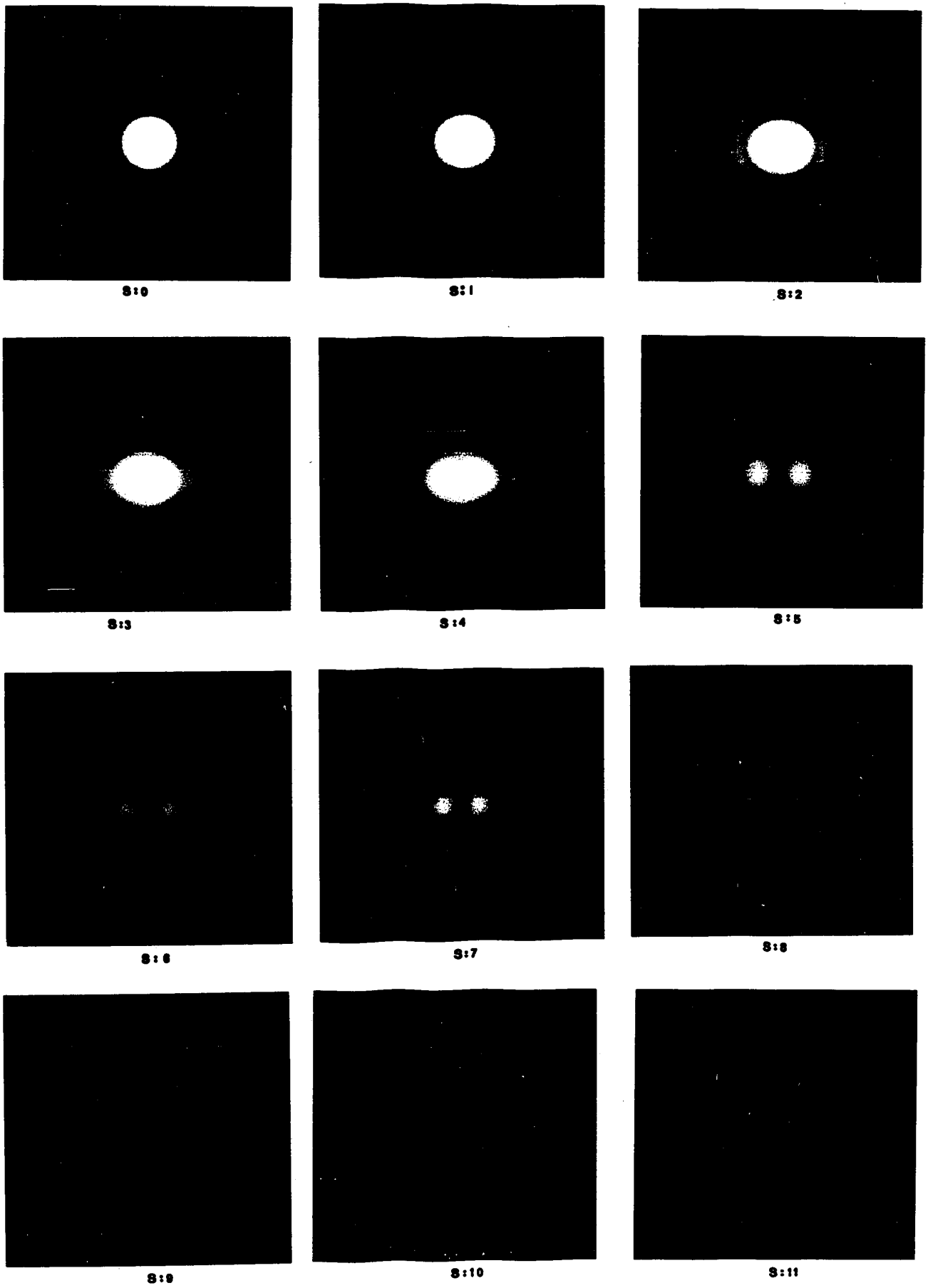

Figure 5.8 Photographs of iterated diffraction patterns in plane 2 for A_1 = 3.054 and for different values of S.

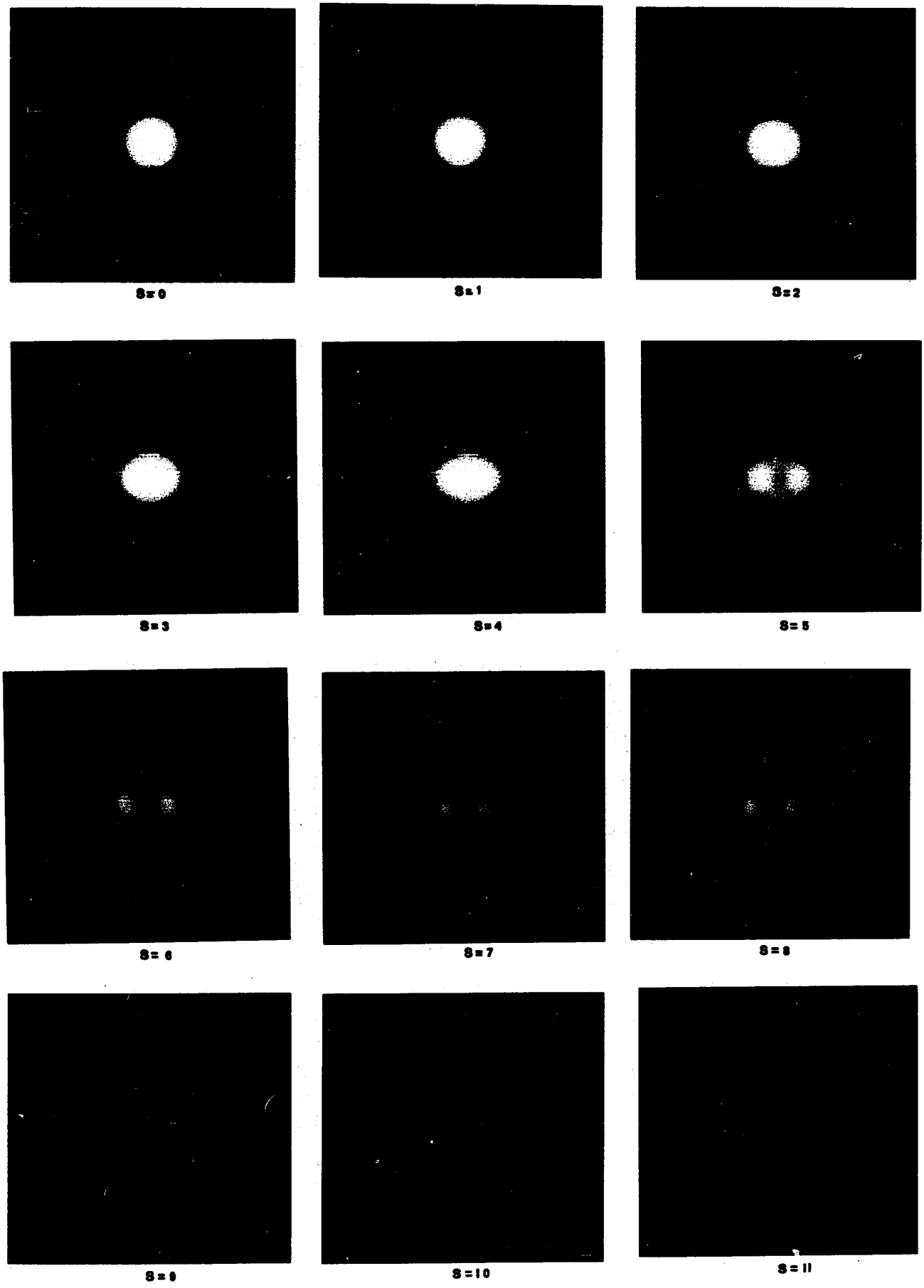

Figure 5.9 Photographs of iterated diffraction patterns in plane 2 for A_1 = 3.832 and for different values of S.

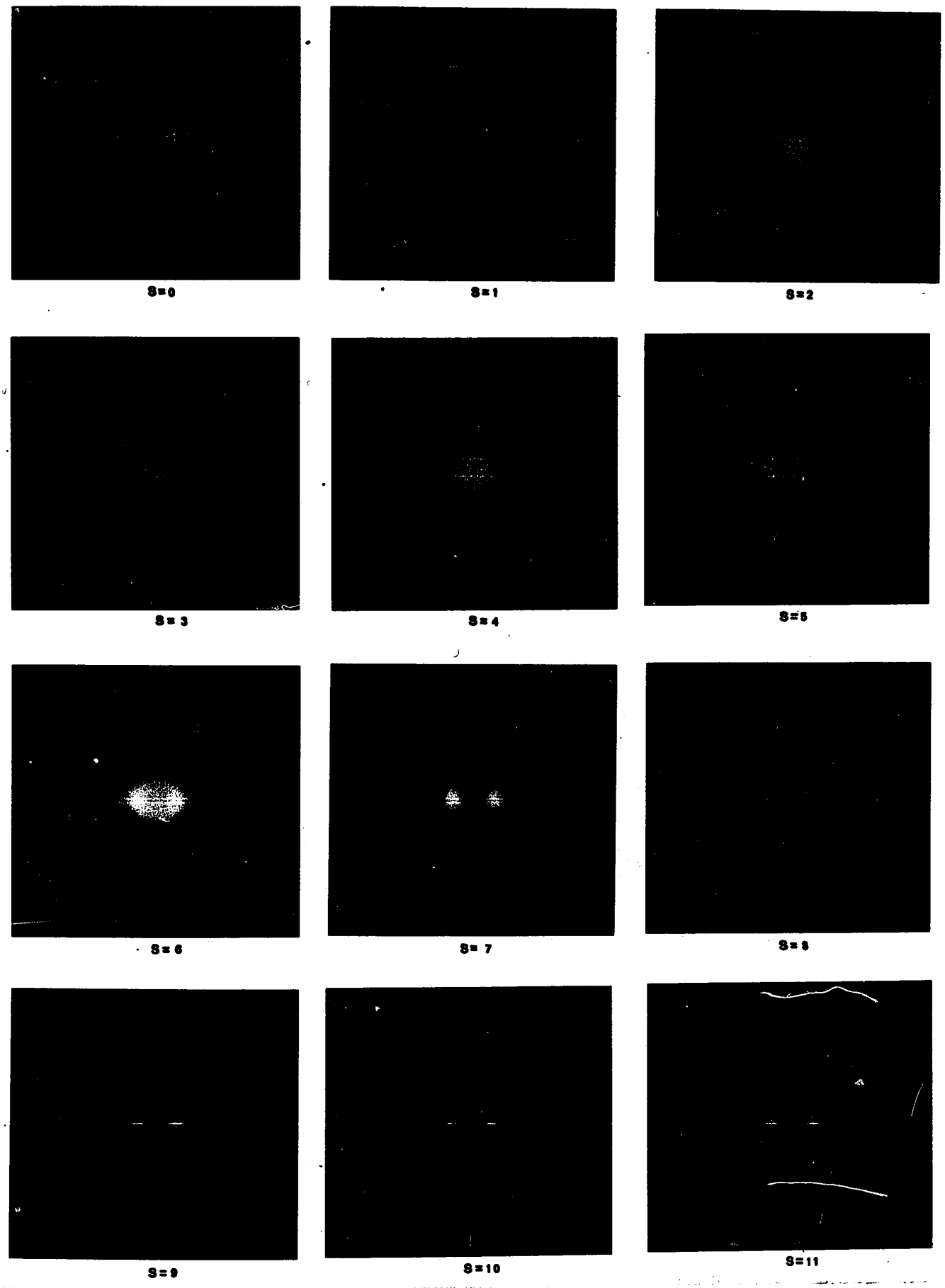

Figure 5.10 Photographs of iterated diffraction patterns in plane 2 for A_1 = 5.136 and for different values of S.

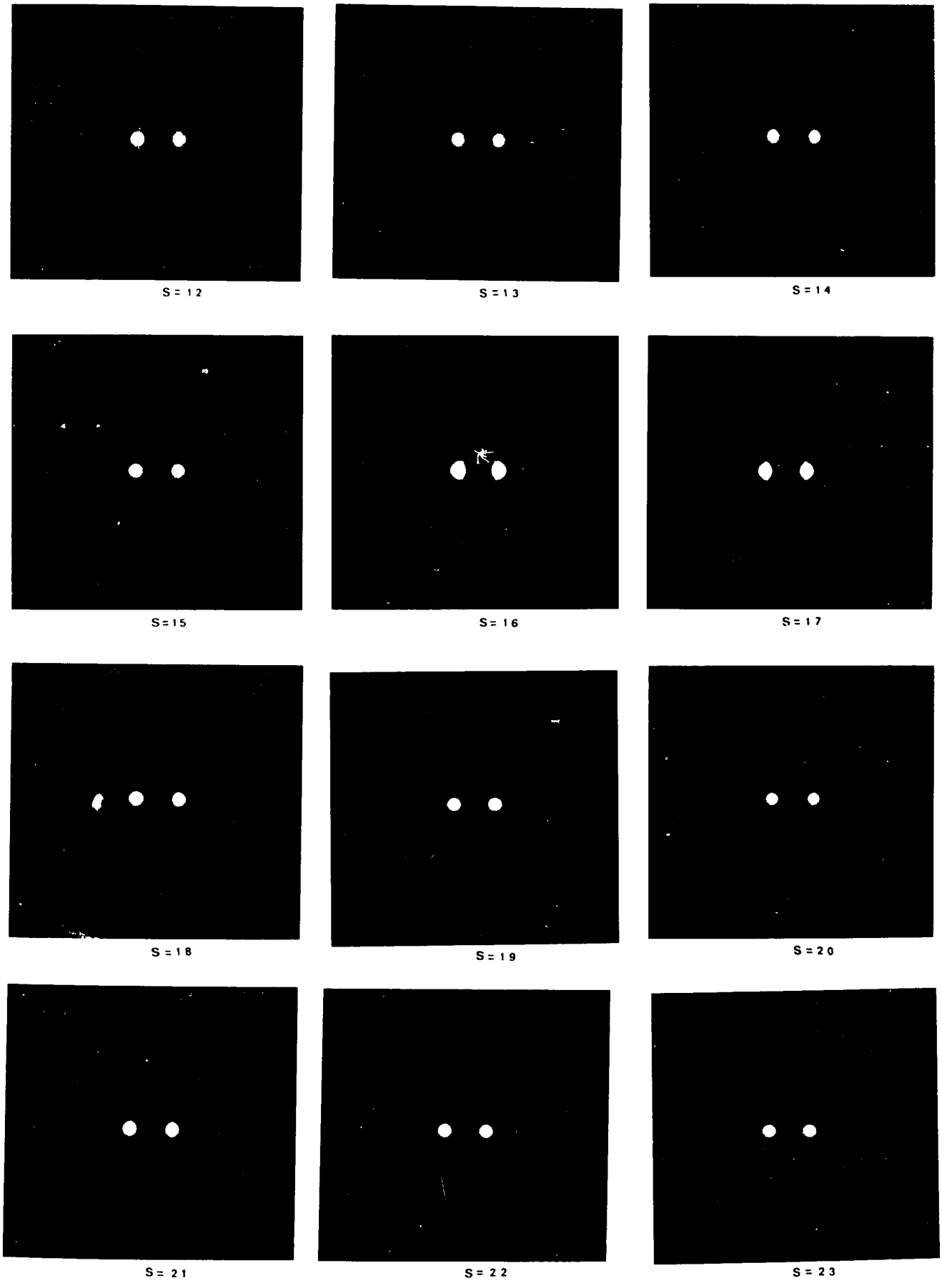

Figure 5.11 Photographs of iterated diffraction patterns in plane z for A_1 = 0.01 and for different values of S.

TABLE 5.7 Parameters of systems with a central diaphram.

plane n	System 1 A_n	System 2 A_n
1	6.706	3.054
2	1.333	1.841
3	7.378	3.570
4	1.405	1.998
5	7.654	3.763
6	1.442	2.075
7	7.816	3.874
8	1.466	2.124
9	7.928	3.949
10	1.484	2.159

TABLE 5.8 Parameters of systems with one annulus

plane n	system 3		system 4	
	A_n	B_n	A_n	B_n
1	6.706	0.000	4.612	0.000
2	1.334	0.282	1.531	0.752
3	7.090	0.000	3.610	0.000
4	1.407	0.238	1.961	1.006
5	7.230	0.000	2.773	0.000
6	1.447	0.208	2.550	1.319
7	7.322	0.000	2.125	0.000
8	1.474	0.188	3.325	1.724
9	7.392	0.000	1.628	0.000
10	1.495	0.172	4.343	2.250

	system 5		system 6	
	A_n	B_n	A_n	B_n
	8.158	0.000	7.015	0.000
	1.421	0.790	2.151	0.546
	7.306	0.000	6.984	0.000
	0.937	0.245	2.237	0.711
	8.700	0.000	6.063	0.000
	0.787	0.112	2.492	0.801

	system 7		system 8	
Plane n	A_n	B_n	A_n	B_n
1	6.706	3.832	3.054	0.000
2	0.453	0.000	2.499	1.841
3	18.082	12.275	1.085	0.000
4			7.541	5.098

TABLE 5.9 Parameters of systems with two annuli

System 9

Plane n	A_n	B_n	C_n	D_n
1	6.541	4.201	2.299	0.000
2	2.383	1.655	1.200	0.392
3	6.493	4.931	3.597	0.000

System 10

Plane n	A_n	B_n	C_n	D_n
1	6.706	4.612	3.054	0.000
2	2.162	1.505	1.294	0.646
3	6.468	4.912	2.617	0.000

System 11

Plane n	A_n	B_n	C_n	D_n
1	8.158	4.612	3.054	0.000
2	3.307	2.297	1.220	0.000
3	8.174	5.066	3.179	0.000
4	3.103	2.282	1.966	0.000

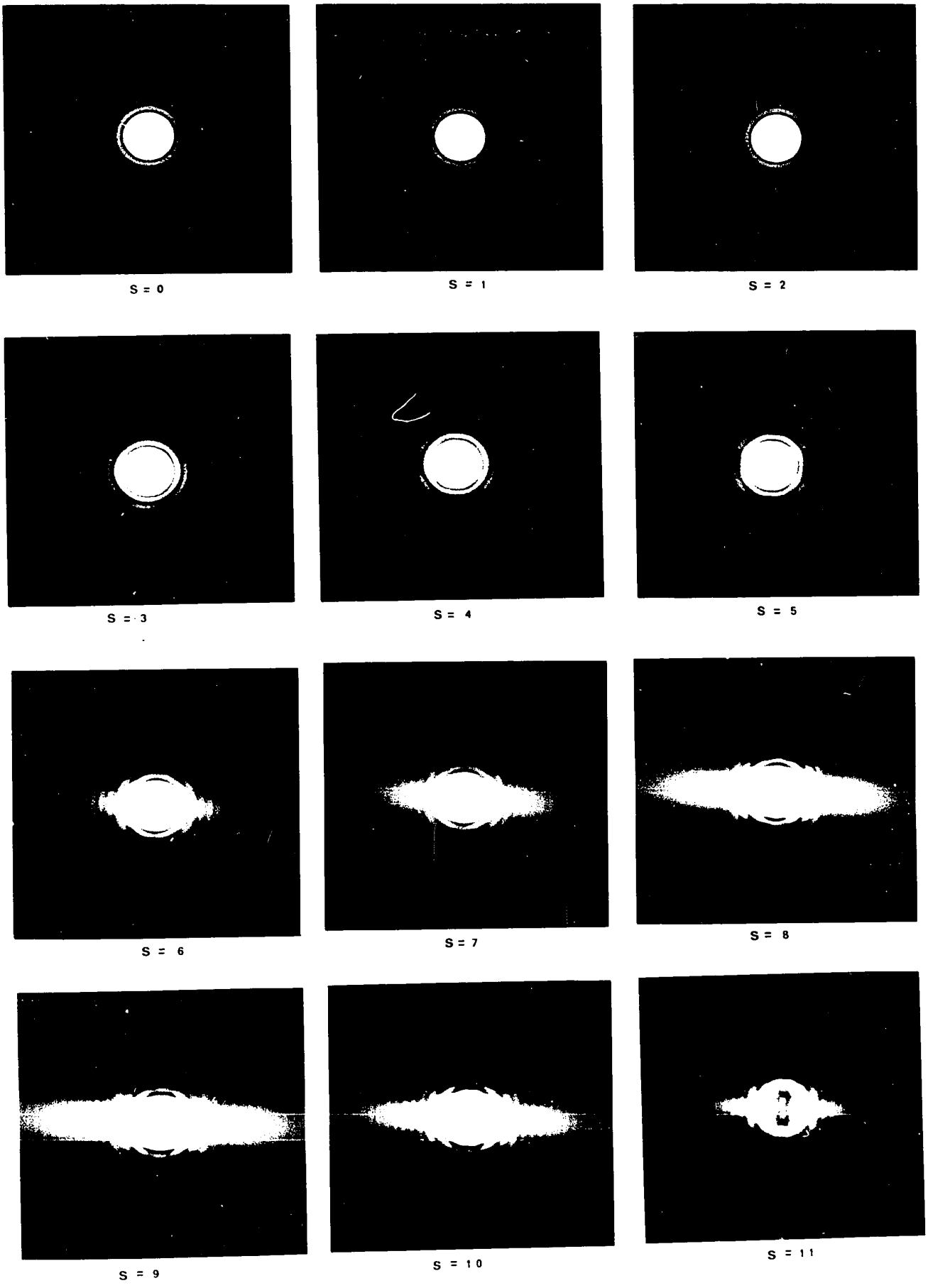

Figure 5.12 Photographs of iterated diffraction patterns formed by the selected system in plane 2 for A_1 = 8.157 and for different values of S.

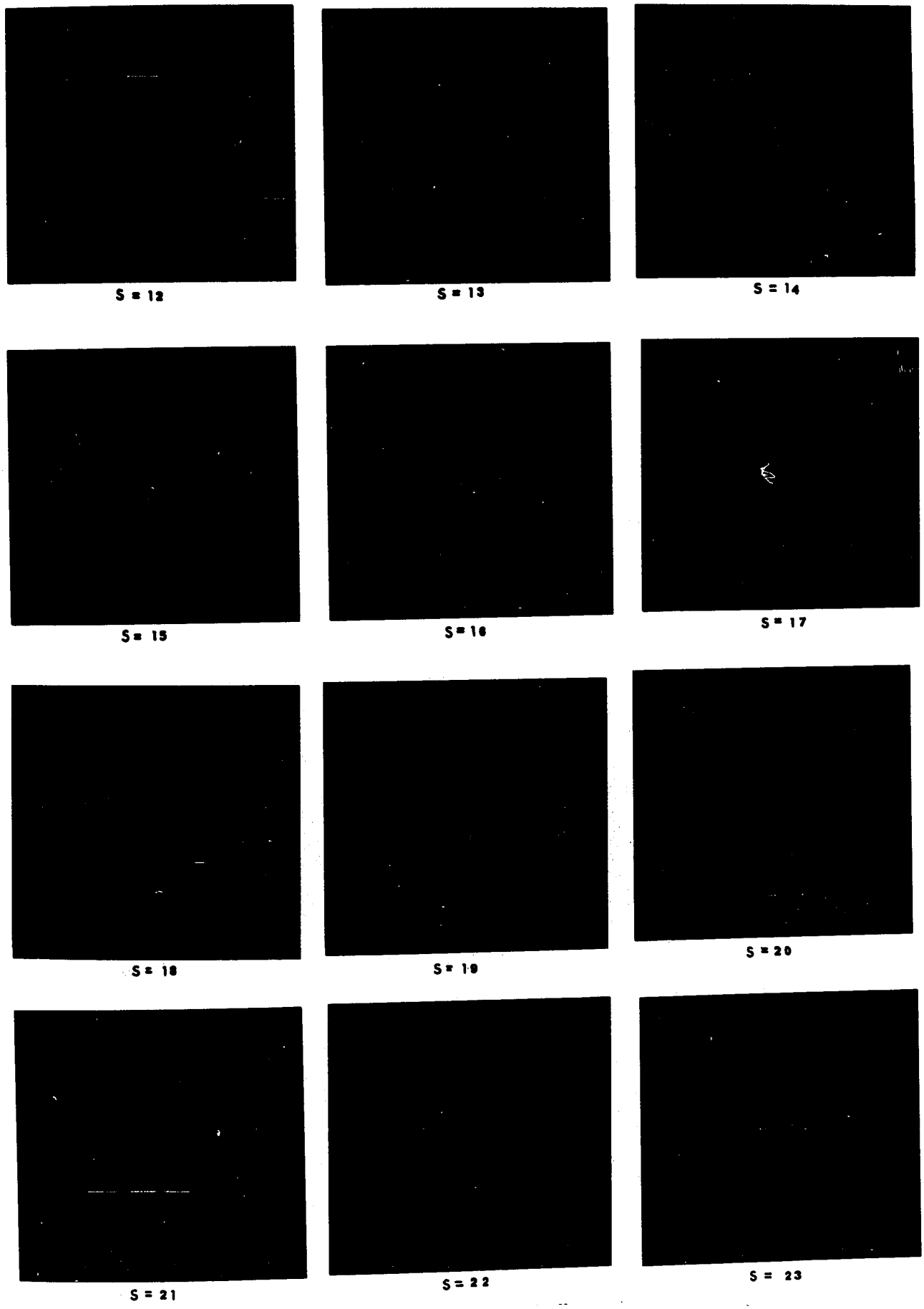

Figure 5.12 Photographs of iterated diffraction patterns formed by the selected system in plane 2 for A_1 = 8.157 and for different values of S.

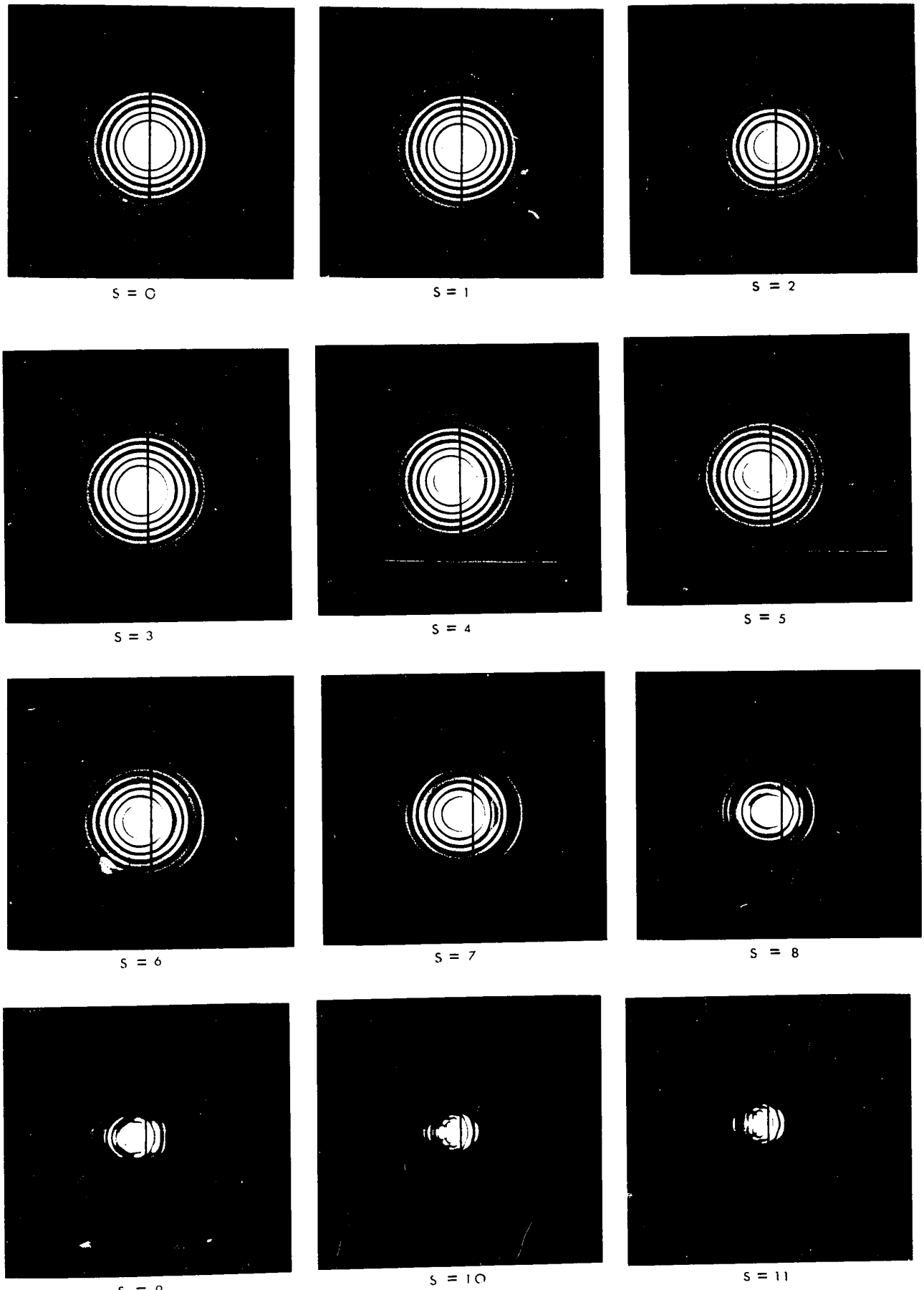

Figure 5.13 Photographs of iterated diffraction patterns formed by the selected system in plane 3 for $A_1 = 8.157$, $B_1 = 0$, $A_2 = 1.421$, $B_2 = 0.790$ and for different values of S.

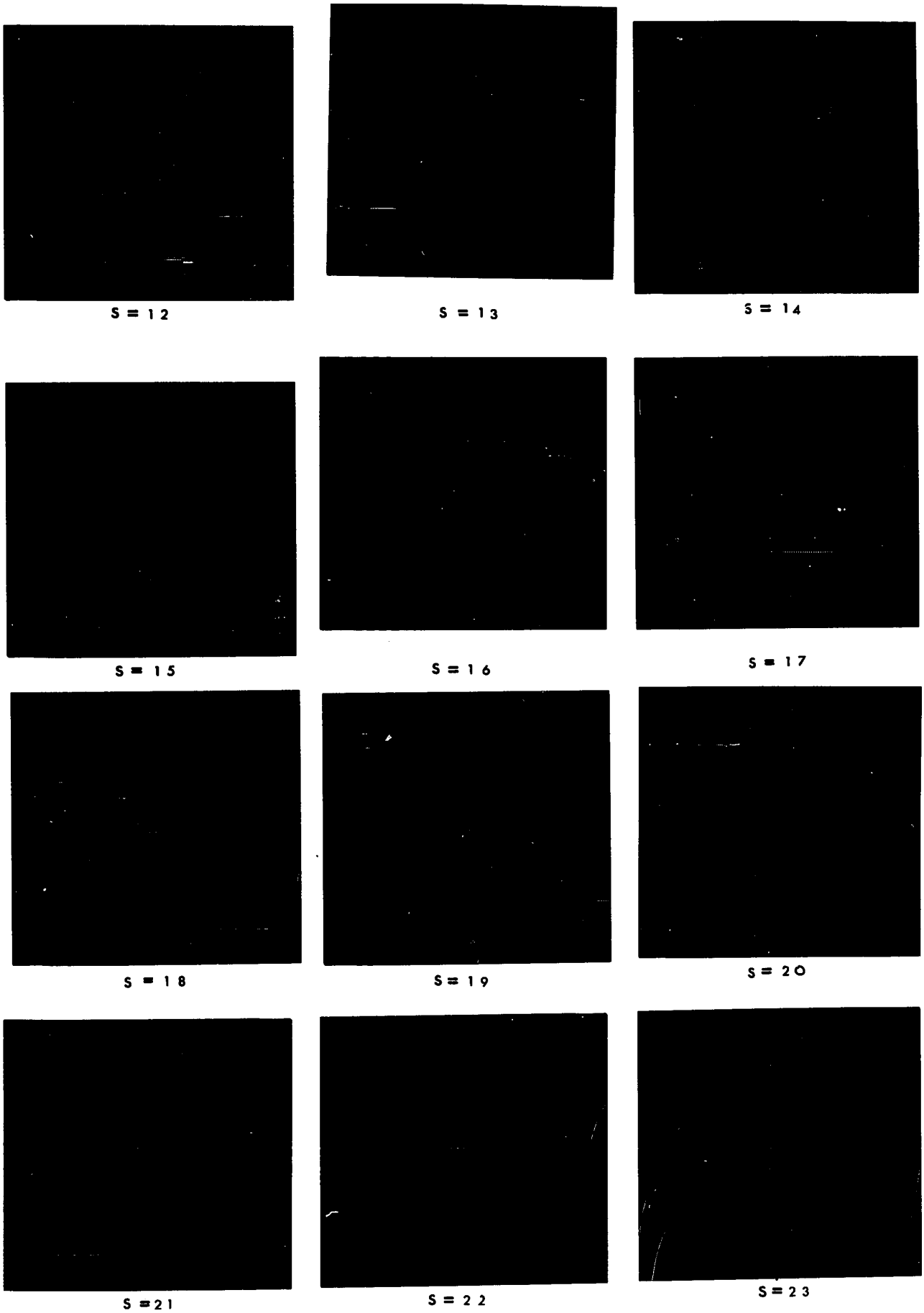

Figure 5.13 Photographs of iterated diffraction patterns formed by the selected system in plane 3 for $A_1 = 8.157$, $B_1 = 0$, $A_2 = 1.421$, $B_2 = 0.790$ and for different values of S.

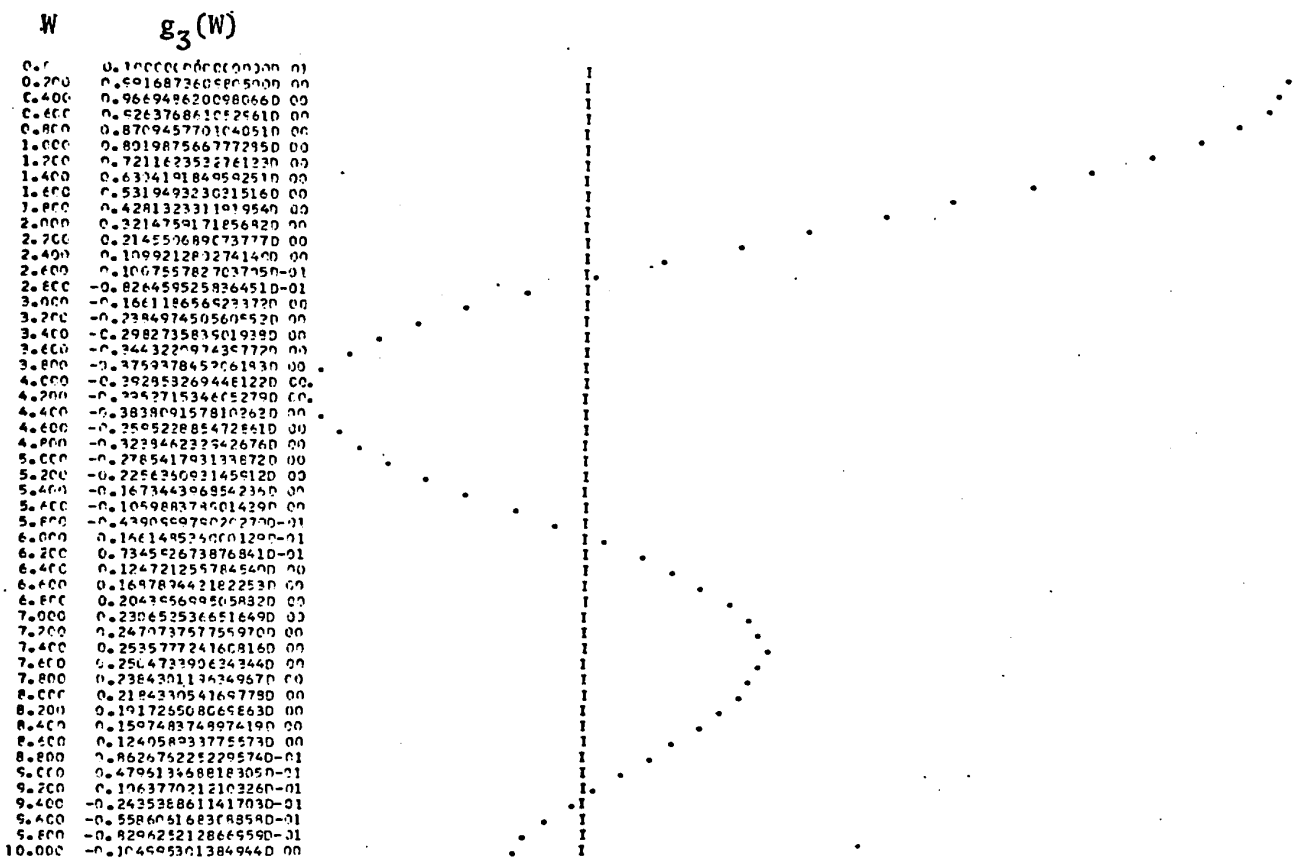

Figure 5.15 Calculation of $g_3(W)$ for the selected system $A_1 = 8.157$, $C_1 = 1.421$, $D_1 = 0.000$ and for S = 0.

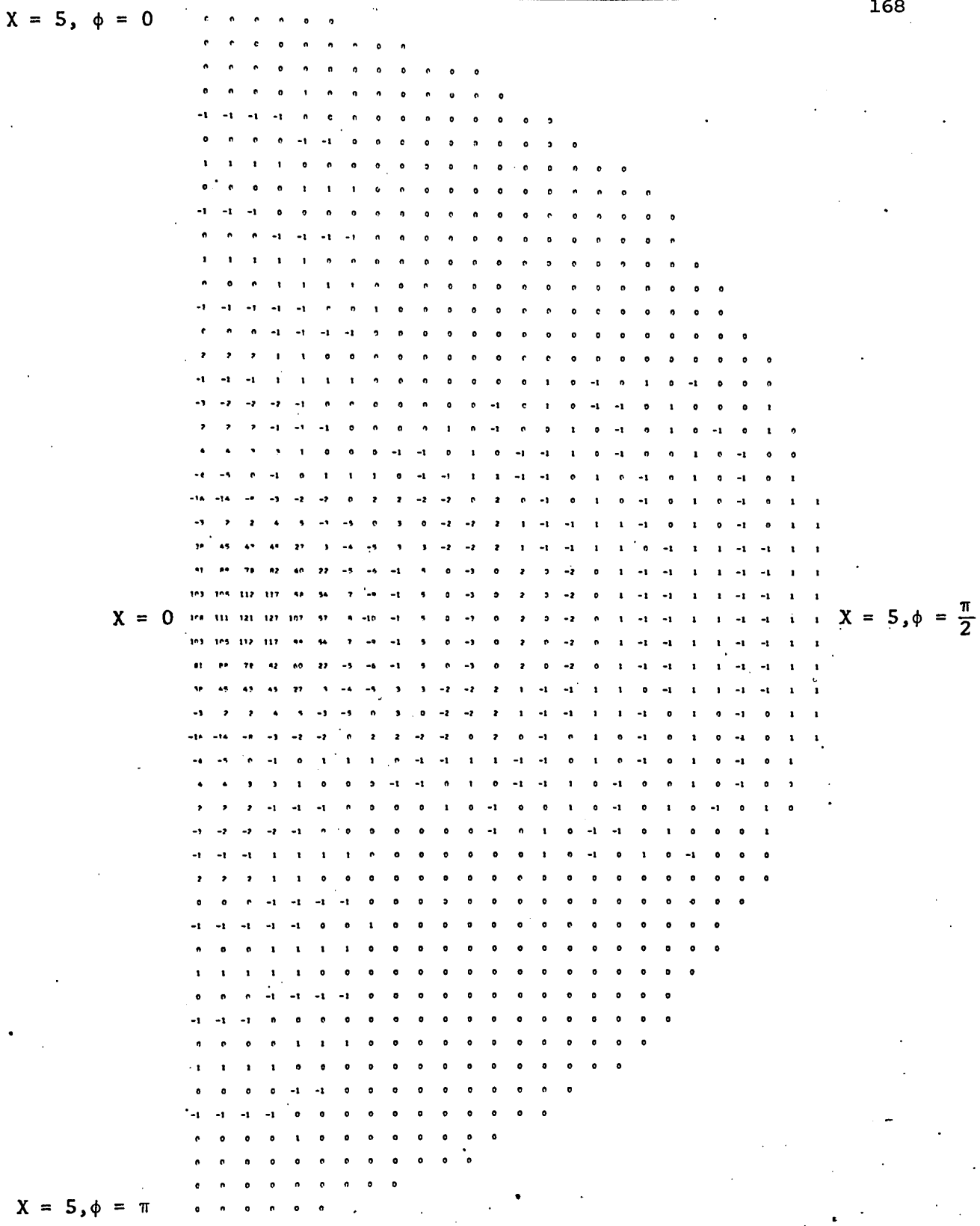

Figure 5.16 Contour map of even amplitude in plane 2 for the selected system $A_1 = 8.157$, $B_1 = 0.000$, $A_2 = 1.421$, $B_2 = 0.790$ for S = 2, for X from 0 to 5 and for ϕ from o to π . The values of even amplitude are normalized so that $g_2(0,0,0)=100$. The construction of contour maps is explained in section 3.6.

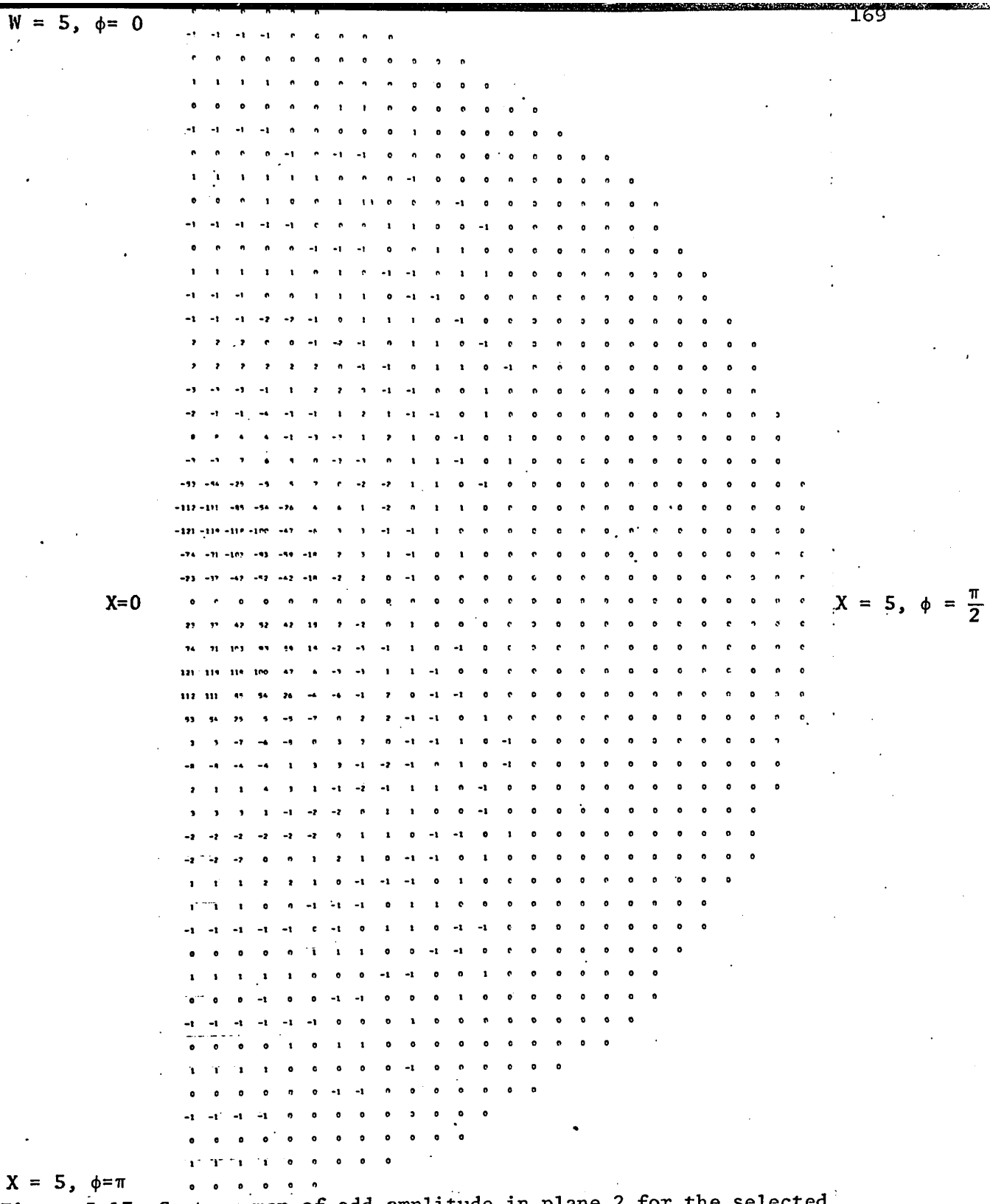

Figure 5.17 Contour map of odd amplitude in plane 2 for the selected system $A_1 = 8.157$, $B_1 = 0.000$, $A_2 = 1.421$, $B_2 = 0.790$, for $S = 2$, for X from 0 to 5 and for ϕ from 0 to π. The values of odd amplitude are normalized so that $g_2(0,0,0) = 100$. The construction of contour maps is explained in section 3.6.

X = 5, ϕ = 0

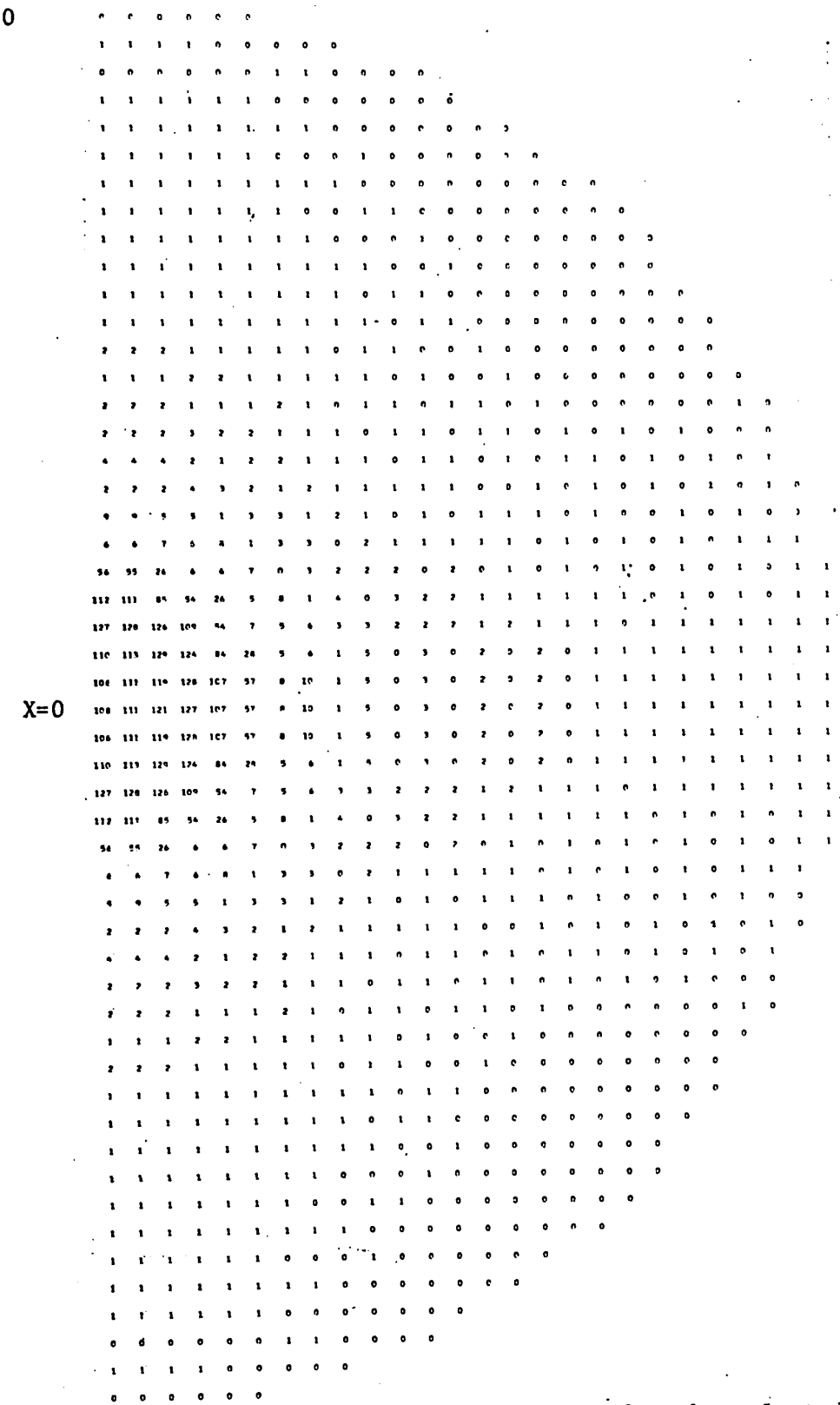

X=0

X = 5, $\phi = \frac{\pi}{2}$

X = 5, $\phi = \pi$

Figure 5.18 Contour map of amplitude in plane 2 for the selected system A_1 = 8.157, B_1 = 0.000, A_2 = 1.421, B_2 = 0.790, for S = 2, for X from 0 to 5 and for ϕ from 0 to π . The values of amplitude are normalized so that $g_2(0,0,0) = 100$. The construction of contour maps is explained in section 3.6.

$X = 5, \quad \phi = 0$

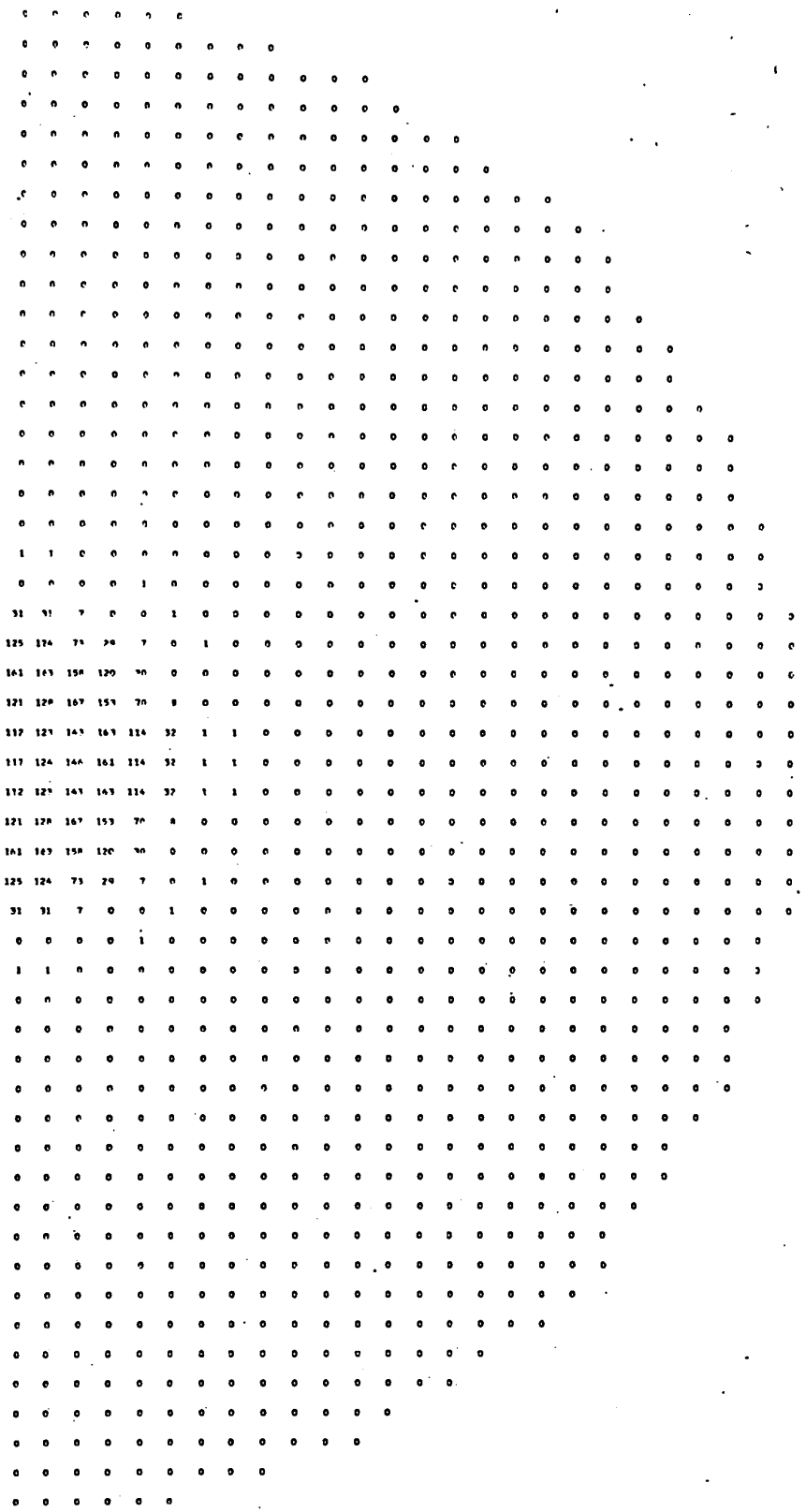

$X=0$

$X = 5, \phi = \frac{\pi}{2}$

$X = 5, \phi = \pi$

Figure 5.19 Contour map of luminous intensity in plane 2 for the selected system $A_1 = 8.157$, $B_1 = 0.000$, $A_2 = 1.421$, $B_2 = 0.790$, for S = 2, for X from 0 to 5 and for ϕ from 0 to π. The values are normalized so that $g_2(0,0,0) = 100$. The construction of contour maps is explained in section 3.6.

$X = 5, \quad \phi = 0$

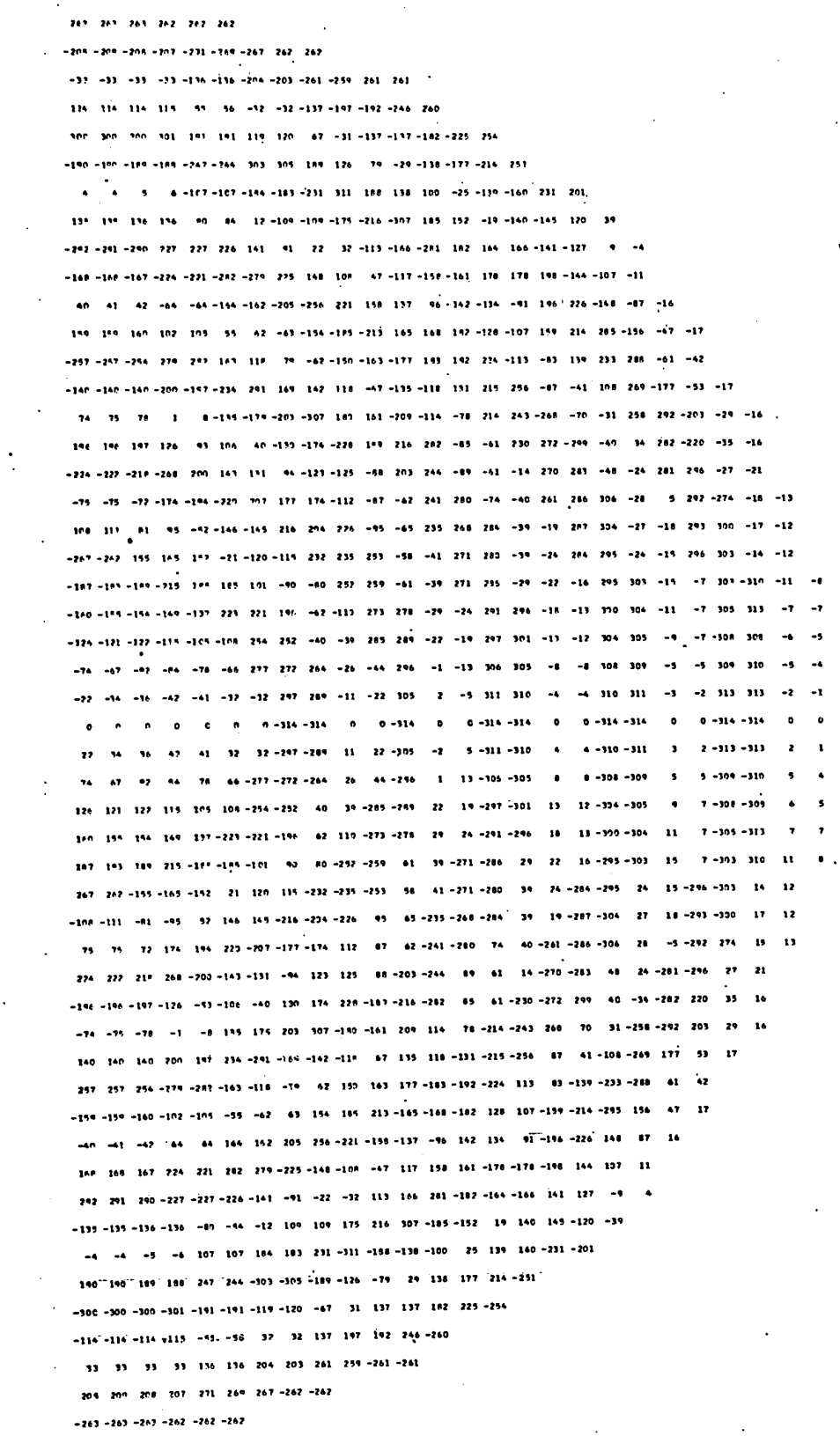

$X = 0$

$X = 5, \phi = \frac{\pi}{2}$

$X = 5, \phi = \pi$

Figure 5.20 Contour map of phase in plane 2 for the selected system $A_1 = 8.157$, $B_1 = 0{,}000$, $A_2 = 1.421$, $B_2 = 0.790$ for S = 2, for X from 0 to 5 and for ϕ from 0 to π. The values are multiplied by 100. The construction of contour maps is explained in section 3.6.

W = 10, θ = 0

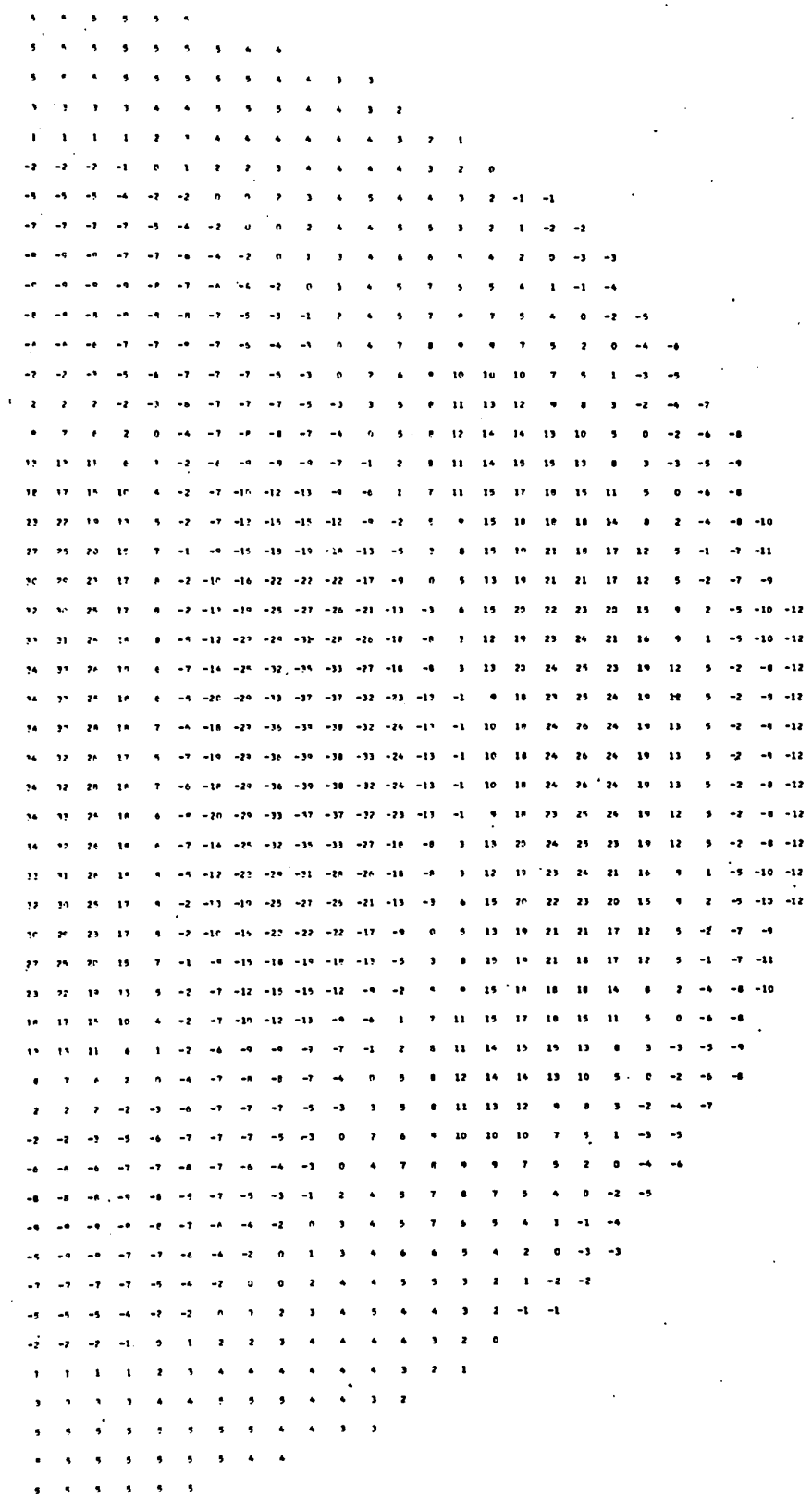

W = 0

X =10, $\phi = \frac{\pi}{2}$

W = 10, θ = π

Figure 5.21 Contour map of even amplitude in plane 3 for the selected system A_1 = 8.157, B_1 = 0.000, A_2 = 1.421, B_2 = 0.790 for S = 2, for W from 0 to 10 and for θ from 0 to π. The values are normalized so that g_3 (0,0,0) = 100. The construction of contour maps is explained in section 3.6.

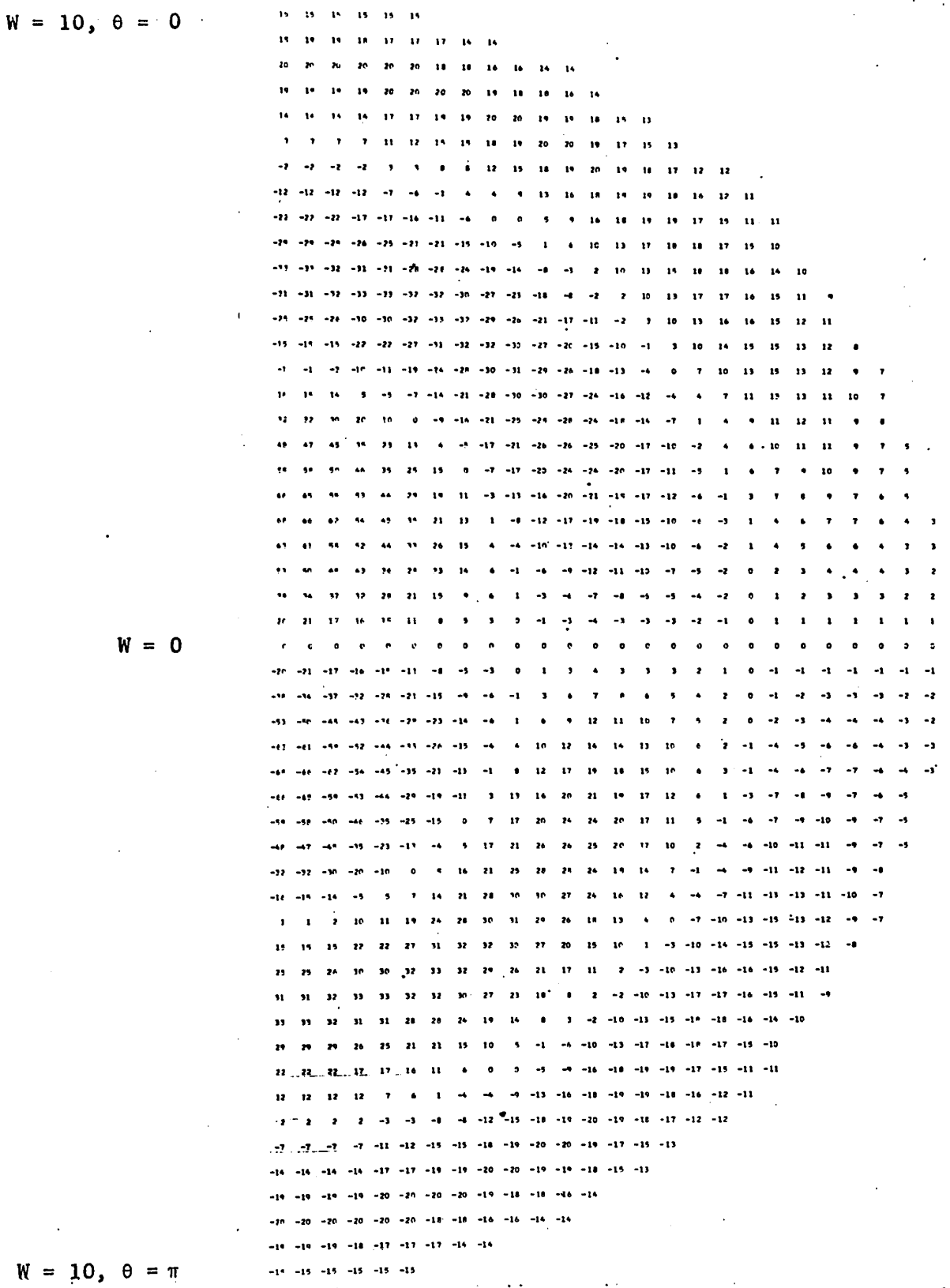

Figure 5.22 Contour map of odd amplitude in plane 3 for the selected system $A_1 = 8.157$, $B_1 = 0.000$, $A_2 = 1.421$, $B_2 = 0.790$ for S = 2, for W from 0 to 10 and for θ from 0 to π. The values are normalized so that $g_3(0,0,0) = 100$. The construction of contour maps is explained in section 3.6.

W = 10, θ = 0

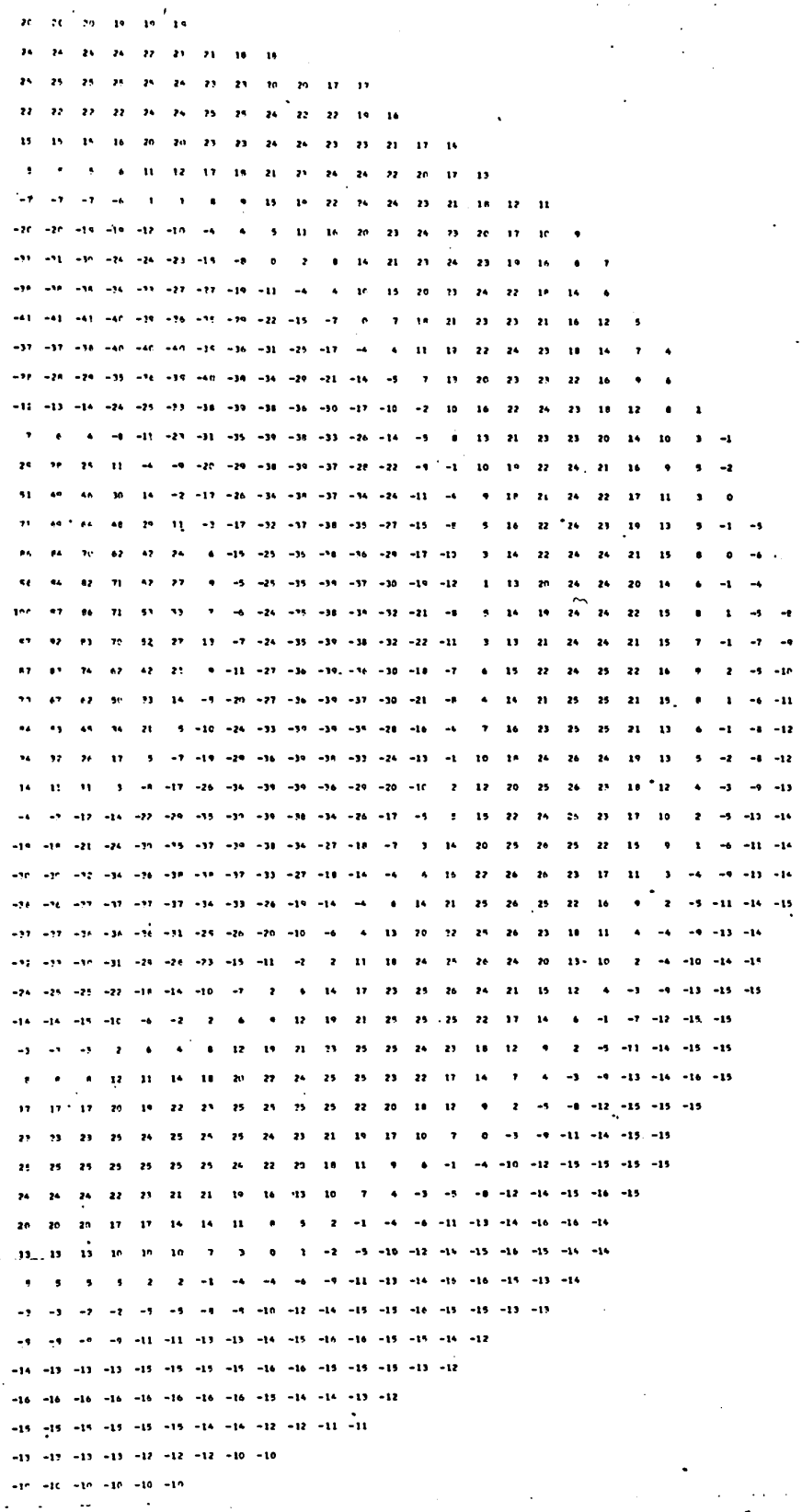

W = 0

W = 10, θ = $\frac{\pi}{2}$

W = 10, θ = π

Figure 5.23 Contour maps of amplitude in plane 3 for the selected system $A_1 = 8.157$, $B_1 = 0.000$, $A_2 = 1.421$, $B_2 = 0.790$ for S = 2, for W from 0 to 10 and for θ from 0 to π. The values are normalized so that $g_3(0,0,0) = 100$. The construction of contour maps is explained in section 3.6.

W = 10, θ = 0

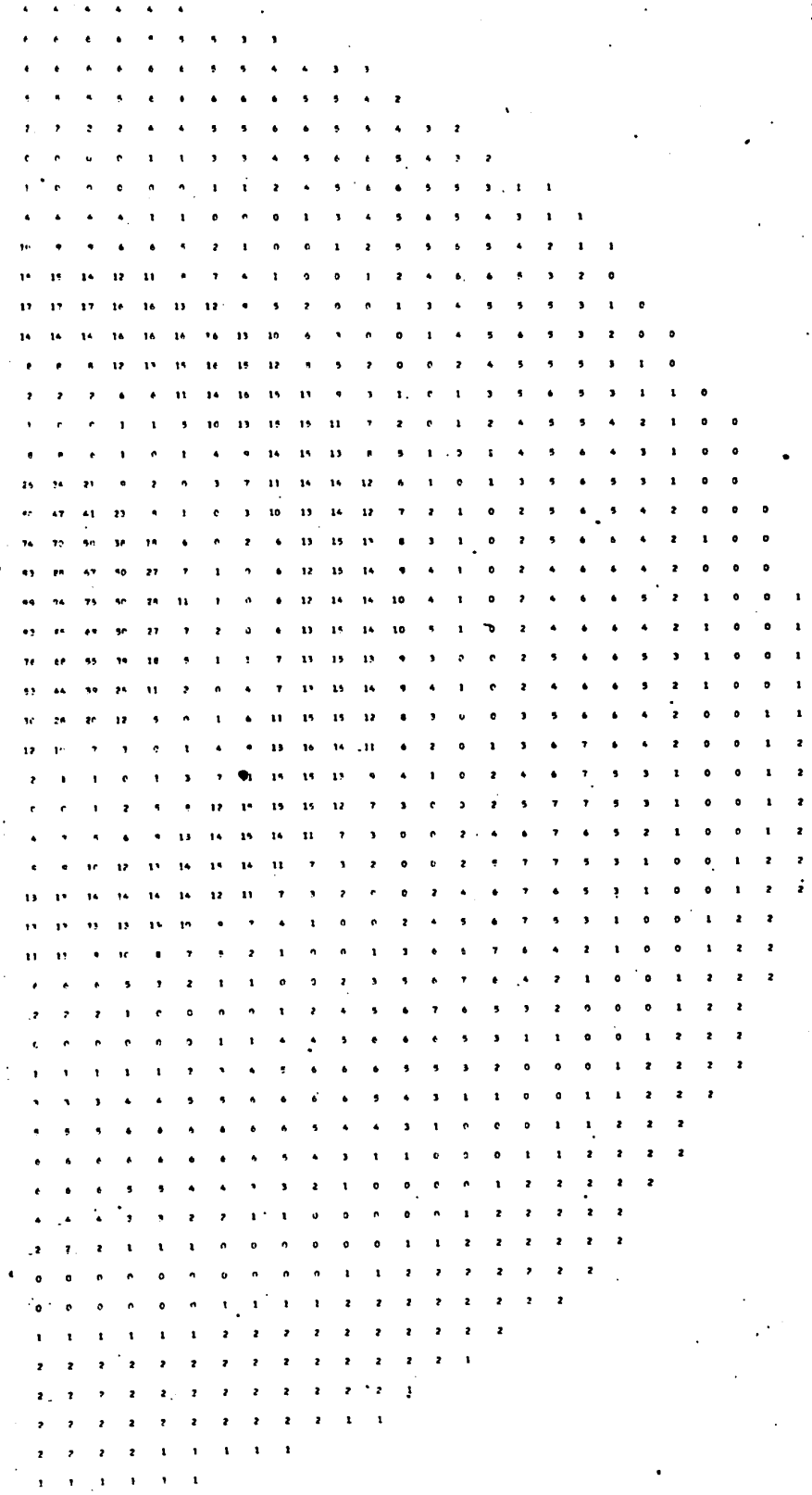

W = 0

W = 10, θ = $\frac{\pi}{2}$

W = 10, θ = π

Figure 5.24 Contour map of luminous intensity in plane 3 for the selected system A_1 = 8.157, B_1 = 0.000, A_2 = 1.421, B_2 = 0.790 for S = 2, for W from 0 to 10, and for θ from 0 to π. The values are normalized so that $g_3(0,0,0) = 100$. The construction of contour maps is explained in section 3.6.

W = 10, θ = 0

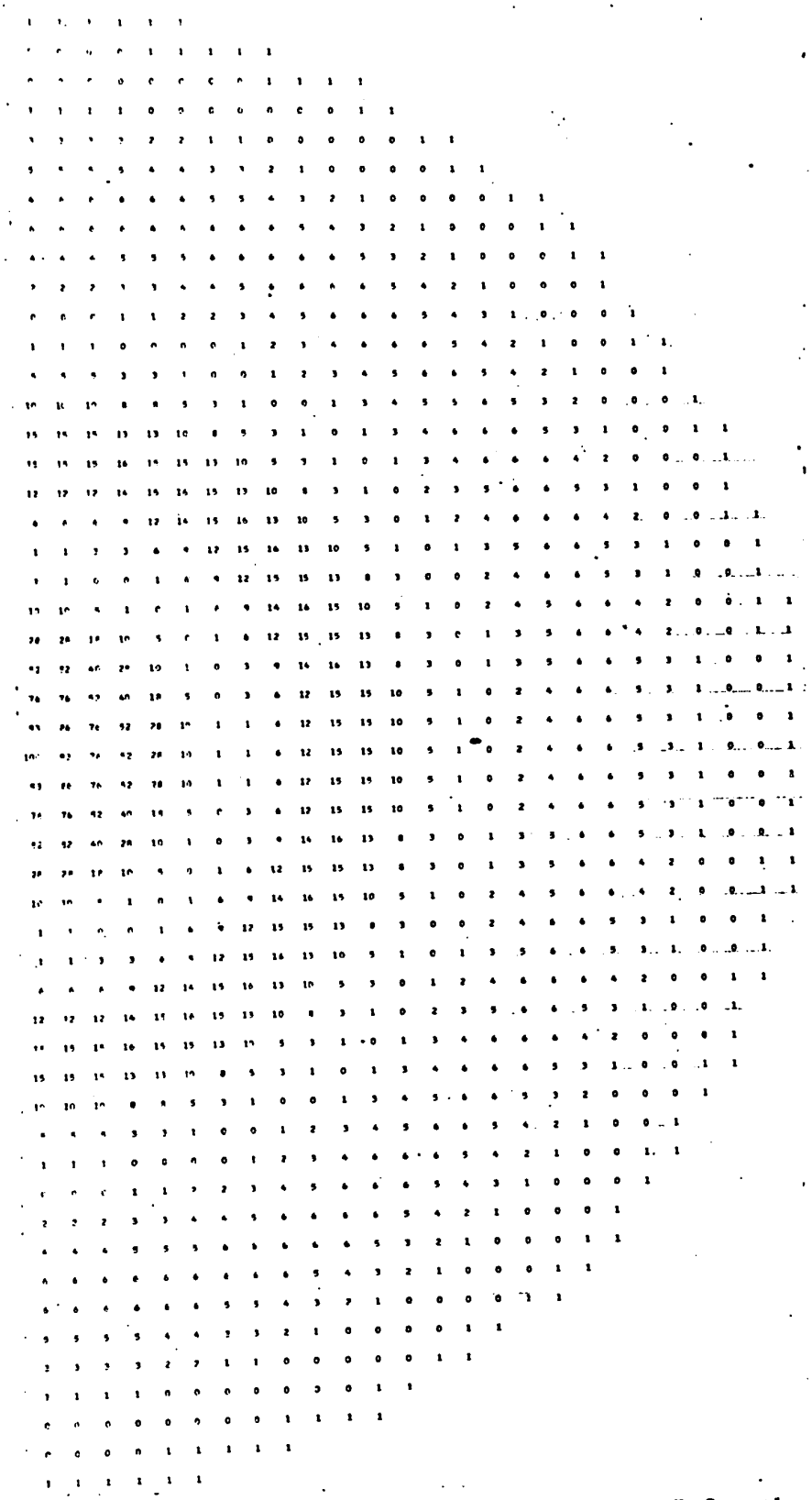

W = 0

W = 10, θ = $\frac{\pi}{2}$

W = 10, θ = π

Figure 5.25 Contour map of luminous intensity in plane 3 for the selected system $A_1 = 8.157$, $B_1 = 0.000$, $A_2 = 1.421$, $B_2 = 0.790$ for $S = 0$, for W from 0 to 10 and for θ from 0 to π. The values are normalized so that $g_3(0,0,0) = 100$. The construction of contour maps is explained in section 3.6.

X	$g_2(X)$
0.0	0.1000000000000000D 01
0.100	0.1013571148551137D 01
0.200	0.1053837852754010 01
0.300	0.1117157855338440 01
0.400	0.1191697541809200 01
0.500	0.1254252441114960 01
0.600	0.1273054075745950 01
0.700	0.1217484010852960 01
0.800	0.1071259025614720 01
0.900	0.8427499707361440 00
1.000	0.5565079638423620 00
1.100	0.2938496778072160 00
1.200	0.7565483268699070-01
1.300	-0.5541827535607350-01
1.400	-0.9548516523900780-01
1.500	-0.6819164933787040-01
1.600	-0.1260954366782720-01
1.700	0.3382518933717990-01
1.800	0.4946510220336670-01
1.900	0.3374493459499430-01
2.000	0.2328451524345390-02
2.100	-0.2425603189251970-01
2.200	-0.3215095839792970-01
2.300	-0.2023407545449870-01
2.400	0.1477019081475570-02
2.500	0.1908844369842260-01
2.600	0.2309548519120310-01
2.700	0.1306348391970090-01
2.800	-0.3354928199665690-02
2.900	-0.1580554944136120-01
3.000	-0.1748296582361990-01
3.100	-0.8628622485652750-02
3.200	0.4398562838537550-02
3.300	0.1347275027223600-01
3.400	0.1362221776460110-01
3.500	0.5625302417711190-02
3.600	-0.4998846602554890-02
3.700	-0.1168128173172880-01
3.800	-0.1077807019492670-01
3.900	-0.3474419313943590-02
4.000	0.5325743431593220-02
4.100	0.1322170011577170-01
4.200	0.8575596103465240-02
4.300	0.1875106196361940-02
4.400	-0.5466508838487240-02
4.500	-0.8969542025930400-02
4.600	-0.6781632310680670-02
4.700	-0.6083774460330520-03
4.800	0.5555303616190930-02
4.900	0.7985238345423670-02
5.000	0.5457877081593100-02

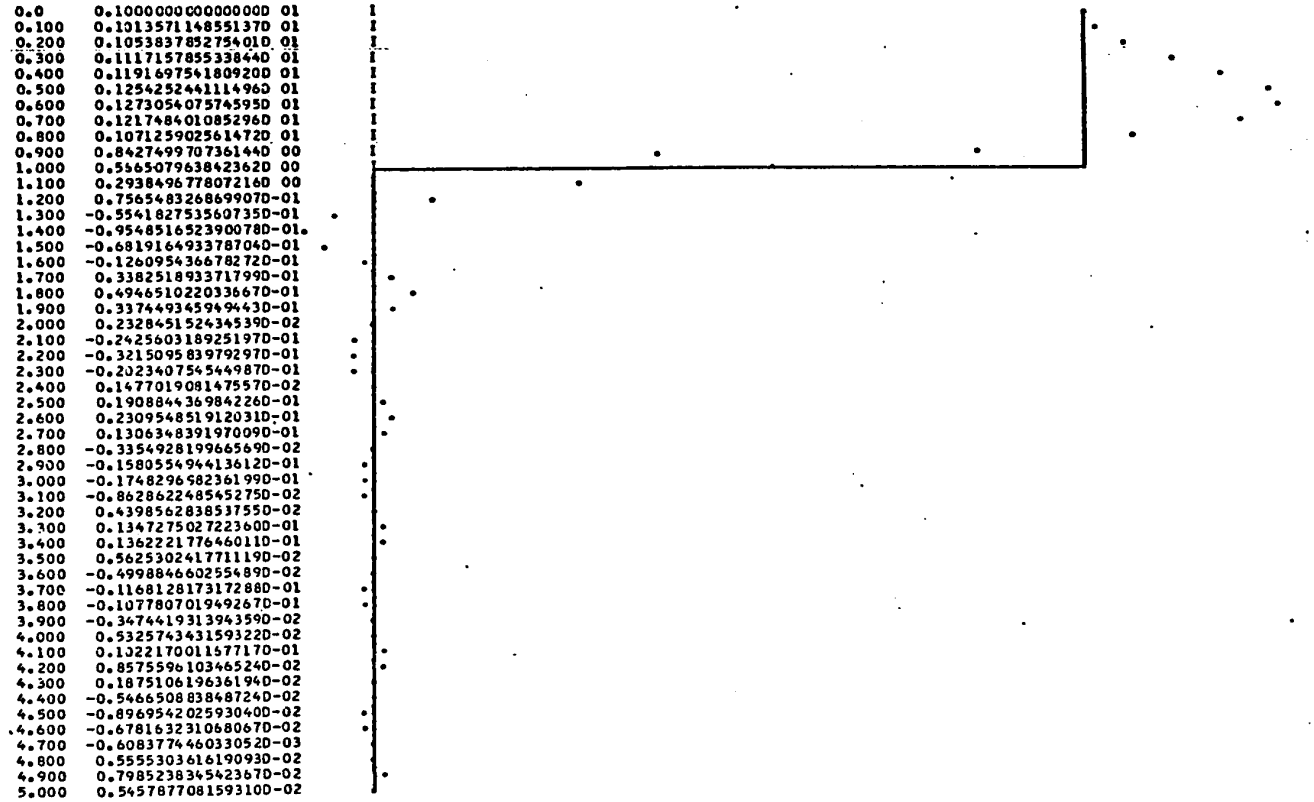

Figure 5.26 & Figure 5.14 Comparison of $g_2(X)$ for the selected system $A_1 = 8.157$, $C_1 = 1.421$, $D_1 = 0.000$ and for S = 0 with the approximating function given by equation 5.40. The solid curve is the approximating function and the dotted curve is the exact function.

5.5.3 The selected system

One of the most successful cases calculated has been selected for illustration both theoretically and experimentally. The system was not extended beyond iteration 2 because there was no further improvement of the energy characteristic for further iterations. However, the system is much better than many which have been extended further. The parameters of the system are:

$A_1 = 8.157$ the abscissa for the second extremum of $4L_1(W) - 3L_2(W)$. This function determines the variation of even amplitude with S as discussed in criterion 2.

$B_1 = 0.000$

$A_2 = 1.421$ the abscissa for the second extremum of $g_2(X,\phi,0)$.

$B_2 = 0.790$ the abscissa for the second extremum of $g_2(X,\phi,0)$.

Photographs of diffraction patterns for this system are shown for plane 2 in figure 5.12 and for plane 3 in figure 5.13. They are shown for integer values of S from 0 to 23 in steps of 1.

For comparison with the photographs, in the special case S = 0, the amplitude function $g_2(X)$ is shown for plane 2 in figure 5.14 of p. 178 and the amplitude function $g_3(W)$ is shown for

plane 3 in figure 5.15. In figures 5.16 to 5.24 contour maps, as explained in section 3.6, are shown of the even function, the odd function, the amplitude, the function of luminous intensity, and the phase for S = 2.0 and for planes 2 and 3. In figure 5.25 a contour map of luminous intensity for S = 0 is shown.

(a) $g_2(X,\phi,S)$ for small S.

Since the chosen value of A_1 is quite large, it encloses about 92% of the total energy of the Airy pattern for small S. Moreover, for $W \geq A_1$, $|g_1(W, ,S)| \leq 0.058$, a reasonably small value. As a result, an approximate expression for $g_2(X,\phi,S)$ can be obtained for small S. That is, when A_1 is very large,

$$g_2(X,\phi,S) \simeq \frac{1}{2\pi} \int_0^{2\pi} \int_0^{\infty} g_1(W,\theta,S)\, e^{iWX\cos(\phi-\theta)} W dW d\theta \qquad 5.39$$

Applying the inverse Fourier transform theorem stated in section 2.11,

$$g_2(X,\phi,S) \simeq g_o(X,\phi,-S) = e^{-iSX\cos\phi} \quad X \leq 1$$
$$= 0 \quad X > 1 \qquad 5.40$$

For S = 0, this result may be compared to the exact computer calculation shown in figure 5.26, and to the corresponding photograph in figure 5.13. In figure 5.26, the approximate distribution is superimposed in the calculated one for easy comparison. Although the approximate distribution is not very close to the calculated one, it is sufficiently close to extend

the analysis to plane 3 for the purpose of gaining greater understanding of the system.

b) $g_2(X,\phi,S)$ for intermediate values of S.

For intermediate values of S, equation 5.39 certainly cannot be used for quantitative analysis since much of the energy is lost outside the diaphram in plane 1. Furthermore, no other exact or approximate expressions could be found.

However, a useful qualitative analysis suggested by the photographs of figure 5.12 can be given. As stated in section 2.9, the amplitude of the light at the diffracting edge has a particularly great influence on the strongly diffracted light; it also has an influence on the light closer to the optical axis. For values of S approximately equal to 8.157, the central spot of the Airy pattern is centered on a small region of the circular diffracting edge. The light emitted from this arc can be compared to the light which would be emitted by a continuous distribution of point sources on a very small arc of the diffracting edge. The light from each point source located at $(A_1,\Delta\theta)$ has in plane 2 at (X,ϕ), a phase given by $e^{iA_1 X \cos(\Delta\theta-\phi)}$. At the point (X,ϕ) in plane 2, the phase difference between the light received from point sources located sufficiently close to each other will be less than π. Under these circumstances there is very little interference and the distribution never reaches zero amplitude. The amplitude distribution appears relatively

uniform although the phase distribution may vary considerably (note that a point source off axis at S gives in plane 0 a uniform amplitude of 1 and a phase which varies as $e^{iSX \cos \phi)}$.

The actual situation does not correspond exactly to this idealized case. Since the angle $\Delta\theta$ limiting the most significant part of the illuminated edge is not extremely small, some interference can be expected. Furthermore, the light inside the diffracting edge is still very significant. But the highest amplitude of the light is relatively concentrated over a small angle $\Delta\theta$ located at the diffracting edge where it has the greatest effect on the diffraction pattern. Therefore, it can be expected that the resultant pattern consists of a relatively uniform amplitude upon which is superimposed an interference pattern. This effect is observable on the photographs of figure 5.12. The effect is highest for S = 8 but it is also quite prominent for S = 7 and S = 9.

c) $g_2(X,\phi,S)$ for large values of S.

The approximate expression for $g_2(X,\phi,S)$ for large S has been derived in section 2.8 (equation 2.28). This equation and its given interpretation agree well with the photographs of figure 5.12

d) Strongly diffracted light for $g_2(X,\phi,S)$ with small S

The light at the circular diffracting edge not only determines the strongly diffracted light but also has a strong influence on the light diffracted nearer the axis. This is readily seen from equation 2.29.

The equation for $g_1(W,\theta,S)$ is given by equation 2.11:

$$g_1(W,\theta,S) = g_{1e}(W,\theta,S) - g_{1o}(W,\theta,S)$$

According to the demonstration is section 5.2, when S is small this can be expressed as,

$$g_1(W,\theta,S) = \Gamma_{1e}(W,S) + \cos 2\theta\, \Gamma'_{1e}(W,S) - g_{1o}(W,\theta,S) \qquad 5.41$$

where

$$\Gamma_{1e}(W,S) = \bar{g}_{1e}(W,\theta,S) = \frac{1}{2}\{L_1(W) - (\frac{S}{2})^2[L_1(W) - \frac{1}{2}L_2(W)]\}$$

$$\Gamma'_{1e}(W,S) = -\frac{1}{2}(\frac{S}{2})^2\ [L_1(W) - L_2(W)]$$

$$g_{1o}(W,\theta,S) = -\frac{WS\cos\theta L_2(W)}{4}$$

At the diffracting edge where $X = A_1 = 8.157$, $L_2(A_1) = 0.0085$ which is negligible. Therefore these equations become,

$$g_1(A_1,\theta,S) = \Gamma_{1e}(A_1,S) + \cos 2\theta\, \Gamma'_{1e}(A_1,S) \qquad 5.42$$

where

$$\Gamma_{1e}(A_1,S) = \frac{1}{2}L_1(A_1)\ [1 - (\frac{S}{2})^2]$$

$$\Gamma'_{1e}(A_1,S) = -\frac{1}{2}(\frac{S}{2})^2\ L_1(A_1)$$

$$g_{10}(A_1,\theta,S) = 0.$$

$$g_{1e}(A_1,\theta,S) = g_1(A_1,\theta,S)$$

Therefore, from equations 2.30, 2.32 and 5.42, the strongly diffracted light in plane 2 is given by,

$$g_{2(far)}(X,\phi,S) = \frac{A_1 L_1(A_1)}{2X} \{[1 - (\frac{S}{2})^2] J_1(A_1X) - (\frac{S}{2})^2 \cos 2\phi \, J_3(A_1X)\} \qquad 5.43$$

$$= \Gamma_{2e}(X,S) - \Gamma'_{2e}(X,S) \cdot \cos 2\phi$$

where

$$\Gamma_{2e}(X,S) = \frac{A_1}{2} L_1(A_1) [1 - (\frac{S}{2})^2] \frac{J_1(A_1X)}{X}$$

$$\Gamma'_{2e}(X,S) = \frac{A_1 L_1(A_1)}{2} (\frac{S}{2})^2 \frac{J_3(A_1X)}{X}$$

This equation for $g_{2(far)}(X,\phi,X)$ is of the form of equation 5.5 as expected. For S = 0, $g_{2(far)}(X,\phi,S)$ simplifies to the distribution of an Airy pattern

$$g_{2(far)}(X) = A_1^2 L_1(A_1) L_1(A_1X) \qquad 5.44$$

A comparison can now be made between the amplitude distribution of the far diffracted light for S = 0 as calculated from equation 5.44 and as calculated from the exact equation 2.13. Table 5.10 shows that

Table 5.10 Comparison of $g_{2(far)}(X)$ as calculated from equation 5.44 and from equation 2.13 with S = 0, A_1 = 8.157.

X	$A_1^2 L_1(A_1)L_1(A_1X)$ equation 5.44	Fourier transform equation 2.13.
0.8	- 0.2209	+ 0.5356
0.9	- 0.1056	0.4213
1.0	+ 0.2580	0.2832
1.1	+ 0.2298	0.1469
1.2	+ 0.0806	0.0378
1.3	- 0.0200	- 0.0277
1.4	- 0.0406	- 0.0477
1.5	- 0.0340	- 0.0340

there is agreement for higher values of X only.

As S increases from 0 to 2, $\Gamma_{2e}(X,S)$ decreases and becomes zero at S = 2. This is a characteristic of the far diffracted light at all values of X. The far diffracted light might therefore contribute to improving the ratios $e_{3e}(0,S)$, particularly at S = 2

(e) $g_3(W,\theta,S)$ for small S.

An approximate expression for $g_3(W,\theta,S)$ may be obtained with S small using the approximating expression 5.40:

$$g_3(W,\theta,S) = \frac{1}{2\pi} \int_0^{2\pi} \int_{B_2}^{A_2} g_2(X,\phi,S)\, e^{iWX\cos(\phi-\theta)} X dX d\phi \qquad 5.45$$

$$\simeq \frac{1}{2\pi} \int_0^{2\pi} \int_{B_2}^{1} e^{-iS\cos\phi}\, e^{iWX\cos(\phi-\theta)} X dX d\phi$$

By equation 2.18,

$$g_3(W,\theta,S) = \frac{J_1(W')}{W'} - B_2^2 \frac{J_1(B_2W')}{B_2W'} \qquad 5.46$$

where

$$W' = \sqrt{W^2 - 2WS\cos\theta + S^2}$$

The result is the superposition of two Airy patterns, each having the same center, W = + S, θ = 0 (see section 2.7). Consequently, the

distribution moves a displacement + S when the point source moves a displacement + S. The photographs in figure 5.13 clearly show this displacement with respect to the dark vertical line, a reference for the position S = 0.

The luminous intensity of the second Airy pattern is 0.38 times the luminous intensity of the first Airy pattern. The abscissae giving the extrema of $\frac{J_1(W')}{W'}$ are 0.000, 5.136, 8.157... whereas the abscissae giving the extrema of $\frac{J_1(B_2W')}{B_2W'}$ are 0.000, 6.501, 10.325... Thus, the extrema of the first diffraction pattern are interlaced with those of the second diffraction pattern which has a lower luminous intensity. The two Airy patterns can therefore be easily distinguished on the photographs of figure 5.13.

(f) $g_3(W,\theta,S)$ for intermediate values of S.

As S increases, the diffraction patterns become progressively more distorted; they eventually change to a stable pattern which is strikingly different from the symmetrical patterns for small S.

(g) $g_3(W,\theta,S)$ for large values of S.

The photographs of figure 5.13 show well localized curved fringes very similar to the distribution $g_1(W,\theta,S)$ for large S given by the approximating equation 2.25:

$$g_1(W,\theta,S) = \sqrt{\frac{2}{\pi}}\left(\frac{1}{S^{3/2}} - \frac{3}{2}\,\frac{W\cos\theta}{S^{5/2}}\right)\cos\left(S + W\cos\theta - \frac{3\pi}{4}\right) \quad W \leq A_1 \qquad 5.47$$

$$= 0 \qquad W > A_1$$

Since the phase term $\frac{1}{2}\frac{W^2}{S}$ was omitted in the cosine argument, this equation describes straight fringes rather than circular fringes.

$g_3(X,\phi,S)$ and $g_1(X,\phi,S)$ will be equal if the Fourier transform inverse theorem explained in section 2.11 can be applied. Therefore it is useful to investigate how closely the integration of $g_2(X,\phi,S)$ from B_2 to A_2 approximates the same integration from 0 to ∞. This depends on the function $g_2(X,\phi,S)$ which, as explained in section 2.8, consists predominantly of two Airy patterns centered at X = +1 and X = -1. The first zero of these Airy patterns is defined by,

$$X_1' = X_2' = \frac{3.832}{A_1} = 0.469$$

where

$$X_1' = \sqrt{X^2 + 2X\cos\phi + 1} \qquad \text{and} \qquad X_2' = \sqrt{X^2 - 2X\cos\phi + 1}$$

For $\phi = 0$, this corresponds to $X = \pm 1.4697$ and $X = \pm 0.5303$. Thus both the inner radius $B_2 = 0.790$ and the outer radius $A_2 = 1.421$ of the annulus in plane 2 cut a small section of these spots. Therefore, the integration from B_2 to A_2 is not a good approximation of the integration from 0 to ∞. Nevertheless, the principle of the Fourier transform inverse theorem is quite evident qualitatively. The complete absence of any apparent light outside the defined fringe region is quite striking.

(h) Effect of the far diffracted light in plane 2 on $g_3(0,S)$

Since the far diffracted light in plane 2 is weighted by large values of X, it is useful to investigate its possible effect on $g_3(0,S)$. As shown by table 5.10, equation 5.44 is not a good representation of $g_2(X,\phi,S)$ in the range of $0.790 \leq X \leq 1$. Therefore, this range is excluded from the expression below. The component of $g_3(0,S)$ due to the far diffracted light is given by,

$$g_{3_{(far)}}(0,S) \approx \frac{1}{2\pi} \int_0^{2\pi} \int_1^{A_2} g_{2_{(far)}}(X,\phi,S)\, X dX d\phi$$

$$\approx A_1^2 L_1(A_1) \left[1 - \left(\frac{S}{2}\right)^2\right] \int_1^{A_2} L_1(A_1 X)\, X dX \qquad 5.48$$

From equation B_4 of appendix B,

$$g_{3_{(far)}}(0,S) \approx -2 L_1(A_1) \left[1 - \left(\frac{S}{2}\right)^2\right] \left[L_o(A_1A_2) - L_o(A_1)\right]$$

$$\approx 0.02256 \left[1 - \left(\frac{S}{2}\right)^2\right] \qquad 5.49$$

(i) Normalized even energy in plane 3.

Table 5.11 shows for integer values of S from 0 to 10, a comparison of the normalized even energy values, $e_{3e}(0,S)$ as calculated from:

(1) The approximating expression of equation 5.46 which is valid for small values of S.

(2) The Fourier transform (FT).

In addition, a table of $e_{3e}(0,S)$ times the modulation function (MF) as defined in section 2.12 is given.

The normalized even energy values calculated by (1) and (2) agree well for values of S from 0 to 5. The normalized even energy values are not within our goal for hyperresolution discussed in the introductory paragraphs of this chapter: $e_{3e}(0,S) \leq 0.05$ for $S \geq 2$. For this system, $e_{3e}(0,S) \leq 0.144$ for $S \geq 2$. However, the values of $e_{3e}(0,S)$x MF are within this goal: $e_{3e}(0,S)$ x MF ≤ 0.039 for $S \geq 2$.

A comparison of the normalized energy values in plane 3 to the normalized energy values of the Airy pattern, $e_{1e}(0,S)$, gives a direct indication of the improvement of the hyperresolving characteristic. Table 5.11 shows that there is a slight improvement since $e_{3e}(0,S) < e_1(0,S)$ for $S \leq 2$. For higher values of S, this inequality does not hold in general. However, the normalized even energy values are negligible in this region.

Table 5.11 Normalized even energy values, $e_{3e}(0,S)$ of the selected system for integer values of S.

S	$e_1(0,S)$	$e_{3e}(0,S)$ from equation 5.46	$e_{3e}(0,S)$ from Fourier transform (FT)	$e_{3e}(0,S)$ x MF From (FT)
0	1.000	1.0000	1.0000	1.0000
1	0.7746	0.6449	0.6532	0.5060
2	0.3326	0.1245	0.1181	0.0392
3	0.0511	0.0141	0.0178	0.0009
4	0.0011	0.1437	0.1435	0.0002
5	0.0171	0.0955	0.0931	0.0016
6	0.0085	0.0442	0.0021	0.0000
7	0.0000	0.0402	0.0438	0.0000
8	0.0034	0.0666	0.0852	0.0000
9	0.0030	0.0174	0.0342	0.0001
10	0.0001	0.0047	0.0000	0.0000

CONSOLIDATION OF THE ANALYSIS

In the theoretical and experimental investigation of this system, analyses were made which led to a greater understanding of the system. As a result, these analyses can now be consolidated and examined for understanding of the normalized even energy values $e_3(0,S)$ of table 5.11.

For small values of S, results predicted by equation 5.46 agree well with both the numerical calculations of $e_3(0,S)$ and photographs of the diffraction patterns. Equation 5.44 for the strongly diffracted light in plane 2 is reasonably accurate in the range $1 \leq x \leq 1.42$. But the effect of the strongly diffracted light on $g_3(0,S)$ with small S is not large enough compared with the error in equation 5.46 to warrant much consideration.

When the point source is moved to a position S, the center of the distribution $g_3(W,\theta,S)$ is moved to a position + S. The amplitude at W = +S of the symmetrical distribution $g_3(W)$ is moved to the channel axis where W = 0. Thus the distribution $g_3(0,0,S)$ at the channel axis is the symmetrical amplitude distribution $g_3(W)$ with W = +S. As a result, the unnormalized even energy function $E_{3e}(0,S)$ varies as the function of luminous intensity $I_3(W)$ with W = +S. This result can be used to understand the decrease in the normalized even energy values for small S. Since the function $I_3(W)$ is the result of the superposition of two Airy patterns, it decreases rapidly to zero for small values of W. Consequently, $e_{3e}(0,S)$, which varies as $I_3(+S)$, also decreases in the same way.

Although the large diaphram $A_1 = 8.157$ does not eliminate much energy from the system for small S, it does eliminate much of it for intermediate and larger values of S. For intermediate values of S, there are two principle effects when the central Airy spot reaches the circular diffracting edge:

(1) The part of the spot beyond the edge is eliminated from the system.

(2) The part of the spot at the diffracting edge contributes to a high component of uniform light well spread out in plane 2 . Much of this light is eliminated from the system by the annulus in plane 2.

As a result of these two effects, there are relatively low normalized even energy values in plane 3 for intermediate values of S.

At large values of S, a small part of the energy of the two spots formed in plane 2 is eliminated from the system by the annulus. But the low energy is mostly due to the low amplitude of that part of the Airy pattern within the diaphram.

In conclusion, the system behaves as expected. Although the normalized even energy values are not within our goal for hyperesolution, the modulation function has brought these values within this goal.

5.6 A system with narrow annuli

The main difficulty in the design of a hyperresolving system is that the Fourier transform does not lend itself to the development of a simple mathematical expression for the diffraction pattern in any plane

for any values of S. This difficulty can be overcome if the annuli are sufficiently narrow so that the integrand of the Fourier transform can be considered constant as the radial coordinate varies over the width of the annulus. It was decided to attempt such a solution with two annuli, this being the simplest nontrivial system. Each annulus is characterized by its radius and by its width relative to other annuli. It is reasonable to expect that these parameters can be used to specify that the axis amplitude of the diffraction patterns is zero for at least two chosen values of S . Hopefully, the values of S close to these chosen values, will also have low axis amplitudes. The theory and experimental results for the solution are explained in this chapter.

5.6.1 Role of the average even amplitude

In criterion 4 of section 5.3, it was shown for small values of S that the energy characteristic on the axis depended only on the average even amplitude. This result will now be shown for all values of S.

Suppose that for any value of S with n even, $g_{ne}(X,\phi,S)$ may be expressed as,

$$g_{ne}(X,\phi,S) = \Gamma_{ne}(X,S) - \sum_{k=1}^{\infty} \Gamma'_{nek}(X,S) \cos 2k\phi \qquad 5.50$$

Then

$$g_{n+1}(W,\theta,S) = \frac{1}{2\pi}\int_0^{2\pi}\int_{B_n}^{A_n} g_{ne}(X,\phi,S)\ e^{iWX\cos(\phi-\theta)}X\,dX\,d\phi \qquad 5.51$$

$$= \int_{B_n}^{A_n} \Gamma_{ne}(X,S)\left[\frac{1}{2\pi}\int_0^{2\pi} e^{iWX\cos(\phi-\theta)}\,d\phi\right]X\,dX$$

$$- \sum_{k=1}^{\infty}\int_{B_n}^{A_n} \Gamma'_{nek}(X,S)\left[\frac{1}{2\pi}\int_0^{2\pi}\cos 2k\phi\ e^{iWX\cos(\phi-\theta)}\,d\phi\right]X\,dX$$

From equation A3 of appendix A, this becomes,

$$g_{n+1,e}(W,\theta,S) = \Gamma_{n+1,e}(W,S) + \sum_{k=1}^{\infty}\Gamma'_{n+1,ek}(X,S)\cos 2k\theta \qquad 5.52$$

where $\Gamma_{n+1,e}(W,S) = \int_{B_n}^{A_n} \Gamma_{ne}(X,S)\,J_0(WX)\,X\,dX$

$$\Gamma'_{n+1,ek}(W,S) = (-1)^k\int_{B_n}^{A_n}\Gamma'_{nek}(X,S)\,J_{2k}(WX)\,X\,dX$$

Similarly for n odd,

if $$g_{ne}(W,\theta,S) = \Gamma_{ne}(W,S) + \sum_{k=1}^{\infty}\Gamma'_{nek}(W,S)\cos 2k\phi \qquad 5.53$$

then,

$$g_{n+1,e}(X,\phi,S) = \Gamma_{n+1,e}(X,S) + \sum_{k=1}^{\infty} \Gamma'_{n+1,e}(X,S) \cos 2k\phi \qquad 5.54$$

where

$$\Gamma_{n+1,e}(X,S) = \int_{B_n}^{A_n} \Gamma_{ne}(W,S)\, J_o(WX)\, WdW$$

$$\Gamma'_{n+1,ek}(X,S) = (-1)^k \int_{B_n}^{A_n} \Gamma'_{nek}(W,S) J_{2k}(WX) WdW$$

In the plane of the lens, from equation A8 of appendix A,

$$g_{oe}(X,\phi) = \cos(XS\cos\phi) = J_o(SX) + 2\sum_{k=1}^{\infty} J_{2k}(XS)\cos 2k\phi \qquad 5.55$$

Therefore,

$$\Gamma_{oe}(X,S) = J_o(SX) \qquad 5.56$$

$$\Gamma_{oek}(X,S) = 2J_{2k}(SX) \qquad 5.57$$

Thus $g_{ne}(X,\phi,S)$ can be expressed in the form given by equation 5.50

As in the case of small S,

$$\Gamma'_{n+1,ek}(0,S) = (-1)^k \int_{B_n}^{A_n} \Gamma'_{nek}(W,S)\, J_{2k}(0) W dW = 0 \qquad n \text{ odd}$$

$$k \geq 1 \qquad 5.58$$

$$\Gamma'_{n+1,ek}(0,S) = (-1)^k \int_{B_n}^{A_n} \Gamma'_{nek}(X,S)\, J_{2k}(0) X dX = 0 \qquad n \text{ even}$$

$$k \geq 1 \qquad 5.59$$

Therefore, the function Γ'_{ne} plays no role in determining the energy characteristic on the channel axis, the energy characteristic depends entirely on the function Γ_{ne}, which is the average even amplitude $\bar{g}_{ne}$ (see criterion 4).

5.6.2 The function $\Gamma_{2e}(X,S)$ with two annuli.

If the annuli in plane 1 have radii defined by W_1 and W_2 with widths ΔW_1 and ΔW_2 respectively, the function $\Gamma_{2e}(X,S)$ is given by,

$$\Gamma_{2e}(X,S) = \Gamma_{1e}(W,S)\, J_o(W_1 X)\, W_1 \Delta W_1 + \Gamma_{1e}(W_2,S)\, J_o(W_2 X) W_2 \Delta W_2 \qquad 5.60$$

For two values of S, S_1 and S_2 we require that

$$\Gamma_{2e}(X,S) = 0$$

That is,

$$\Gamma_{1e}(W_1,S_1)J_o(W_1X)W_1\Delta W_1 + \Gamma_{1e}(W_2,S_1)J_o(W_2X)W_2\Delta W_2 = 0$$

$$\Gamma_{1e}(W_1,S_2)J_o(W_1X)W_1\Delta W_1 + \Gamma_{1e}(W_2,S_2)J_o(W_2X)W_2\Delta W_2 = 0 \qquad 5.61$$

A solution of this Cramer system will exist only if,

$$\begin{vmatrix} \Gamma_{1e}(W_1,S_1) & \Gamma_{1e}(W_2,S_1) \\ \Gamma_{1e}(W_1,S_2) & \Gamma_{1e}(W_2,S_2) \end{vmatrix} = 0 \qquad 5.62$$

That is, W_1 and W_2 must be chosen to satisfy the equation,

$$\Gamma_{1e}(W_1,S_1)\,\Gamma_{1e}(W_2,S_2) = \Gamma_{1e}(W_2,S_1)\,\Gamma_{1e}(W_1,S_2) \qquad 5.63$$

Assuming equation 5.63 can be satisfied, equations 5.61 have the solution,

$$\frac{J_o(W_1X)\,W_1\Delta W_1}{J_o(W_2X)\,W_2\Delta W_2} = -\frac{\Gamma_{1e}(W_2,S_2)}{\Gamma_{1e}(W_1,S_2)} \qquad 5.64$$

This equation must be satisfied by the proper choice of X and the ratio $\Delta W_1/\Delta W_2$.

Substituting equation 5.64 in equation 5.60,

$$\Gamma_{2e}(X,S) = [\Gamma_1(W_2,S) - \frac{\Gamma_1(W_1,S)\Gamma_1(W_2,S_2)}{\Gamma_1(W_1,S_2)}] J_o(W_2X)\, W_2\Delta W_2 \qquad 5.65$$

This equation is valid only for the chosen values of X satisfying equation 5.64.

The normalized even energy is given by,

$$e_{2e}(X,S) = [\frac{\Gamma_{2e}(X,S)}{\Gamma_{2e}(X,O)}]^2 = [\frac{\Gamma_1(W_2,S)\Gamma_1(W_1S_2) - \Gamma_1(W_1S)\Gamma_1(W_2,S_2)}{\Gamma_1(W_2,O)\Gamma_1(W_1,S) - \Gamma_1(W_1,O)\Gamma_1(W_2,S_2)}]^2$$

$$= 0 \text{ for } S = S_1 \text{ and } S = S_2 \qquad 5.66$$

To repeat the process in another iteration, it is necessary to have in plane 2, two annuli located at values X_1 and X_2 which satisfy equation 5.64. At these values of X, $\Gamma_{2e}(X,S) = 0$ for $S = S_1$ and S_2. However, since the ratio $e_{2e}(X,S)$ is identical for the annulus at $X = X_1$ and the annulus at $X = X_2$, there is no possibility to change the normalized even energy values by repeating the process. The analysis was therefore restricted to plane 2.

The analysis was aided by the fact that there is an analytical expression for $\Gamma_{1e}(W,S)$:

From equation A7 of appendix A,

$$\Gamma_{1e}(W,S) = \int_0^1 J_o(SX)\, J_o(WX)\, XdX \qquad 5.67$$

$$= \frac{1}{S^2-W^2}\,[SJ_o(W)J_1(S) - WJ_o(S)J_1(W)] \qquad S \neq W$$

$$= \frac{1}{2}\,[J_o^2(W) + J_1^2(W)] \qquad S = W$$

5.6.3 System parameters

Using the analytical expression 5.67 for $\Gamma_{1e}(W,S)$, the computer was used to calculate the sets of values W_1 and W_2 satisfying equation 5.63 for various chosen values of S_1 and S_2. For each pair of values S_1 and S_2, domains of solutions for W_1 and W_2 were found. Of these solutions, it was decided to choose $W_1 = 0$ and an associated value of W_2 which maximizes the bracket quantity in equation 5.65. The choice $W = 0$ makes easier the construction of the two annuli, and the choice of W_2 enables easier detection of the signal. Since the ratio $\frac{\Gamma_1(W_2,S_2)}{\Gamma_1(0,S_2)}$ in equation 5.64 is negative for this solution, it is possible to choose $X = 0$. With this choice the signal can be received on the axis of plane 2, eliminating the necessity to make a special annulus for this purpose. In addition, the function $\Gamma_{2e}(X,S)$ is maximized.

For the solution with $W_1 = 0$, equations 5.64 and 5.65 must be modified:

As $$W_1 \to 0 \int_0^{\Delta W_1} J_o(W_1 X)\, W_1 dW_1 \to \frac{\Delta W_1^2}{2} L_1(\Delta W_1 X) \qquad 5.69$$

With $W_1 = 0$, $X = 0$, equations 5.63, 5.64 and 5.65 becomes, respectively,

$$\Gamma_{1e}(0,S_1)\, \Gamma_{1e}(W_2 S_2) = \Gamma_{1e}(W_2 S_1)\, \Gamma_{1e}(0,S_2) \qquad 5.69$$

$$\frac{\Delta W_1^2}{2W_2 \Delta W_2} = - \frac{\Gamma_1(W_2,S_2)}{\Gamma_1(0,S_2)} \qquad 5.70$$

$$\Gamma_{2e}(0,S) = \left[\Gamma_1(W_2,S) - \frac{\Gamma_1(0,S)\, \Gamma_1(W_2,S_2)}{\Gamma_1(0,S_2)}\right] W_2 \Delta W_2 \qquad 5.71$$

Choice of S_1 and S_2

Table 5.12 shows a comparison of the normalized even energy values of systems designed according to equations 5.69, 5.70 and 5.71 for various values of S_1 and S_2. At least one value of S_1 or S_2 was always chosen close or equal to the chosen limit for hyperesolution, $S = 2$.

For low values of S_1 and S_2 (for example $S_1 = 1.0$, $S_2 = 2.0$), the normalized even energy is low for narrow domains of S close to S_1 and S_2; and it is prohibitively high for certain large values of S.

Table 5.12 Normalized even energy values of two narrow light transmitting annuli in plane 1 for various values of S_1 and S_2 and for values of S from 0 to 20.

S_1	1.0	2.0	2.0	2.0	2.5	2.5
S_2	2.0	3.0	3.5	4.0	4.0	4.5
W_1	0.0000	0.0000	0.0000	0.0000	0.0000	0.0000
W_2	6.5199	6.7550	6.8906	7.0941	7.0807	7.3469
ΔW_2	0.1×10^{-5}	0.1×10^{-5}	0.1×10^{-5}	0.1×10^{-5}	0.1×10^{-5}	0.1×10^{-5}
S	Normalized even energy					
0	1.0000	1.0000	1.0000	1.0000	1.0000	1.0000
0.5	0.4852	0.8155	0.8280	0.8363	0.8769	0.8830
1.0	0.0000	0.4126	0.4407	0.4596	0.5765	0.5934
1.5	0.2523	0.0910	0.1080	0.1199	0.2565	0.2752
2.0	0.0000	0.0000	0.0000	0.0000	0.0543	0.0625
2.5	50.062	0.0000	0.0559	0.1533	0.0190	0.0309
3.5	208.32	0.2176	0.0000	0.0934	0.0202	0.0583
4.0	578.80	1.5856	0.2482	0.0000	0.0000	0.0326
4.5	1230.5	5.3185	1.4715	0.2484	0.0754	0.0000
5.0	2134.6	12.094	4.2188	1.2649	0.4122	0.0741
5.5	3127.0	21.231	8.4092	3.1909	1.0909	0.3501
6.0	3940.3	30.508	13.1107	5.6864	2.0064	0.8202
6.5	4305.1	36.921	16.823	7.9674	2.8787	1.3519
7.0	4074.4	38.062	18.1647	9.1939	3.3806	1.7471
7.5	3303.7	33.359	16.5799	8.8814	3.3086	1.8461
8.0	2235.8	24.430	12.6414	7.1578	2.6920	1.6129
8.5	1190.2	14.318	7.7680	4.6896	1.7748	1.1499
9.0	432.02	6.0478	3.5232	2.3347	0.8855	0.6382
9.5	61.353	1.3140	0.9055	0.7314	0.2757	0.2426
10.0	8.1726	0.0001	0.0173	0.0571	0.0202	0.0392
10.5	104.71	0.6778	0.2386	0.0606	0.0256	0.0021
11.0	191.09	1.6559	0.7285	0.3060	0.1232	0.0453
11.5	190.28	1.8993	0.9125	0.4470	0.1784	0.0851
12.0	117.99	1.3352	0.6875	0.3749	0.1488	0.0826
12.5	37.552	0.5210	0.2961	0.1851	0.0729	0.0477
13.0	0.71678	0.0408	0.0349	0.0336	0.1290	0.0126
13.5	14.522	0.0793	0.0242	0.0042	0.0019	0.0000
14.0	48.476	0.3994	0.1702	0.0678	0.0279	0.0096
14.5	66.397	0.6207	0.2922	0.1358	0.0553	0.0247
15.0	54.330	0.5685	0.2800	0.1426	0.0577	0.0294
15.5	25.413	0.3019	0.1589	0.0892	0.0359	0.0207
16.0	3.4254	0.0596	0.0370	0.0257	0.0102	0.0074
16.5	1.9652	0.0068	0.0012	0.0000	0.0000	0.0002
17.0	15.921	0.1262	0.0524	0.0200	0.0083	0.0027
17.5	29.230	0.2687	0.1228	0.0554	0.0228	0.0099
18.0	29.708	0.2981	0.1434	0.0703	0.0288	0.0140
18.5	18.008	0.1980	0.1000	0.0529	0.0215	0.0116
19.0	4.7257	0.0627	0.0347	0.0209	0.0084	0.0053
19.5	0.0452	0.0002	0.0006	0.0011	0.0004	0.0006
20.0	5.5036	0.0414	0.0166	0.0059	0.0025	0.0007

Table 5.12 Normalized even energy values of two narrow light transmitting annuli in plane 1 for various values of S_1 and S_2 and for values of S from 0 to 20.

S_1	1.0	2.0	2.0	2.0	2.5	2.5
S_2	2.0	3.0	3.5	4.0	4.0	4.5
W_1	0.0000	0.0000	0.0000	0.0000	0.0000	0.0000
W_2	6.5199	6.7550	6.8906	7.0941	7.0807	7.3469
ΔW_2	0.1×10^{-5}	0.1×10^{-5}	0.1×10^{-5}	0.1×10^{-5}	0.1×10^{-5}	0.1×10^{-5}
S	Normalized even energy					
0	1.0000	1.0000	1.0000	1.0000	1.0000	1.0000
0.5	0.4852	0.8155	0.8280	0.8363	0.8769	0.8830
1.0	0.0000	0.4126	0.4407	0.4596	0.5765	0.5934
1.5	0.2523	0.0910	0.1080	0.1199	0.2565	0.2752
2.0	0.0000	0.0000	0.0000	0.0000	0.0543	0.0625
2.5	50.062	0.0000	0.0559	0.1533	0.0190	0.0309
3.5	208.32	0.2176	0.0000	0.0934	0.0202	0.0583
4.0	578.80	1.5856	0.2482	0.0000	0.0000	0.0326
4.5	1230.5	5.3185	1.4715	0.2484	0.0754	0.0000
5.0	2134.6	12.094	4.2188	1.2649	0.4122	0.0741
5.5	3127.0	21.231	8.4092	3.1909	1.0909	0.3501
6.0	3940.3	30.508	13.1107	5.6864	2.0064	0.8202
6.5	4305.1	36.921	16.823	7.9674	2.8787	1.3519
7.0	4074.4	38.062	18.1647	9.1939	3.3806	1.7471
7.5	3303.7	33.359	16.5799	8.8814	3.3086	1.8461
8.0	2235.8	24.430	12.6414	7.1578	2.6920	1.6129
8.5	1190.2	14.318	7.7680	4.6896	1.7748	1.1499
9.0	432.02	6.0478	3.5232	2.3347	0.8855	0.6382
9.5	61.353	1.3140	0.9055	0.7314	0.2757	0.2426
10.0	8.1726	0.0001	0.0173	0.0571	0.0202	0.0392
10.5	104.71	0.6778	0.2386	0.0606	0.0256	0.0021
11.0	191.09	1.6559	0.7285	0.3060	0.1232	0.0453
11.5	190.28	1.8993	0.9125	0.4470	0.1784	0.0851
12.0	117.99	1.3352	0.6875	0.3749	0.1488	0.0826
12.5	37.552	0.5210	0.2961	0.1851	0.0729	0.0477
13.0	0.71678	0.0408	0.0349	0.0336	0.1290	0.0126
13.5	14.522	0.0793	0.0242	0.0042	0.0019	0.0000
14.0	48.476	0.3994	0.1702	0.0678	0.0279	0.0096
14.5	66.397	0.6207	0.2922	0.1358	0.0553	0.0247
15.0	54.330	0.5685	0.2800	0.1426	0.0577	0.0294
15.5	25.413	0.3019	0.1589	0.0892	0.0359	0.0207
16.0	3.4254	0.0596	0.0370	0.0257	0.0102	0.0074
16.5	1.9652	0.0068	0.0012	0.0000	0.0000	0.0002
17.0	15.921	0.1262	0.0524	0.0200	0.0083	0.0027
17.5	29.230	0.2687	0.1228	0.0554	0.0228	0.0099
18.0	29.708	0.2981	0.1434	0.0703	0.0288	0.0140
18.5	18.008	0.1980	0.1000	0.0529	0.0215	0.0116
19.0	4.7257	0.0627	0.0347	0.0209	0.0084	0.0053
19.5	0.0452	0.0002	0.0006	0.0011	0.0004	0.0006
20.0	5.5036	0.0414	0.0166	0.0059	0.0025	0.0007

As S_1 and S_2 increase, the domains broaden and the values of normalized even energy decrease substantially for larger values of S. For these reasons, the system with $S_1 = 2.5$ and $S_2 = 4.5$ was chosen for experimental investigation. The domain of S which has low values of normalized even energy is broad. It extends from slightly less than S_1 to slightly more than S_2: $2.0 \leq S \leq 5.0$. For the domain $5 \leq S \leq 10$, the values of normalized even energy are high but not so prohibitively high as for the other systems. The modulation function (MF) described in section 2.12 may reduce these to acceptable values.

Choice of Annulus Widths

Although smaller widths more accurately satisfy the design equations, defects of the physical annuli are more prominent and difficulties in detecting the signal are greater. Therefore, it is useful to consider the variation of the normalized even energy with a change in width ΔW_2 and its associated width ΔW_1. Table 5.13 shows that the normalized even energy values for this system do not change much with a change in parameter widths, especially for low values of S. The normalized even energy values for larger values of S can be reduced to acceptable levels by the modulation function (MF) as defined in section 2.12. Therefore, in the choice of width of S, the widths ΔW_1 and ΔW_2 which are chosen for the experimental system, are not very critical.

Table 5.13 Normalized even energy values of two narrow annuli in plane 1 for $S_1 = 2.5$, $S_2 = 4.5$, for various width ΔW_2 of annuli and for various values of S. The parameters A_1 and B_1 are given by $A_1 = W_2 + \frac{\Delta W_2}{2}$, $B_1 = W_2 - \frac{\Delta W_2}{2}$, $C_1 = \Delta W_1$ where $W_2 = 7.3469$, and $W_1 = 7.5969$

ΔW_2	0.1×10^{-5}	0.5000	1.0000	2.0000	2.2125	3.0000
A_1	7.5969	7.5969	7.8469	8.3469	8.4097	8.8469
B_1	7.3469	7.0969	6.8469	6.3469	6.1972	5.8469
C_1	0.0000	0.5473	0.7740	1.0946	1.1411	0.0000
S	Normalized even energy					
0	1.0000	1.0000	1.0000	1.0000	1.0000	1.0000
0.5	0.8830	0.8828	0.8831	0.8853	0.8847	0.8903
1.0	0.5934	0.5928	0.5938	0.6008	0.5992	0.6168
1.5	0.2752	0.2745	0.2760	0.2862	0.2849	0.3099
2.0	0.0625	0.0621	0.0634	0.0718	0.0718	0.0920
2.5	0.0000	0.0000	0.0000	0.0007	0.0010	0.0058
3.0	0.0309	0.0308	0.0288	0.0194	0.0163	0.0059
3.5	0.0583	0.0574	0.0537	0.0046	0.0295	0.0147
4.0	0.0326	0.0312	0.0277	0.0152	0.0074	0.0018
4.5	0.0000	0.0000	0.0004	0.0046	0.0148	0.0236
5.0	0.0741	0.0793	0.0882	0.1222	0.1773	0.1918
5.5	0.3501	0.3645	0.3865	0.4597	0.5853	0.5887
6.0	0.8202	0.8466	0.8839	0.9993	1.2066	1.1871
6.5	1.3519	1.3899	1.4416	1.5948	1.8712	1.8323
7.0	1.7471	1.7927	1.8539	2.0331	2.3430	2.3062
7.5	1.8461	1.8927	1.9561	2.1437	2.4400	2.4319
8.0	1.6129	1.6536	1.7111	1.8871	2.1281	2.1656
8.5	1.1499	1.1800	1.2254	1.3715	1.5351	1.6140
9.0	0.6382	0.6565	0.6867	0.7911	0.8796	0.9760
9.5	0.2426	0.2510	0.2668	0.3270	0.3610	0.4437
10.0	0.0392	0.0414	0.0466	0.0695	0.0759	0.1222
10.5	0.0021	0.0019	0.0012	0.0000	0.0000	0.0061
11.0	0.0453	0.0450	0.0426	0.0316	0.0353	0.0143
11.5	0.0851	0.0855	0.0838	0.0736	0.0812	0.0533
12.0	0.0826	0.0835	0.0831	0.0784	0.0858	0.0663
12.5	0.0417	0.0485	0.0490	0.0489	0.0531	0.0463
13.0	0.0126	0.0129	0.0134	0.0148	0.0157	0.0166
13.5	0.0000	0.0000	0.0000	0.0001	0.0001	0.0007
14.0	0.0096	0.0096	0.0092	0.0073	0.0083	0.0043
14.5	0.0247	0.0248	0.0243	0.0215	0.0239	0.0163
15.0	0.0294	0.0297	0.0294	0.0272	0.0300	0.0225
15.5	0.0207	0.0209	0.0209	0.0210	0.0219	0.0178
16.0	0.0074	0.0075	0.0076	0.0078	0.0083	0.0076
16.5	0.0002	0.0002	0.0003	0.0004	0.0004	0.0007
17.0	0.0027	0.0027	0.0026	0.0020	0.0024	0.0012
17.5	0.0099	0.0099	0.0097	0.0086	0.0096	0.0065
18.0	0.0140	0.0141	0.0139	0.0128	0.0142	0.0105
18.5	0.0116	0.0117	0.0116	0.0110	0.0120	0.0095
19.0	0.0053	0.0053	0.0053	0.0052	0.0057	0.0048
19.5	0.0006	0.0006	0.0006	0.0007	0.0007	0.0008
20.0	0.0007	0.0007	0.0007	0.0005	0.0006	0.0003

Table 5.14 Effect of the modulation function (MF) defined in section 2.12 on the normalized even energy values of two narrow annuli in plane 1 with $A_1 = 8.4097$, $B_1 = 6.1972$, $C_1 = 1.1411$, $D_1 = 0.0000$

S	$e_2(0,S)$	$e_2(0,S) \times MF$	$e_1(0,S)$
0	1.0000	1.0000	1.0000
0.5	0.8847	0.8308	0.9391
1.0	0.5992	0.4641	0.7746
1.5	0.2849	0.1577	0.5534
2.0	0.0718	0.0239	0.3326
2.5	0.0010	0.0002	0.1581
3.0	0.0163	0.0008	0.0511
3.5	0.0295	0.0002	0.0062
4.0	0.0074	0.0000	0.0011
4.5	0.0148	0.0002	0.0105
5.0	0.1773	0.0030	0.0172
5.5	0.5853	0.0090	0.0154
6.0	1.2066	0.0103	0.0085
6.5	1.8712	0.0042	0.0022
7.0	2.3430	0.0000	0.0000
7.5	2.4400	0.0032	0.0013
8.0	2.1281	0.0073	0.0034
8.5	1.5351	0.0063	0.0041
9.0	0.8796	0.0026	0.0030
9.5	0.3610	0.0004	0.0011
10.0	0.0759	0.0000	0.0000
10.5	0.0000	0.0000	0.0002
11.0	0.0353	0.0000	0.0010
11.5	0.0812	0.0001	0.0016
12.0	0.0858	0.0001	0.0014
12.5	0.0531	0.0000	0.0007
13.0	0.0157	0.0000	0.0002
13.5	0.0001	0.0000	0.0000
14.0	0.0083	0.0000	0.0004
14.5	0.0239	0.0000	0.0007
15.0	0.0300	0.0000	0.0007
15.5	0.0219	0.0000	0.0005
16.0	0.0083	0.0000	0.0001
16.5	0.0004	0.0000	0.0000
17.0	0.0024	0.0000	0.0001
17.5	0.0096	0.0000	0.0003
18.0	0.0142	0.0000	0.0004
18.5	0.0120	0.0000	0.0003
19.0	0.0057	0.0000	0.0001
19.5	0.0007	0.0000	0.0000
20.0	0.0006	0.0000	0.0000

This is within the goal for hyperesolution discussed in the introductory paragraphs to Chapter 5. For the purposes of direct comparison, to the Airy pattern, the values of $e_1(0,S)$ are also shown. It will be noticed that for $S \leq 3$, $e_2(0,S) < e_1(0,S)$. However, for $3 \leq S \leq 10$, $e_2(0,S) > e_1(0,S)$. Thus, without the effect of the modulation function, there is an improvement in the energy characteristic for values of S greater than 3 and a deterioration for values of S between 3 and 10.

5.6.4 Photographs taken with the narrow annuli system.

Three series of photographs were taken - with the central diaphram separately, with the annulus separately, and with the composite system of the central diaphram and the annulus:

(1) For S = 0, 0.5, 1.5, 2.5, 3.5, 4.5, photographs of diffraction patterns taken with the annulus separately are shown in figure 5.27 For S = 0, there is a maximum of luminous intensity in the center of a rapidly varying pattern. As S increases, this central region becomes deformed and its amplitude decreases to zero at S = 2.5. This is followed by greater deformation in the outer regions, especially for S = 3.5 and 4.5

(2) For S = 0, 0, 0.5, 1.5, 2.5, 3.5, 4.5, photographs of diffraction patterns with the central diaphram separately are shown in figure 5.28 It can be expected that for most values of S, the amplitude within the domain of this small diaphram is approximately uniform. As a result most of the diffraction patterns are Airy patterns given by,

$$g_1(W,\theta,S) = \frac{J_1(S)}{S} \times \frac{J_1(W')}{W'} \qquad 5.72$$

where from section 2.7, $W' = \sqrt{W^2 + S^2 + 2WS\cos\phi}$

All the photographs except S = 3.5, appear to be Airy patterns which gradually decrease in intensity with S. Since at S = 3.5, the amplitude at the central diaphram changes from positive to negative, it cannot give an Airy pattern.

(3) For values of S from 0 to 22.5, photographs of diffraction patterns taken with the composite system of the central diaphram and the annulus are shown in figure 5.29. From S = 0 to 4.5, these diffraction patterns may be considered as the superposition of two diffraction patterns - one due to the central diaphram and the other due to the annulus. Except for this superposition, the interesting features of the diffraction patterns in this range of S are the same as for the diffraction patterns taken with the annulus separately. The discussion of these features is therefore not repeated.

From S = 6.5 to S = 8.5, the central spot of the Airy pattern is located at the circular diffracting edges of the annulus. The coherent light emitted from these two edges interfere, giving slowly varying interference fringes.

For large values of S, the diffraction patterns do not change very much and tend toward a steady pattern having two small spots. The mathematical analysis in section 2.8 can easily be used to deduce the approximating expression for this diffraction pattern.

For comparison with the photographs, contour maps of even amplitude, odd amplitude, amplitude, phase and luminous intensity are shown for S = 2.5 in figures 5.30 to 5.34. In addition, the contour map of luminous intensity for S = 0 is shown in figure 5.35 and the amplitude function $g_2(X)$ for S = 0 is shown in figure 5.36

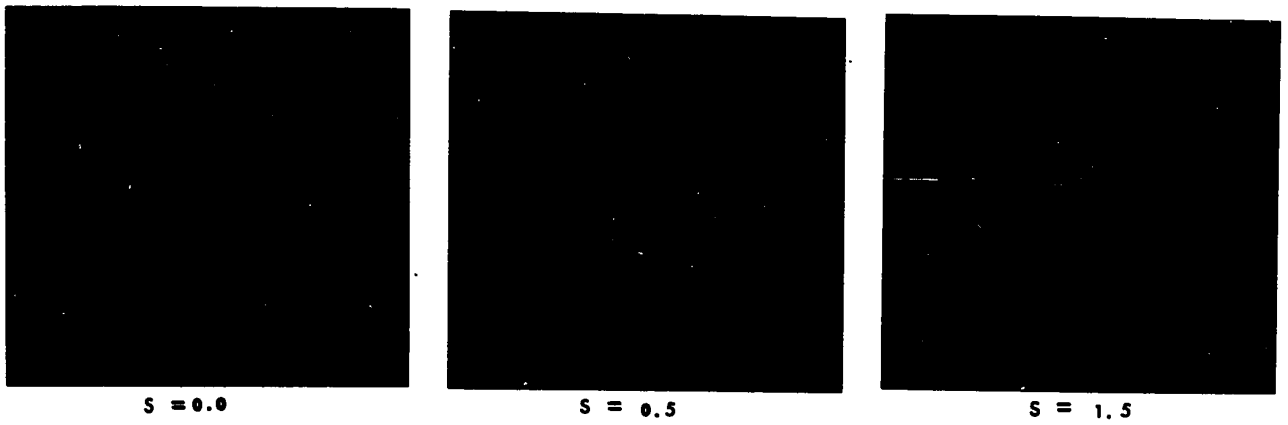

Fig. 5.27 Photographs of iterated diffraction patterns formed in plane 2 by a narrow annulus in plane 1 for A_1 = 8.4097, B_1 = 6.1972 and for different values of S.

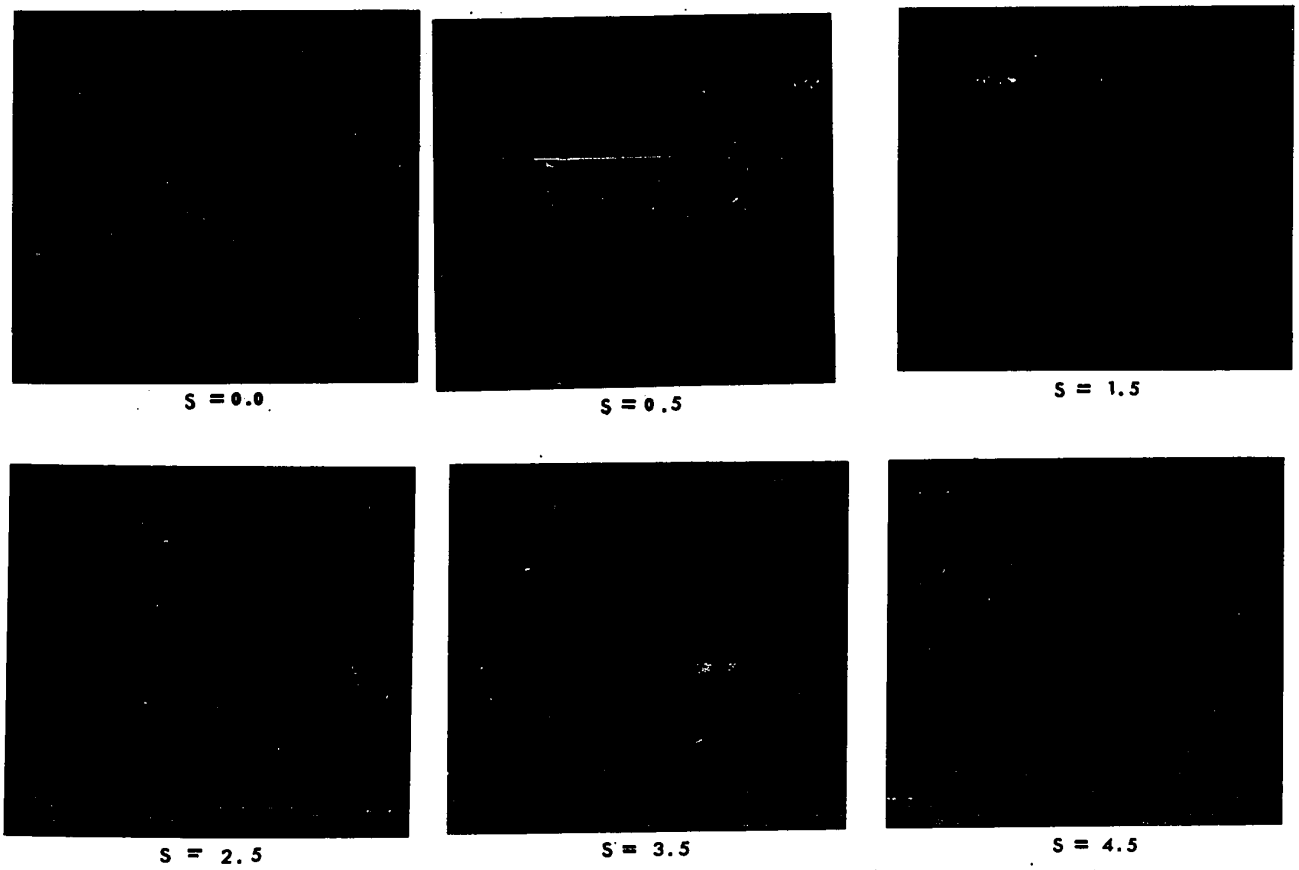

Figure 5.28 Photographs of iterated diffraction patterns formed in plane 2 by a central diaphram in plane 1 for A_1 = 1.1411 and for different values of S.

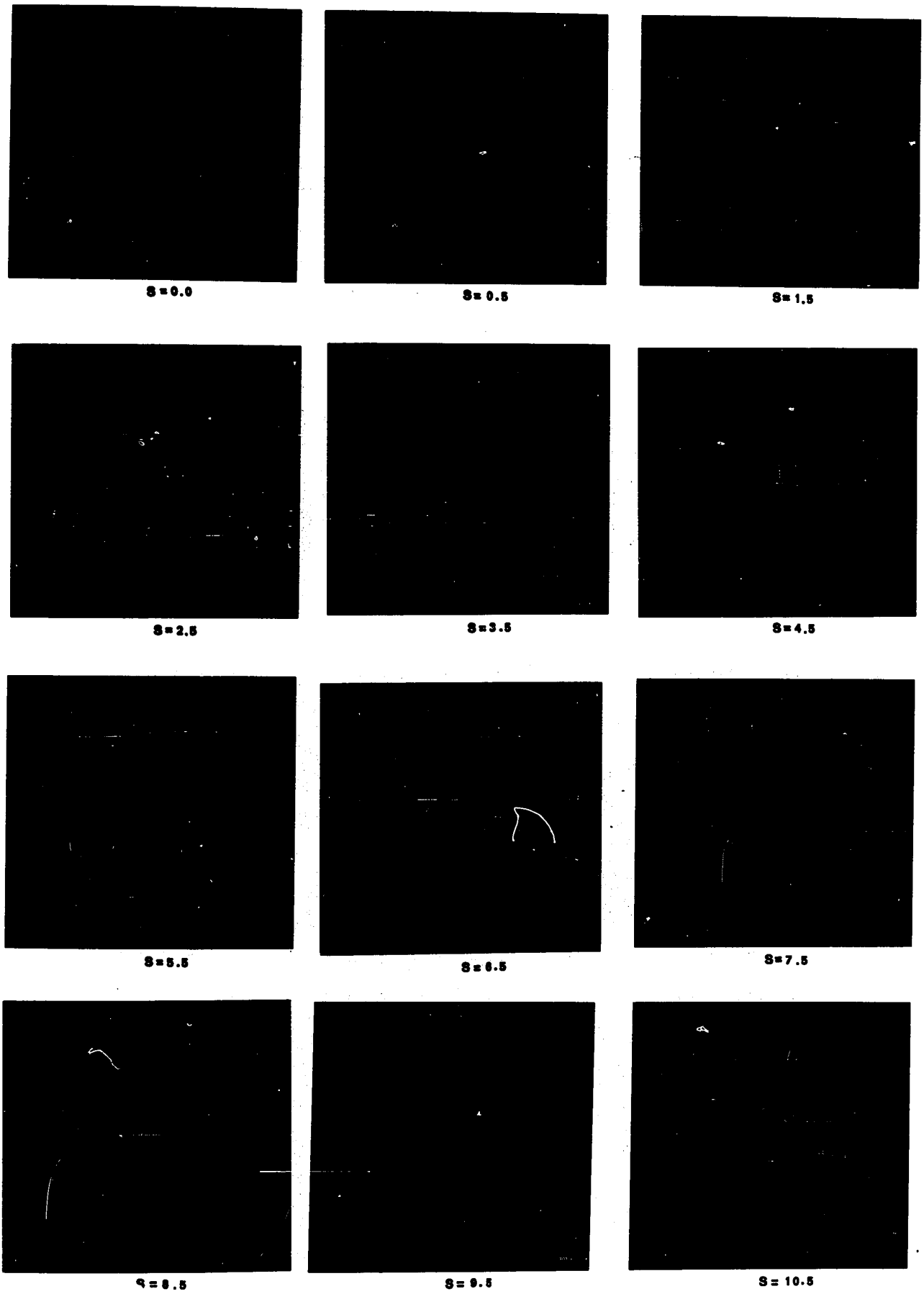

Figure 5.29 Photographs of iterated diffraction patterns formed in plane 2 by the narrow annuli system for A_1 = 8.4097, B_1 = 6.1972, C_1 = 1.411, D_1 = 0.0000 and for different values of S.

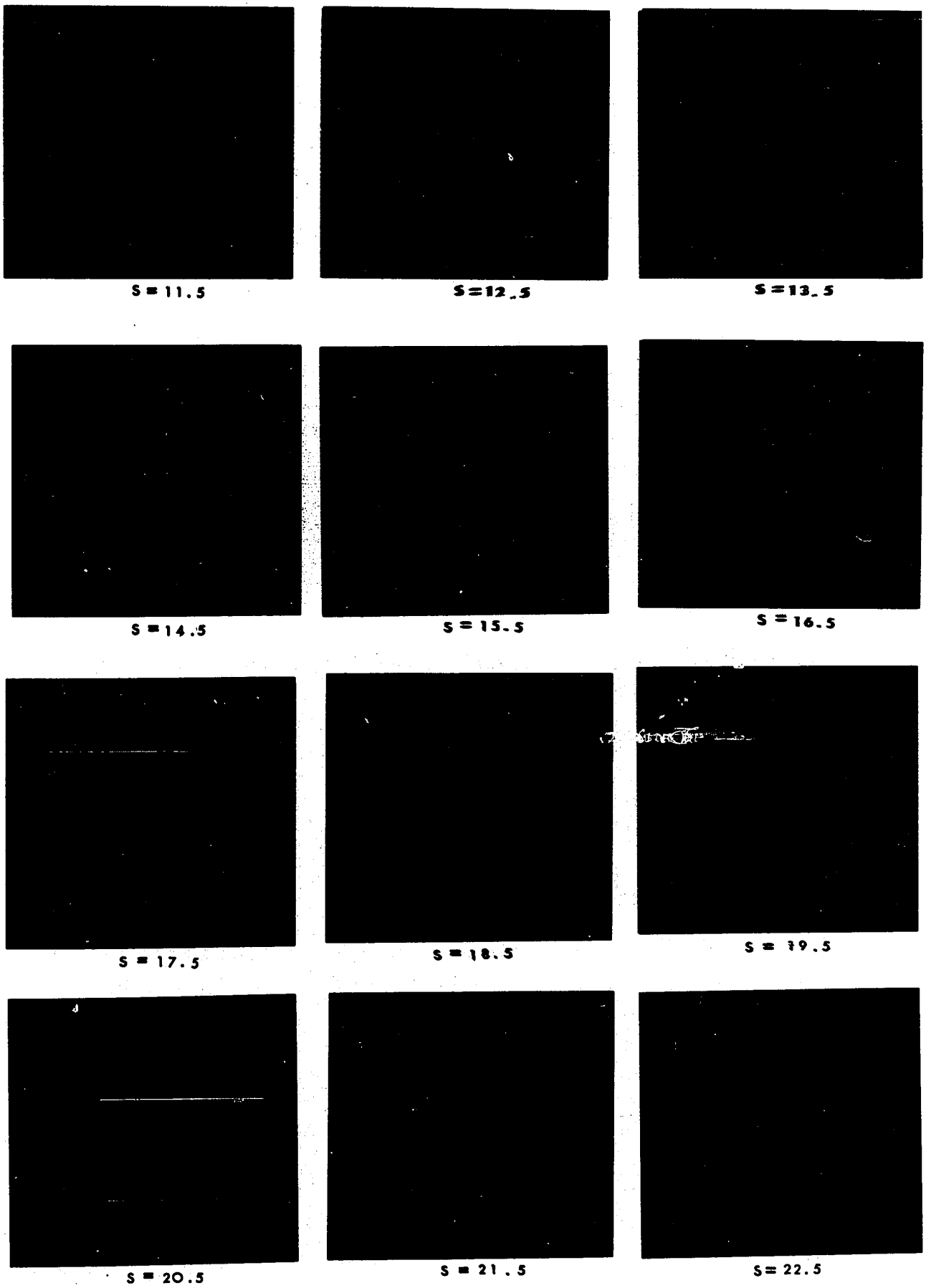

Figure 5.29 Photographs of iterated diffraction patterns formed in plane 2 by the narrow annuli system for A_1 = 8.4097, B_1 = 6.1972, C_1 = 1.411, D_1 = 0.0000 and for different values of S.

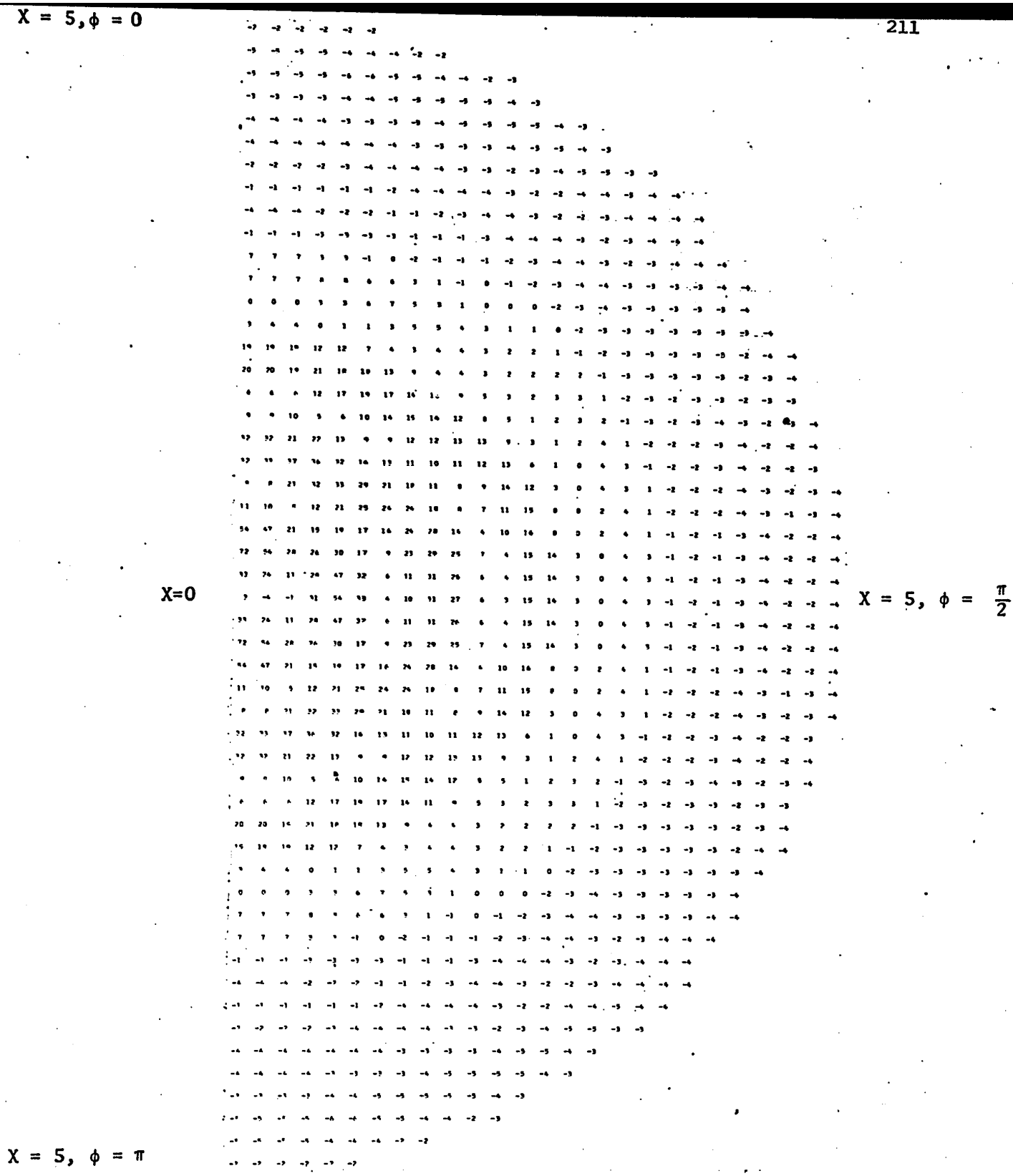

Figure 5.30 Contour map of even amplitude in plane 2 for the narrow annuli system $A_1 = 8.410$, $B_1 = 6.197$, $C_1 = 1.141$, $D_1 = 0.000$ for $S = 2.5$, for X from 0 to 5 and for ϕ from 0 to π. The values of even amplitude are normalized so that $g_2(0,0,0) = 100$. The construction of contour maps is explained in section 3.6.

X = 5, ϕ = 0

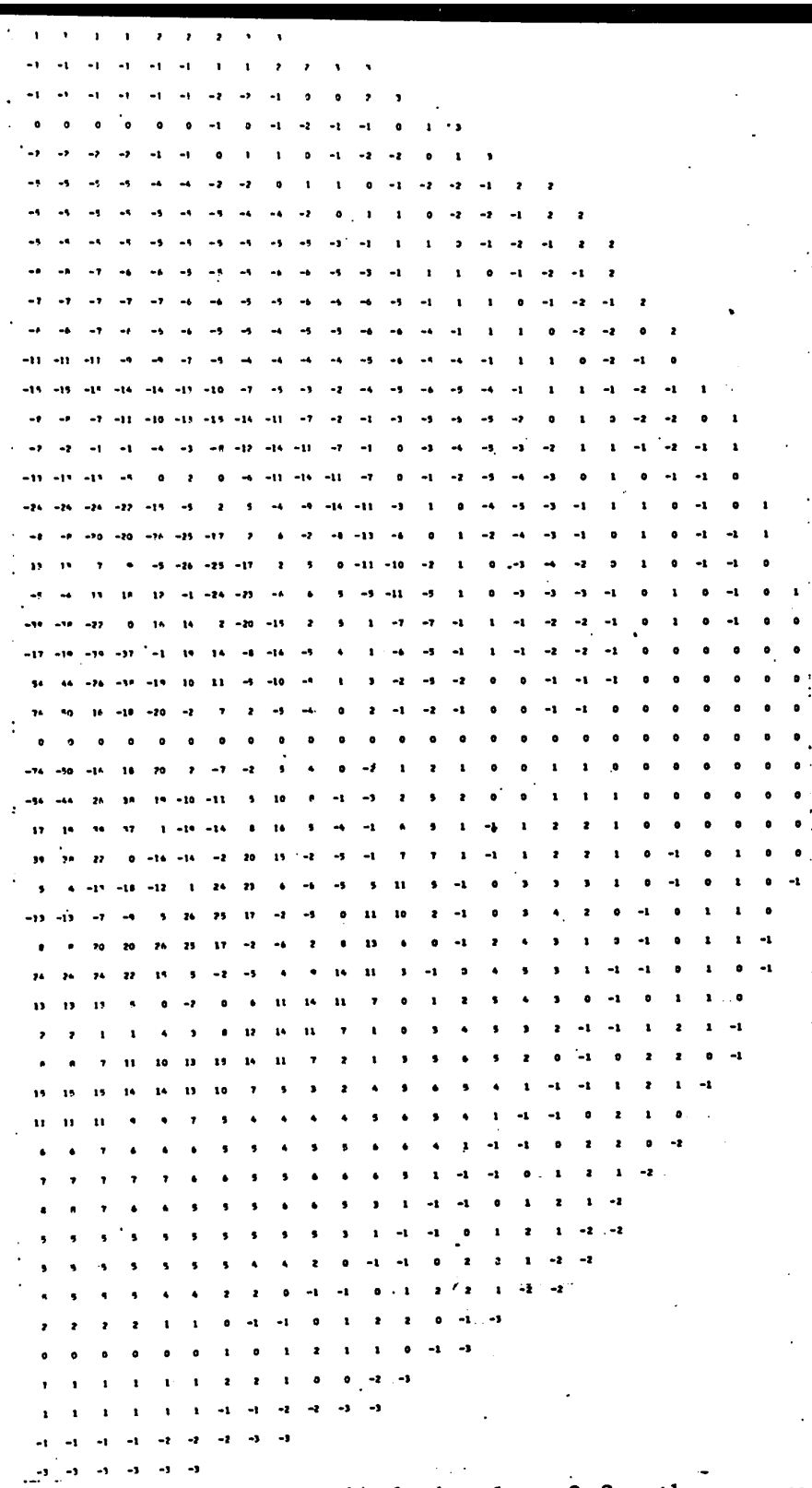

X = 0

X = 5, ϕ = π/2

X = 5, ϕ = π

Figure 5.31 Contour map of odd amplitude in plane 2 for the narrow annuli system $A_1 = 8.410$, $B_1 = 6.197$, $C_1 = 1.141$, $D_1 = 0.000$ for S = 2.5, for X from 0 to 5 and for ϕ from 0 to π. The values of odd amplitude are normalized so that $g_2(0,0,0) = 100$. The construction of contour maps is explained in section 3.6.

X = 5, ϕ= 0

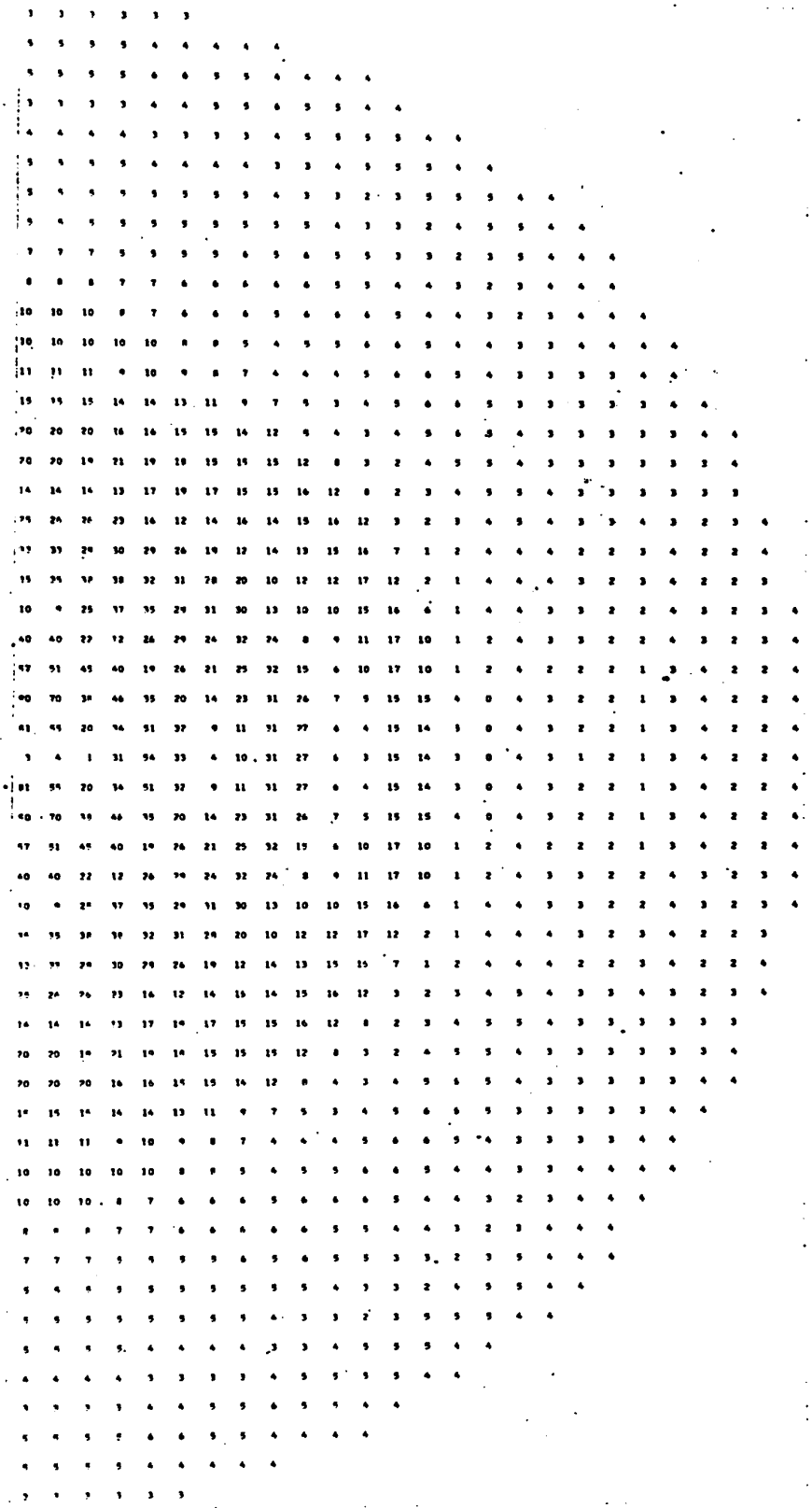

X = 0

X = 5, $\phi = \frac{\pi}{2}$

X = 5, ϕ = π

Figure 5.32 Contour map of amplitude in plane 2 for the narrow annuli system A_1 = 8.410, B_1 = 6.197, C_1 = 1.141, D_1 = 0.000 for S = 2.5, for X from 0 to 5 and for ϕ from 0 to π. The values of amplitude are normalized so that $g_2(0,0,0)$ = 100. The construction of contour maps is explained in section 3.6.

X = 5, ϕ = 0

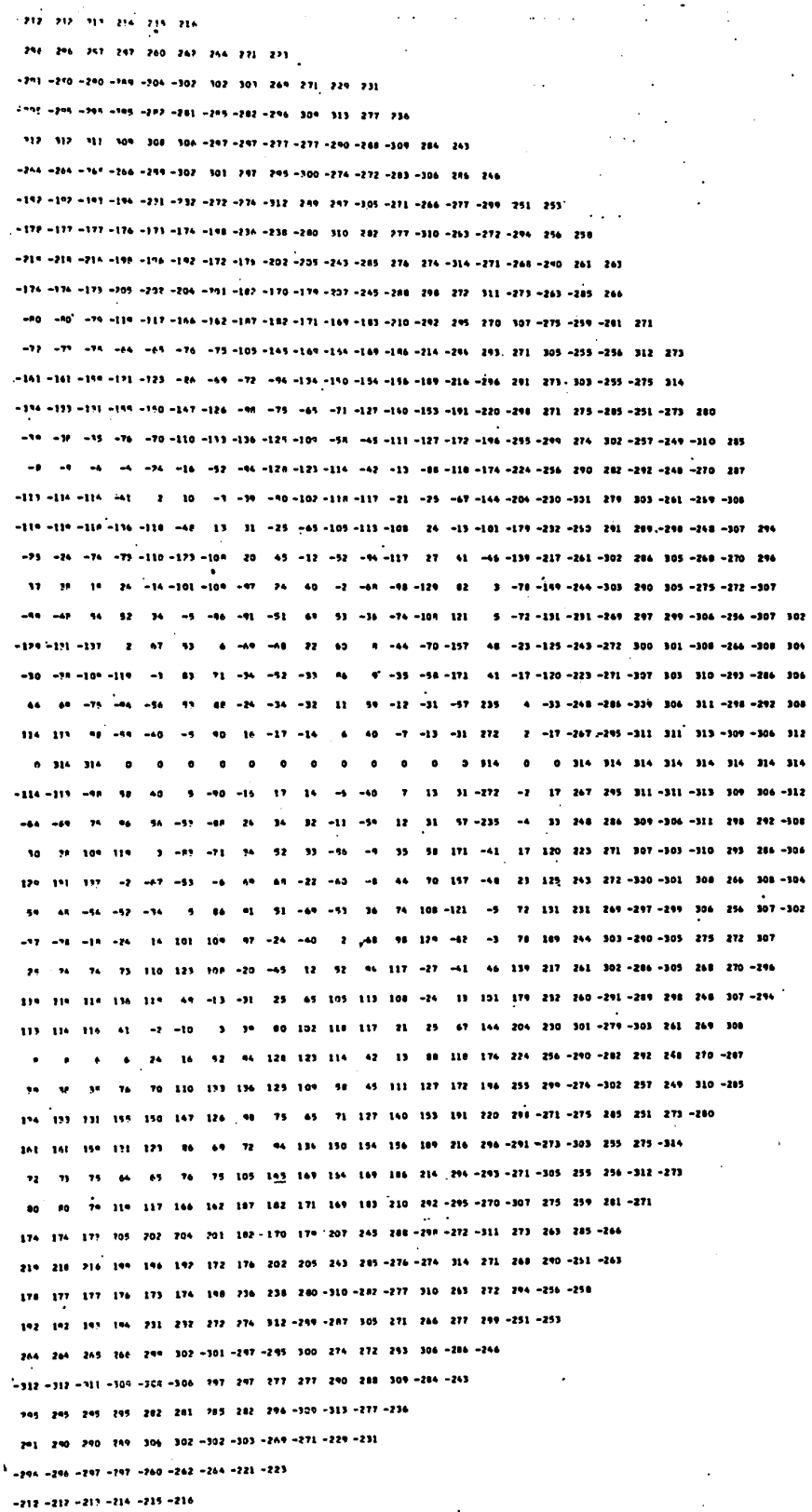

X = 0

X = 5, $\phi = \frac{\pi}{2}$

X = 5, $\phi = \pi$

Figure 5.33 Contour map of phase in plane 2 for the narrow annuli system $A_1 = 8.410$, $B_1 = 6.197$, $C_1 = 1.141$, $D_1 = 0.000$ for S = 2.5, for X from 0 to 5 and for ϕ from 0 to π. The values of phase are multiplied by 100. The construction of contour maps is explained in section 3.6.

X = 5, ϕ= 0

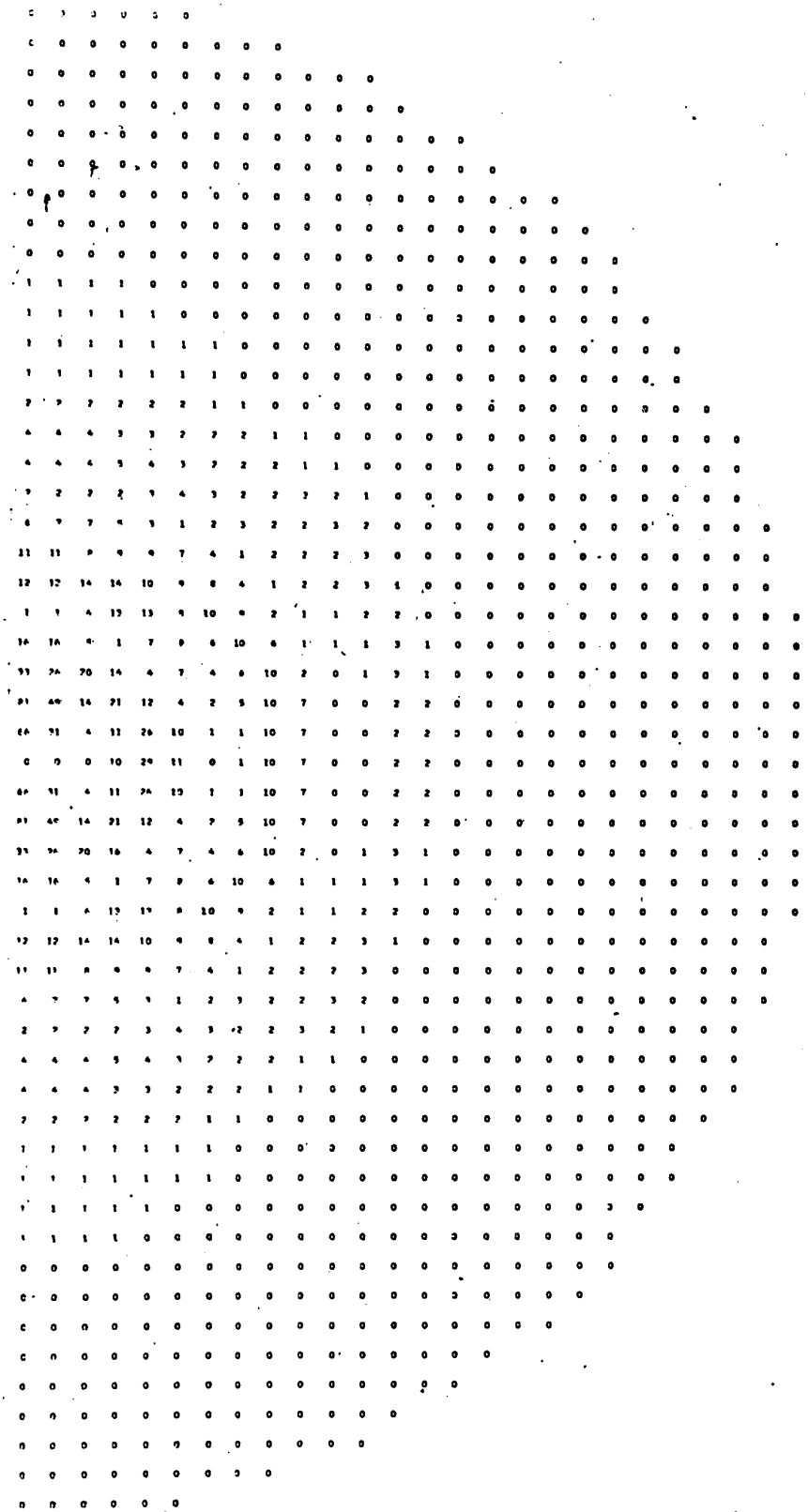

X = 0

X = 5, $\phi = \frac{\pi}{2}$

X = 5, $\phi = \pi$

Figure 5.34 Contour map of luminous intensity in plane 2 for the narrow annuli system $A_1 = 8.410$, $B_1 = 6.197$, $C_1 = 1.141$, $D_1 = 0.000$, for S = 2.5, for X from 0 to 5 and for ϕ from 0 to π. The values of intensity are normalized so that $g_2(0,0,0) = 100$. The construction of contour maps is explained in section 3.6.

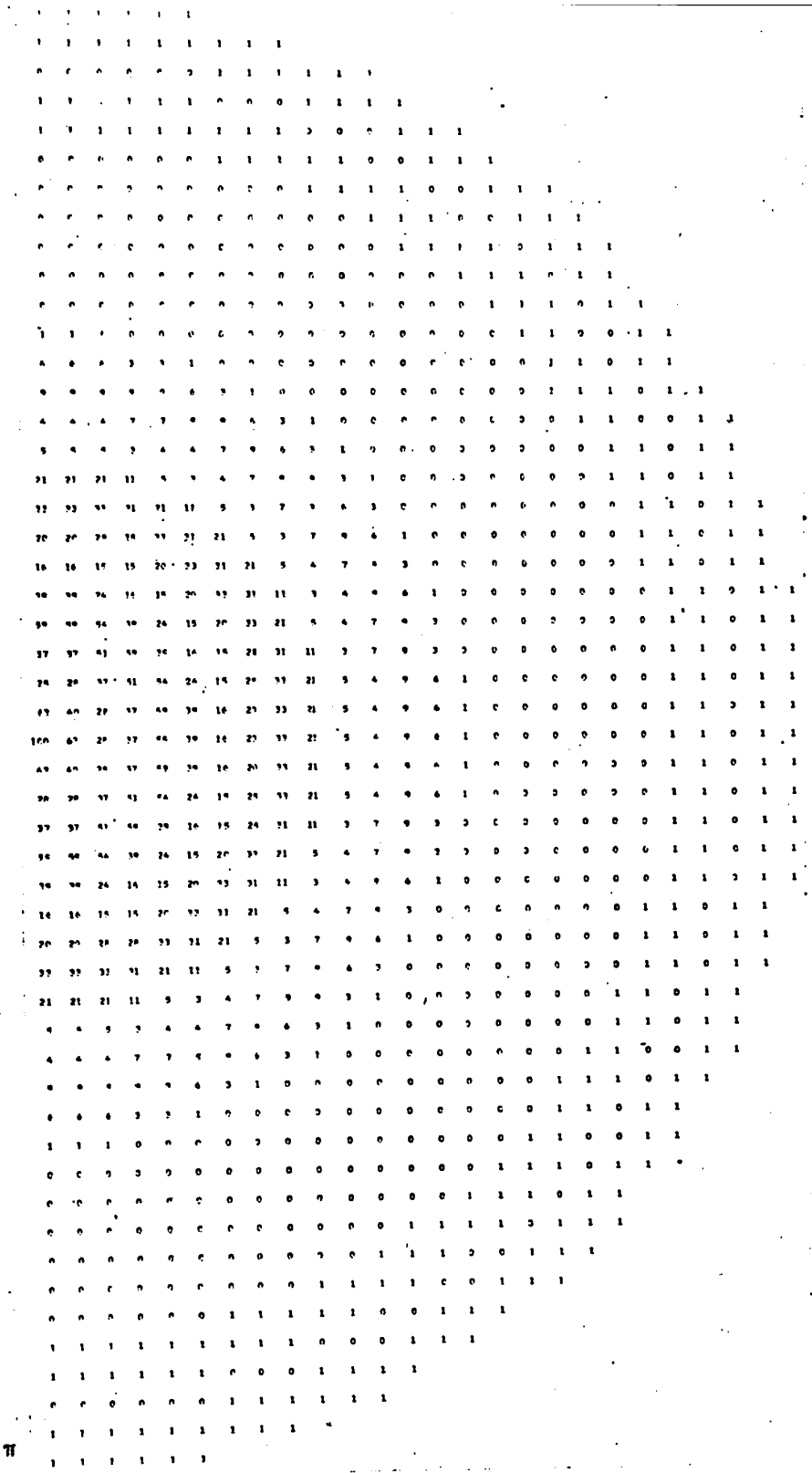

Figure 5.35 Contour map of luminous intensity in plane 2 for the narrow annuli system $A_1 = 8.410$, $B_1 = 6.197$, $C_1 = 1.141$, $D_1 = 0.000$, for $S = 0$, for X from 0 to 5 and for ϕ from 0 to π. The values of intensity are normalized so that $g_2(0,0,0) = 100$. The construction of contour maps is explained in section 3.6.

X	$g_2(X)$
0.0	0.1000000000000000 01
0.100	0.941289853903555D 00
0.200	0.794484505805138D 00
0.300	0.631679835763419D 00
0.400	0.528934923788590 00
0.500	0.526036694784219D 00
0.600	0.606889032765941D 00
0.700	0.710805266177040D 00
0.800	0.767659938916218D 00
0.900	0.736816050506538D 00
1.000	0.628224546410129D 00
1.100	0.494678069676135D 00
1.200	0.400618216338810D 00
1.300	0.385748323653730D 00
1.400	0.443889363423575D 00
1.500	0.528189046206815D 00
1.600	0.578637857436404D 00
1.700	0.555614047087574D 00
1.800	0.460610315189CC8D 00
1.900	0.333372942545996D 00
2.000	0.228341550992576D 00
2.100	0.184558581603277D 00
2.200	0.205937394786610D 00
2.300	0.261934746307967D 00
2.400	0.306717677117582D 00
2.500	0.304890967559708D 00
2.600	0.249230248813150 00
2.700	0.161542738835834D 00
2.800	0.778994804682085D-01
2.900	0.278801437019620-01
3.000	0.205457921720840-01
3.100	0.403926363876193D-01
3.200	0.634298583479490-01
3.300	0.676594572408750D-01
3.400	0.454024390649920D-01
3.500	0.856255732C567920-02
3.600	-0.294836440157461D-01
3.700	-0.547155141980810D-01
3.800	-0.641883035546767D-01
3.900	-0.643234707832823D-01
4.000	-0.645015616492546D-01
4.100	-0.700027235154590D-01
4.200	-0.790517087811730-01
4.300	-0.854086776018845D-01
4.400	-0.840650197565653D-C1
4.500	-0.756651336539266D-01
4.600	-0.664984393593221D-01
4.700	-0.641312949557401D-01
4.800	-0.718168714017190D-01
4.900	-0.856931976126270-01
5.000	-0.964277999322310-01

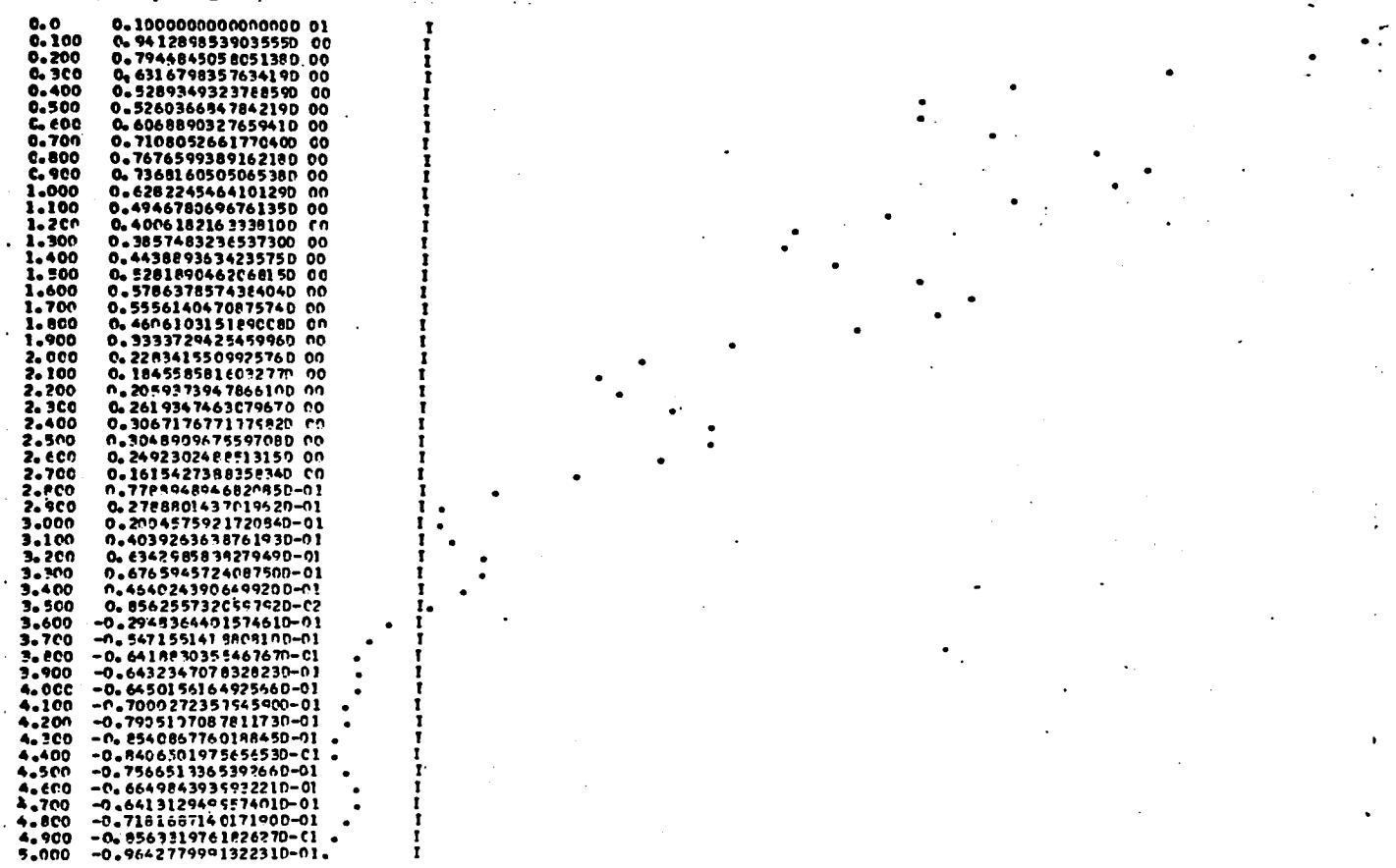

Figure 5.36 Calculation of $g_2(X)$ for the narrow annuli system A_1 = 8.4097, B_1 = 6.1972, C_1 = 1.141, D_1 = 0.000, for S = 0, and for X from 0 to 5.

CHAPTER 6

EXPERIMENTAL INVESTIGATION

6.1 Photographs

Diffraction patterns have been observed experimentally up to plane 4. Three series of photographs are presented:

(1) Figures 5.8 to 5.11 show the diffraction patterns formed in plane 2. with diaphrams in plane 1 having radii equal to the abscissae of the special points 3.054, 3.832, 5.136, 7.016. For the special points 3.054,3.832 and 5.136, the diffraction patterns are shown for values of S from 0 to 11 in steps of 1. For the special point 7.016, the diffraction patterns are shown for values of S from 0 to 23 in steps of 1.

(2) Figures 5.12 and 5.13 show the diffraction patterns of planes 2 and 3 for the selected system defined in section 5.6.3. The diffraction patterns are shown for values of S from 0 to 23 in steps of 1.

(3) Figures 5.29 show the diffraction patterns of plane 2 for the narrow annulus system as defined in section 5.5. The diffraction patterns are shown for values of S from 0.5 to 22.5 in steps of 1 and for S = 0. The corresponding diffraction patterns in plane 2 for the first annulus separately are shown in figure 5.28 and for the second annulus separately in figure 5.27. These diffraction patterns are shown for values of S from 0.5 to 4.5 in steps of 1 and for S = 0.

6.2 Experimental Optical System

The introductory theory of hyperresolving systems is given in Chapter 1 where a schematic diagram of a hyperesolving system is given by figure 1.2. The point source and lenses equipped with diaphrams or annuli were aligned on stands and spaced a distance D equal to twice the focal length of the lenses. In this experimental investigation, D was chosen to be 200 cm corresponding to a focal length of 100 cm. A general view of the system as described below is shown in figure 6.1.

6.2.1 Light Source

We could have chosen for the experimental work a mercury arc lamp or a laser. The advantage of a laser is that it has a much higher luminance than the mercury lamp. This would permit easier observation of the diffraction patterns and shorter exposure times when photographs are taken. However, the high coherence of laser light has a serious disadvantage in optical systems. Internal reflections of highly coherent light in lenses often result in spurious diffraction and interference patterns. Taking into account the advantage and disadvantage of each light source, we chose a mercury lamp. The lamp was an Osram HBO 100 watt mercury super pressure lamp which was the brightest mercury source available.

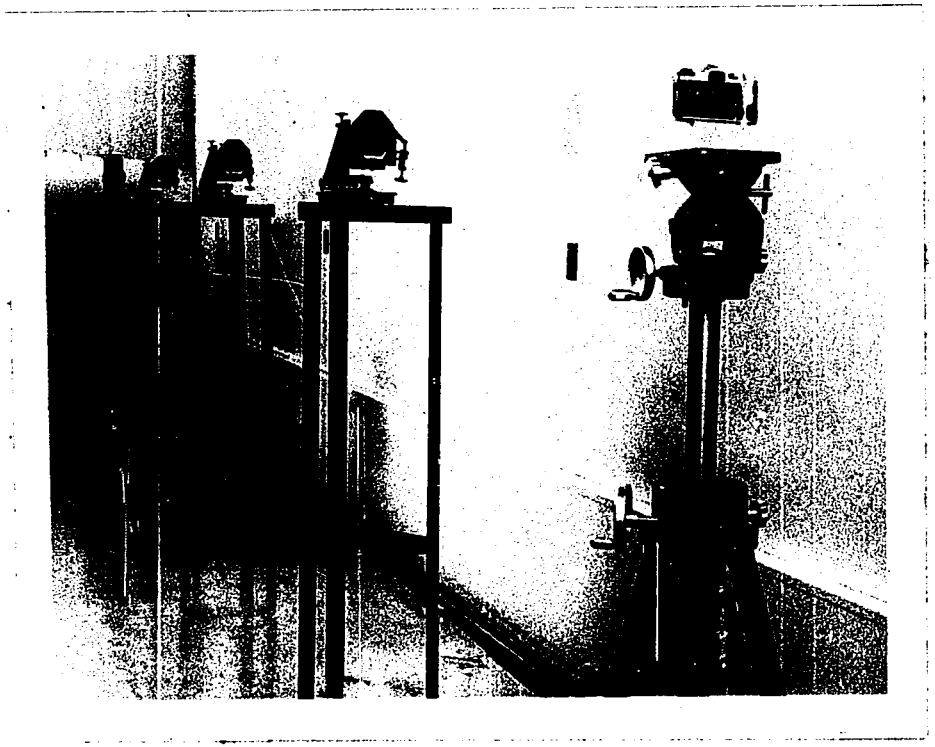

Figure 6.1 A general view of the experimental system.

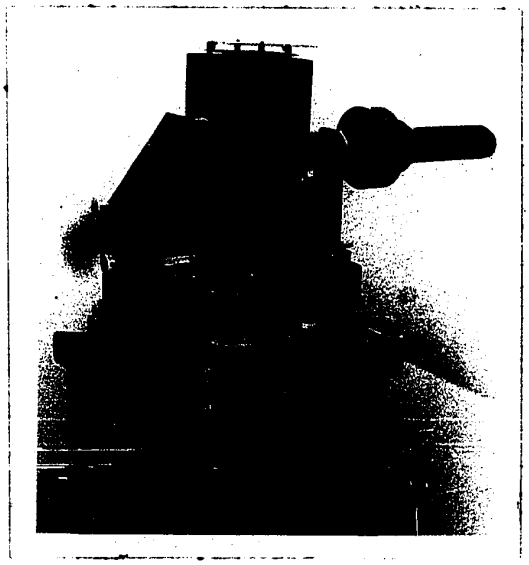

Figure 6.2 Photograph of point source

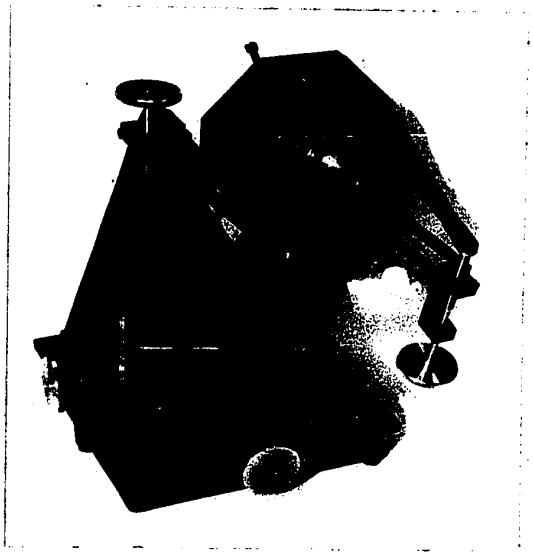

Figure 6.3 Photograph of lens holder

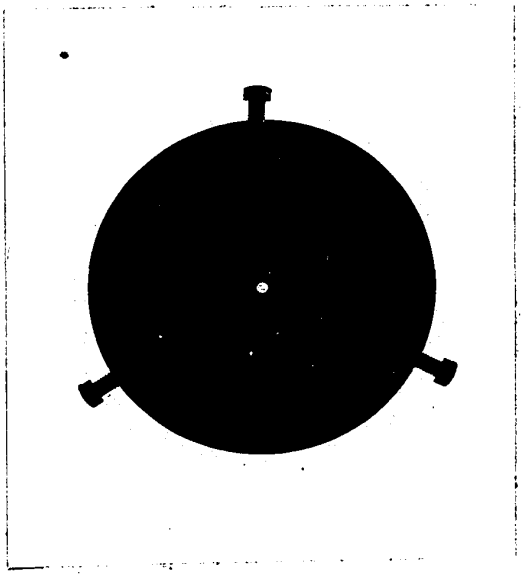

Figure 6.4 Photograph of cup holder with cup and diaphram

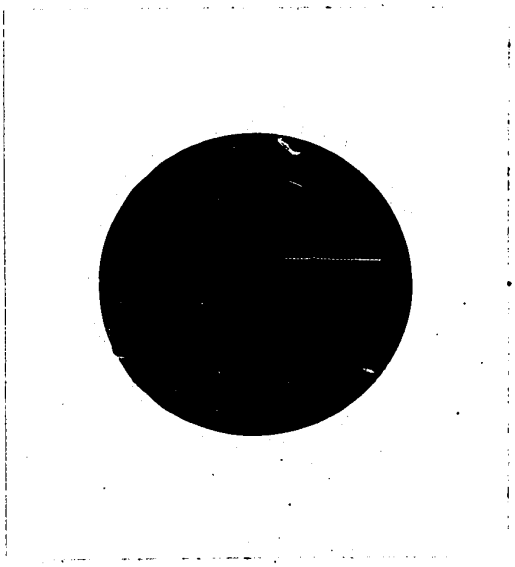

Figure 6.5 Photograph of lens cell with lens, and one annulus for the selected system.

A photograph of the light source, which was designed and constructed at N.R.C. for the mercury arc lamp, is shown in figure 6.2. It is mounted on a platform in such a way that its angular position can be changed by three levelling screws. The light source consists of:

(1) a light cavity which contains the lamp.

(2) a mechanism for positioning the light cavity.

(3) a collimating tube with a lens.

(4) an interference filter and a diaphram

(5) a focussing tube with a lens.

(6) a pinhole.

The lamp is housed inside a parallelepiped light cavity. The cavity has at the top and bottom a series of baffles which permit circulation of air to cool the lamp and at the same time the cavity remains light tight.

Diverging light emitted by the lamp is collimated by the lens of the collimating tube and then filtered by an interference filter located inside a disc shaped filter housing. The interference filter isolates the strongest line of the mercury spectrum - the green line of wavelength 5461A. The light is then focussed by a lens on the pinhole which serves as a point source for the system. An iris diaphram mounted in front of the focussing lens is used to limit the angle of the conical beam emerging from the pinhole.

It is also important that the image of the mercury lamp be properly centered on the pinhole. The mercury lamp has two conical electrodes spaced a distance of approximately 0.3 mm. The image of the arc across these electrodes should be correctly focussed and exactly positioned on the pinhole. However, since the arc is not absolutely steady, it may move with respect to the electrodes of the lamp. In this case, the pinhole is no longer strongly illuminated. Thus, either the pinhole or the lamp must be moved so that the image of the arc is recentered on the pinhole. Unfortunately, if the pinhole is moved, the S coordinates of the optical system are changed. Therefore, the light source was designed so that the lamp could be accurately positioned while the pinhole remained fixed. The cavity with the lamp can be moved in the x, y, z directions of a rectangular coordinate system by means of three dovetails. Accurate positioning is obtained by means of threaded rods, gears and positioning knobs.

The size of the pinhole was based on considerations of brightness and image quality of the Airy pattern. When the pinhole is larger, the source is brighter and consequently, the diffraction pattern is easier to detect. However, a large pinhole is not a very good approximation to a point source. Consider a pinhole centered on the axis of the hyperesolving system as a very small extended source consisting of an infinite set of point sources. As explained in section 2.7, each of these point sources gives an Airy pattern displaced from the axis by an amount equal and opposite to the displacement of the point source. The resultant diffraction pattern

therefore is a superposition of Airy patterns with various displacements from the axis. Thus, the image quality of the resultant diffraction pattern depends on the pinhole radius since it determines the maximum displacement. The image quality also depends on the radius of the diaphram limiting the pupil of the lens which forms this diffraction pattern. The size of this diffraction pattern is inversely proportional to the radius of the diaphram. Therefore, for a given size of the pinhole, the displaced Airy patterns forming the resultant diffraction patterns will considerably overlap if the radius of the diaphram increases. In conclusion, when the pinhole and the radius of the diaphram are both smaller, the image quality of the resultant diffraction pattern is higher.

The radius of the pinhole was chosen to be the largest for which there was no observable deterioration of the Airy pattern. A pinhole of radius 99 microns was used for all the experimental work except the study of the selected system defined in section 5.4.1. Since a larger diaphram was used in plane 0 for the selected system, a smaller pinhole was necessary in this case. A pinhole of radius 33 microns was used. The pinholes were drilled in brass foil 0.005" thick and mounted on cups which were placed at the end of the focussing tube.

The light source is mounted on a platform which can move with roller bearings along two parallel rods made of hardened steel. The direction of these rods is perpendicular to the optical axis of the hyperesolving system. The platform is moved by a motor driven screw

controlled remotely. In this way, the point source could be moved to any desired position while observing the diffraction patterns. Two types of switches are placed near the end of travel of the platform - reversing switches for reversing the direction of travel and safety switches which would stop the motor in case the reversing switches failed to operate properly. The distance d of the point source is measured by a dial indicater to an accuracy of 1 micron. The value of S can be calculated from d by equation 1.2.

6.2.2. Lenses and Diaphrams

Identical lenses having a cross sectional diameter of three inches and a focal length of 1 meter were used for the optical system. Each lens was mounted in a ring shaped cell and then placed in a lens holder as shown in figure 6.3. The lens holders, which were designed and constructed at N.R.C., were securely fastened to triangular stands welded out of steel angle. Each holder can move its lens in the x, y, z directions of a rectangular coordinate system by means of three dovetails. Accurate positioning is obtained by means of threaded rods and positioning knobs. It can also swivel the lens in two angular motions by means of two lever arms controlled by threaded rods.

The lens holders enabled good control on the positioning of the lenses with respect to an optical axis defined as follows. The light beam emitted by the point source is a conical divergent beam having a symmetry of revolution. The axis of revolution of this light beam

was used as a reference optical axis and all optical parts of the system were positioned with respect to this axis. The lenses were aligned as follows:

a) Each lens was adjusted so that the light reflected from its front surface was collinear with the axis of the conical beam emitted by the point source. For the first or primary lens, this was done by swivelling the lens so that the reflected light received on a white screen surrounding the point source was centered with respect to the pinhole. For the other lenses, the adjustment was made with the aid of a white screen in front of one quadrant of the lens. In this way both the incident and reflected beams could be observed simultaneously.

b) The positions of the lenses were adjusted to make the system confocal. That is, the lenses were spaced a distance of twice their focal length. The distance between the point source and the first lens was adjusted with the aid of a meter stick to be 200 cm, twice the focal length of the lens. At this stage, two experimental processes described below were tried to adjust the other lenses of the system.

Plane 1 of the hyperresolving system is the plane where the image of the point source is formed by the primary lens. The next lens, which has to be placed in plane 1, was moved by means of its lens holder so that the previous image was sharply focussed on the front surface of the lens. A similar procedure was used to adjust the distance between the lenses for planes 2 and 3. However, in this case it was necessary to place a small diaphram (described later), about one millimeter in diameter, on the primary

lens in plane 0. The diaphram, illuminated by the point source, served as an object for the lens in plane 1.

In the second experimental process, the lenses were positioned with only the aid of a meter stick. In practice, this procedure was at least as accurate as the first one, as explained below: The depth of focus of a lens is associated with the angle Ω subtended by the lens in the image plane. The smaller the angle Ω, the greater the depth of focus. In the experimental system, the cross sectional diameter of the lens was 7.62 cm and the distance from the lens to the image plane was 200 cm. Therefore, the angle subtended by the lens was 0.0361 radians. Because of this small value of Ω, the image formed by the lens did not change very much in the vicinity of the image plane. As a result, it was not possible to focus the lenses to a precision better than a few millimeters. Since this precision could easily be obtained with a meter stick, we prefered the second method which is much simpler.

c) A microscope was used to aid in adjusting the position of each lens so that its diaphram (described later) was centered with respect to the symmetrical diffraction pattern for S = 0.

The radii a_n of the diaphrams were determined by the parameters A_n used to design the system, the focal length f of the lenses and the wavelength λ : $a_n = A_n \sqrt{\frac{f\lambda}{\pi}}$.

In principle, any focal length may be used for a given system but a long focal length has the advantage that the diaphrams are large, thus simplifying their construction. It has the disadvantage

that the hyperresolving system will be long; consequently it may be affected by mechanical stability and air turbulance along the optical path. Taking into account various characteristics of the tunnel at N.R.C. where the experiment was carried out: total length, stability of the floor, constant temperature well within 1°C, reduced air turbulance....., it was decided to use a focal length of 1 meter with diaphram radii in the order of millimeters or tenths of millimeters.

The diaphrams were made with brass foil 0.001 inch thick, to obtain very sharp edges of the circular holes. During the drilling process, the foil was clamped tightly between two sheets of steel. After the hole was drilled, it was carefully polished with a needle to eliminate the remaining burrs. Each diaphram was observed with a travelling microscope to check the quality of the hole and to measure its diameter. It was then mounted on a specially designed cup which could easily be inserted and held in the central hole of a disc shaped cup holder. This cup holder was mounted to the lens cell by means of three screws. A cup and its holder are shown in figure 6.4.

A different procedure was used in the case of two annuli consisting of a central circular aperture and a concentric light transmitting annulus. In this case, a hole was drilled in the foil as described above giving the central circular aperture. This diaphram was then machined on a lathe so as to make an opaque annulus having an outer radius equal to the required inner radius of the light transmitting annulus. It was then accurately positioned by a method described later

and cemented with glyptol on the front surface of the lens.

Separately, a circular hole was drilled in a large disc which could be positioned accurately just inside the inner radius of the lens cell. The radius of the hole was equal to the required outer radius of the light transmitting annulus. By construction, the disc was accurately centered with respect to the opaque annulus described above, so as to form the composite light transmitting pupil. It was held against the front surface of the lens by a large "O" ring. A photograph of the lens with the two annuli and the lens cell is shown in figure 6.5.

A "centering guide", for centering the opaque circular annulus to be cemented on the lens, was designed and made. It consisted of two parts: The first, a circular disc of brass with a radius of 7.62 cm, exactly equal to the inner radius of the lens cell. This disc could be accurately positioned on the lens cell. The second part was a cylindrical rod, having the diameter of the outer edge of the opaque annulus. It could be inserted through a hole of the same size at the center of the large disc described above.

The procedure was as follows: The cylindrical rod was inserted through the central hole of the large disc so that its end was slightly recessed with respect to the surface. The assembly then formed a circular cavity in which the opaque annulus could be exactly inserted. A small drop of glyptol was deposited on the surface of the opaque annulus.

The centering guide was mounted on the lens cell, and, as a result of the design, the cylindrical rod and the opaque annulus were then positioned so as to be concentric with the optical axis of the lens. By construction, a small clearance distance was allowed between the opaque annulus and the lens. The circular rod was then pushed so as to move the opaque annulus towards the lens and to maintain it against the front surface of the lens while the cement was drying. Finally, the centering guide was removed.

Experimental determination of the composite light transmitting pupil

For plane n, the parameters A_n, B_n, C_n, D_n and their corresponding radii a_n, b_n, c_n, d_n are given by equation 1.4:

$A_n = a_n\sqrt{\frac{2\pi}{D\lambda}}$ where a_n is the outer radius of the largest annulus

$B_n = b_n\sqrt{\frac{2\pi}{D\lambda}}$ where b_n is the inner radius of the largest annulus

$C_n = c_n\sqrt{\frac{2\pi}{D\lambda}}$ where c_n is the outer radius of the smallest annulus.

$D_n = d_n\sqrt{\frac{2\pi}{D\lambda}}$ where d_n is the inner radius of the smallest annulus.

$D = 200$ cm.

$\lambda = 5460.74 \times 10^{-8}$ cm.

For convenience of calculations, A_o was normalized to 1 corresponding to a central diaphram of radius $a_o = \sqrt{\frac{D\lambda}{2\pi}} = 0.0417$ cm. However, since this radius is not convenient experimentally, a homothetic system, which merely changes the magnification and intensity of the diffraction pattern as indicated in section 2.3, was constructed. If the actual radius of the diaphram in plane 0 is a_o', the system is transformed homothetically according to a ratio of similitude given by,

$$k = \frac{a_o'}{a_o}$$

The selection of a_o' was based on the following considerations:

(1) It is more difficult to make small holes free of defects.

(2) Since the size of the Airy pattern is inversely proportional to the size of a_o', a large value of a_o' will result in a small Airy pattern. Consequently, annuli in the planes of odd order will be small.

(3) Since the energy entering the system is proportional to $(a_o')^2$, a small hole will form diffraction patterns having a low illumination. Consequently it may be difficult to observe and photograph such diffraction patterns.

(4) The possible radii are dictated by the available drill sizes.

After considering all these factors, the value chosen was $a_o' = 0.0701$ cm giving a ratio of similitude $k = 1.68$. Consequently, the theoretical radii in plane 1 are determined by equations of the type,

$$a_1' = A_1 \sqrt{\frac{D\lambda}{2\pi}} \frac{a_o}{a_o'} = \frac{A_1 D\lambda}{2\pi a_o'} = 0.02480\, A_1 \text{ cm} \qquad 6.2$$

Pupils based on the special points

For diaphrams in plane 1 having radii equal to the abscissae of special points, the theoretical and experimental radii and parameters are:

theoretical parameter	experimental parameter	theoretical radius a_1' (cm)	experimental radius a_1' (cm)
3.054	3.105	0.0758	0.0770
3.832	3.729	0.0950	0.0924
5.135	5.135	0.1273	0.1273
7.016	7.019	0.1740	0.1741
8.158	8.220	0.4046	0.4077

Radii of the narrow annuli system

In the case of a narrow annuli system, a much greater experimental precision is required in the width of each annulus than on its average radius. The parameter widths ΔW_1 and ΔW_2 are related by equation 5.70 which for $W_1 = 0$ and $W_2 = 7.3469$ becomes,

$$\Delta W_1 = \sqrt{0.5991\ \Delta W_2} \qquad 6.3$$

From equation 6.2, the corresponding radii widths are given by,

$$a_1' - b_1' = 0.02480\ \Delta W_2$$
$$c_1' = 0.02480\ \sqrt{0.5991 \Delta W_2} \qquad 6.4$$

To achieve the maximum accuracy in the widths, holes with radii c_1' and a_1' were first drilled with available drill sizes and measured (the method was given previously). b_1' was then machined to a diameter which would accurately satisfy equation 6.3. The theoretical and experimental radii and parameters are:

radii	theoretical radii (cm)	experimental radii (cm)
a_1'	0.2068	0.2085
b_1'	0.1537	0.1537
c_1'	0.0271	0.0283
d_1'	0	0

parameter	theoretical parameter	experimental parameter
A_1	8.3469	8.4097
B_1	6.1972	6.1972
C_1	1.0946	1.1411
D_1	0	0

Radii of the selected system

radii	theoretical radii (cm)	experimental radii (cm)
a_o'	0.1946	0.1942
a_1'	0.0729	0.0733
a_2'	0.2766	0.2776
b_2'	0.1537	0.1537

CONCLUSIONS.

As a result of the analytical and experimental study of diffraction channels, we have obtained various properties of mode formation and of iterated diffraction. This has led to the investigation of two systems of iterated diffraction.

In the study of mode formation, we have shown the successive structural modifications of iterated diffraction patterns when they tend towards the dominant mode, iteration by iteration.

The study of diffraction channels for hyperresolution was approached analytically, numerically and computationally: A significant step in our analytical study of hyperresolution was to point out the fundamental role of the even function and of the average even amplitude. We established certain properties of iterated diffraction patterns which were useful tools for a complete understanding of these optical systems. For example, the development of the analytical expression for the diffraction pattern in plane 2 when S is large. Also, the expression developed for strongly diffracted light. The concept of a homothetic diffraction channel was developed, and used in our experimental systems.

The work reported in this thesis gives very little indication of the extensiveness of the computational investigation, which resulted literally in tons of computer output.

The numerical study and experimental work gave complementary information. For example, we obtained numerically some information that the experimental work could not give on phase and therefore functions associated with amplitude. On the contrary, visual observation and photography were far superior to computation for the study of energy distribution in the diffraction patterns. Photographs were particularly useful in the analysis of the experimental systems. For example, the selected systems were studied by means of analytical equations suggested by certain photographs.

To the best of our knowledge, the work in this thesis is the first broad study of diffraction channels; we were not able to find any literature which can be used as a starting point. Therefore, the analytical, numerical and experimental investigations in this thesis are a first step to further progress in this area. In this work, various properties of diffraction channels have been found and an investigation has been made into the possible use of diffraction channels for hyperresolution. As a result, two systems were designed, constructed and studied both theoretically and experimentally for their hyperresolving properties.

The selected system gave some improvement in the energy characteristic for plane 3 over that in plane 1 but the improvement was slight and it did not satisfy the goal set for hyperesolution. This goal was only achieved with the use of the modulation function. For the narrow

annuli system, the improvement in the energy characteristic for low values of S was associated with a deterioration of the characteristic for higher values of S. This can be compared with the work by Toraldo di Francia 1952 mentioned in Chapter 1: The narrowing of the central spot was associated with an increase of the luminous energy in the outer rings.

Based on the comparison of the energy characteristic for the selected system in planes 3 and 1, it may be said that hyperresolution has been achieved theoretically to a certain degree. However, it has not been achieved to the extent that a practical hyperresolving system should be constructed.

The prospects for achieving a practical hyperresolving system by this method do not appear great. Nevertheless, one cannot overlook the possibility that an approach different from those studied would lead to a practical system. It would seem however, that before other approaches are attempted, it is necessary to consider the fundamental requirements for hyperresolution. Since information theory has been used by various authors to prove the principle of hyperresolution, this theory might also give useful information on how a practical diffraction channel can be designed for hyperresolution.

APPENDIX A

Bessel function formulas.

The following equations involving Bessel functions are used in this thesis. The derivations for these equations may be obtained from standard references, one of which is given in each case. In many cases, a simple algebraic substitution is necessary to obtain the form given here from the equation given in the reference.

The Bessel function of order n can be defined in its series form as,

$$J_n(Z) = \sum_{k=o}^{\infty} \frac{(-1)^k (\frac{Z}{2})^{n+2k}}{k!\ (k+n)!} \qquad \text{A1}$$

Watson, pg. 15, eq. 1

Integrals

$$\frac{1}{2\pi} \int_o^{2\pi} e^{iWX \cos(\phi-\theta) - im\phi} = e^{im(\frac{\pi}{2}-\theta)} J_m(WX) \qquad \text{A2}$$

Stratton, pg. 372, eq. 59

$$\frac{1}{2\pi} \int_o^{2\pi} \cos m\phi\ e^{iWX \cos(\phi-\theta)}\, d\phi = i^m \cos m\theta\ J_m(WX) \qquad \text{A3}$$

derived from eq. A2

$$\frac{1}{2\pi} \int_o^{2\pi} e^{iWX \cos(\phi-\theta)}\, d\phi = J_o(WX) \qquad \text{A4}$$

derived from eq. A2

$$\int_0^1 X^{m+1} J_m(WX)\,dX = \frac{J_{m+1}(W)}{W} \qquad \text{A5}$$

McLachlan, pg. 192, eq. 30

$$\int_0^{2\pi}\int_0^1 X^{m+1} \cos m\phi \; e^{iWX\cos(\phi-\theta)}\,dX d\phi = i^m \cos m\theta \; \frac{J_{m+1}(W)}{W} \qquad \text{A6}$$

derived from eq. A3 and A5.

$$\int_0^1 J_n(SX)\, J_n(WX)\, X\,dX = \frac{1}{S^2-W^2}\,[SJ_n(W)J_{n+1}(S) - WJ_n(S)J_{n+1}(W)] \quad S\neq W \qquad \text{A7}$$

$$= \frac{1}{2}\,[J_n^2(W) - J_{n-1}(W)\, J_{n+1}(W)] \quad S=W$$

McLachlan, pg. 195, eq. 79 & 80.

Series Formula

$$\cos(SX\cos\phi) = J_o(SX) + 2\sum_{k=1}^{\infty} J_{2k}(SX)\cos 2k\phi \qquad \text{A8}$$

Watson, pg. 22, eq. 1

$$e^{iSX\cos\phi} = J_o(SX) + 2\sum_{k=1}^{\infty} i^k J_k(SX)\cos k\phi \qquad \text{A9}$$

McLachlan, pg. 57, eq. 12

Differential equation

$$\frac{1}{X}\frac{d}{dW}\left[W^k J_k(WX)\right] = W^k J_{k-1}(WX) \qquad \text{A10}$$

McLachlan, pg. 192, eq. 32

Recursion formula

$$\frac{2n}{Z} J_n(Z) = J_{n+1}(Z) + J_{n-1}(Z) \qquad \text{A11}$$

McLachlan, pg. 191, eq. 29

APPENDIX B

Formulas involving the function $L_n(W)$

The following formulas involving the function $L_n(W)$ are used in this thesis. The equations are easily derived from the Bessel function equations indicated. Tables of values for the functions $L_n(W)$ are available in Jahnke, Emde, Losch.

The function $L_n(W)$ is defined by,

$$L_n(W) = 2^n n! \frac{J_n(W)}{W^n} = \sum_{k=o}^{\infty} \frac{(-1)^k n!}{k!\ (n+k)!} \left(\frac{W}{2}\right)^{2k} \qquad \text{B1}$$

Recursion formula

$$L_{n-1}(W) = L_n(W) - \frac{W^2}{4n(n+1)} L_{n+1}(W) \qquad \text{B2}$$

derived from A10 and B1

Derivative

$$\frac{dL_n(W)}{dW} = -\frac{WL_{n+1}(W)}{2(n+1)} \qquad \text{B3}$$

derived from A9 and B1

Integrals

$$\int_0^W L_n(W)\ W dW = -2nL_{n-1}(W) \qquad \text{B4}$$

derived from A5 and B1

$$\int_0^W L_n(W) L_m(W)\ W dW = \left[\frac{2nm}{n+m-1}\right]\left[1-L_{n-1}(W)L_{m-1}(W) - \frac{W^2}{4nm} L_n(W)L_m(W)\right] \qquad \text{B5}$$

derived from eq. 11.105, 11.107 of Wheelon and eq. B1

BIBLIOGRAPHY.

Barnes, C.W., Object Restoriation in a Diffraction-Limited Imaging System, Journal of the Optical Society of America, Vol. 56, No. 5, May 1966.

Christian, J.R. and G. Goubau, Experimental Studies on a Beam Waveguide for Millimeter Waves, IRE Transactions on Antennas and Propagation, Volume AP-9, Number 3, May 1961.

Goodman, J.W., Introduction to Fourier Optics, McGraw Hill 1968.

Goubau, G., and Schwering, F., On the Guided Propagation of Electromagnetic Wave Beams, IRE Transactions on Antenna and Propagation, Volume AP-9, Number 3, May 1961.

Hamming, R.W. Numerical Methods for Scientists and Engineers, McGraw Hill, 1962.

Harris, J.L. Diffraction and Resolwing Power, Journal of the Optical Society of America, Vol. 54, No. 7, July 1964.

Jahnke, Emde, Losch, Tables of Higher Functions, 6th edition, McGraw Hill, 1960.

McLachlan, N.W., Bessel Functions for Engineers, 2nd edition, Oxford, 1955.

Stratton, J.A. Electromagnetic Theory, McGraw Hill, 1941.

Toraldo di Francia , Super-Gain Antennas and Optical Resolving Power, Nuovo Cimento Suppl. 9, 426, 1952.

Watson, G.N. A treatise on the Theory of Bessel Functions, Cambridge University Press, 1966.

Wheelon, Albert Dewell, Tables of summable series and integrals involving Bessel functions, Holden-Day, 1968.

Lansraux, G. Japan, J. Appl. Phys. 4, Suppl. (1965) 261

Lansraux, G. Metrologia 1, (1965) 31.

Boivin, C.-P., Ph.D. Thesis, Unpublished, University of Ottawa, 1969.

ERRATA

The word "diaphram" throughout the whole thesis should be spelled "diaphragm".